



**UNIVERSIDADE FEDERAL DE UBERLÂNDIA**  
**INSTITUTO DE BIOTECNOLOGIA**  
**PÓS-GRADUAÇÃO EM GENÉTICA E BIOQUÍMICA**

**NANOCRYSTALS IN GLYPHOSATE DETECTION**

**Aluno:** Anderson Luis do Valle

**Orientador:** Luiz Ricardo Goulart Filho

**Co-Orientador:** Luciano Pereira Rodrigues

**UBERLÂNDIA-MG**

**2019**



**UNIVERSIDADE FEDERAL DE UBERLÂNDIA**  
**INSTITUTO DE BIOTECNOLOGIA**  
**PÓS-GRADUAÇÃO EM GENÉTICA E BIOQUÍMICA**

**Aluno:** Anderson Luis do Valle

**Orientador:** Luiz Ricardo Goulart Filho

**Co-Orientador:** Luciano Pereira Rodrigues

Tese apresentada à Universidade Federal de Uberlândia como parte dos requisitos para obtenção do Título de Doutor em Genética e Bioquímica (Nanobiotecnologia)

UBERLÂNDIA-MG

2019



Ficha Catalográfica Online do Sistema de Bibliotecas da UFU  
com dados informados pelo(a) próprio(a) autor(a).

V181  
2019 Valle, Anderson Luis do, 1979-  
NANOCRYSTALS IN GLYPHOSATE DETECTION [recurso  
eletrônico] / Anderson Luis do Valle. - 2019.

Orientador: Luiz Ricardo Goulart Filho.  
Coorientador: Luciano Pereira Rodrigues.  
Tese (Doutorado) - Universidade Federal de Uberlândia, Pós-  
graduação em Genética e Bioquímica.  
Modo de acesso: Internet.  
Disponível em: <http://dx.doi.org/10.14393/ufu.te.2019.2229>  
Inclui bibliografia.

1. Genética. I. Goulart Filho, Luiz Ricardo , 1962-, (Orient.). II.  
Pereira Rodrigues, Luciano, 1976-, (Coorient.). III. Universidade  
Federal de Uberlândia. Pós-graduação em Genética e Bioquímica.  
IV. Título.

CDU: 575

Bibliotecários responsáveis pela estrutura de acordo com o AACR2:  
Gizele Cristine Nunes do Couto - CRB6/2091  
Nelson Marcos Ferreira - CRB6/3074



UNIVERSIDADE FEDERAL DE UBERLÂNDIA

**ATA DE DEFESA - PÓS-GRADUAÇÃO**

Programa de Pós-Graduação em:	Genética e Bioquímica - PPGGB				
Defesa de:	Tese de Doutorado Acadêmico				
Data:	Vinte e três de setembro de 2019	Hora de início:	14:00h	Hora de encerramento:	19:00h
Matrícula do Discente:	11523GBI021				
Nome do Discente:	Anderson Luis do Valle				
Título do Trabalho:	O uso de nanocristais na detecção de glifosato.				
Área de concentração:	Genética				
Linha de pesquisa:	Biologia Molecular				
Projeto de Pesquisa de vinculação:	Desenvolvimento de sensores biológicos para o controle ambiental.				

Aos vinte e três dias do mês de setembro de dois mil e dezenove, às 14:00 horas no Anfiteatro 4K, Campus Umuarama da Universidade Federal de Uberlândia, reuniu-se a Banca Examinadora, designada pelo Colegiado do Programa de Pós-graduação em Genética e Bioquímica, assim composta: Prof. Dr. Marcos Vinícius Dias Vermelho, Prof. Dr. Marcelo Porto Bemquerer, Prof. Dr. Eduardo De Faria Franca, Prof. Dr. Foued Salmen Espíndola e Prof. Dr. Luiz Ricardo Goulart Filho, orientador (a) do (a) candidato (a) e demais convidados presentes conforme lista de presença. Iniciando os trabalhos o (a) presidente da mesa, o Prof. Dr. Luiz Ricardo Goulart Filho, apresentou a Comissão Examinadora e o (a) candidato (a), agradeceu a presença do público, e concedeu o (à) Discente a palavra para a exposição do seu trabalho. A duração da apresentação do (a) Discente e o tempo de arguição e resposta foram conforme as normas do Programa de Pós-graduação em Genética e Bioquímica. A seguir o (a) senhor (a) presidente concedeu a palavra, pela ordem sucessivamente, aos examinadores, que passaram a arguir o (a) candidato (a). Ultimada a arguição, que se desenvolveu dentro dos termos regimentais, a Banca, em sessão secreta, atribuiu os conceitos finais. Em face do resultado obtido, a Banca Examinadora considerou o candidato (a):

APROVADO (A).

Esta defesa de Tese de Doutorado é parte dos requisitos necessários à obtenção do título de Doutor. O competente diploma será expedido após cumprimento dos demais requisitos, conforme as normas do Programa, a legislação pertinente e a regulamentação interna da UFU. Nada mais havendo a tratar foram encerrados os trabalhos. Foi lavrada a presente ata que após lida e achada conforme foi assinada pela Banca Examinadora.

Documento assinado eletronicamente por **Luiz Ricardo Goulart Filho, Professor(a) do Magistério Superior**, em 23/09/2019, às 19:02, conforme horário oficial de Brasília, com fundamento no art. 6º, § 1º, do [Decreto nº 8.539, de 8 de outubro de 2015](#).



Documento assinado eletronicamente por **Marcos Vinícius Dias Vermelho, Usuário Externo**, em 23/09/2019, às 19:04, conforme horário oficial de Brasília, com fundamento no art. 6º, § 1º, do [Decreto nº 8.539, de 8 de outubro de 2015](#).



Documento assinado eletronicamente por **Eduardo de Faria Franca, Professor(a) do Magistério Superior**, em 23/09/2019, às 19:05, conforme horário oficial de Brasília, com fundamento no art. 6º, § 1º, do [Decreto nº 8.539, de 8 de outubro de 2015](#).



Documento assinado eletronicamente por **Marcelo Porto Bemquerer, Usuário Externo**, em 23/09/2019, às 19:09, conforme horário oficial de Brasília, com fundamento no art. 6º, § 1º, do [Decreto nº 8.539, de 8 de outubro de 2015](#).



Documento assinado eletronicamente por **Foued Salmen Espíndola, Membro de Comissão**, em 24/09/2019, às 09:59, conforme horário oficial de Brasília, com fundamento no art. 6º, § 1º, do [Decreto nº 8.539, de 8 de outubro de 2015](#).



A autenticidade deste documento pode ser conferida no site [https://www.sei.ufu.br/sei/controlador\\_externo.php?acao=documento\\_conferir&id\\_orgao\\_acesso\\_externo=0](https://www.sei.ufu.br/sei/controlador_externo.php?acao=documento_conferir&id_orgao_acesso_externo=0), informando o código verificador **1488185** e o código CRC **ED5B94B2**.



**UNIVERSIDADE FEDERAL DE UBERLÂNDIA**  
**INSTITUTO DE BIOTECNOLOGIA**  
**PÓS-GRADUAÇÃO EM GENÉTICA E BIOQUÍMICA**

**NONOCRISTAIS NA DETECÇÃO DE GLIFOSATO**

**ALUNO:** Anderson Luis do Valle

**COMISSÃO EXAMINADORA**

**Presidente:** Prof. Dr. Luiz Ricardo Goulart Filho (Orientador)

**Examinadores:**

Membro Externo: Marcos Vinícius Dias Vermelho

Membro Externo: Marcelo Porto Bemquerer

Membro Interno: Eduardo de Faria Franca

Membro Interno: Foued Salmen Spíndola

**Data da Defesa:** \_\_\_\_ / \_\_\_\_ / \_\_\_\_

As sugestões da Comissão Examinadora e as Normas PGGB para o formato da Dissertação/Tese foram contempladas

---

Luiz Ricardo Goulart Filho

## AGRADECIMENTOS

Esse foi um desafio pessoal. Entretanto, esta tese foi um desafio compartilhado. A primeira linha surgiu com toda a amizade e apoio que Francielli me deu. Na sequência alguns amigos como William Mendonça, um entusiasta, professor de química, que me convenceu que um doutorado sobre aplicação da nanobiotecnologia no combate ao uso de agrotóxicos seria um desafio e uma forma de agradecer à Mãe Terra. Luiz Ricardo Goulart que aceitou este desafio, agregando mais uma linha de pesquisa. Meu chefe, Rodrigo Herles dos Santos, que compreendeu a importância deste passo para termos melhor qualidade na gestão pública, e meus colegas de trabalho, que por vezes ficaram sobrecarregados. Minha esposa, que absorveu muitas de nossas tarefas. Meu coorientador, paciente e dedicado, Luciano Pereira Rodrigues, muito presente em cada capítulo desta tese. Meus pais que investiram no meu potencial. Em alguns momentos pensei em desistir. Eu não queria um título mais que um desafio pessoal. Eis que me lembrei de Kelson, um porteiro que conheci em Natal. Ele ganhava a metade de minha bolsa de mestrado, que naquela época já era vergonhosa. Na casa dele encontrei uma coleção com umas 20 revistas da National Geographic empilhadas ao lado do sofá. Casa de chão cimento queimado e telhado cerâmica exposta. Lhe disse: termine o fundamental. E ele o fez. Termine o ensino médio. Preste o vestibular na Federal. E passo por passo, vítima de todos os preconceitos sociais, da cor de sua pele às escolhas diversas, de porteiro a professor e a doutorando na Universidade Federal do Rio Grande do Norte. Vida irônica do grande homem que dedicava seus finais de semana a projetos sociais, lhe entregou via postal o aceite para concluir seu doutorado no exterior junto do resultado conclusivo de exames médicos das dores recentes que havia sentido na barriga. Previamente mal diagnosticado, faleceu dias depois. Nas linhas finais, lembrei de muitos de meus professores, em especial à Profa. Cecília De Martino, que lá no fundamental foi capaz de me convencer que estudar era algo divertido. Os outros passos vieram na sequência. Meus filhos pela grande compreensão. Àqueles que dedicaram o próprio tempo para prestigiar esta defesa. No ponto final eu dedico à mãezona dos meus filhos. Essa é uma mulher que merece todos os agradecimentos. Começo, meio e fim.



“Não acredito em níveis seguros enquanto são os próprios fabricantes que fornecem os estudos toxicológicos às autoridades reguladoras;  
Não acredito nas autoridades reguladoras se elas desconhecem os componentes que constituem as formulações comerciais de tais produtos protegidas por patentes;  
Não acredito na fiscalização quando os custos das análises laboratoriais impedem políticas públicas;  
Não acredito em políticas públicas que não consideram o modo de trabalho do homem do campo. O homem do campo, sábio, corajoso e crédulo, aponta seu borrifador a favor do vento e nos serve a comida;  
Eu não tenho mesmo acreditado em muitas coisas, mas em uma única eu queria acreditar: sábios gestores se posicionando ao lado do princípio da precaução, e freando a máquina.  
Assim como o filme fotográfico desapareceu no tempo e levou à falência gigantes da indústria, haverá o dia em que tecnologias aplicadas à agricultura irão retirar do Brasil o pseudo título de celeiro do mundo. Pragas agrícolas resistentes aos agrotóxicos trarão sede às indústrias por novos químicos de prateleira. Entretanto hortas verticais e processos automatizados trarão alimento saudável às cidades. Os mercados consumidores serão locais e exigentes. Serão nesses dias que olharemos para a nossa terra e o nosso passado e perceberemos o quanto fomos ignorantes.  
Eu vejo esse futuro, mas sou a minoria.”

# Table of Contents

<b>LISTA DE FIGURAS.....</b>	<b>XI</b>
<b>LISTA DE TABELAS.....</b>	<b>XIV</b>
<b>LISTA DE SIGLAS.....</b>	<b>XV</b>
<b>APRESENTAÇÃO.....</b>	<b>17</b>
<b>CAPÍTULO I .....</b>	<b>19</b>
<b><i>Glyphosate detection: methods, needs and challenges</i> .....</b>	<b>19</b>
<b>ABSTRACT .....</b>	<b>21</b>
<b>INTRODUCTION .....</b>	<b>22</b>
General considerations.....	22
Environmental risks and animal's health.....	22
Reasons to determine precise levels of glyphosate .....	24
Glyphosate: metabolites and analogues, formulation toxicity and detection problems .....	26
<b>MEASUREMENT METHODS .....</b>	<b>28</b>
Chromatography techniques .....	28
Liquid chromatography .....	28
Spectroscopic methods .....	33
Electrochemical sensors .....	40
Capillary electrophoresis .....	43
Enzyme-linked immunosorbent assays .....	45

Cell biosensor .....	46
Cross-responses from multiple sensors.....	47
<b>DISCUSSION.....</b>	<b>48</b>
<b>CONCLUSION .....</b>	<b>48</b>
<b>Acknowledgements .....</b>	<b>50</b>
<b>Supplementary Material – Comparative techniques for Glyphosate detection .....</b>	<b>51</b>
<b>References.....</b>	<b>59</b>
<b><i>CAPÍTULO II .....</i></b>	<b><i>86</i></b>
<b><i>Glyphosate:ZnO Nanocrystal Interaction Controlled by pH Changes.....</i></b>	<b><i>86</i></b>
<b>ABSTRACT.....</b>	<b>88</b>
<b>INTRODUCTION .....</b>	<b>89</b>
<b>MATERIAL AND METHODS .....</b>	<b>91</b>
Synthesis and Characterization of ZnO Nanocrystals .....	91
Glyphotal TR® with ZnO Nanocrystals Solution .....	91
Fourier transform infrared spectroscopy (FTIR) .....	91
Scanning Electron Microscope (SEM) .....	91
Atomic Force Microscopy (AFM) .....	92
<b>RESULTS AND DISCUSSION.....</b>	<b>93</b>
The pH effect on Glyphosate FTIR spectra.....	93
FTIR spectra changes under different pH on Glyphosate-ZnO Nanocrystals.....	95
FTIR Glyphosate-ZnO Nanocrystals Spectra at pH 14 .....	99



FTIR Glyphosate-ZnO Nanocrystals Spectra at pH 5 .....	99
FTIR Glyphosate-ZnO Nanocrystals Spectra at pH 2 .....	100
The micrometric level structure under different pH on Glyphosate-ZnO Nanocrystals .....	101
The nanometric level structure under different pH on Glyphosate-ZnO Nanocrystals .....	105
A predicted model .....	107
<b>CONCLUSION .....</b>	<b>111</b>
<b>Acknowledgements .....</b>	<b>112</b>
<b>Supplements.....</b>	<b>113</b>
<b>References.....</b>	<b>114</b>
<b><i>CAPÍTULO III .....</i></b>	<b><i>122</i></b>
<b><i>Application of ZnO Nanocrystals as a Surface-Enhancer FTIR for Glyphosate</i></b>	
<b><i>Detection .....</i></b>	<b><i>122</i></b>
<b>ABSTRACT.....</b>	<b>124</b>
<b>INTRODUCTION .....</b>	<b>125</b>
<b>MATERIALS AND METHODS .....</b>	<b>128</b>
Synthesis and Characterization of Nanocrystals.....	128
Characterization of the GLYPHOTAL TR® with Nanocrystals .....	128
Fourier transform infrared spectroscopy (FTIR) .....	128
Atomic force microscopy (AFM) .....	129
Enhancement properties analysis.....	129
<b>RESULTS .....</b>	<b>130</b>

DISCUSSION .....	138
CONCLUSION .....	142
References.....	144
<b>CAPÍTULO IV .....</b>	<b>155</b>
<b><i>Smartphone-based surface plasmon resonance device for glyphosate detection</i></b> .....	<b>155</b>
ABSTRACT.....	157
INTRODUCTION .....	158
MATERIAL AND METHODS.....	164
Smartphone-based SPR sensor .....	164
Samples.....	166
Microscopy Analysis of the Glyphosate-CuO interaction .....	166
Analysis of the absorbance spectrum of glyphosate samples.....	167
EXPERIMENTAL RESULTS.....	168
Performance analysis .....	171
DISCUSSION.....	181
CONCLUSIONS .....	184
References.....	185

# LISTA DE FIGURAS

Chapter II, Figure 1. FTIR spectra of Glyphotal TR <sup>®</sup> in three different pH (A) and ZnO nanocrystals (B), all in ultrapure water [10 <sup>-2</sup> v/v]. The area highlighted in the spectrum corresponds to vibrational modes and chemical bonds of glyphosate spectra. ....	94
Chapter II, Figure 2. FTIR spectra of Glyphotal TR <sup>®</sup> when interacting with ZnO in three different pH, all in ultrapure water [10 <sup>-2</sup> v/v]. The area highlighted in the spectrum corresponds to vibrational modes and chemical bonds of glyphosate spectra. ....	95
Chapter II, Figure 3. Glyphotal TR <sup>®</sup> and Glyphosate-ZnO [10 <sup>-2</sup> v/v] spectra in 3 different pH.....	96
Chapter II, Figure 4 Heat map of the transmittance's vibrations modes energy of Glyphosate [10 <sup>-2</sup> v/v] and Glyphosate-ZnO [10 <sup>-2</sup> v/v] interaction after spectra normalization. Ratio represents the relation between Glyphosate-ZnO and Glyphosate by pH evidencing the freedom and reactive structures in solution. As bluer, as more energy, as less interaction with another molecules. ....	97
Chapter II, Figure 5. Schematic representations of the ZnO-Glyphosate interaction process. As transmittance decrease, as more energy was absorbed by the sample. The transmitted energy is detected by FTIR by vibrating mode of the structures. As more bonded as less a structure is able to vibrate. Hence, as bigger the transmittance as bigger interaction. ....	98
Chapter II, Figure 6. Glyphotal TR <sup>®</sup> vibrating modes after H <sub>2</sub> SO <sub>4</sub> addition showing a great concentration of glyphosate in the inferior phase. ....	101
Chapter II, Figure 7. SEM of Glyphotal TR <sup>®</sup> -ZnO [10 <sup>-4</sup> v/v] at pH 13-14.....	102
Chapter II, Figure 8. SEM of Glyphotal TR <sup>®</sup> -ZnO [10 <sup>-4</sup> v/v] pH 9.....	103
Chapter II, Figure 9. SEM of Glyphotal TR <sup>®</sup> -ZnO [10 <sup>-4</sup> v/v] pH 6-7. ....	103
Chapter II, Figure 10 SEM of Glyphotal TR <sup>®</sup> -ZnO [10 <sup>-4</sup> v/v] pH 3-4. ....	104
Chapter II, Figure 11. SEM of Glyphotal TR <sup>®</sup> -ZnO [10 <sup>-4</sup> v/v] pH 0-1. Like stars ZnO NCs are dispersed on the solution (A). Black holes are imperfections of the carbon tape. The end of a star is represented in (B) containing many ZnO NCs. ....	104
Chapter II, Figure 12. Figure 11. AFM of Glyphotal TR <sup>®</sup> and Glyphotal TR <sup>®</sup> -ZnO [10 <sup>-4</sup> v/v] pH 13-14. ....	106
Chapter II, Figure 13. AFM of Glyphotal TR <sup>®</sup> and Glyphotal TR <sup>®</sup> -ZnO [10 <sup>-4</sup> v/v] pH 9.....	106
Chapter II, Figure 14. AFM of Glyphotal TR <sup>®</sup> and Glyphotal TR <sup>®</sup> -ZnO [10 <sup>-4</sup> v/v] pH 6-7. ....	106
Chapter II, Figure 15. AFM of Glyphotal TR <sup>®</sup> and Glyphotal TR <sup>®</sup> -ZnO [10 <sup>-4</sup> v/v] pH 3-4 at 4.00 μm <sup>2</sup> and 2.00 μm <sup>2</sup> . ....	107
Chapter II, Figure 16. AFM of Glyphotal TR <sup>®</sup> and Glyphotal TR <sup>®</sup> -ZnO [10 <sup>-4</sup> v/v] pH 0-1 at 4.00 μm <sup>2</sup> and 2.00 μm <sup>2</sup> . ....	107

Chapter II, Figure 17. AFM of Glyphotal TR <sup>®</sup> and Glyphotal TR <sup>®</sup> -ZnO [ $10^{-4}$ v/v] pH 6-7. ....	109
Chapter II, Figure 18. A hypothesis about glyphosate's clouds around ZnO NCs in pH 6-10. ....	110
Chapter II, Figure 19. Glyphosate-ZnO model in accordance to pH changes. ....	111
Chapter II, Figure 20. Controls for AFM figures. A. Mica surface: The flattest known surface made by silica sheet. B. Glyphotal TR <sup>®</sup> above mica surface. ....	113
Chapter III, Figure 1. (A) XRD of ZnO, Ag-doped ZnO and Ag <sub>2</sub> O nanocrystals. (B) The inset shows a zoom around the peak (100) of ZnO. ....	131
Chapter III, Figure 2. A) ZnO, ZnO:0.3Ag, ZnO:1.0Ag and Ag <sub>2</sub> O. (B) GLYPHOTAL TR <sup>®</sup> at [ $10^{-2}$ v/v], [ $10^{-4}$ v/v] and [ $10^{-6}$ v/v], and GLYPHOTAL TR <sup>®</sup> -NCs interacted at $10^{-6}$ v/v, (C) zoom of the glyphosate in GLYPHOTAL TR <sup>®</sup> spectra. ....	132
Chapter III, Figure 3. FTIR nanocrystals' spectra comparison of GLYPHOTAL TR <sup>®</sup> at [ $10^{-2}$ v/v] and GLYPHOTAL TR <sup>®</sup> - Ag <sub>2</sub> O. ....	133
Chapter III, Figure 4. Energy color scale. ....	134
Chapter III, Figure 5. Structures formed by four different kinds of nanocrystals interacted with GLYPHOTAL TR <sup>®</sup> ( $10^{-4}$ ) ....	138
Chapter IV, Figure 1. The basic configuration of a biosensor based on the SPR phenomenon. N1 – Non-conductive layer of the biochip (polymer), N2 - Metallic layer (a thin film of gold), N3 - Sensitive layer (biochemical). ....	160
Chapter IV, Figure 2. SPR characteristic curve. Reflections in function of the angle of incidence. For each sensitive layer type, we have a refractive index associated with a different resonance angle (res). ....	161
Chapter IV, Figure 3. Portable multi-analytic detection platform hardware architecture. Camera - photodetector, Processor - image processing, Display - light source, User Interface (Display) - information input and output and Biochip - Transducer (converts biochemical signal to electrical signal). ....	165
Chapter IV, Figure 4. Smartphone-based Portable Multi-analytical SPR Biosensor Device. The screen of the smartphone sends the signal that light in the entrance of the biochip is transmitted to its exit and captured by the camera of the smartphone in image form. The captured images are stored in the internal memory of the smartphone and processed, for extraction of the characteristic information to the SPR technique of analysis. ....	165
Chapter IV, Figure 5. Investigation of the influence of different nanoparticles on the absorbance spectrum of glyphosate-containing samples. Acronyms: UP - ultrapure water, GL - glyphosate, Ag <sub>2</sub> O - silver oxide nanoparticle, CuO-nanoparticle of copper oxide and ZnO - nanoparticle of zinc oxide. The red curves represent the samples with glyphosate in the dilution of $10^{-2}$ (v/v), the green curves represent the samples with glyphosate in the dilution of $10^{-6}$ (v/v) and the blue curves represent the samples with glyphosate in the dilution of $10^{-8}$ (v/v). Full line curves are related to samples without the influence of nanoparticles, dashed curves with the influence of Ag <sub>2</sub> O nanoparticles, traces curves with points with the influence of CuO nanoparticles and dotted curves with the influence of ZnO nanoparticles. ....	168

Chapter IV, Figure 6. Investigation of the influence of pH on the absorbance spectrum of substances containing glyphosate at a dilution of $10^{-8}$ (v/v) and copper oxide nanoparticles. Following the legend: pH 1 - acid, pH 7 - neutral, pH 10 - basic.....	170
Chapter IV, Figure 7. Investigation of the influence of pH 1-acid in UP-ultrapure water on the absorbance spectrum of glyphosate-containing substances in the dilutions of $10^{-2}$ , $10^{-4}$ , $10^{-6}$ and $10^{-8}$ (v/v) and CuO-oxide nanoparticles copper.....	171
Chapter IV, Figure 8. Curves resulting from the analysis of the intensity of the pixels of the images. Following the legend: REF - Reference signals of the pixels intensity for the channels (R, G and B). Signal - signals of the intensity of the pixels relative to the analysis of the samples for the channels (R, G and B)..	173
Chapter IV, Figure 9. Curves of the energy signals for the channels (R, G and B) of the images resulting from the analysis of the substances. $\Delta E_R$ - Energy variation for the red channel. $\Delta E_G$ - Energy variation for the green channel. $\Delta E_B$ - Energy variation for the blue channel.....	174
Chapter IV, Figure 10. Energy signal curve for the red channel of the images resulting from the analysis of the samples containing different concentrations of the glyphosate and CuO nanoparticle.....	175
Chapter IV, Figure 11. Signals referring to the analysis of samples containing glyphosate in the solutions of $10^{-6}$ , $10^{-4}$ and $10^{-2}$ (v/v) in neutral pH. a-) Signal obtained by the biosensor platform presented the energy of the channel (R) in relation to the concentration of glyphosate. b-) Signal obtained by UV-Vis showing the maximum absorbance in relation to the glyphosate concentration.....	176
Chapter IV, Figure 12. Signals pertaining to the analysis of glyphosate-containing substances in the dilutions of $10^{-8}$ , $10^{-6}$ , $10^{-4}$ and $10^{-2}$ (v/v) in acidic pH. a-) Signal obtained by the biosensor platform presented the energy of the channel (R) in relation to the glyphosate concentration. b-) Signal obtained by UV-Vis showing the maximum absorbance in relation to glyphosate concentration.....	177
Chapter IV, Figure 13. Calculated sensitivity to the sample analysis with glyphosate diluted at dilution of $10^{-6}$ , $10^{-4}$ and $10^{-2}$ , considering acidic and neutral pH. a-) Calculated sensitivity for the proposed sensor. b-) Calculated sensitivity for UV-Vis approach.....	178
Chapter IV, Figure 14 AFM of the (A) mica sheet used to support (B) Glyphosate, (C1 and C2) CuO nanocrystals in water and (C3 and C4) Glyphosate-CuO interacted.....	179
Chapter IV, Figure 15. SEM of Glyphotol TR-CuO ( $10^{-2}$ v/v) in pH 1, 6 and 14. Like stars CuO nanocrystals are shown interacted with Glyphosate. The starry structure is missed as the pH increases. EDS results: mean - C (65.15), O (16.87), Cu (12.63), Au (5.35); Std. deviation: C (3.17), O (2.39), Cu (3.31), Au (0.44). .....	180

## LISTA DE TABELAS

1 - Chapter, Table 1 - Comparative detection methods. ....	51
2- Chapter 2, Table 1 - Energy color scale. ....	134

## LISTA DE SIGLAS

- 2-mercapto-5-nitrobenzi-midazole-capped silver nanoparticles (MNBZ-Ag NPs)
- 2-mercapto-5-nitrobenzi-midazole-capped silver nanoparticles (MNBZ-Ag NPs) and  $Mg^{2+}$  ions (MNBZ-Ag NPs– $Mg^{2+}$ )
- 3,3',5,5'-tetra- methylbenzidine (TMB)
- 9-fluorenylmethyl chloroformate (FMOC)
- Atemoya peroxidase (ES-Ate- moya)
- Attention-deficit/hyperactive disorder (ADHD)
- Average recovery analytes (ARA)
- Background electrolytes (BGEs)
- Bacteriophages (SPR-pd)
- Bioelectric Recognition Assay (BERA)
- Capacitively coupled contactless conductivity system (CE-C(4)D)
- Capillary electrophoresis (CE)
- Carbon dot-labeled antibodies (IgG-CDs)
- Chemiluminescence (CL)
- Chemiluminescence-molecular imprinting sensor (CL-MIS)
- Chromatography–mass spectrometry (LC/MS), or (HPLC/MS)
- Cross-responses from multiple sensors (CRMS)
- Energy-Dispersive X-Ray Spectroscopy (EDS)
- Electron capture detector (GC/ECD)
- Electrospray ionization (ESI)
- Enzyme-linked immunosorbent assay (ELISA)
- European Glyphosate Task Force (GTF)
- European Union (EU)
- Flame ionization detector (GC/FID)
- Flame photometric detector (GC/FPD)
- Fluorescence detector (FLD)
- Fluorescence magnetic nanoparticles (FMPs)
- Fluorescence magnetic nanoparticles (FMPs) coupled to specific DNA probe (FS- FPMs/DNA)
- Fluorescence resonance energy transfer (FRET)
- Fluorometric sensor (FS)
- Gas chromatography (GC)
- GC–CI (chemical ionization)–MS
- GC–EI (electron impact)–MS
- GC–FID (flame ionization detector)–MS
- Glutathione (GSH)
- Glutathione S-transferase (GST)
- GLY-dsDNA-gold conjugate nanoparticles (FS-AU/DNA)
- Glyphosate [(N-phosphonomethyl) glycine] (GLY)
- Gold nanoparticles (NPs) with Cysteamine (CS-AuNPs)
- High-performance liquid chromatography (HPLC)
- Hollow-core metal-cladded waveguide (HCMW)

- Horseradish peroxidase (ES-HRP)
- Hydrophilic interaction chromatography (HILIC)
- Immunosensor (IS)
- Indirect ELISA (CI-ELISA)
- Integrated pulsed amperometric detection (IC/IPAD)
- Intramolecular Indicator Displacement Assay (IIDA)
- Ion chromatography (IC)
- Laser-induced fluorescence (LIF)
- Limits of Detection (LOD)
- Linker-assisted enzyme-linked immunosorbent assay (L'ELISA)
- Liquid chromatography (LC)
- Lowest Observed Adverse Effect Level or (LOAEL)
- Mass spectrometer (MS) detectors (LC/MS)
- Maximum residue limit (MRL)
- Micro-electrospray interface (mESI)
- Molecular imprinting sensor (MI)
- NiAl-LDH ( $\text{Ni}_1\text{-Al}_x(\text{OH})_2\text{NO}_3 \cdot n\text{H}_2\text{O}$ - layered double hydroxides)
- No Observed Adverse Effect Level (NOAEL)
- Nitrogen phosphorus detector (GC/NPD)
- Nuclear magnetic resonance spectroscopy (NMR)
- *o*-phthalaldehyde (OPA)
- Optical chemosensors (OC)
- Oxidation–reduction potential (ORP)
- QDs capped with thioglycolic acid (TGA-CdTe-QDs)
- Quantum dots (QDs)
- Reactive oxygen species (ROS)
- Reflectance spectroscopy (DRS)
- Reporter spacer receptors (RSR)
- Reversed phase (RP)
- Scanning electron microscope (SEM)
- Small dimension microspheres (MIMs)
- Superoxide dismutase (SOD)
- Surface plasmon resonance (SPR)
- Surface-enhanced Raman scattering (SERS)
- Tandem mass spectrometry (MS/MS)
- Tetradecyltrimethylammonium bromide (TTAB)
- The algal biosensor-chlorophyll fluorescence-based and isolated photosystem II (PSII)
- US Environmental Protection Agency (EPA)
- Voltammetric electronic tongue (VET)



## APRESENTAÇÃO

O glifosato é um herbicida toxicologicamente nocivo com potencial associação com a carcinogênese humana e outras doenças crônicas, incluindo comportamentos mentais e reprodutivos. As dificuldades para detectar e demonstrar sua toxicidade são provavelmente devido às suas propriedades quelantes de metais, à interferência de compostos orgânicos no meio ambiente e à similaridade com seus subprodutos. Como consequência, custos elevados para a detecção deste agrotóxico resultam em ausência de políticas públicas.

Uma vez as propriedades quelantes do glifosato, testamos a capacidade de detecção do complexo formado por esse herbicida e alguns nanocristais de óxidos metálicos em diversas condições de pH, usando métodos espectroscópicos através de um Equipamento de Infravermelho, cujos resultados são apresentados após a Transformada de Fourier (FTIR) e em um Sensor de Ondas Evanescentes Acopladas.

O primeiro capítulo foi publicado pela *Environmental Chemistry Letters* e apresenta a maior revisão bibliográfica contendo todas as tecnologias disponíveis para detecção e quantificação de glifosato dos últimos 36 anos, incluindo suas desvantagens e vantagens. O objetivo deste capítulo é criar uma fundamentação teórica demonstrando o status atual de conhecimento sobre métodos de detecção do glifosato que possa justificar a utilização de nanocristais em sua detecção.

O segundo capítulo, foi submetido para o *The Journal of Physical Chemistry Letters*. Investigou-se o complexo Glifosato-nanocristal de ZnO através de FTIR, microscopia eletrônica de varredura (SEM) e microscopia de força atômica (AFM) para teorizar suas propriedades químico-físicas. Este estudo fundamenta os ensaios experimentais dos próximos capítulos.

O terceiro capítulo foi submetido à *Analytical Chimica Acta* em agosto de 2019. Neste capítulo demonstra-se que nanocristais de óxido de zinco são potentes promotores espectrais de FTIR para amostras com glifosato enquanto

nanocristais de óxido de prata têm propriedades quelantes superiores em pH neutro.

O quarto capítulo foi submetido à *Sensors and Actuators Reports* em setembro de 2019. O objetivo deste estudo foi demonstrar a possibilidade de o Glifosato ser detectado através de um equipamento portátil de superfície plasmônica de ressonância acoplado a um celular através da complexação do herbicida com nanocristais de óxido de cobre, e em uma determinada condição específica de protonação.

## CAPÍTULO I

### Glyphosate detection: methods, needs and challenges

Publicado em: Environmental Chemistry Letters ISSN 1610-3653  
Environ Chem Lett DOI 10.1007/s10311-018-0789-5  
<http://link.springer.com/article/10.1007/s10311-018-0789-5>  
Reformatado para se adequar às regras de publicação da Tese

---

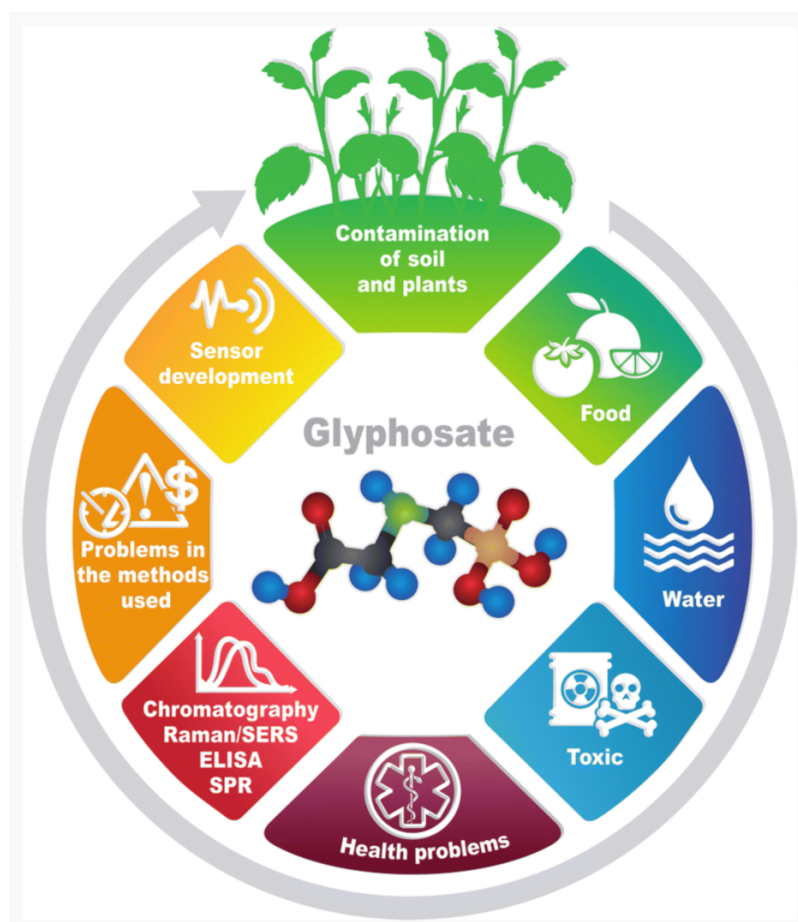
## *Glyphosate detection: methods, needs and challenges*

---

A.L. Valle<sup>1</sup> · F. C. C. Mello<sup>1</sup> · R. P. Alves-Balvedi<sup>1</sup> · L. P. Rodrigues<sup>2</sup> · L. R. Goulart<sup>1</sup>

<sup>1</sup> Laboratory of Nanobiotechnology, Institute of Biotechnology, Federal University of Uberlândia, Uberlândia, MG, Brazil.

<sup>2</sup> Institute of Engineering, Science and Technology, Federal University of Jequitinhonha and Mucuri's Valleys, Janaúba, MG, Brazil.



Desenho de Paula Cristina Brígido Tavares

## ABSTRACT

Glyphosate is considered toxicologically harmful and presents potential association with human carcinogenesis and other chronic diseases, including mental and reproductive behaviors. The challenges to analyze and demonstrate its toxicity are likely due to its metal-chelating properties, the interference of organic compounds in the environment, and similarity with its by-products. Whereas there is a link with serious health and environmental problems, there is an absence of public health policies, which is probably due to the difficulties in detecting glyphosate in the environment, further complicated by the undetectable hazard in occupational safety and health. The historical lenient use of glyphosate in transgenic-resistant crops, corroborated by the fact that it is not easily detected, creates the “Glyphosate paradox”, by which it is the most widely used herbicide and one of the most hardly determined. In this review, we revisited all available technologies for detection and quantification of glyphosate, including their drawbacks and advantages, and we further discuss the needs and challenges. Briefly, most of the technologies require high-end equipments and resources in low throughput, and none of them are adequate for real-time field tests, which may explain the lack of studies on occupational health associated with the chemical hazard. The real-time detection is an urgent and highly demanded need to improve public policies.

**Keywords:** Glyphosate, Detection, Methods, Environment and health

## INTRODUCTION

### General considerations

Glyphosate [(*N*-phosphonomethyl) glycine] (GLY) is a non-selective and broad-spectrum herbicide and is the most widely used worldwide (Castle et al. 2004; Woodburn 2000). Since the introduction of genetically modified GLY-resistant crops at the end of the twentieth century, its use has increased dramatically (Giesy et al. 2000). The main commercial formulation of GLY is “Roundup”, which consists of isopropyl amine salt, and the surfactant polyoxymethylene amine is also added according to the manufacturer to increase its efficiency (Tsui and Chu 2003). World Health Organization et al. (1994) had considered GLY as “toxicologically harmless” for humans, other mammals, birds and environment (Tsui and Chu 2003, 2008; Williams et al. 2000) due to its degradability by soil microbes (Zhang et al. 2015a; Napoli et al. 2015) and binding ability to soil colloids (González-Martínez et al. 2005). However, new studies have pointed out GLY as a possibly carcinogenic agent due to its accumulation in the water at the environment. It is believed that this poisonous is probably related to the ability of GLY to form metal complex (Coutinho et al. 2007; Tsui et al. 2005). Actually, the diagnostic strategies and tools have frequently failed to detect GLY and its by-products, and therefore such assumptions need to be confirmed (Simonetti et al. 2015). This review summarizes methods most used during the past 36 years for GLY detection.

### Environmental risks and animal’s health

The European Glyphosate Task Force (GTF) published an enormous list of scientific citations about toxicological effects of GLY. Interestingly, GLY has been associated with fungus infestation in wheat plantations (Ho and Cherry 2010), and additionally, it has been related to more than 30 plant diseases (Johal and Huber 2009; Huang et al. 2015). An extensive review has compiled evidences for the widespread contamination of GLY and its derivatives in groundwater, surface waters (creeks, brooks, lakes, rivers and drains), marine sediments, seawater and

rain (Watts 2009; Allinson et al. 2016; Bradley et al. 2017; Okada et al. 2018). Furthermore, GLY can also be transported by particles in the air (Humphries et al. 2005) and be deposited in the snow (European Commission 2002). GLY may also affect the marine microbial community (Stachowskihaberkorn et al. 2008). The observed concentration of GLY found in coastal areas may be enough to cause considerable changes in the ecosystem, including the obstruction of biomass trophic transfer to different levels (DeLorenzo et al. 1999).

Chronic exposure of GLY is associated with many human health hazards that include: endocrine function disruption (Gasnier et al. 2009; Chalubinski and Kowalski 2006; Ejaz et al. 2004), attention-deficit/hyperactive disorder (ADHD), colitis, diabetes, heart disease, inflammatory bowel disease, amyotrophic lateral syndrome, multiple sclerosis, obesity, depression, non-Hodgkin lymphoma and Alzheimer's disease (Samsel and Seneff 2013a), anencephaly (Rull 2004), autism (Beecham and Seneff 2015), pineal gland disorders (Seneff et al. 2015), birth defects (Paganelli et al. 2010), brain and breast cancers (Shim et al. 2009; Cattani et al. 2014; Thongprakaisang et al. 2013), celiac disease and gluten intolerance (Samsel and Seneff 2013b), chronic kidney disease (Jayasumana et al. 2014, 2015), Parkinson's disease (Gui et al. 2012), pregnancy problems (Richard et al. 2005; Garry et al. 2002; Benachour and Séralini 2009; Hokanson et al. 2007; Poletta et al. 2009), abnormal cell cycle (Marc et al. 2004), allergies (Slager et al. 2010; Heras-Mendoza et al. 2008; Nielsen et al. 2007) and intestine problems (Shehata et al. 2013).

In fish, GLY has affected the energy metabolism, free radical processes, acetylcholinesterase activity (Gluszczak et al. 2006, 2007; do Carmo Langiano and Martinez 2008), modified parameters of the micronucleus test and caused DNA damage as evidenced by the comet assay (Grisolia 2002; Cavalcante et al. 2008; Cavaş and Könen 2007) and caused significant alterations in the immune response (El-Gendy et al. 1998) and in hepatocytes histology (Jiraungkoorskul et al. 2003; Szarek et al. 2000). Besides such effects, preference and avoidance reactions of rainbow trout could also be induced by different GLY concentrations (Tierney et al. 2007). It has been demonstrated that low GLY exposure may induce mild oxidative stress in goldfish tissues by sup- pressing molecules that

modulate reactive oxygen species (ROS), such as superoxide dismutase (SOD), glutathione reductase, glutathione S-transferase (GST) and glucose 6-phosphate dehydrogenase (Winfield 1990). Additionally, the increase in alkaline phosphatase activity at the heart and liver of fish with sublethal GLY doses has also affected the oxaloacetic and glutamic-pyruvic transaminases activities, leading to epithelial hyperplasia and subepithelial edema in gills, and morphological changes in the liver (Nešković et al. 1996; Lushchak et al. 2009). In amphibians, it has induced morphological changes on tadpole development, probably breaking their antipredator responses (Relyea 2012). A very broad review on the impact of GLY on native amphibians was published in 2008 (Govindarajulu 2008).

### Reasons to determine precise levels of glyphosate

Detection and quantification of glyphosate is expensive and slow; consequently, governmental control measures are ineffective since GLY usually cannot be detected by methods that simultaneously analyze different kinds of chemical and their metabolites in the same assay, in a unique multiresidue method. Therefore, the impact of this knowledge gap on public economy and in the health- system is not known. Hence, the concept of the “Glyphosate paradox” is raised, which means that besides GLY being the most widely used agrochemical in the world, it is also the most hardly determined by analytical methods.

Currently, there is no continuous monitoring of GLY or any systematic information about environmental contaminated areas worldwide. The European Union (EU) authorities conducted 186,852 tests in 2009 on cereal samples for pesticide residues, but such survey was performed in only five countries, reaching only 462 sites, from which 42 tested positive. Since 2010, EU authorities have performed regular monitoring of GLY in cereals, but the challenge still remains in testing GLY residues on imported genetically modified soybeans, in which Brazil is one of the biggest producers in the world with indiscriminate use of GLY. Even in the EU, only a small number of testing laboratories are able to detect this chemical (Poulsen et al. 2009). The consequence of this lack of information means greater difficulties to find out how much GLY people have been daily exposed, and how



governments should protect human and environment health from the adverse effects of it.

Our perception is that the Europe Community is more concerned in applying the precautionary principle than many other countries. For example, the Codex Alimentarius Commission and the US Environmental Protection Agency (EPA) established the maximum residue limit (MRL) of 20 mg kg<sup>-1</sup> for GLY in soybean and, in a most preventive way, the National Health Surveillance Agency (ANVISA) in Brazil set the MRL of 10 mg kg<sup>-1</sup>. For drinking water, the regulatory rules adopted by each country differ significantly. The EU has set a MRL of pesticides independently of the chemical structure or biological activity of the compound in 0.1 ng mL<sup>-1</sup>. The EPA established the MRL in terms of persistence and toxicity of each pesticide individually at 700 ng mL<sup>-1</sup> (Winfield 1990). The Canadian Drinking Water Guideline recommends a maximum level of 280 ng mL<sup>-1</sup>. In Brazil, the ANVISA and the Ministry of Health has established the MRL in water of max 500 ng mL<sup>-1</sup>. The level of exposure that is deemed safe for humans over a long period of time is called ADI. It has been set at 0.3 mg kg<sup>-1</sup> of body-weight per day (bw/d) in EU and Canada and 1.75 mg kg<sup>-1</sup> bw/d in the USA. The ADI is the highest dose at which no adverse effect is found (the No Observed Adverse Effect Level or NOAEL), which is also lower than the lowest dose that has a toxic effect (the Lowest Observed Adverse Effect Level or LOAEL). However, it is important to emphasize that analyses on the current approvals by the EU and in the USA regarding GLY levels suggest that the established ADIs are questionable (Antoniou et al. 2012), especially because agencies used the information provided by studies performed by the industries, which support regulators to calculate and approve the application of chemical levels without adverse effects. All these facts have raised questions about how safe GLY levels are, which is further complicated by the fact that many approaches present Limits of Detection (LOD) far away from Agency's control interest. GLY has some special characteristics that go far from the fact that it has been broadly used. It is usually applied to soils in the form of aqueous solutions, in high concentrations of around 0.03 mol L<sup>-1</sup> (Candela et al. 2010; Laitinen et al. 2009; Tuesca and Puricelli 2007).

So, to understand and predict the transport of GLY in soils, one needs to measure it in a wide spectrum of concentrations, focusing on how GLY interacts with the soil complexity under variable conditions. In fact, this challenge is quite difficult, both technically and financially, which is mainly due to the complexity of molecular interactions among GLY, metals, nutrients and organic matter, and also because there is no good technology for real-time and sensitive measurements of GLY. Simple, portable and low-cost methods and instruments are highly desirable, but difficult to attain for all different environmental conditions.

### Glyphosate: metabolites and analogues, formulation toxicity and detection problems

Glyphosate (GLY) is generally formulated by a series of zwitterions with adjuvants or surfactants to improve its activity. It is an aminophosphonic analogue of the natural amino acid glycine, which is protonated and presented in different ionic states depending on pH. The carboxylic and the phosphonic acid can be ionized, and the amine group can be protonated (Winfield 1990; Chenier 2002). The GLY primary natural decomposition pathway occurs through degradation by soil microflora under both aerobic and anaerobic conditions (Franz et al. 1997). The main deactivation path is the hydrolysis to aminoethyl phosphonic acid (AMPA). This compound presents a low toxicity weak organic acid with a phosphoric acid group (Winfield 1990; Schuette 1998). AMPA is then broken down further by manganese oxide, which naturally occurs in soil (Barrett and McBride 2005), or to phosphoric acid via bacterial action (Forlani et al. 1999; Pipke and Amrhein 1988), and ultimately to carbon dioxide and inorganic phosphate (Winfield 1990; Tuesca and Puricelli 2007). The second catabolic pathway is sarcosine as intermediate metabolite. In hard water, the decomposition process is slower, and GLY forming salt, mainly by complexation to  $\text{Ca}^{2+}$  (Coutinho and Mazo 2005). GLY has more than one thousand analogues (Winfield 1990; Pollegioni et al. 2011), but seems that there are only two, very similar analogues, which are as effective to the same extent as GLY, the *N*-hydroxy-glyphosate and *N*-amino-glyphosate (Winfield 1990; Laitinen et al. 2009; Singh 1998).

Interestingly, the oxidative stress generated by GLY, AMPA and its commercial formulation was examined in a hepatocyte cell line (HepG2) under dilution levels below agricultural applications, but surprisingly, the AMPA exposure produced an increase in glutathione (GSH) levels only, and no effects were observed for GLY. However, the GLY formulation induced a significant increase in reactive oxygen species, nitrotyrosine formation, superoxide dismutase activity and GSH levels, suggesting that adjuvants associated with the active GLY may be causing part of the toxic effects (Chaufan et al. 2014).

The challenge to detect GLY residue using a simple analytical method is due to its ionic character, high polarity and solubility in water, difficult evaporation, poor solubility in common organic solvents, low volatility, low mass and favored complexing behavior (Ibáñez et al. 2006; de Llasera et al. 2005; Koskinen et al. 2016; Skeff et al. 2016). The photometric and fluorometric detection of these substances is not viable due to the absence of chromophore or fluorophore groups in GLY structures. Moreover, similarity with amino acids or other natural plant components can cause interferences. The GLY capacity to adsorb strongly on clay minerals (Hance 1976; Arroyave et al. 2016) and organic (Zheng et al. 2015) or mineral particles in water (Thompson et al. 1989; Rueppel et al. 1977) and its high affinity to metal cations that complex with it, make it hard to detect without a pretreatment method (Glass 1984).

## MEASUREMENT METHODS

### Chromatography techniques

Chromatography can be used to break apart mixtures into their components allowing each part to be analyzed separately. Many approaches to detect glyphosate (GLY) residues use liquid chromatography (LC) or high-performance liquid chromatography (HPLC), gas chromatography (GC) and ion chromatography (IC) (Zelenkova and Vinokurova 2008). Alternatively, the eluates from the chromatographic columns can be fed into mass spectrometer (MS) detectors (LC/MS).

### Liquid chromatography

Liquid chromatography (LC) is the most suitable method to detect GLY. It needs derivatization procedure, for which several approaches have been used, such as pre-column, e.g., and post-column (Winfield 1990; Patsias et al. 2001; Hogendoorn et al. 1999; Mallat and Barceló 1998). Normally, LC has been used in combination with fluorescence and UV/ visible (LC/UV–Vis) detection after derivatization and has also been used with fluorescence detector (LC–FLD) (Khrolenko and Wieczorek 2005; Merás et al. 2005; Nedelkoska and Low 2004; Ridlen et al. 1997). The recommended EPA method for GLY in drinking water uses LC with direct injection of the sample, post-column derivatization and fluorescence detection without pre-concentration (Barcelo 2000). The derivatization reagents for UV detector are *p*-toluenesulfonyl chloride (Si et al. 2009; Kawai et al. 1991), *o*-nitrobenzenesulfonyl chloride (Fang et al. 2011) and 2,5-dimethoxy-benzenesulfonyl chloride (Fang et al. 2014). LC methods for GLY often adopt pre-column 9-fluorenylmethyl chloro- format (FMOC-Cl) derivatization and fluorometric detection. On FLD detections used 9-fluorenylmethyl chloroformate (FMOC) and *o*-phthalaldehyde (OPA) in post-column (Nedelkoska and Low 2004; Zhou et al. 2007; Hidalgo et al. 2004; Sancho et al. 1996; Sun et al. 2017). The pre-column is more precise than post-column derivatization due to the difficulty in controlling reaction in the reflux system of HPLC for post-column.

Pre-column derivatization reaches LOD as low as  $0.02 \text{ ng mL}^{-1}$  in water and  $0.02 \text{ mg kg}^{-1}$  in soil, while post-column derivatization reaches on aqueous sample  $2.0 \text{ ng mL}^{-1}$ . LC is a fast, sensitive and repeatable method to GLY residue detection, but it needs derivatization processes and requires high-end equipments.

#### Gas chromatography

Gas chromatography (GC) is not commonly used to detect GLY due to the complicated derivatization procedure, but the evaporation properties have been improved through esterification and acylation. Generally, GC is performed after pre-column derivatization of GLY to convert it to volatile and thermally stable derivative (Hu et al. 2008; Kudzin et al. 2002, 2003; Börjesson and Torstensson 2000; Tadeo et al. 2000). The C, P and H in the GLY molecule permit the use of associated techniques as flame photometric detector (GC/FPD) (Tseng et al. 2004; Kataoka et al. 1996), flame ionization detector (GC/FID) (Kudzin et al. 2003), electron capture detector (GC/ECD) and nitrogen phosphorus detector (GC/NPD) (Hu et al. 2008). The most used derivatization reagents are *N*-methyl-*N*-*tert*-butyldimethylsilyltrifluoroacetamide and dimethylformamide (Tsunoda 1993), trifluoroacetic anhydride and 4,4,4-trifluoro-1-butanol (Hu et al. 2007; Lou et al. 2001; Ding et al. 2015), isopropyl chloroformate and diazomethane (Kataoka et al. 1996), trifluoroacetic acid, trifluoroacetic anhydride and trimethyl orthoformate (Kudzin et al. 2002), propionic anhydride and methanol (Ding et al. 2015; Pei and Lai 2004).

Quantification of GLY in soil and water through NPD has reached LOD equivalents of  $0.02 \text{ mg kg}^{-1}$  (Ding et al. 2015; Pei and Lai 2004) and  $0.5 \text{ ng L}^{-1}$ , respectively (Hu et al. 2007). One point that should be emphasized is the use of less toxic acetone, ethyl acetate and methanol instead of the carcinogenic chloroform, dichloromethane and neurotoxic *n*-hexane as eluent solvents (Tseng et al. 2004). Therefore, GC and LC can determine GLY derivatives in a sensitive and selective way, but the steps to transform GLY in a product that could be read are quite complicated, besides generating unstable products.

## Ion chromatography

Ion chromatography (IC) is a type of LC in which retention of molecules is based on the attraction between solute ions and charged sites bonded to the stationary phase. Once GLY is an ionic compound ( $pK_{a1} = 2.27$ ,  $pK_{a2} = 5.58$  and  $pK_{a3} = 10.25$ ), an anion-exchange column can be used followed by elution with an alkaline buffer. IC was used to measure GLY in a simple and sensitive method with emphasis on a simple clean-up procedure based on IC with suppressed conductivity detection (Zhu et al. 1999). The highlight of this study was the very short retention time of common inorganic anions of GLY, such as chloride, phosphate, nitrate and sulfate, without any interference. In a few cases, GLY could be determined directly by IC with UV (Ibáñez et al. 2005) or by suppressing conductivity detection due to its limited sensitivity. Furthermore, an IC method with integrated pulsed amperometric detection (IC/IPAD) could determine GLY with the advantages of not requiring derivatization, pre-concentration and mobile-phase conductivity inhibition (Sato et al. 2001). It is important to consider the complexity of soils, which includes the presence of several competing ions in different concentrations and other environmental variations, such as pH, organic matter and microorganisms that make the extraction methods harder to be attained and leading to unreproducible results.

## Chromatography–mass spectrometry

Chromatography–mass spectrometry (LC/MS), or alternatively HPLC/MS, is the most common method to detect GLY in environmental samples due to its higher sensitivity (Liao et al. 2018). Low analysis time has been achieved using solid-phase extractions with LC–SPE (Delmonico et al. 2014), but with higher LOD. LC/MS methods are already used with a technique called electrospray ionization (ESI) that works as an ion source (LC/ESI–MS) (Sato et al. 2009). Sensitivity can be significantly improved by LC/MS–MS, which also avoids the derivatization procedure. MS/MS combines two mass analyzers in one instrument, in which the first MS filters the precursor ion followed by its fragmentation with high energy, and the second MS analyzer then filters the produced ions generated by

fragmentation. The advantage of the MS/MS is the increased sensitivity due to the noise reduction.

It was reported that the LC/MS–MS method sufficiently detects GLY, but this method requires longer equilibration time, suffers from poor robustness and still has adverse impacts on column lifetime (Liao et al. 2018). Kaczyński and Łozowicka compared LC/MS–MS and LC/FLD to detect traces of GLY in rapeseeds. Good results have been achieved with LC/MS–MS, but some factors may have affected the method's performance such as metal ions, sample preservation and storage time (Kaczyński and Łozowicka 2015). However, while LC/FLD requires less expensive equipment, the LC/MS–MS presents simpler sample preparation, easier procedure, faster and more sensitive (Hao et al. 2011). Routine analysis can be performed without laborious instrumental changes using this technique. The results suggest that LC/MS–MS may also be used to analyze residues of these compounds in oil plants, where GLY is widely used. Flow injection associated with tandem mass spectrometry (MS/MS) was researched for the rapid detection of polar pesticides, such as GLY (Mol and van Dam 2014).

Searching for an analysis without derivatization procedures has led to the development of an alternative methodology to determine GLY and AMPA residues using a fast-chromatographic analysis with sensitive detection, with calibration curves prepared in the matrix after a simple sample extraction and liquid–liquid partition followed by protein precipitation step with organic solvent to minimize the complexity of the sample (Martins-Júnior et al. 2009, 2011). These authors investigated the potential of reversed-phase LC–ESI/MS/MS for the quantification of these residues in soybean-spiked samples, suggesting that this method could be expanded to corn and cotton crops. LC–ESI–MS/MS does not need derivatization procedure, but the instrumentation demands are substantial (Byer et al. 2008). A fully automated SPE–LC–ESI–MS/MS was developed and validated to analyze potable water, surface water and waste-water with good LOD, but with derivatizations (Vreeken et al. 1998). Similarly, a selective and sensitive online SPE–LC–ESI–MS/MS approach reached incredible LOD for GLY and AMPA in soil and water samples, reaching as low as  $50 \text{ ng g}^{-1}$  and  $0.0005 \text{ ng mL}^{-1}$ ,

respectively (Ibáñez et al. 2005, 2006; Hanke et al. 2008). It is also interesting to highlight that using labeled GLY as internal standard, even applying powerful approaches as SPE–LC–ESI–MS/ MS detection, its application to real-world samples failed. Most reported methods for GLY analysis did not perform acidification of sample before derivatization, and some data reported on GLY concentrations in water might be questionable due to the presence of some organic compounds and metal ions that were neglected, which act as chelating agents that form complexes with GLY, becoming unavailable for the derivatization step. The nature of the formed complex was not elucidated yet, and more studies are necessary to establish whether acidification of samples is a general approach that should be applied to all water samples (Ibáñez et al. 2006).

GC/MS is another method that requires derivatization to confer volatility to GLY (de Llasera et al. 2005; Kudzin et al. 2003). Three technologies based on GC/MS have been used to detect GLY: GC–CI (chemical ionization)–MS, GC–FID (flame ionization detector)–MS and GC–EI (electron impact)–MS. Generally, the methods are time-consuming, tedious and require a substantial amount of sample manipulation. Although these methods present high sensitivity and capability of detecting very low GLY concentrations, they are laborious and require the use of high- end specialized equipments. Tsunoda developed a sensitive GC/ion-trap-MS (GC/IT-MS) method to determine simultaneously GLY, glufosinate (GLU) and bialaphos (BIA), their major metabolites, besides other nineteen amino acids (Tsunoda 1993). Royer et al. (2000) used this method to determine GLY and AMPA in water with different hard- nesses. Börjesson and Torstensson (2000) reached LOD as low as  $0.1 \text{ ng mL}^{-1}$  in groundwater and  $6 \text{ ng g}^{-1}$  for both compounds in soil. The preferred detection system according to many scientists is MS (Kudzin et al. 2002; Börjesson and Torstensson 2000; Royer et al. 2000; Alferness and Iwata 1994).

Another approach based on by ion-pairing reversed- phase liquid (RP-LC) coupled to inductively coupled plasma mass spectrometry with octapole (ICP/MS) did not require derivation and obtained lower sensitivity with LOD at  $25\text{--}32 \text{ ng mL}^{-1}$  (Sadi et al. 2004). Guo and colleagues also built an IC/ICP–MS method in



order to determine the GLY in water. The method was sensitive, simple, did not require sample pre-concentration or mobile-phase conductivity suppression and did not suffer anions' interference (nitrate, nitrite, sulfate, chloride, etc.) and metallic ions from the matrix (Guo et al. 2005). Later in 2007, they developed an IC/ICP–MS method to determine simultaneously four water-soluble organophosphorus herbicides. The detection was fast, simple, selective and free from tedious sample preparation or chemical derivatization and was applicable to highly polluted water samples. However, environmental water applicability depends on further research using instrumental upgrading or applying a pre-concentration step to improve its sensitivity (Guo et al. 2007). Yoshioka and colleagues also avoided derivatization and ion-pair reagents and aimed the study to the emergency medicine, where time is the utmost aim, especially in poisonings cases. In this situation, a rapid method for detecting multiple herbicides would allow rapid treatment. Besides GLY, this method could also detect GLU, BIA, AMPA and 3-methylphosphinopropionic acid (3-MPPA) in human serum. These amphoteric and polar phosphorus herbicides contain amino acids. Their detection without derivatization or ion-pair reagents, and under the use of conventional columns, such as reversed-phase (RP) or ion-exchange column may lead to poor peak shapes and insufficient peak separation in LC chromatograms (Yoshioka et al. 2011). In order to solve this problem, hydrophilic interaction chromatography (HILIC) columns were used (Coutinho et al. 2007; Li et al. 2009; Vass et al. 2016). Once hydrophilic and polar compounds cannot be retained by conventional RP chromatography, the HILIC column is suitable. The greatest advantage of IC testing is the simple treatment for samples. However, it is only applied in water and soil analysis.

### Spectroscopic methods

Spectroscopy analysis studies the interaction between matter and electromagnetic radiation as a function of its wave-length or frequency. The data are represented by a plot of the response of interest as a function of the wavelength, wave-number or frequency.

Although accurate and sensitive, the technologies related to atomic absorption spectrometry, electrothermal atomization atomic absorption spectrometry, flame atomic absorption spectrometry, fluorimetry and fading spectrophotometry, suffer from the requirement of well-established laboratory settings, high complexity and long testing times. However, a simple and cost-effective fluorometric sensor (FS) has been developed, which is based on the detection of oligonucleotides by fluorescence. It is based on fluorescence magnetic nanoparticles (FMPs) coupled to specific DNA probe (FS- FMPs/DNA). The principle of detection was based on a competitive inhibition of conjugated GLY-double target/ probe-FMP (Lee et al. 2013). GLY could be easily quantified using confocal laser scanning microscopy and low-cost UV photometric analysis. Unfortunately, this study did not explore the possible cross-reactions with GLY analogues and possible environmental interferents. This study further improves the previous report by the same authors, who developed a competitive inhibition assay by free GLY using GLY-dsDNA-gold conjugate nanoparticles, which was used to quantify fluorescence intensity through an immunoassay (FS-AU/DNA) (Lee et al. 2010).

Another immunosensor (IS) was developed using carbon dot-labeled antibodies (IgG-CDs) that were able to specifically recognize GLY (Wang et al. 2016a). The fluorescent properties of this IS allowed the visualization of the GLY distribution into plant tissues. The excess of IgG-CDs is removed from the system using magnetic nanoparticles  $\text{Fe}_3\text{O}_4$  allowing a linear relationship between the fluorescence intensity of IgG-CDs and the logarithmic concentration of GLY.

Silva and colleagues employed diffuse reflectance spectroscopy (DRS) using a spot test on a filter paper (da Silva et al. 2011; Metzger 1997). Although the technique is simple, precise, inexpensive, environmentally friendly, requires minimal amounts of samples and reagents and is applicable to environmental, drinking water and commercial formulations, it presents very low sensitivity and may not be applicable to soil samples.

Most of the spectrophotometric methods require colored reagents and chromophore groups. To surpass this difficulty, a simple and rapid method was developed by transforming the amino group of GLY into a dithiocarbamate derivative. A copper (I) perchlorate reaction formed a yellowish green- colored complex with maximum absorbance at 392 nm (Sharma et al. 2012). The color intensity and stability were obtained at 60 s, and remained for at least 90 min, which was an advantage over the commonly used spectrophotometric methods. In some cases, it is useful to apply a low-cost, simple and fast method, despite its lower sensitivity, when compared with chromatographic methods or CE. For example, some researchers have used UV–Vis spectroscopy for GLY quantification in laboratory experiments to evaluate the adsorption capacity in soil sample under different pH values by performing adsorption isotherms under well-controlled conditions and was able to quantify GLY in the range from 0.084 to 21.8 mg L<sup>-1</sup> (Waiman et al. 2012). However, a derivatization step was performed, in which the GLY amine group was modified by Fmoc-Cl in acetonitrile at pH 9.0. Besides, a non-characterized soil sample was incubated overnight in buffer solution and adjusted to different pH values, and therefore, the potential use for field conditions with different soils is yet to be demonstrated, since differences in the concentration of organic compounds and metal ions were not referred to, or considered (Waiman et al. 2012). Another method has also been proposed, which uses carbon disulfide to convert the GLY amine group into dithiocarbamic acid. Dithiocarbamate by-product is then used as a copper-chelating group that results in a yellowish-colored complex used for measurements (Jan et al. 2009).

Another colorimetric sensor for GLY detection has specifically been made by aggregating 2-mercapto-5-nitrobenzimidazole-capped silver nanoparticles (MNBZ-Ag NPs) and Mg<sup>2+</sup> ions. This structure suffers a reduction in the distance of its interparticle complex formation between MNBZ-Ag NPs–Mg<sup>2+</sup> ion and GLY, which promotes a color switch from yellow to orange-red (Rawat et al. 2016). The colorimetric property was based on the inhibition of peroxidase- like activity of Cu<sup>2+</sup> through the oxidation of 3,3',5,5'-tetra- methylbenzidine (TMB). The color solution changed according to the concentration of GLY when complexed with

$\text{Cu}^{2+}$  (Chang et al. 2016a). The indirect colorimetric determination method of GLY was developed after its oxidation with hydrogen peroxide to orthophosphate, reaching levels between 1000 and 20,000  $\text{ng mL}^{-1}$  (Glass 1981). Although the complex is pH dependent and needs a pre-concentration step before measurement, it can detect GLY in different samples.

Recently, the dithiocarbamic acid was used as an optical color changer of the polyvinyl alcohol (cd-PVA; copper-doped polyvinyl alcohol) nanofiber from blue to yellow (De Almeida et al. 2015). Although advantageous, requiring small sample volume, with a fast response time ( $\sim 1\text{--}3$  s), good color spot stability (4 h) and low cross-reactivity with GLY derivatives and structural analogues, AMPA and glycine, respectively, the sensor was not very sensitive and could not keep stability for longer periods ( $> 20$  days). Another drawback was the system susceptibility to compounds and ions commonly found in environmental waters at a lower concentration (60,000  $\text{ng mL}^{-1}$ ), which could require pre-treatment, besides being strongly dependent on pH 11–12.

An additional colorimetric sensor strip was capable to detect not only GLY, but also three other organophosphorus compounds: dimethoate, dichlorvos and chlorpyrifos (Liu et al. 2015). It presents some advantages, such as easy read-out, fast analysis, easy operation, low cost, simple transportation and storage. However, although its detection limit has met the maximum residue limits reported in the EU pesticides database, naked eyes cannot distinguish very large ranges, so specific photonic equipments are required for measurements. Briefly, stabilized gold nanoparticles (NPs) with cysteamine (CS-AuNPs) without aggregation present a red color, and when GLY aggregates to these NPs, the color switches to blue or purple color (Zheng et al. 2013).

Another optical sensor was designed using hollow-core metal-cladded waveguide (HCMW) with double-metal surface. The insertion of chromogenic GLY in the hollow core promoted the orientation for the wave propagation exciting highly sensitive ultra-high-order modes, through small incident angle coupling (Dai et al. 2014). Detection of GLY concentrations as low as 0.23  $\text{ng mL}^{-1}$  was

unambiguously identified within several minutes. Several interesting advantages are mentioned, such as the small analyte volume required, environmentally friendly, compactness, inexpensive, label-free and real-time detection. However, the system behavior is unknown in field samples since detection was performed only in ultrapure water.

Reporter spacer receptors (RSR), both colorimetric- and also luminescence-based systems, are the most widely used optical chemosensors (OC) (Roberts 1989). But, the sensor synthesis requirement is very expensive. To overcome this setback, Minami et al. (2014) developed an optical chemosensor named "Intramolecular Indicator Displacement Assay (IIDA)" (OC-IIDA). In this sensor, an attached dye works as an anionic chromophore, which is bonded to the receptor. The anionic analyte GLY competes for receptor binding leading to changes in photophysical properties of the dye. Besides the possibility of reusing it, one of the benchmarks of this work is the study of phosphate-type anions, e.g., phosphate (Pi), pyrophosphate (PPi), AMPA and phosphonate GLY in aqueous solutions with and without excess of NaCl as a competing electrolyte, which showed no differences (Minami et al. 2014).

Quantum dots (QDs) are also used to develop bioanalytical methods based on fluorescence resonance energy transfer (FRET) (Algar and Krull 2008). QDs act as donor fluorophore to a proximal ground-state acceptor (Guo et al. 2014). In this work, gold NPs stabilized with cysteamine (CS- AuNPs) were used as acceptors of fluorescence emission by QDs capped with thioglycolic acid (TGA-CdTe-QDs). The presence of GLY created electrostatic interactions with CS-AuNPs, promoting disaggregation between CS-AuNPs and TGA-CdTe-QDs, and consequently generating fluorescence.

#### Surface-enhanced Raman scattering

Surface-enhanced Raman scattering (SERS) can magnify molecular vibrations in a system. The enhancement factor can be as much  $10^{14}$  or  $10^{15}$ , which is sufficient to allow even a single molecule to be detected. The enhancement takes place at a nanoscale roughness reflective metal surface

where the molecules are adsorbed. Gold nanorod particles can be synthesized with controllable size and numerous surface functionalities, and due to its tunable optical properties, it can be used as SERS substrates. Therefore, GLY was detected in attomol levels through gold nanorods derivatized with 4-mercaptophenylboronic acid (Torul et al. 2010). At the range of  $1\text{--}10^{-16}$  mM the SERS signal exhibited a linear dependence within the GLY. A disadvantage was that all solutions were prepared using deionized water, free of any organic matter, and considering the high complexity of organic compounds and metal ions interactions with GLY, studies should be performed to better understand and discriminate such complex profiles.

#### Surface plasmon resonance

Surface plasmon resonance (SPR) can be used as an optical biosensor that monitors the interactions between an analyte in a solution and a bioelement immobilized on the SPR sensor surface through special electromagnetic waves—surface plasmon polaritons. One of the advantages provided by SPR biosensors is its label-free real-time analytical technology in which the main application is to detect biological analytes through biomolecular interactions (Homola 2003). Using bacteriophages (SPR-pd), it has been developed a specific oligopeptide that presents good specificity against glycine, thiacloprid and imidacloprid (Ding and Yang 2013). SPR is much more sensitive than nuclear magnetic resonance spectroscopy (NMR); however, the immobilization of binding partners creates several undesirable issues. In particular, the molecular binding site may be near the surface and induce steric hindrances that could affect binding energy and/or kinetics, and the surface layers often exhibit decreased activity during the analysis (Ding and Yang 2013).

#### Nuclear magnetic resonance

NMR provides detailed information about the molecular structure through the exploration of magnetic properties of certain atomic nuclei. Using  $^{31}\text{P}$  NMR it was possible to determine GLY in blood, liver and urine in postmortem samples, reaching levels of  $1\text{ mg mL}^{-1}$  in less than a minute (Dickson et al. 1988). Using

$^{31}\text{P}$  and  $^1\text{H}$  NMR, GLY could be detected in biological fluids in between 10 and 20 min in a small sample size without any pretreatment (Cartigny et al. 2004). In fact,  $^{31}\text{P}$  NMR has been used to detect organophosphorus compounds as endogenous phosphorus metabolites present in plasma or urine. Interestingly, other components can be detected in the same NMR spectrum, e.g., the occurrence of metabolic acidosis in salicylate and alcohol/glycol poisonings (Cartigny et al. 2004). The main limitation of NMR analysis is the quantification analysis, particularly when therapeutic agents are administered, because several signals can overlap. However, in the clinical emergency context, the diagnostic problem is partially solved when only detection is needed, as is the case of monitoring the effectiveness of drug elimination. In an emergency clinical context, the diagnosis problem could be at least partly solved if a rapid identification procedure was available. The NMR method should be useful in rapidly confirming the diagnosis of poisoning and in evaluating the effectiveness of elimination procedures such as gastric lavage, forced diuresis or hemodialysis (Cartigny et al. 2004).

#### Chemiluminescence-molecular imprinting sensor

Chemiluminescence-molecular imprinting sensor (CL-MIS) can be made using small dimension microspheres (MIMs) as a molecular printer, reaching extremely high surface-to- volume ratio (Zhao et al. 2011). It was synthesized onto a molecularly imprinted polymer base, using precipitation polymerization with GLY as template. A circular glass sheet was used as a form to be coated by GLY-MIMs suspension. After, placing it into the well, the microplate is prepared as a recognition element, acting as a chemiluminescence (CL)-molecular imprinting (MI) sensor able to perform 96 sequentially independent measurements in just 10 min. Stability tests showed around 90% of its initial CL intensity for 3 months when stored in air at 4 °C. The authors pointed out that CL-MIS may become a useful and quick analytical technology for molecular recognition due to its excellent selectivity for GLY determination; however, they did not compare the GLY recognition sensor capacity with its derivatives as AMPA. Therefore, specificity was not considered.

## Electrochemical sensors

### Amperometric and voltammetric methods

To access a simple and fast way to determine GLY residue in soil samples, a single sweep oscillopolarographic method was developed (Sun et al. 2007). This is an adaptation of an old method (Brønstad and Friestad 1976) that detected GLY in natural water by nitrosation, converting GLY in *N*-nitroso-*N*-(phosphonomethyl) glycine after derivatization with sodium nitrite, followed by detection with differential pulse polarography. This derivative showed a sensitive cathodic peak at  $-0.81$  V against saturated calomel electrode in pH 0.7 and resulted inefficient determination of GLY in formulations and soil samples. However, the presence of concomitant metal ions or organic compounds may have probably affected the analysis, and interference of any potential confounding effect should be further investigated to validate the proposed method for GLY quantification.

Glyphosate could be detected electrochemically in 20 min by its ability to bind to horseradish peroxidase (ES-HRP). Although the LOD of  $1.70 \text{ ng mL}^{-1}$  achieved was very good, it is not known its applicability to real samples. Another ES-HRP with good reproducibility was also developed using a gold disk electrode. It is a sensitive, simple and low-cost method. Besides it can detect AMPA too. One interesting characteristic of this biosensor is the possibility to reuse it for up to three measurements before surface saturation (Songa et al. 2009a). Another proposed sensor also uses HRP electrostatically immobilized onto the surface of a rotating gold disk electrode modified with PDMA-PSS [poly(2,5-dimethoxyaniline)-poly(4-styrenesulfonic acid) nanoparticles for amperometric detection. Before the exposure of GLY onto the electrolyte solution the activity of the enzyme was measured with hydrogen peroxide. The stability of this enzymatic electrode was very good and could be used for over 60 measurements (Songa et al. 2009b).

Another electrochemical sensor study uses enzymatic inhibition method to determine GLY through a modified nanoclay that immobilizes atemoya peroxidase (ES-Ate- moya). It is applicable to real water samples, stable for 8 weeks, and



does not need pretreatment process. Unfortunately, there is no information regarding its portability and cross-reactivities with analogues (Oliveira et al. 2012).

Other two reports have been published on nanofilm-modified amperometric sensors. One used an electrogenerated NiAl-LDH ( $\text{Ni}_1\text{-Al}_x(\text{OH})_2\text{NO}_3 \cdot n\text{H}_2\text{O}$ -layered double hydroxides) thin film by electrodeposition on the Pt electrode surface. The principle of detection is based on oxidation of amine group by Ni (III). The electrocatalytic efficiency and morphology of the obtained LDH film was strongly dependent on the electrodeposition time. It is important to note that this sensor could not properly work at strong alkaline pH (Khenifi et al. 2009). Despite these electroactive NiAl-LDH films easily electrodeposited, lower LODs could not be achieved. The second sensor was capable of detecting chemicals in soil, human serum samples and water simultaneously without cross-reaction. However, a derivatization by nitrosation is needed for GLY in order to distinguish herbicides, leading to an *N*-nitroso Glyphosate derivative (Prasad et al. 2014).

Toward a sensor fabrication, (*N*-methacryloyl-L-cysteine) monomers through S–Au bonds were used to immobilize a nanostructured polymer film that was grown directly onto the electrode surface. These molecules were polymerized in the presence of templates, cross-linker, initiator and carbon nanotubes as pre-polymer mixture. It reached limits as low as  $0.35 \text{ ng mL}^{-1}$ . Although it is clear there is no cross-reaction between GLY and GLU, there is no information about other possible cross-reactions among its metabolites. However, these procedures are generally very slow, need laboratory apparatus of high cost and are inadequate for on-site or in situ monitoring (Prasad et al. 2014).

A voltammetric electronic tongue (VET) was used in the determination of GLY. The VET consisted of three metallic electrodes of cobalt, copper and platinum, which produced a signal pattern when subjected to GLY in aqueous sample. Besides its simplicity, speed (2 s) and low cost, the electronic tongue was also capable of detecting this analyte, even in the presence of different concentrations of potential interferents, such as  $\text{Ca}^{2+}$  and humic acids (Bataller et al. 2012). Another voltammetry-based detection system used rhodium, cobalt and

copper electrodes coupled to a mathematical model to predicted GLY concentration, but despite the presence of fertilizers (ammonium nitrate) and organic substances, the system proved to be effective (Martínez Gil et al. 2013). Finally, voltammetric determination of GLY using a copper electrode in natural waters was performed in agreement with the green chemistry concept. The optimization showed ideal condition in neutral pH, reaching an LOD of  $59 \mu\text{g L}^{-1}$  (Garcia and Rollemberg 2007). Still with copper electrode, an electrochemical determination of the AMPA in drinking waters was demonstrated (Pintado et al. 2012). Electrochemical and spectroscopic investigations of GLY and AMPA were performed successfully on pure samples of GLY and commercial products (Habekost 2015). Electrochemical behavior of GLY on nickel and copper electrode was measured in the development of a sensor by cyclic voltammetry (Sierra et al. 2008).

Interestingly, despite the success of several electrochemical sensors in the last decade, none of them has become a reality, and it is still questionable their reliability and reproducibility in real-time detection without controlled complex environments, especially because of variations and complexity of production of such electrodes, and also because of the complex interactions of GLY with other compounds. Although the proof of concepts was presented, one should be able to demonstrate the production cost-effectiveness, sensitivity and reproducibility in field detections for final validation.

A photoelectrochemical sensor (PEC) using a glassy carbon electrode (GCE) firstly modified with nanosheets graphitic carbon nitride g-C<sub>3</sub>N<sub>4</sub> NSs (g-C<sub>3</sub>N<sub>4</sub>/GCE) and then self-assembled with Ag<sup>+</sup> onto the g-C<sub>3</sub>N<sub>4</sub>/GCE was performed (Li et al. 2016). The pyridine nitrogen units on g-C<sub>3</sub>N<sub>4</sub> backbone could absorb chemically the Ag<sup>+</sup> and then photogenerated electrons would be used to reduce Ag<sup>+</sup>/Ag, leading to the inhibition of electrons transfer and decrement of photocurrent. However, GLY can displace the Ag to form a very stable chelate, promoting an increase in current in a process called “Binding-induced internal-displacement of signal-on photoelectrochemical response.” Response was given

in 5–15 min. The PEC sensor possesses fine fabrication reproducibility, detection precision and excellent selectivity, even in the presence of the interferences, such as sulfluramid, glucose, vitamin B1, carbendazim, starch, sucrose and acetochlor. Even with excess of other interfering ions, such as  $\text{Ca}^{2+}$ ,  $\text{Zn}^{2+}$ ,  $\text{Al}^{3+}$ ,  $\text{Pd}^{2+}$ ,  $\text{Fe}^{2+}$ ,  $\text{Fe}^{3+}$ ,  $\text{Na}^{+}$ ,  $\text{K}^{+}$ ,  $\text{Cd}^{2+}$ , and all interferences mixed in  $\text{Ag}^{+}$  solution, the photocurrent remained practically constant. Moreover, the mixture of the nine metal ions did not influence the signal response to  $\text{Ag}^{+}$ . The question that remains is could  $\text{Ag}^{+}$  of the electrode be strong enough to displace other chemicals that commonly bind GLY? This sensor still needs to be tested in the presence of humic acid. Some drawbacks of it are the pH- and time-dependent responses, besides losing its photocurrent response very quickly, even if stored in ideal conditions (dark sealed environment at 4 °C). Lastly, it is not known its behavior in the presence of GLY analogues main (Li et al. 2016).

### Capillary electrophoresis

Capillary electrophoresis (CE) is a common method to detect GLY or AMPA. This method requires derivatization for the same reasons cited before. CE is generally associated with UV–Vis (Cikalo et al. 1996; Chang and Wei 2005), fluorescence (Molina and Silva 2002) and MS (Goodwin et al. 2003) detectors, and in this latter method, derivatization is not required. A rapid and direct pre-concentration technique followed by CE was utilized, and detection was based on a capacitively coupled contactless conductivity system (CE-C(4)D). The method showed good reproducibility for GLY and its derivatives and analogues, AMPA and GLU, respectively (See et al. 2010). Comparing CE with LC, in samples of low to medium conductivity, the GLY concentration might be effectively determined, but there is the necessity to adjust the sample volume to the required sensitivity. Considering this and the fact that CE is much cheaper and less time-consuming than LC, CE should be the preferred method. On the other hand, in samples with high concentration of salts, AMPA is poorly extracted by the strong anion-exchange resin that was used to pre-concentrate both analytes in environmental aqueous samples (Corbera et al. 2005). Cikalo et al. (1996) used the same CE/UV procedure, however using tetradecyltrimethylammonium bromide (TTAB) as

an electro-osmotic flow modifier and reached LOD with gains of 85 ng mL<sup>-1</sup> to GLY and 60 ng mL<sup>-1</sup> to AMPA in pure water samples in contrast, with 5000 ng mL<sup>-1</sup> for and 4000 ng mL<sup>-1</sup> reached by the previous report. Molina and Silva also reached even better LOD, from 0.06 to 0.16 ng mL<sup>-1</sup> (Molina and Silva 2002), by using a non-ionic surfactant MEKC-LIF as a selective agent, which was fast and sensitive tool for the determination of GLY, GLU and their metabolites. Besides, once it does not need a previous enrichment steps, it increases its potential for analysis of environmental samples. Chang and Liao (2002) also used indirect fluorescence as a detection method in commercial formulations and showed that this technique can be applied in routine analysis, but direct analysis of GLY in ground- water is still problematic. Finally, Goodwin et al. (2003) combined CE with MS for simultaneous determination of GLY, GLU and their metabolites using a simple micro-electrospray interface (mESI). To drive separation and generate the electrospray, the interface uses the voltage applied to the CE capillary, thus avoiding sample dilution. Other advantage of mESI in relation an ESI is that it has no physical contact between the capillary outlet and the ground-state electrode because electrical contact is achieved by placing the capillary tip 1 mm away from the MS, that is, under these conditions the voltage generates the electrospray and promotes the necessary electrophoretic separation (Mazereeuw et al. 1997). This technique presents a hindrance, because only high resistivity background electrolytes (BGEs) can be used. Besides, if the BGE concentration is too high, interference may occur during detection due to electrical discharges. Some of the operational limitations of the “homemade” mESI used were the restricted range of acceptable sample matrices. On the other hand, when compared to the typical sheath liquid interface systems, it has the advantage that analyte dilution is not required. The microchip electrophoresis system with laser-induced fluorescence (LIF) was also used as detection system for fast and sensitive analysis of GLY and GLU residues. In order to minimize the cost of the technology, a low-cost LIF detector with disposable cyclic olefin copolymer microchips was used (Mazereeuw et al. 1997); moreover, the technology is portable and user-friendly.

## Enzyme-linked immunosorbent assays

The enzyme-linked immunosorbent assay (ELISA) has been presented as an alternative approach to the drawbacks exposed in the other techniques, such as the requirement of derivatization procedures, hard sample pre-treatments, high-cost end equipments and reactions and time for analysis. Immunoassay offers some advantages over chemistry methods, since labeled antibodies can be used in competitive reactions to detect herbicides. It is also selective and sensitive to determine GLY and enables prompt environmental surveys. Besides, the ELISAs's LOD are higher than those typically achieved by LC/MS/MS, better than GC/MS methods, and even similar of those obtained by HPLC (Rubio et al. 2003). Two kinds of ELISA have been used to identify GLY. The first includes a derivatization step with acetic anhydride followed by detection with immobilized antibodies, resulting in an LOD equal to or less than  $0.6 \text{ ng mL}^{-1}$  (Rubio et al. 2003). The second, an indirect ELISA (CI-ELISA) just needs water pretreatment. Moreover, it was found to be highly specific for GLY detection with cross-reactivity less than 0.1%, even in the presence of related compounds, e.g., AMPA and GLU (Clegg et al. 1999). A so-called linker-assisted enzyme-linked immunosorbent assay (L'ELISA) method that first derivatized GLY with succinic anhydride achieved LOD values as low as  $0.1 \text{ ng mL}^{-1}$  (Lee et al. 2002). Additionally, González-Martínez et al. (2005) also improved the LOD to  $0.021 \text{ ng mL}^{-1}$  by using a GLY ELISA sensor. In contrast, the drawback of ELISA methods is the high limits of AMPA detection, which under certain circumstances may be present in the absence of its parent pesticide (e.g., high use of GLY and vulnerable hydrogeological settings) (Scribner et al. 2007). Therefore, the quantification of AMPA through conventional analytical methods should be concurrently applied along with determination of GLY by ELISA (Sanchís et al. 2012). The difficulty of monitoring mixed herbicides is due to the requirement of specific antibodies, which are not always available, because generation of antibodies against poisonous chemicals cannot be produced by conventional methods. In conclusion, ELISA is the most cost-effective method for routine analysis, but the commercially available kits are still high

relatively expensive (González-Martínez et al. 2005), and applications for soil samples in field conditions have not been demonstrated.

### Cell biosensor

A cyanobacterium sensor was developed based on the luciferase activity present in a modified *cyanobacterium Synechocystis* sp. cell. The results showed that the decrease in bioluminescence could be correlated with the herbicide concentration and with increasing incubation time. The reduction bioluminescence by 20% and 50% (EC20 and EC50) of the herbicide Glyphosate was determined at 6 h and 1 day, respectively. The EC20 at 6 h was  $3.62 \times 10^3 \pm 0.79 \text{ ng L}^{-1}$ , and the EC50 at 1 day was  $3.10 \times 10^3 \pm 0.17 \text{ ng L}^{-1}$ . One of the major restrictions of this method is its low selectivity, presenting cross-reactions with other herbicides as diuron, paraquat, mcpa, mecoprop, atrazine, propazine and simazine. Besides, the pH conditions must be optimized in order to obtain reproducible responses (Shao et al. 2002). The use of the green alga *Selenastrum capricornutum* demonstrated to be less sensitive to GLY when two parameters are considered: sensitivity and reaction time. The EC50 of  $1050 \text{ ng mL}^{-1}$  could only be reached after 4 days (Abdel- Hamid 1996).

In comparison with other methods, such as the algal biosensor, chlorophyll fluorescence-based and isolated photosystem II (PSII) (Campanella et al. 2001; Frense et al. 1998; Koblizek et al. 1998), it is simpler, faster, economical and accurate. It is more suitable for prediction of long- term effects of chronic toxicity of pollutants, because of the longer doubling time of cyanobacteria. Unfortunately, to decrease the detection limit, it is necessary to increase the assay time (Schafer et al. 1994). Other cell biosensors preserve cell “physiological” functions by the utilization of an agarose gel matrix with immobilized cell components, to access electrophysiological interactions by measuring its potential. This method was called Bioelectric Recognition Assay (BERA). In a preliminary work it was able to specifically detect GLY in 3–5 min in concentrations lower than  $0.1 \text{ ng mL}^{-1}$ , even among other compounds with similar structure in water solution (Kintzios et al. 2001).

BERA biosensors can determine GLY in a fast and cost-efficient way without prior knowledge of the sample. Besides, it has kept its stability even after a 2-month storage in low temperature. This method responds differently to GLY and AMPA herbicides. Another characteristic of this sensor is that, rather than operating the biosensor electrode in direct contact with a single cell, BERA's electrodes are inserted into the matrix of a group of cells. It approaches the measurements made in natural tissues. It is expected that an evolution of this type of sensors should be made with the interface of luminescent cells with optical transducers. Finally, the factors that can affect the biosensor response are, among others, gel density, cell density in the matrix, and cell size, because it has a direct correlation with gel porosity (Frense et al. 1998). However, it is not known how the bio- sensor will behave in field samples. An important drawback of this method is that the sensor depends on many careful and detailed steps, including cell culture.

#### Cross-responses from multiple sensors

Different detection methods using data from conventional measurements of water quality have been published in numerous publications, which include artificial intelligence, statistical analyses and data mining. Cross-responses from multiple sensors (CRMS) are also a proposed method to detect some contaminants. An online water quality monitoring system can detect GLY from simultaneous and continuous measurements of eight parameters: UV-254, pH, temperature, conductivity, turbidity, oxidation–reduction potential (ORP), nitrate-nitrogen and phosphate, even if the contaminant in concentrations as low as 2000 ng mL<sup>-1</sup> had been introduced 1 min before (Che and Liu 2014). However, for each contaminant it is necessary to optimize the analytical parameters. Another drawback of such algorithm is the use of conventional parameters that are highly affected by other environmental factors, such as different soil compositions, different fertilizer formulations, among others.

## DISCUSSION

Commercial glyphosate contains toxic agents called adjuvants (Mesnage et al. 2013). Most investigators have neglected the analysis of these toxic products. This is clear from analyzing Table 1 where basically only AMPA and GLU are the most common chemicals simultaneously analyzed with glyphosate. In clinical tests, immunosensors are usually more sensitive than ELISA; however, for GLY analysis, ELISA has shown to be more sensitive than most of the methods presented in this review. Among chromatographic methods, the most sensitive one for GLY detection is liquid chromatography using solid-phase extraction coupled to mass spectrometry with electrospray ionization (LC–SPE–ESI/MS/MS). However, SERS was much more sensitive reaching attomole levels of GLY using gold nanorods, far surpassing the other methods, although it is not yet applicable to field conditions. Recovery studies are a classical technique for validating the performance of an analytical method, mainly in the absence of a reliable comparison method. Average recovery analytes (ARA) showed superior performance for diffuse reflectance spectroscopy. The detection of Glyphosate in living tissues with high protein content appears to exhibit a systematic negative error. Studies with bluegill sunfish exposed to  $^{14}\text{C}$ -radiolabeled Glyphosate showed subsequent contamination in which the amount of radiolabeled extracted with EDTA was greater than the GLY content detected in these fish. After the digestion procedure of these samples with protein K and a new extraction with EDTA, a significant increase of radiolabeled occurred, suggesting that the GLY is strongly incorporated to the protein. Probably GLY is misleadingly replacing the amino acid coding for glycine during protein synthesis (Anthony and Stephanie 2017). Generally, the analytical chemistry is faced with problems in method development, reachable detection and quantification limits, for GLY (Huhn 2018).

## CONCLUSION

Nowadays, many kinds of glucometers are known as reference platforms for detection, due to their sensitivity, portability, reproducibility, fastness, specificity, selectivity, stability, low cost and easiness to operate. However, these



characteristics cannot be found in Glyphosate detectors. There are three classes of security levels for food and potable water in which a detector can operate: below the  $0.1 \text{ ng mL}^{-1}$  limit (EU), above  $700 \text{ ng mL}^{-1}$  limit (US) and between both. Most of the sensors that reach EU values fail in other aspects as reproducibility, possible use in real samples, stability, portability or selectivity. It should be pointed out, however, that sometimes the method of choice should be cheaper and less time-consuming, instead of being highly sensitive. Sensors that do not need pre- or post-derivatization, or pretreatment of samples, are the most needed characteristic, and this is one of the drawbacks of the current methods. There is an urgent need to investigate residual applications of GLY directly in environmental samples on site, and for this, sensitivity, specificity, portability and speed are essential. Interestingly, such characteristics have been reported for GLY sensing using colorimetric or electrochemical biosensors, but these biosensors are difficult to prepare and maintain, due to the use of antibodies as probes, which require controlled conditions for optimal operation. In this sense, the major concern is the shelf life of such sensors, and solutions must search for greater stability prior to detection. Several authors have also claimed the development of low-cost methods to detect GLY, but none of them have published their costs or compared with other methods. Real-time detection at lower cost, faster, with good sensitivity is important issues, and at the moment no method can reach the required parameters for field tests with environmental samples.

Another important issue is that GLY is never used alone, which means that commercial formulations contain adjuvants as additional toxic agents. They are used to increase Glyphosate toxicity by allowing its penetration into plants and in some cases are more toxic than GLY, but they are never included in GLY long-term toxicity tests and are considered to be inert. They constitute a “black hole” in pesticide toxicology, because they are often kept secret by companies, and are never measured in the environment, and so, they are not included in the establishment of pesticide acceptable daily intakes. So, pure GLY purchased from chemical companies is not the commercial form used, and the pure form is the one used for the development of sensors. Therefore, the true need is the ability to quantify GLY in real environmental complex matrices and not as a pure GLY form

dissolved in ultrapure water. The ability to quantify GLY bonded to metal ions and cations ( $\text{Ca}^{2+}$ ) in soil or in water in a fast, simple and sensitive way using a stable portable device is still a challenge.

## Acknowledgements

The authors are grateful for the financial support of the state funding agencies Fundação de Amparo à Pesquisa do Estado de Minas Gerais (FAPEMIG-Process: 01/17 CEX APQ 02633/17), Conselho Nacional de Desenvolvimento Científico e Tecnológico (CNPq) and Coordenação de Aperfeiçoamento de Pessoal de Nível Superior (CAPES).

# Supplementary Material – Comparative techniques for Glyphosate detection

1 - Chapter, Table 1 - Comparative detection methods.

**Table 1** Comparative analysis among glyphosate detection methods

Method	Samples	Simultaneous identification	LOD ng mL <sup>-1</sup> or ng g <sup>-1</sup> (RSD)	Other analytical characteristics	References
HPLC	Pregnant women Umbilical cord	Paraquat	0.4	94.33–99.03% (ARA) Fluorescence (detection)	Kongtip et al. (2017)
HPLC	General water	–	0.02–6.25 × 10 <sup>3</sup>	–	Ding et al. (2013)
HPLC	Soils and sludges	–	10 (< 15%)	9-Fluorenyl methoxycarbonyl chloride (derivatization) 75–110% (ARA)	Sun et al. (2017)
HPLC	Seawater	AMPA	0.6	Fluorescence (detection) 9-Fluorenyl methoxycarbonyl chloride (derivatization)	Wang et al. (2016b)
HPLC/MS (HILIC–MS/MS)	Olive oil and olives	Amitrol, cyromazine, diquat, paraquat, mepiquat, tri-methylsulfonium, fosetyl aluminum	50	Borate buffer Fluorescence (detection) Liquid partitioning with methanol	Nortes-Méndez et al. (2016)
HPLC/MS	Milk and urine produced by lactating women	AMPA	0.28 (urine)	The products aren't detectable in milk	Nortes-Méndez et al. (2016)
HPLC/MS/MS	Water matrices (drinking, surface and groundwater)	AMPA	0.1	No derivatization 85–113% (ARA)	Guo et al. (2016)
LC–ESI/MS/MS	Soybean	AMPA, GLU	300 (5.3–13%)	73.9–109.1% (ARA)	Martins-Júnior et al. (2009)
LC–ESI/MS/MS	Soybean	AMPA	5 (5.3–13%)	73.9–109.1% (ARA)	Martins-Júnior et al. (2011)
LC/FLD	Fatty matrix (rapeseed)	AMPA	20 (12.8–14.7%)	70.8–74.1% (ARA)	Kaczyński and Łozowicka (2015)
LC–SPE–ESI/MS/MS	General water	AMPA, GLU	0.0002 (< 7%)	91–107% (ARA)	Ibáñez et al. (2005, 2006), Vreeken et al. (1998)
LC–SPE–ESI/MS/MS	Surface, drinkable and waste water	AMPA, GLU	0.03 (< 8.4%)	50 samples (62 min run <sup>-1</sup> ) in a sequence (analysis time) 96% (ARA) 9-Fluorenyl methoxycarbonyl chloride (derivatization)	Vreeken et al. (1998)
LC/MS–ESI	Urine and serum	BIA, GLU, AMPA, 3-MPPA	0.05	–	Sato et al. (2009)
LC/MS/MS	Water	AMPA, GLU	1.2 (6.3–10.2%)	12 min (analysis time) 77.0–102% (ARA) Metal ions, sample preservation, and storage time (interferents)	Hao et al. (2011)
LC/MS/MS	Water	AMPA	0.025 (groundwater) 0.066 (surface water) 0.105 (WWTP effluent)	Fluorenylmethyl chloroformate (derivatization) 97.0–100% (ARA)	Poiger et al. (2017)
LC/MS/MS	Fatty matrix (rapeseed)	AMPA	5 (6.9–9.2%)	88.8–95.0% (ARA)	Kaczyński and Łozowicka (2015)

Table 1 (continued)

Method	Samples	Simultaneous identification	LOD ng mL <sup>-1</sup> or ng g <sup>-1</sup> (RSD)	Other analytical characteristics	References
LC/MS/MS	Serum	AMPA, GLU, BIA, AMPA, 3-MPPA	30 (5.9%)	30 min (analysis time) 94–108% (ARA) Often observed (interferents) Filter (pretreatment) pH (4–8)	Yoshioka et al. (2011)
LC/MS/MS	Blood, urine and gastric content samples	Paraquat, diquat, GLU	100		Tsao et al. (2016)
LC-MS	Coffee leaves	AMPA	41	FMOC (derivatization)	Schribbers et al. (2016)
LC-FLD+MS/MS	Water canals	AMPA	0.058	Lyophilization (3–4 days for 72 samples) pH 9 FMOC-Cl (derivatization) 8 min (analysis time) 67.1–104.0% (ARA) TFA-Gly (OMe) <sub>2</sub> (derivatization)	Ramirez et al. (2014) Kudzin et al. (2003)
LC-SPE	Tap, filtered and river water	AMPA	200		Delmonico et al. (2014)
GC/CU/MS	Biological	Phosphonoglycine, phosphonosarcosine, phosphonoalanine, phosphono- <i>b</i> -alanine, phosphonohomocysteine, phosphono- $\gamma$ -homocysteine, GLU	1		
GC/FID	Biological	Phosphonoglycine, phosphonosarcosine, phosphonoalanine, Phosphono- <i>b</i> -alanine, phosphonohomocysteine, phosphono- $\gamma$ -homocysteine, GLU	30	TFA-Gly (OMe) <sub>2</sub> (derivatization)	Kudzin et al. (2003)
GC/FPD	Rice, soybean sprouts	GLU, AMPA, 3-MPPA	20	Trimethyl orthoacetate (TMOA) (derivatization)	Tseng et al. (2004)
GC/FPD	River water, soil, carrot	GLU, AMPA	8, 1.2 and 20 pg, respectively/injection	20 min (analysis time) 91–106% (ARA) <i>N</i> -isopropoxycarbonylmethyl (derivatization)	Kataoka et al. (1996)
GC/MS	Biological	Phosphonoglycine, phosphonosarcosine, phosphonoalanine, phosphono- <i>b</i> -alanine, phosphonohomocysteine, phosphono- $\gamma$ -homocysteine, GLU	1.5	TFA-Gly (OMe) <sub>2</sub> (derivatization)	Kudzin et al. (2003)
GC/MS	Human serum	AMPA	250	<i>t</i> -BDMS (derivatization) > 73% (ARA)	de Liasera et al. (2005)

Table 1 (continued)

Method	Samples	Simultaneous identification	LOD ng mL <sup>-1</sup> or ng g <sup>-1</sup> (RSD)	Other analytical characteristics	References
GC/MS	Groundwater	AMPA	0.1 (10%)	103% (ARA) Trifluoroacetic anhydride (TFAA) and trifluoroethanol (TFE) (derivatization)	Kudzin et al. (2002)
GC/MS	Soil	AMPA	6 (23%)	78% (ARA) Trifluoroacetic anhydride (TFAA) and trifluoroethanol (TFE) (derivatization)	Kudzin et al. (2002)
GC/MS/MS	Deionized water	–	0.24	Trifluoroacetic anhydride (TFAA) and 2,2,3,3,4,4,4-heptafluoro-1-butanol (HFB) (derivatization) Nitrite nitroso ion and amylum and iodine (pre-treatment)	Lou et al. (2001), Ding et al. (2015) and Pei and Lai (2004)
GC/IT-MS	GLY, GLU and bialaphos	GLU, BIA, their metabolites and nineteen amino acids	10–20	<i>N</i> -methyl- <i>N</i> -( <i>tert</i> -butyldimethylsilyl) trifluoroacetamide in dimethylformamide (derivatization)	Tsunoda (1993)
IC	Water	Bentazone and picloram	1.54	11.0–106.0% (ARA) 50 min per assay (analysis time)	Luo et al. (2015)
IC	Aquatic environment	Not informed	0.04 (1.94%)	96.4–103.2% (ARA) inorganic ion and organic acids (no interferences)	Zhu et al. (1999)
IC/ICP-MS	Water	AMPA, polyphosphates	0.7 ( $\leq 7.4\%$ for $n=3$ )	97.1–107.0% (ARA) 500 $\mu$ L (sample injection volume)	Guo et al. (2005)
IC/ICP-MS	Reservoir and treated water, and clean water reclaimed from waste water	GLU, fosamine, ethephon	1.1–1.4	95–109% (ARA)	Guo et al. (2007)
FS-FPMs/DNA DRS	Distilled water Commercial formulations, environmental and drinking waters	– –	0.04 7280 (4.6–5.4%)	Unknown (interferences) 93.2–102.6% (ARA) Cu <sup>2+</sup> , Fe <sup>3+</sup> , Zn <sup>2+</sup> , Mn <sup>2+</sup> and SO <sub>4</sub> <sup>2-</sup> , CO <sub>3</sub> <sup>2-</sup> , C <sub>6</sub> H <sub>5</sub> O <sub>7</sub> <sup>3-</sup> , PO <sub>4</sub> <sup>3-</sup> , NO <sub>3</sub> <sup>-</sup> (Interferences) 20 $\mu$ L (sample volume)	Lee et al. (2013) da Silva et al. (2011)

Table 1 (continued)

Method	Samples	Simultaneous identification	LOD ng mL <sup>-1</sup> or ng g <sup>-1</sup> (RSD)	Other analytical characteristics	References
IS	Water	–	0.021	25 min per assay (analysis time) Automated (derivatization) Occasionally (Pretreatment) > 500 × (reusability) 500 µL (sample volume) 48 h (stability)	González-Martínez et al. (2005)
IS	Soil (min. 10 g)	–	7.9	25 min (analysis time) Automated (derivatization) Occasionally (Pretreatment) > 500 × (reusability) 48 h (stability)	González-Martínez et al. (2005)
IS	Pearl River water, tea and soil	–	8	87.4–103.7% (ARA)	Wang et al. (2016a)
Spectrophotometric	Groundwater	Gibberellins	0.82	–	Zhang et al. (2015b)
Spectrophotometric	Commercial formulation in soil and water samples	–	3380 (0.5–1.02%)	60 s (analysis time) 90.3–96.5% (ARA) Dithiocarbamate (derivatization)	Sharma et al. (2012)
Spectrophotometric	Soil	–	1100 (2.7%)	80.0–87.0% (ARA)	Jan et al. (2009)
Spectrophotometric	Wheat grain	–	1100 (2.7%)	95.0–102.0% (ARA)	Jan et al. (2009)
Spectrophotometric	Distilled water	–	1100 (2.7%)	92.0–95.0% (ARA)	Jan et al. (2009)
Spectrophotometric	Legume	–	210	98.0–102.0% (ARA)	Çetin et al. (2017)
Fluorescence	Agricultural products	GLU	–	Laser-induced fluorescence Microchip electrophoresis	Wei and Pu (2015)
Fluorescence	Water	–	670	Sensor synthesized by combining copper (II) oxide and multiwall carbon nano-tubes (MWCNTs) 96–107% (ARA)	Chang et al. (2016b)
Fluorescence	Milli-Q water	–	12	Fluorescence (CDs/AgNPs)	Wang et al. (2016c)
Fluorescence	Water, tea, soil	–	8	Carbon dot-labeled antibodies (CD-IgG) Antigen and magnetics beads (GLY-Fe <sub>3</sub> O <sub>4</sub> ) 87.4–103.7% (ARA)	Wang et al. (2016a)
UV-Vis spectroscopy	Aqueous media	–	84	9-Fluorenylmethoxycarbonyl chloride (FMOC-Cl) (derivatization) Organic matter (interferents)	Waiman et al. (2012)

**Table 1** (continued)

Method	Samples	Simultaneous identification	LOD ng mL <sup>-1</sup> or ng g <sup>-1</sup> (RSD)	Other analytical characteristics	References
UV-Vis spectroscopy	Aqueous solution	–	3200	Tungsten halogen lamp coupled to the cuvette holder by a 500 µm core diameter optical fiber	De Góes et al. (2017)
FS-AU/DNA	Distilled water	Pesticides and target materials containing carboxyl groups	10	2 h (analysis time)	Lee et al. (2010)
SERS	Tomato juice	–	16.9 × 10 <sup>12</sup> (2.48)	90% (ARA) 4-Mercaptophenylboronic acid (derivatization)	Torul et al. (2010)
SERS	Water Spiked beer	–	0.1 (water) 0.01 (spiked beer)	Thiocholine-induced aggregation of OsCO-Au NPS	Tan et al. (2017)
SERS	Aqueous solution	–	900	He-Ne laser 632.8 nm Silver nanoparticles	De Góes et al. (2017)
SPR-pd	Buffer solution	–	98	Glycine, thiocloprid, and imidacloprid (no interferences)	Ding and Yang (2013)
NMR <sup>31</sup> P	Biological fluids and tissue digest	–	1 × 10 <sup>6</sup>	1 min (analysis time) Just an enzymic digestion of the liver (pretreatment)	Dickson et al. (1988)
NMR <sup>1</sup> H- <sup>31</sup> P Colorimetric assay	Biological fluids Water and food	Salicylate, alcohol/glycol	33.814 2.9	10–20 min (analysis time) 2-Mercapto-5-nitrobenzimidazole-capped silver nanoparticles adding Mg <sup>2+</sup>	Cartigny et al. (2004) Rawat et al. (2016)
Colorimetric sensor	Drinkable, lake and ground water	–	169	20 min (analysis time) H <sub>2</sub> PO <sub>4</sub> <sup>2-</sup> , HPO <sub>4</sub> <sup>2-</sup> , SO <sub>4</sub> <sup>2-</sup> , C <sub>2</sub> O <sub>4</sub> <sup>2-</sup> , CO <sub>3</sub> <sup>2-</sup> , F <sup>-</sup> , Cl <sup>-</sup> , NO <sub>3</sub> <sup>-</sup> , chloride salts of ion Na <sup>+</sup> , K <sup>+</sup> , Ca <sup>2+</sup> , Ba <sup>2+</sup> and Mg <sup>2+</sup> , KNO <sub>3</sub> , KBr, and Pb(NO <sub>3</sub> ) <sub>2</sub> , dicamba, AMPA, acetochlor (at 4 µg mL <sup>-1</sup> ), atrazine (at 4 µg mL <sup>-1</sup> ) (not interferences) Concentrations can be differentiated by naked eyes	Chang et al. (2016a)
Strip colorimetric cdPVA	Environmental water	–	100	1–3 s (analysis time) AMPA and glycine (no interferences)	De Almeida et al. (2015)
Strip colorimetric test	River water	AChE inhibitors	100	30 µL (sample volume) 20 days (stability) 30–60 min (analysis time)	Liu et al. (2015)

Table 1 (continued)

Method	Samples	Simultaneous identification	LOD ng mL <sup>-1</sup> or ng g <sup>-1</sup> (RSD)	Other analytical characteristics	References
CS-AuNPs	Tap water with chloro	–	1	0.1 mM of GLU, AMPA, dicamba, acetochlor, atrazine, and trifluralin (not interferents) SO <sub>4</sub> <sup>2-</sup> , Al(III) and Cu(II) (interferents)	Zheng et al. (2013)
TR-FRET	Water	–	131.9	Lanthanide (Ln <sup>3+</sup> )-doped nanoparticles	Wang et al. (2016d)
FRET	Apple	–	9.8 × 10 <sup>-3</sup>	Vitamin C, Vitamin B <sub>2</sub> , AMPA and GLU (not interferents) 2–15 min (analysis time) pH 7.0	Guo et al. (2014)
OC-IIDA	Water, salted water	–	200	12 simultaneous tests	Minami et al. (2014)
CL-MIS-MIMs	Foodstuff, water	–	46 (4.68% for n = 11)	96 independent measurements sequentially in 10 min (analysis time)	Zhao et al. (2011)
Oscillo-polarographic	Formulations and soil	–	96 (1.7)	N-nitroso-N-(phosphonomethyl) glycine (derivatization)	Sun et al. (2007)
DPP (differential pulse polarography)	Crops, soil, and water	–	500–1000	> 60% (ARA) aminomethylyphosphonic acid (not interferents)	Friestad and Brønstad (1985)
Amp-HRP	Corn	GLU	0.1	60 × (reusability)	Songa et al. (2009c)
DIPN-GNPs-PGE	Water	GLU	0.34 (0.13%)	97.8–102.3% (ARA) N-nitroso (derivatization) 20 × (reusability) 60 days (stability)	Prasad et al. (2014)
DIPN-GNPs-PGE	Soil	GLU	0.35 (0.48%)	98.6–102.8% (ARA) N-nitroso (derivatization) 20 × (reusability) 60 days (stability)	Prasad et al. (2014)
DIPN-GNPs-PGE	Human serum	GLU	0.35 (5.49%)	98.1–110.2% (ARA) N-nitroso (derivatization) 50-fold dilution (Pretreatment)	Prasad et al. (2014)
ES-Atenoya	Environmental water	–	30 (5.5%)	20 × (reusability) 60 days (stability) 94.9–108.9% (ARA) 8 weeks (Stability)	Oliveira et al. (2012)



Table 1 (continued)

Method	Samples	Simultaneous identification	LOD ng mL <sup>-1</sup> or ng g <sup>-1</sup> (RSD)	Other analytical characteristics	References
ES-HRP	Doubly distilled water	–	1.7	20 min (analysis time) Unknown (interferents)	Songa et al. (2009b)
ES-HRP	Phosphate buffer solution (0.1 M, pH 6.10)	AMPA	0.16	20 min (analysis time) Unknown (interferents) 3 × (reusability)	Songa et al. (2009b)
NiAl-LDH	Deionised water	GLU	169	20 s (analysis time)	Khenifi et al. (2009)
VET	Aqueous environments	–	16,905	Humic acids and Ca <sup>2+</sup> (not interferents)	Battaller et al. (2012)
Spectroelectrochemical Electrochemical	Double-distilled water	AMPA	16,905	Screen-printed electrode (SPE)	Habekost (2017)
DPV (differential pulse voltammetry)	Nature water	–	59	Signal of [Ru(bpy) <sub>3</sub> ] <sup>2+</sup> (ECL) Copper electrode Phosphate buffer 0.05 mol L <sup>-1</sup> and pH 7.3	Garcia and do Carmo Rollemberg (2007)
DPV	GLY 99.9% pure diluted	–	2.02	Copper phthalocyanine/multiwalled carbon nanotube film-modified glassy carbon	Moraes et al. (2010)
SWV (square wave voltammetry)	GLY 99.9% pure diluted	–	25	Mercury drop electrode N-nitroso (derivatization)	Teófilo et al. (2004)
SWV	Soil	–	25	Carbon fiber microelectrode Phosphate buffer 0.2 mol L <sup>-1</sup> and pH 5.3 (pretreatment) 88.5–102.3% (ARA)	Tapsoba et al. (2012)
PEC	Orange juice	–	0.004 (2.9–3.6%)	94.5–114.9% (ARA) pH and time dependent (pretreatment)	Li et al. (2016)
CE	Marijuana	Paraquat and AMPA	8000	Starch, carbendazim, PMG, vitamin B1, glucose, sulfiramid, blank, sucrose and acetochlor (not interferents)	Sharma et al. (2012)
CE	Natural waters	AMPA	85 (< 6%)	Indirect UV/VIS detection 84–87% (ARA) p-toluenesulfonyl chloride (derivatization) Salts in water (interferents)	Corbera et al. (2005)
CE-C(4)D	Drinking water	GLU, AMPA	0.1–2.2 (10%)	Not informed	See et al. (2010)
CE/LIF	River water, broccoli, soybean	GLU	0.34	84.0–101.0% (ARA)	Wei et al. (2013)
CE/MS/mESI	Wheat	GLU, AMPA, 3-MPPA	169.07 (1–2%)	–	Goodwin et al. (2003)
CE/UV-Vis	Ground and lake water	GLU, AMPA	16.9	9-Fluorenylmethyl chloroformate (derivatization)	Chang and Wei (2005)

**Table 1** (continued)

Method	Samples	Simultaneous identification	LOD ng mL <sup>-1</sup> or ng g <sup>-1</sup> (RSD)	Other analytical characteristics	References
CF-ELISA	Water	–	76	Glyphosate, AMPA (interferents)	Clegg et al. (1999)
L-ELISA	Surface and ground waters	–	0.1 (0.2%)	Succinic anhydride (derivatization)	Lee et al. (2002)
Cyan-sensor	Water, soil, environmental	–	450	Minutes till some days (analysis time) Other herbicides, heavy metals copper and zinc and a representative volatile organic 3,5-DCP (interferents)	Shao et al. (2002)
BERA	Distilled water	–	0.1	3–5 min (analysis time)	Kintzios et al. (2001)
CRMS	Water for treatment	Atrazine, lead nitrate, cadmium nitrate	2000	1 min (analysis time)	Che and Liu (2014)

LOD lower detection limit, RSD relative standard deviations

## References

Abdel-Hamid MI (1996) Development and application of a simple procedure for toxicity testing using immobilized algae. *Water Sci Technol* 33:129–138

Alferness PL, Iwata Y (1994) Determination of glyphosate and (aminomethyl)phosphonic acid in soil, plant and animal matrixes, and water by capillary gas chromatography with mass-selective detection. *J Agric Food Chem* 42:2751–2759

Algar WR, Krull UJ (2008) Quantum dots as donors in fluorescence resonance energy transfer for the bioanalysis of nucleic acids, proteins, and other biological molecules. *Anal Bioanal Chem* 391:1609–1618

Allinson G, Allinson M, Bui A et al (2016) Pesticide and trace metals in surface waters and sediments of rivers entering the Corner Inlet Marine National Park, Victoria, Australia. *Environ Sci Pollut Res Int* 23:5881–5891

Anthony S, Stephanie S (2017) Glyphosate pathways to modern diseases VI: prions, amyloidosis and autoimmune neurological diseases. *J Biol Phys Chem* 17:8–32

Antoniou M, Habib M, Howard CV et al (2012) Teratogenic effects of glyphosate-based herbicides: divergence of regulatory decisions from scientific evidence. *J Environ Anal Toxicol* S4:006

Arroyave JM, Waiman CC, Zanini GP, Avena MJ (2016) Effect of humic acid on the adsorption/desorption behavior of glyphosate on goethite. Isotherms and kinetics. *Chemosphere* 145:34–41

Barcelo D (2000) Sample handling and trace analysis of pollutants. Techniques, applications and quality assurance, vol 21, 1st edn. Elsevier, Amsterdam Barrett KA, McBride MB (2005) Oxidative degradation of glyphosate and aminomethylphosphonate by manganese oxide. *Environ Sci Technol* 39:9223–9228

Bataller R, Campos I, Laguarda-Miro N et al (2012) Glyphosate detection by means of a voltammetric electronic tongue and discrimination of potential interferents. *Sensors* 12:17553–17568

Beecham JE, Seneff S (2015) The possible link between autism and glyphosate acting as glycine mimetic—a review of evidence from the literature with analysis. *J Mol Genet Med*. <https://doi.org/10.4172/1747-0862.1000187>

Benachour N, Séralini G-E (2009) Glyphosate formulations induce apoptosis and necrosis in human umbilical, embryonic, and placental cells. *Chem Res Toxicol* 22:97–105

Börjesson E, Torstensson L (2000) New methods for determination of glyphosate and (aminomethyl)phosphonic acid in water and soil. *J Chromatogr A* 886:207–216

Bradley PM, Journey CA, Romanok KM et al (2017) Expanded target-chemical analysis reveals extensive mixed-organic-contaminant exposure in U.S. streams. *Environ Sci Technol* 51:4792–4802

Brånstad JO, Friestad HO (1976) Method for determination of glyphosate residues in natural waters based on polarography of the *N*-nitroso derivative. *Analyst* 101:820–824

Byer JD, Struger J, Klawunn P et al (2008) Low cost monitoring of glyphosate in surface waters using the ELISA method: an evaluation. *Environ Sci Technol* 42:6052–6057

Campanella L, Cubadda F, Sammartino MP, Saoncella A (2001) An algal biosensor for the monitoring of water toxicity in estuarine environments. *Water Res* 35:69–76

Candela L, Caballero J, Ronen D (2010) Glyphosate transport through weathered granite soils under irrigated and non-irrigated conditions—Barcelona, Spain. *Sci Total Environ* 408:2509–2516

Cartigny B, Azaroual N, Imbenotte M et al (2004) Determination of glyphosate in biological fluids by  $^1\text{H}$  and  $^{31}\text{P}$  NMR spectroscopy. *Forensic Sci Int* 143:141–145

Castle LA, Siehl DL, Gorton R et al (2004) Discovery and directed evolution of a glyphosate tolerance gene. *Science* 304:1151–1154  
Cattani D, de Liz Oliveira Cavalli VL, Heinz Rieg CE et al (2014) Mechanisms underlying the neurotoxicity induced by glyphosate-based herbicide in immature rat hippocampus: involvement of glutamate excitotoxicity. *Toxicology* 320:34–45

Cavalcante DGSM, Martinez CBR, Sofia SH (2008) Genotoxic effects of Roundup® on the fish *Prochilodus lineatus*. *Mutat Res Genet Toxicol Environ Mutagen* 655:41–46

Cavaş T, Könen S (2007) Detection of cytogenetic and DNA damage in peripheral erythrocytes of goldfish (*Carassius auratus*) exposed to a glyphosate formulation using the micronucleus test and the comet assay. *Mutagenesis* 22:263–268

Çetin E, Şahan S, Ülgen A, Şahin U (2017) DLLME-spectrophotometric determination of glyphosate residue in legumes. *Food Chem* 230:567–571

Chalubinski M, Kowalski ML (2006) Endocrine disrupters–potential modulators of the immune system and allergic response. *Allergy* 61:1326–1335

Chang SY, Liao C-H (2002) Analysis of glyphosate, glufosinate and aminomethylphosphonic acid by capillary electrophoresis with indirect fluorescence detection. *J Chromatogr A* 959:309–315

Chang SY, Wei M-Y (2005) Simultaneous determination of glyphosate, glufosinate, and aminomethylphosphonic acid by capillary electrophoresis after 9-fluorenylmethyl chloroformate derivatization. *J Chin Chem Soc* 52:785–792

Chang Y, Zhang Z, Hao J et al (2016a) A simple label free colorimetric method for glyphosate detection based on the inhibition of peroxidase-like activity of Cu(II). *Sens Actuators B Chem* 228:410–415

Chang Y-C, Lin Y-S, Xiao G-T et al (2016b) A highly selective and sensitive nanosensor for the detection of glyphosate. *Talanta* 161:94–98

Chaufan G, Coalova I, Ríos de Molina MDC (2014) Glyphosate commercial formulation causes cytotoxicity, oxidative effects, and apoptosis on human cells: differences with its active ingredient. *Int J Toxicol* 33:29–38

Che H, Liu S (2014) Contaminant detection using multiple conventional water quality sensors in an early warning system. *Proc Eng* 89:479–487

Chenier PJ (2002) Sulfuric acid and its derivatives. In: Chenier PJ (ed) *Survey of industrial chemistry*. Springer, Boston, pp 23–40  
Cikalo MG, Goodall DM, Matthews W (1996) Analysis of glyphosate using capillary electrophoresis with indirect detection. *J Chromatogr A* 745:189–200

Clegg BS, Stephenson GR, Hall JC (1999) Development of an enzyme-linked immunosorbent assay for the detection of glyphosate. *J Agric Food Chem* 47:5031–5037

Corbera M, Hidalgo M, Salvadó V, Wieczorek PP (2005) Determination of glyphosate and aminomethylphosphonic acid in natural water using the capillary electrophoresis combined with enrichment step. *Anal Chim Acta* 540:3–7

Coutinho CFB, Mazo LH (2005) Complexos metálicos com o herbicida glifosato: revisão. *Quim Nova* 28:1038

Coutinho CFB, Coutinho LFM, Mazo LH et al (2007) Direct determination of glyphosate using hydrophilic interaction chromatography with coulometric detection at copper microelectrode. *Anal Chim Acta* 592:30–35

da Silva AS, Fernandes FCB, Tognolli JO et al (2011) A simple and green analytical method for determination of glyphosate in commercial formulations and

water by diffuse reflectance spectroscopy. *Spectrochim Acta A Mol Biomol Spectrosc* 79:1881–1885

Dai H, Sang M, Wang Y et al (2014) Determination of trace glyphosate in water with a prism coupling optical waveguide configuration. *Sens Actuators A Phys* 218:88–93

De Almeida LKS, Chigome S, Torto N et al (2015) A novel colorimetric sensor strip for the detection of glyphosate in water. *Sens Actuators B Chem* 206:357–363

De Góes RE, Muller M, Fabris JL (2017) Spectroscopic detection of glyphosate in water assisted by laser-ablated silver nanoparticles. *Sensors* 17(954):1–15

de Llasera MPG, Gómez-Almaraz L, Vera-Avila LE, Peña-Alvarez A (2005) Matrix solid-phase dispersion extraction and determination by high-performance liquid chromatography with fluorescence detection of residues of glyphosate and aminomethylphosphonic acid in tomato fruit. *J Chromatogr A* 1093:139–146

Delmonico EL, Bertozzi J, Evelázio de Souza N, Celestino Oliveira C (2014) Determination of glyphosate and aminomethylphosphonic acid for assessing the quality tap water using SPE and HPLC. *Acta Sci Technol* 36:513–519

DeLorenzo ME, Lauth J, Pennington PL et al (1999) Atrazine effects on the microbial food web in tidal creek mesocosms. *Aquat Toxicol* 46:241–251

Dickson SJ, Meinhold RH, Beer ID, Koelmeyer TD (1988) Rapid determination of glyphosate in postmortem specimens using <sup>31</sup>P NMR. *J Anal Toxicol* 12:284–286

Ding X, Yang K-L (2013) Development of an oligopeptide functionalized surface plasmon resonance biosensor for online detection of glyphosate. *Anal Chem* 85:5727–5733

Ding J, Guo H, Liu W-W et al (2013) Current progress on the detection of glyphosate in environmental samples. J Sci Appl Biomed 2014:2015

Ding J, Guo H, Liu W-W, Zhang W-W, Wang J-W (2015) Current progress on the detection of glyphosate in environmental samples. J Sci Appl Biomed 3(6):88–95

do Carmo Langiano CV, Martinez CBR (2008) Toxicity and effects of a glyphosate-based herbicide on the Neotropical fish *Prochilodus lineatus*. Comp Biochem Physiol C Toxicol Pharmacol 147:222–231

Ejaz S, Akram W, Lim CW et al (2004) Endocrine disrupting pesticides: a leading cause of cancer among rural people in Pakistan. Exp Oncol 26:98–105

El-Gendy KS, Aly NM, El-Sebae AH (1998) Effects of edifenphos and glyphosate on the immune response and protein biosynthesis of bolti fish (*Tilapia nilotica*). J Environ Sci Health B 33:135–149

European Commission (2002) Review report for the active substance glyphosate. European Commission 6511/VI/99-final. <https://big.assets.huffingtonpost.com/ec.2002.pdf>. Accessed 20 April 2018

Fang F, Xu H, Wei RQ et al (2011) Determination of glyphosate by high performance liquid chromatography with *o*-nitrobenzene- sulfonyl chloride as derivatization reagent. Fenxi Ceshi Xuebao 30:683–686

Fang F, Wei RQ et al (2014) Determination of glyphosate by HPLC with a novel pre-column derivatization reagent. Chin J Bio- process Eng 12(3):69–73

Forlani G, Mangiagalli A, Nielsen E, Suardi CM (1999) Degradation of the phosphonate herbicide glyphosate in soil: evidence for a possible involvement of unculturable microorganisms. Soil Biol Biochem 31:991–997

Franz JE, Mao MK, Sikorski JA (1997) Glyphosate: a unique global herbicide. ACS Monograph 189



Frense D, Müller A, Beckmann D (1998) Detection of environmental pollutants using optical biosensor with immobilized algae cells. *Sens Actuators B Chem* 51:256–260

Friestad HO, Brønstad JO (1985) Improved polarographic method for determination of glyphosate herbicide in crops, soil, and water. *J Assoc Off Anal Chem* 68:76–79

Garcia AF, do Carmo Rollemberg M (2007) Determinação voltamétrica do herbicida glifosato em águas naturais utilizando eletrodo de cobre. *Quim Nova* 30(7):1592–1596

Garcia AF, Rollemberg MC (2007) Voltammetric determination of glyphosate in natural waters with a copper electrode. *Quím Nova* 30:1592–1596

Garry VF, Harkins ME, Erickson LL et al (2002) Birth defects, season of conception, and sex of children born to pesticide applicators living in the Red River Valley of Minnesota, USA. *Environ Health Perspect* 110(Suppl 3):441–449

Gasnier C, Dumont C, Benachour N et al (2009) Glyphosate-based herbicides are toxic and endocrine disruptors in human cell lines. *Toxicology* 262:184–191

Giesy JP, Dobson S, Solomon KR (2000) Ecotoxicological risk assessment for roundup<sup>®</sup> herbicide. In: Ware GW (ed) *Reviews of environmental contamination and toxicology*. Springer, New York, pp 35–120

Glass RL (1981) Colorimetric determination of glyphosate in water after oxidation to orthophosphate. *Anal Chem* 53:921–923 Glass RL (1984) Metal complex formation by glyphosate. *J Agric Food Chem* 32:1249–1253 Gluszcak L, dos Santos Miron D, Crestani M et al (2006) Effect

of glyphosate herbicide on acetylcholinesterase activity and metabolic and hematological parameters in piava (*Leporinus obtusidens*). *Ecotoxicol Environ Saf* 65:237–241

Gluszczak L, dos Santos Miron D, Moraes BS et al (2007) Acute effects of glyphosate herbicide on metabolic and enzymatic parameters of silver catfish (*Rhamdia quelen*). Comp Biochem Physiol C Toxicol Pharmacol 146:519–524

González-Martínez MA, Brun EM, Puchades R et al (2005) Glyphosate immunosensor. Application for water and soil analysis. Anal Chem 77:4219–4227

Goodwin L, Startin JR, Keely BJ, Goodall DM (2003) Analysis of glyphosate and glufosinate by capillary electrophoresis–mass spectrometry utilising a sheathless microelectrospray interface. J Chromatogr A 1004:107–119

Govindarajulu PP (2008) Literature review of impacts of glyphosate herbicide on amphibians: what risks can the silvicultural use of this herbicide pose for amphibians in B.C.? B.C. Ministry of Environment, Victoria, BC. Wildlife Report No. R-28

Grisolia CK (2002) A comparison between mouse and fish micronucleus test using cyclophosphamide, mitomycin C and various pesticides. Mutat Res 518:145–150

Gui Y-X, Fan X-N, Wang H-M et al (2012) Glyphosate induced cell death through apoptotic and autophagic mechanisms. Neurotoxicol Teratol 34:344–349

Guo Z-X, Cai Q, Yang Z (2005) Determination of glyphosate and phosphate in water by ion chromatography–inductively coupled plasma mass spectrometry detection. J Chromatogr A 1100:160–167

Guo Z-X, Cai Q, Yang Z (2007) Ion chromatography/inductively coupled plasma mass spectrometry for simultaneous determination of glyphosate, glufosinate, fosamine and ethephon at nanogram levels in water. Rapid Commun Mass Spectrom 21:1606–1612

Guo J, Zhang Y, Luo Y et al (2014) Efficient fluorescence resonance energy transfer between oppositely charged CdTe quantum dots and gold nanoparticles for turn-on fluorescence detection of glyphosate. Talanta 125:385–392

Guo H, Riter LS, Wujcik CE, Armstrong DW (2016) Direct and sensitive determination of glyphosate and aminomethylphosphonic acid in environmental water samples by high performance liquid chromatography coupled to electrospray tandem mass spectrometry. *J Chromatogr A* 1443:93–100

Habekost A (2015) Spectroscopic and electrochemical investigations of *N*-(phosphonomethyl)glycine (glyphosate) and (aminomethyl) phosphonic acid (AMPA). *World J Chem Educ* 3(6):134–140

Habekost A (2017) Rapid and sensitive spectroelectrochemical and electrochemical detection of glyphosate and AMPA with screen- printed electrodes. *Talanta* 162:583–588

Hance RJ (1976) Herbicide usage and soil properties. *Plant Soil* 45:291–293

Hanke I, Singer H, Hollender J (2008) Ultratrace-level determination of glyphosate, aminomethylphosphonic acid and glufosinate in natural waters by solid-phase extraction followed by liquid chromatography–tandem mass spectrometry: performance tuning of derivatization, enrichment and detection. *Anal Bioanal Chem* 391:2265–2276

Hao Chunyan, Morse David, Morra Franca, Zhao Xiaoming, Yang Paul, Nunn Brian (2011) Direct aqueous determination of glyphosate and related compounds by liquid chromatography/tandem mass spectrometry using reversed-phase and weak anion-exchange mixed-mode column. *J Chromatogr A* 1218(33):5638–5643

Heras-Mendoza F, Casado-Fariñas I, Paredes-Gascón M, Conde- Salazar L (2008) Erythema multiforme-like eruption due to an irritant contact dermatitis from a glyphosate pesticide. *Contact Dermat* 59:54–56

Hidalgo C, Rios C, Hidalgo M et al (2004) Improved coupled-column liquid chromatographic method for the determination of glyphosate and

aminomethylphosphonic acid residues in environmental waters. *J Chromatogr A* 1035:153–157

Ho MW, Cherry B (2010) Glyphosate tolerant crops bring diseases and death. *Sci Soc* 47:12–15

Hogendoorn EA, Ossendrijver FM, Dijkman E, Baumann RA (1999) Rapid determination of glyphosate in cereal samples by means of pre-column derivatisation with 9-fluorenylmethyl chloroformate and coupled-column liquid chromatography with fluorescence detection. *J Chromatogr A* 833:67–73

Hokanson R, Fudge R, Chowdhary R, Busbee D (2007) Alteration of estrogen-regulated gene expression in human cells induced by the agricultural and horticultural herbicide glyphosate. *Hum Exp Toxicol* 26:747–752

Homola J (2003) Present and future of surface plasmon resonance biosensors. *Anal Bioanal Chem* 377:528–539

Hu J-Y, Zhao D-Y, Ning J et al (2007) Determination of glyphosate residues in soil and apple by capillary gas chromatography with nitrogen-phosphorus detection. *Chin J Pestic Sci* 3:016

Hu J-Y, Chen C-L, Li J-Z (2008) A simple method for the determination of glyphosate residues in soil by capillary gas chromatography with nitrogen phosphorus. *J Anal Chem* 63:371–375

Huang Y, Reddy KN, Thomson SJ, Yao H (2015) Assessment of soy- bean injury from glyphosate using airborne multispectral remote sensing. *Pest Manag Sci* 71:545–552

Huhn C (2018) More and enhanced glyphosate analysis is needed. *Anal Bioanal Chem* 410:3041–3045

Humphries D, Anderson A-M, Byrtus G (2005) Glyphosate residues in Alberta's atmospheric deposition, soils and surface waters. Alberta Environment no. T/806

Ibáñez M, Pozo ÓJ, Sancho JV et al (2005) Residue determination of glyphosate, glufosinate and aminomethylphosphonic acid in water and soil samples by liquid chromatography coupled to electrospray tandem mass spectrometry. *J Chromatogr A* 1081:145–155

Ibáñez M, Pozo OJ, Sancho JV et al (2006) Re-evaluation of glyphosate determination in water by liquid chromatography coupled to electrospray tandem mass spectrometry. *J Chromatogr A* 1134:51–55

Jan MR, Shah J, Muhammad M, Ara B (2009) Glyphosate herbicide residue determination in samples of environmental importance using spectrophotometric method. *J Hazard Mater* 169:742–745

Jayasumana C, Gunatilake S, Senanayake P (2014) Glyphosate, hard water and nephrotoxic metals: are they the culprits behind the epidemic of chronic kidney disease of unknown etiology in Sri Lanka? *Int J Environ Res Public Health* 11:2125–2147

Jayasumana C, Gunatilake S, Siribaddana S (2015) Simultaneous exposure to multiple heavy metals and glyphosate may contribute to Sri Lankan agricultural nephropathy. *BMC Nephrol* 16:103

Jiraungkoorskul W, Upatham ES, Kruatrachue M et al (2003) Biochemical and histopathological effects of glyphosate herbicide on Nile tilapia (*Oreochromis niloticus*). *Environ Toxicol* 18:260–267

Johal GS, Huber DM (2009) Glyphosate effects on diseases of plants. *Eur J Agron* 31:144–152

Kaczyński P, Łozowicka B (2015) Liquid chromatographic determination of glyphosate and aminomethylphosphonic acid residues in rapeseed with MS/MS detection or derivatization/fluorescence detection. *Open Chem* 13:1011–1019

Kataoka H, Ryu S, Sakiyama N, Makita M (1996) Simple and rapid determination of the herbicide glyphosate and glufosinate in river water, soil and

carrot samples by gas chromatography with flame photometric detection. J Chromatogr A 726:253–258

Kawai S, Uno B, Tomita M (1991) Determination of glyphosate and its major metabolite aminomethylphosphonic acid by high- performance liquid chromatography after derivatization with *p*-toluenesulphonyl chloride. J Chromatogr A 540:411–415

Khenifi A, Derriche Z, Forano C et al (2009) Glyphosate and glufosinate detection at electrogenerated NiAl-LDH thin films. Anal Chim Acta 654:97–102

Khrolenko MV, Wieczorek PP (2005) Determination of glyphosate and its metabolite aminomethylphosphonic acid in fruit juices using supported-liquid membrane preconcentration method with high-performance liquid chromatography and UV detection after derivatization with *p*-toluenesulphonyl chloride. J Chromatogr A 1093:111–117

Kintzios S, Pistola E, Panagiotopoulos P et al (2001) Bioelectric recognition assay (BERA). Biosens Bioelectron 16:325–336

Koblizek M, Masojidek J, Komenda J et al (1998) A sensitive photo- system II-based biosensor for detection of a class of herbicides. Biotechnol Bioeng 60:664–669

Kongtip P, Nankongnab N, Phupancharoensuk R et al (2017) Glyphosate and Paraquat in maternal and fetal serums in Thai women. J Agromed 22:282–289

Koskinen WC, Marek LJ, Hall KE (2016) Analysis of glyphosate and aminomethylphosphonic acid in water, plant materials and soil. Pest Manag Sci 72:423–432

Kudzin ZH, Gralak DK, Drabowicz J, Luczak J (2002) Novel approach for the simultaneous analysis of glyphosate and its metabolites. J Chromatogr A 947:129–141

Kudzin ZH, Gralak DK, Andrijewski G et al (2003) Simultaneous analysis of biologically active aminoalkanephosphonic acids. *J Chromatogr A* 998:183–199

Laitinen P, Rämö S, Nikunen U et al (2009) Glyphosate and phosphorus leaching and residues in boreal sandy soil. *Plant Soil* 323:267–283

Lee EA, Zimmerman LR, Bhullar BS, Thurman EM (2002) Linker-assisted immunoassay and liquid chromatography/ mass spectrometry for the analysis of glyphosate. *Anal Chem* 74:4937–4943

Lee HU, Shin HY, Lee JY et al (2010) Quantitative detection of glyphosate by simultaneous analysis of UV spectroscopy and fluorescence using DNA-labeled gold nanoparticles. *J Agric Food Chem* 58:12096–12100

Lee HU, Jung DU, Lee JH et al (2013) Detection of glyphosate by quantitative analysis of fluorescence and single DNA using DNA-labeled fluorescent magnetic core–shell nanoparticles. *Sens Actuators B Chem* 177:879–886

Li X, Xu J, Jiang Y et al (2009) Hydrophilic-interaction liquid chromatography (HILIC) with dad and mass spectroscopic detection for direct analysis of glyphosate and glufosinate residues and for product quality control. *Acta Chromatogr* 21:559–576

Li Y, Zhang S, Zhang Q et al (2016) Binding-induced internal- displacement of signal-on photoelectrochemical response: a glyphosate detection platform based on graphitic carbon nitride. *Sens Actuators B Chem* 224:798–804

Liao Y, Berthiona J-M, Coleta I et al (2018) Validation and application of analytical method for glyphosate and glufosinate in foods by liquid chromatography–tandem mass spectrometry. *J Chromatogr A* 1549:31–38

Liu Q, Jiang X, Zhang Y et al (2015) A novel test strip for organo-phosphorus detection. *Sens Actuators B Chem* 210:803–810

Lou ZY, Zhu GN, Wu HM (2001) Study on the detection method of glyphosate in pond water. *Chin J Ningbo Acad* 13(Suppl):142–145

Luo X, Chen L, Zhao Y (2015) Simultaneous determination of three chloroacetic acids, three herbicides, and 12 anions in water by ion chromatography. *J Sep Sci* 38:3096–3102

Lushchak OV, Kubrak OI, Storey JM et al (2009) Low toxic herbicide Roundup induces mild oxidative stress in goldfish tissues. *Chemosphere* 76:932–937

Mallat E, Barceló D (1998) Analysis and degradation study of glyphosate and of aminomethylphosphonic acid in natural waters by means of polymeric and ion-exchange solid-phase extraction columns followed by ion chromatography-post-column derivatization with fluorescence detection. *J Chromatogr A* 823:129–136

Marc J, Mulner-Lorillon O, Bellé R (2004) Glyphosate-based pesticides affect cell cycle regulation. *Biol Cell* 96:245–249

Martínez Gil P, Laguarda-Miro N, Camino JS, Peris RM (2013) Glyphosate detection with ammonium nitrate and humic acids as potential interfering substances by pulsed voltammetry technique. *Talanta* 115:702–705

Martins-Júnior HA, Lebre DT, Wang AY et al (2009) An alternative and fast method for determination of glyphosate and aminomethylphosphonic acid (AMPA) residues in soybean using liquid chromatography coupled with tandem mass spectrometry. *Rapid Commun Mass Spectrom* 23:1029–1034

Martins-Júnior HA, Lebre DT, Wang AY et al (2011) Residue analysis of glyphosate and aminomethylphosphonic acid (AMPA) in Soybean using liquid chromatography coupled with tandem mass spectrometry. In: Ng T-B (ed) *Soybean - biochemistry, chemistry and physiology*. InTech. [https://www.intechopen.com/books/soybean-biochemistry-chemistry-and-](https://www.intechopen.com/books/soybean-biochemistry-chemistry-and-physiology)



physiology/residue-analysis-of-glyphosate-and-aminomethylphosphonic-acid-  
amphipathic- soybean-using-liquid-chromatography

Mazereeuw M, Hofte AJP, Tjaden UR, van der Greef J (1997) A novel sheathless and electrodeless microelectrospray interface for the on-line coupling of capillary zone electrophoresis to mass spectrometry. *Rapid Commun Mass Spectrom* 11:981–986

Merás ID, Díaz TG, Franco MA (2005) Simultaneous fluorimetric determination of glyphosate and its metabolite, aminomethylphosphonic acid, in water, previous derivatization with NBD-Cl and by partial least squares calibration (PLS). *Talanta* 65:7–14

Mesnage R, Bernay B, Séralini G-E (2013) Ethoxylated adjuvants of glyphosate-based herbicides are active principles of human cell toxicity. *Toxicology* 313:122–128

Metzger JO (1997) *Green Chemistry. Designing Chemistry for the Environment*. Herausgegeben von PT Anastas und TS Williamson. American Chemical Society, Washington, DC, 1996. 251 S., geb. 89.95£.-ISBN 0-8412-3399-3. *Angew Chem Int Ed Engl* 109:812–813

Minami T, Liu Y, Akdeniz A et al (2014) Intramolecular indicator displacement assay for anions: supramolecular sensor for glyphosate. *J Am Chem Soc* 136:11396–11401

Mol HGJ, van Dam RCJ (2014) Rapid detection of pesticides not amenable to multi-residue methods by flow injection–tandem mass spectrometry. *Anal Bioanal Chem* 406:6817–6825

Molina M, Silva M (2002) Analytical potential of fluorescein analogues for ultrasensitive determinations of phosphorus-containing amino acid herbicides by micellar electrokinetic chromatography with laser-induced fluorescence detection. *Electrophoresis* 23:1096–1103

Moraes FC, Mascaro LH, Machado SAS, Brett CMA (2010) Direct electrochemical determination of glyphosate at copper phthalocyanine/multiwalled carbon nanotube film electrodes. *Electroanalysis* 22:1586–1591

Napoli M, Cecchi S, Zanchi CA, Orlandini S (2015) Leaching of glyphosate and aminomethylphosphonic acid through silty clay soil columns under outdoor conditions. *J Environ Qual* 44:1667–1673

Nedelkoska TV, Low GK-C (2004) High-performance liquid chromatographic determination of glyphosate in water and plant material after pre-column derivatization with 9-fluorenylmethyl chloroformate. *Anal Chim Acta* 511:145–153

Nešković NK, Poleksić V, Elezović I et al (1996) Biochemical and histopathological effects of glyphosate on carp, *Cyprinus carpio* L. *Bull Environ Contam Toxicol* 56:295–302

Nielsen JB, Nielsen F, Sørensen JA (2007) Defense against dermal exposures is only skin deep: significantly increased penetration through slightly damaged skin. *Arch Dermatol Res* 299:423–431

Nortes-Méndez R, Robles-Molina J, López-Blanco R et al (2016) Determination of polar pesticides in olive oil and olives by hydrophilic interaction liquid chromatography coupled to tandem mass spectrometry and high-resolution mass spectrometry. *Talanta* 158:222–228

Okada E, Pérez D, De Gerónimo E et al (2018) Non-point source pollution of glyphosate and AMPA in a rural basin from the southeast Pampas, Argentina. *Environ Sci Pollut Res*. <https://doi.org/10.1007/s11356-018-1734-7>

Oliveira GC, Moccelini SK, Castilho M et al (2012) Biosensor based on atemoya peroxidase immobilized on modified nanoclay for glyphosate biomonitoring. *Talanta* 98:130–136

Paganelli A, Gnazzo V, Acosta H et al (2010) Glyphosate-based herbicides produce teratogenic effects on vertebrates by impairing retinoic acid signaling. *Chem Res Toxicol* 23:1586–1595

Patsias J, Papadopoulou A, Papadopoulou-Mourkidou E (2001) Automated trace level determination of glyphosate and aminomethyl phosphonic acid in water by on-line anion-exchange solid-phase extraction followed by cation-exchange liquid chromatography and post-column derivatization. *J Chromatogr A* 932:83–90

Pei MQ, Lai J (2004) Qualitative and quantitative analysis of glyphosate. *Chin J Guangdong Police Sci Technol* 1:14–15

Pintado S, Amaro RR, Mayén M, Mellado JMR (2012) Electrochemical determination of the glyphosate metabolite aminomethylphosphonic acid (AMPA) in drinking waters with an electrodeposited copper electrode. *Int J Electrochem Sci* 7:305–312

Pipke R, Amrhein N (1988) Isolation and characterization of a mutant of *Arthrobacter* sp. Strain GLP-1 which utilizes the herbicide glyphosate as its sole source of phosphorus and nitrogen. *Appl Environ Microbiol* 54:2868–2870

Poiger T, Buerge IJ, Bächli A et al (2017) Occurrence of the herbicide glyphosate and its metabolite AMPA in surface waters in Switzerland determined with on-line solid phase extraction LC-MS/MS. *Environ Sci Pollut Res Int* 24:1588–1596

Poletta GL, Larriera A, Kleinsorge E, Mudry M (2009) Genotoxicity of the herbicide formulation Roundup® (glyphosate) in broad- snouted caiman (*Caiman latirostris*) evidenced by the Comet assay and the Micronucleus test. *Mutat Res Genet Toxicol Environ Mutagen* 672:95–102

Pollegioni L, Schonbrunn E, Siehl D (2011) Molecular basis of glyphosate resistance—different approaches through protein engineering. *FEBS J* 278:2753–2766

Poulsen ME, Christensen HB, Herrmann SS (2009) Proficiency test on incurred and spiked pesticide residues in cereals. *Accredit Qual Assur* 14:477–485

Prasad BB, Jauhari D, Tiwari MP (2014) Doubly imprinted polymer nanofilm-modified electrochemical sensor for ultra-trace simultaneous analysis of glyphosate and glufosinate. *Biosens Bioelectron* 59:81–88

Ramirez CE, Bellmund S, Gardinali PR (2014) A simple method for routine monitoring of glyphosate and its main metabolite in surface waters using lyophilization and LC–FLD + MS/MS. Case study: canals with influence on Biscayne National Park. *Sci Total Environ* 496:389–401

Rawat KA, Majithiya RP, Rohit JV et al (2016) Mg<sup>2+</sup> for colorimetric sensing of glyphosate with improved sensitivity via the aggregation of 2-mercapto-5-nitrobenzimidazole capped silver nanoparticles. *RSC Adv* 6:47741–47752

Relyea RA (2012) New effects of Roundup on amphibians: predators reduce herbicide mortality; herbicides induce antipredator morphology. *Ecol Appl* 22:634–647

Richard S, Moslemi S, Sipahutar H et al (2005) Differential effects of glyphosate and roundup on human placental cells and aromatase. *Environ Health Perspect* 113:716–720

Ridlen JS, Klopff GJ, Nieman TA (1997) Determination of glyphosate and related compounds using HPLC with tris(2,2'-bipyridyl) ruthenium (II) electrogenerated chemiluminescence detection. *Anal Chim Acta* 341:195–204

Roberts SM (1989) Molecular recognition: chemical and biochemical problems: the proceedings of an International Symposium, University of Exeter, April 1989. CRC Press  
Lluc Royer A, Beguin S, Tabet JC et al (2000) Determination of glyphosate and aminomethylphosphonic acid residues in water by gas chromatography with tandem mass spectrometry after exchange ion resin purification and derivatization. Application on vegetable matrixes. *Anal Chem* 72:3826–3832

Rubio F, Veldhuis LJ, Clegg BS et al (2003) Comparison of a direct ELISA and an HPLC method for glyphosate determinations in water. *J Agric Food Chem* 51:691–696

Rueppel ML, Brightwell BB, Schaefer J, Marvel JT (1977) Metabolism and degradation of glyphosate in soil and water. *J Agric Food Chem* 25:517–528

Rull RP (2004) Neural tube defects and maternal residential proximity to agricultural pesticide applications and crops. *Am J Epidemiol* 163:743–753

Sadi B, Vonderheide AP, Caruso JA (2004) Analysis of phosphorus herbicides by ion-pairing reversed-phase liquid chromatography coupled to inductively coupled plasma mass spectrometry with octapole reaction cell. *J Chromatogr A* 1050:95–101

Samsel A, Seneff S (2013a) Glyphosate's suppression of cytochrome P450 enzymes and amino acid biosynthesis by the gut microbiome: pathways to modern diseases. *Entropy* 15:1416–1463

Samsel A, Seneff S (2013b) Glyphosate, pathways to modern diseases II: celiac sprue and gluten intolerance. *Interdiscip Toxicol* 6:159–184

Sanchís J, Kantiani L, Llorca M et al (2012) Determination of glyphosate in groundwater samples using an ultrasensitive immunoassay and confirmation by on-line solid-phase extraction followed by liquid chromatography coupled to tandem mass spectrometry. *Anal Bioanal Chem* 402:2335–2345

Sancho JV, Hernández F, López FJ et al (1996) Rapid determination of glufosinate, glyphosate and aminomethylphosphonic acid in environmental water samples using precolumn fluorogenic labeling and coupled-column liquid chromatography. *J Chromatogr A* 737:75–83

Sato K, Jin JY, Takeuchi T et al (2001) Integrated pulsed amperometric detection of glufosinate, bialaphos and glyphosate at gold electrodes in anion-exchange chromatography. *J Chromatogr A* 919:313–320

Sato M, Yamashita A, Kikuchi M et al (2009) Simultaneous analysis of phosphorus-containing amino acid type herbicides and their metabolites in human samples using *N*-acetyl, *O*-methyl derivatives by LC/MS. *Jpn J Forensic Sci Tech* 14:35–43

Schafer H, Hettler H, Fritsche U et al (1994) Biotests using unicellular algae and ciliates for predicting long-term effects of toxicants. *Ecotoxicol Environ Saf* 27:64–81

Schrübbers LC, Masís-Mora M, Rojas EC et al (2016) Analysis of glyphosate and aminomethylphosphonic acid in leaves from *Coffea arabica* using high performance liquid chromatography with quadrupole mass spectrometry detection. *Talanta* 146:609–620

Schuetz J (1998) Environmental fate of glyphosate. Published by Environmental Monitoring & Pest Management. Department of Pesticide Regulation Sacramento, California ISSN 95824–95624

Scribner EA, Battaglin WA, Gilliom RJ, Meyer MT (2007) Concentrations of glyphosate, its degradation product, aminomethylphosphonic acid, and glufosinate in ground-and surface-water, rainfall, and soil samples collected in the United States, 2001–06. Geological Survey (US). <https://pubs.usgs.gov/sir/2007/5122/pdf/SIR2007-5122.pdf>

See HH, Hauser PC, Ibrahim WAW, Sanagi MM (2010) Rapid and direct determination of glyphosate, glufosinate, and aminophosphonic acid by online preconcentration CE with contactless conductivity detection. *Electrophoresis* 31:575–582

Seneff S, Swanson N, Li C (2015) Aluminum and glyphosate can synergistically induce pineal gland pathology: connection to gut dysbiosis and neurological disease. *Agric Sci China* 6:42

Shao CY, Howe CJ, Porter AJR, Glover LA (2002) Novel cyanobacterial biosensor for detection of herbicides. *Appl Environ Micro- biol* 68(10):5026–5033

Sharma DK, Gupta A, Kashyap R, Kumar N (2012) Spectrophotometric method for the determination of Glyphosate in relation to its environmental and toxicological analysis. Arch Environ Sci 6:42–49

Shehata AA, Schrödl W, Aldin AA et al (2013) The effect of glyphosate on potential pathogens and beneficial members of poultry microbiota in vitro. Curr Microbiol 66:350–358

Shim YK, Mlynarek SP, van Wijngaarden E (2009) Parental exposure to pesticides and childhood brain cancer: U.S. Atlantic coast childhood brain cancer study. Environ Health Perspect 117:1002–1006

Si YB, Sang ZY, Cheng FX et al (2009) Determination of glyphosate in soil by high performance liquid chromatography after derivatization with *p*-toluenesulphonyl chloride. J Anhui Agric Univ 36:136–139

Sierra EV, Méndez MA, Sarria VM, Cortés MT (2008) Electro-oxidación de glifosato sobre electrodos de níquel y cobre. Quim Nova 31:220–226

Simonetti E, Cartaud G, Quinn RM et al (2015) An interlaboratory comparative study on the quantitative determination of glyphosate at low levels in wheat flour. J AOAC Int 98:1760–1768

Singh BK (1998) Plant amino acids: biochemistry and biotechnology. CRC Press, Boca Raton Skeff W, Recknagel C, Schulz-Bull DE (2016) The influence of salt matrices on the reversed-phase liquid chromatography behavior and electrospray ionization tandem mass spectrometry detection of glyphosate, glufosinate, aminomethylphosphonic acid and 2-aminoethylphosphonic acid in water. J Chromatogr A 1475:64–73

Slager RE, Simpson SL, Levan TD et al (2010) Rhinitis associated with pesticide use among private pesticide applicators in the agricultural health study. J Toxicol Environ Health A 73:1382–1393

Songa EA, Waryo T, Jahed N et al (2009a) Electrochemical nanobiosensor for glyphosate herbicide and its metabolite. Electroanalysis 21:671–674

Songa EA, Arotiba OA, Owino JHO et al (2009b) Electrochemical detection of glyphosate herbicide using horseradish peroxidase immobilized on sulfonated polymer matrix. *Bioelectrochemistry* 75:117–123

Songa EA, Somerset VS, Waryo T, Baker PG, Iwuoha EI (2009c) Amperometric nanobiosensor for quantitative determination of glyphosate and glufosinate residues in corn samples. *J Macromol Sci Part A Pure Appl Chem* 81:123–139

Stachowskihaberkorn S, Becker B, Marie D et al (2008) Impact of Roundup on the marine microbial community, as shown by an in-situ microcosm experiment. *Aquat Toxicol* 89:232–241

Sun N, Hu B-X, Mo W-M (2007) Single sweep oscillopolarographic technique for the determination of glyphosate after derivatization with sodium nitrite. *PESTICIDES-SHENYANG* 46:609

Sun L, Kong D, Gu W et al (2017) Determination of glyphosate in soil/sludge by high performance liquid chromatography. *J Chromatogr A* 1502:8–13

Szarek J, Siwicki A, Andrzejewska A et al (2000) Effects of the herbicide Roundup<sup>TM</sup> on the ultrastructural pattern of hepatocytes in carp (*Cyprinus carpio*). *Mar Environ Res* 50:263–266

Tadeo JL, Sánchez-Brunete C, Pérez RA, Fernández MD (2000) Analysis of herbicide residues in cereals, fruits and vegetables. *J Chromatogr A* 882:175–191

Tan MJ, Hong Z-Y, Chang M-H et al (2017) Metal carbonyl-gold nanoparticle conjugates for highly sensitive SERS detection of organophosphorus pesticides. *Biosens Bioelectron* 96:167–172

Tapsoba I, Paré S, Toé AM et al (2012) SWV determination of glyphosate in Burkina Faso soils using carbon fiber microelectrode. *Int J Biol Chem Sci* 6:2211–2220



Teófilo RF, Reis EL, Reis C et al (2004) Experimental design employed to square wave voltammetry response optimization for the glyphosate determination. J Braz Chem Soc 15:865–871

Thompson DG, Cowell JE, Daniels RJ et al (1989) Liquid chromatographic method for quantitation of glyphosate and metabolite residues in organic and mineral soils, stream sediments, and hardwood foliage. J Assoc Off Anal Chem 72:355–360

Thongprakaisang S, Thiantanawat A, Rangkadilok N et al (2013) Glyphosate induces human breast cancer cells growth via estrogen receptors. Food Chem Toxicol 59:129–136

Tierney KB, Singh CR, Ross PS, Kennedy CJ (2007) Relating olfactory neurotoxicity to altered olfactory-mediated behaviors in rainbow trout exposed to three currently-used pesticides. Aquat Toxicol 81:55–64

Torul H, Boyaci İH, Tamer U (2010) Attomole detection of glyphosate by surface-enhanced Raman spectroscopy using gold nanorods. FABAD J Pharm Sci 35:179–184

Tsao Y-C, Lai Y-C, Liu H-C et al (2016) Simultaneous determination and quantitation of paraquat, diquat, glufosinate and glyphosate in postmortem blood and urine by LC–MS–MS. J Anal Toxicol 40:427–436

Tseng S-H, Lo Y-W, Chang P-C et al (2004) Simultaneous quantification of glyphosate, glufosinate, and their major metabolites in rice and soybean sprouts by gas chromatography with pulsed flame photometric detector. J Agric Food Chem 52:4057–4063

Tsui MTK, Chu LM (2003) Aquatic toxicity of glyphosate-based formulations: comparison between different organisms and the effects of environmental factors. Chemosphere 52:1189–1197

Tsui MTK, Chu LM (2008) Environmental fate and non-target impact of glyphosate-based herbicide (Roundup®) in a subtropical wet- land. *Chemosphere* 71:439–446

Tsui MTK, Wang W-X, Chu LM (2005) Influence of glyphosate and its formulation (Roundup®) on the toxicity and bioavailability of metals to *Ceriodaphnia dubia*. *Environ Pollut* 138:59–68

Tsunoda N (1993) Simultaneous determination of the herbicides glyphosate, glufosinate and bialaphos and their metabolites by capillary gas chromatography—ion-trap mass spectrometry. *J Chromatogr A* 637:167–173

Tuesca D, Puricelli E (2007) Effect of tillage systems and herbicide treatments on weed abundance and diversity in a glyphosate resistant crop rotation. *Crop Prot* 26:1765–1770

Vass A, Robles-Molina J, Pérez-Ortega P et al (2016) Study of different HILIC, mixed-mode, and other aqueous normal-phase approaches for the liquid chromatography/mass spectrometry- based determination of challenging polar pesticides. *Anal Bio- anal Chem* 408:4857–4869

Vreeken RJ, Speksnijder P, Bobeldijk-Pastorova I, Noij TH (1998) Selective analysis of the herbicides glyphosate and aminomethylphosphonic acid in water by on-line solid-phase extraction– high-performance liquid chromatography–electrospray ionization mass spectrometry. *J Chromatogr A* 794:187–199

Waiman CV, Avena MJ, Garrido M et al (2012) A simple and rapid spectrophotometric method to quantify the herbicide glyphosate in aqueous media. Application to adsorption isotherms on soils and goethite. *Geoderma* 170:154–158

Wang D, Lin B, Cao Y et al (2016a) A highly selective and sensitive fluorescence detection method of glyphosate based on an immune reaction strategy of carbon dot labeled antibody and antigen magnetic beads. *J Agric Food Chem* 64:6042–6050

Wang S, Liu B, Yuan D, Ma J (2016b) A simple method for the determination of glyphosate and aminomethylphosphonic acid in sea- water matrix with high performance liquid chromatography and fluorescence detection. *Talanta* 161:700–706

Wang L, Bi Y, Hou J et al (2016c) Facile, green and clean one-step synthesis of carbon dots from wool: application as a sensor for glyphosate detection based on the inner filter effect. *Talanta* 160:268–275

Wang M, Ye H, You L, Chen X (2016d) A supramolecular sensor array using lanthanide-doped nanoparticles for sensitive detection of glyphosate and proteins. *ACS Appl Mater Interfaces* 8:574–581

Watts M (2009) Glyphosate, monograph, Pesticide Action Network Asia and the Pacific, Penang, Malaysia. Available via PAN ASIA PACIFIC. [http://www.panap.net/sites/default/files/attachments/monograph\\_glyphosate.pdf](http://www.panap.net/sites/default/files/attachments/monograph_glyphosate.pdf). Accessed 13 March 16

Wei X, Pu Q (2015) Microchip electrophoresis for fast and interference-free determination of trace amounts of glyphosate and glufosinate residues in agricultural products. *Methods Mol Biol* 1274:21–29

Wei X, Gao X, Zhao L et al (2013) Fast and interference-free determination of glyphosate and glufosinate residues through electrophoresis in disposable microfluidic chips. *J Chromatogr A* 1281:148–154

Williams GM, Kroes R, Munro IC (2000) Safety evaluation and risk assessment of the herbicide Roundup and its active ingredient, glyphosate, for humans. *Regul Toxicol Pharmacol* 31:117–165

Winfield TW (1990) Determination of glyphosate in drinking water by direct-aqueous-injection HPLC, post-column derivatization, and fluorescence detection: test method 547. U.S. Environmental Protection Agency. <https://www.o2si.com/docs/epa-method-547.pdf>

Woodburn AT (2000) Glyphosate: production, pricing and use world- wide. Pest Manag Sci 56:309–312

World Health Organization et al (1994) Glyphosate environmental health criteria no. 159. WHO, Geneva

Yoshioka N, Asano M, Kuse A et al (2011) Rapid determination of glyphosate, glufosinate, bialaphos, and their major metabolites in serum by liquid chromatography–tandem mass spectrometry using hydrophilic interaction chromatography. J Chromatogr A 1218:3675–3680

Zelenkova NF, Vinokurova NG (2008) Determination of glyphosate and its biodegradation products by chromatographic methods. J Anal Chem 63:871–874

Zhang C, Hu X, Luo J et al (2015a) Degradation dynamics of glyphosate in different types of citrus orchard soils in China. Molecules 20:1161–1175

Zhang L, Chen L, Liu F (2015b) Mutual effect on determination of gibberellins and glyphosate in groundwater by spectrophotometry. Guang Pu Xue Yu Guang Pu Fen Xi 35:966–970

Zhao P, Yan M, Zhang C et al (2011) Determination of glyphosate in foodstuff by one novel chemiluminescence-molecular imprinting sensor. Spectrochim Acta A Mol Biomol Spectrosc 78:1482–1486

Zheng J, Zhang H, Qu J et al (2013) Visual detection of glyphosate in environmental water samples using cysteamine-stabilized gold nanoparticles as colorimetric probe. Anal Methods 5:917–924

Zheng J, Wang Y, Feng Z et al (2015) Preparation of cationic starch microspheres and study on their absorption to anionic-type substance. Water Sci Technol 71:1545–1553

Zhou Y-M, Li N, Niu S et al (2007) Detection glyphosate residues in water by LC. China Meas Technol 3:036

Zhu Y, Zhang F, Tong C, Liu W (1999) Determination of glyphosate by ion chromatography. J Chromatogr A 850:297–301

## CAPÍTULO II

### Glyphosate:ZnO Nanocrystal Interaction Controlled by pH Changes

Journal: The Journal of Physical Chemistry Letters  
Manuscript ID: jz 2019-02640y  
Manuscript Status: Submitted

## Glyphosate:ZnO Nanocrystal Complexes Controlled by pH Changes

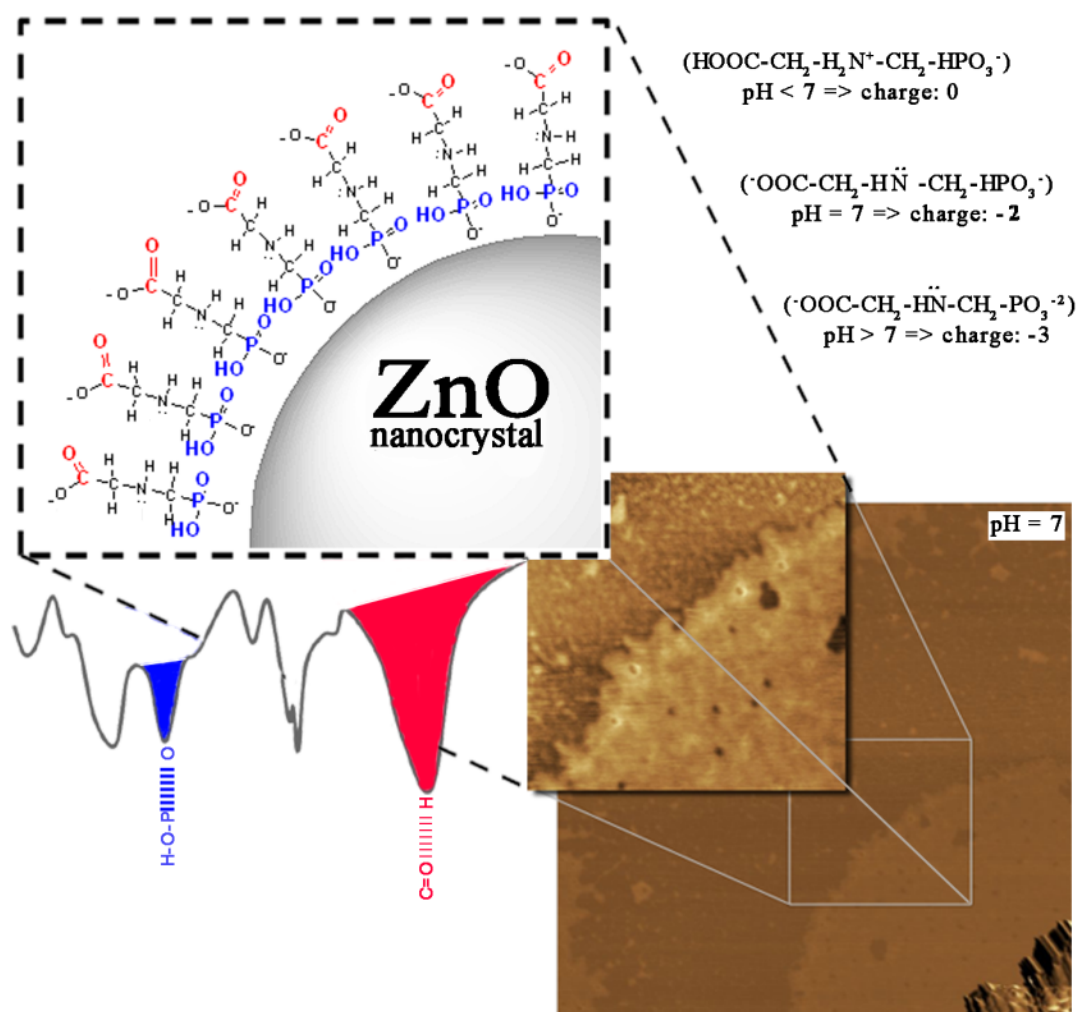
Anderson L. Valle<sup>a</sup>, Anielle C. A. Silva<sup>b</sup>, Francielli, C. C. Melo<sup>a</sup>, Guilherme de L. Fernandes<sup>b</sup>, Guedmiller S. Oliveira<sup>c</sup>, Luciano P. Rodrigues<sup>d\*</sup>, Luiz R. Goulart<sup>a\*</sup>

<sup>a</sup> Laboratory of Nanobiotechnology, Institute of Biotechnology, Federal University of Uberlândia, Uberlândia, MG, Brazil.

<sup>b</sup> Laboratory of New Nanostructured and Functional Materials, Institute of Physics, Federal University of Alagoas, Maceió, AL, Brazil.

<sup>c</sup> Institute of Chemistry, Federal University of Uberlândia, Uberlândia, MG, Brazil.

<sup>d</sup> Institute of Engineering, Science and Technology, Federal University of Jequitinhonha and Mucuri's Valleys, Janaúba, MG, Brazil.



*Graphical Abstract - Schematic representation of glyphosate molecules arrangement around ZnO nanocrystal according to infrared spectroscopy and AFM/SEM images evidence.*

## ABSTRACT

The interaction of the herbicide glyphosate with ZnO nanocrystals (NCs) was studied by FTIR under controlled pH conditions, supported by SEM and AFM images. Our previous studies showed that at low concentrations, glyphosate is undetectable in the FTIR spectra. However, under the mixture with ZnO NCs, FTIR signals were significantly amplified. Here we have shown that this NC-glyphosate complex was strong, but under pH modifications, its structural assembly suffered specific conformational changes. Such alterations were evidenced by intense vibrational energy transfer raised from carbon backbone, phosphonic, and carboxyl groups to CO and OH groups, according to FTIR spectra. We concluded that glyphosate is organized as a mycelium around ZnO NCs at neutral pH, but as the pH varies from acidic to alkaline environment new crystal structures occur, which goes from star-like to volcano-like shapes, respectively, both bound to Glyphosate.

**Keywords:** Glyphosate:ZnO interaction; pH influence, FTIR spectroscopy, AFM, SEM, Zinc Oxide.

## HIGHLIGHTS

- FTIR vibrational modes and AFM/SEM images suggest different structural conformations under variable pH values;
- ZnO nanocrystals interaction with Glyphosate improving its detection in different pH conditions with significant changes in the FTIR vibrational modes;
- ZnO behaves as an FTIR enhancer in glyphosate detection.



## INTRODUCTION

Glyphosate [(N-phosphonomethyl) Glycine] is the most commercialized herbicide worldwide<sup>1</sup>. Its formulation has been dramatically contested in the last century due to provoking glyphosate-resistant crops<sup>2</sup>. Considered “toxicologically harmless” for animals and the environment,<sup>3 4 5</sup> people are debating its potential carcinogenic effects.<sup>6</sup> In 2016, the Environmental Protection Agency (EPA) published a full review in this concern to discuss human safety since glyphosate can accumulate in water<sup>7</sup> causing problems to live beings<sup>8 9 10</sup>.

When applied directly to soils, it shows little herbicidal activity due to inactivation provoked by adsorption<sup>11 12</sup>. This adsorption to the various cation-saturated bentonite clays increases as follows:  $\text{Al}^{+3} > \text{Fe}^{+3} > \text{Mg}^{+2} > \text{Zn}^{+2} > \text{Mn}^{+2} > \text{Ca}^{+2}$ <sup>12</sup>. In fact, most agricultural soils contain Zn ( $10\text{--}300 \text{ mg kg}^{-1}$ )<sup>13</sup>, and the presence of glyphosate can have a significant effect on Zn availability<sup>14</sup>.

The glyphosate molecular ability to coordinate has been investigated by several research groups, which includes the mechanism: the tendency of transitions among trivalent and divalent metal ions<sup>15 16 17</sup>, chelation with metals in solution<sup>18</sup>, and polyvalent cations in interlayer of montmorillonite<sup>19</sup>. DFT molecular modeling methods showed that there is a stability order for tetrahedral and octahedral complexes between metals and glyphosate as  $\text{Zn} > \text{Cu} > \text{Co} > \text{Fe} > \text{Cr} > \text{Al} > \text{Ca} > \text{Mg}$ <sup>21</sup>, what means that ZnO nanocrystals (NCs) are a promising photocatalyst, too<sup>22</sup>.

The first description of Fourier transforms infrared spectroscopy (FTIR) spectra modifications caused by glyphosate pH-induced variations were observed in 1981<sup>19</sup> and in 1993<sup>20</sup>. They verify glyphosate structures vibrating modes between  $916 \text{ cm}^{-1}$  and  $1732 \text{ cm}^{-1}$ . Glyphosate forms weak acid due to its three dissociation constants at the  $\text{pK}_{\text{a}1}$  2.27-2.35,  $\text{pK}_{\text{a}2}$  5.58-5.89 and  $\text{pK}_{\text{a}3}$  10.25-10.89 assuming four forms while the pH enhanced losing  $\text{H}^+$  follow the sequence  $\text{COOH}$ ,  $\text{PO}_3$ ,  $\text{NH}_2$ <sup>12 23</sup>. According to this theory, metallic complexes along with glyphosate were proposed<sup>24 25</sup>. An alternative theory where the amino group should be the

last to be protonated and the complexation should occur first on the COOH group, then on  $\text{NH}_2$  and finishing on  $\text{H}_2\text{PO}_3$  <sup>26</sup> .

Considering the high glyphosate's capacity to adsorb strongly on clay minerals <sup>27</sup> and organic or mineral particles <sup>28 29</sup> and its high affinity to metal cations, it is hard to detect this herbicide without pretreatment methods <sup>30</sup>. In order to supply such information, we have investigated mechanisms related to glyphosate-ZnO nanocrystals (NCs) complexes using Fourier transform infrared spectroscopy (FTIR), scanning electron microscope (SEM) and atomic force microscopy (AFM) techniques. Our study supports the alternative and most recent theory.

## MATERIAL AND METHODS

### Synthesis and Characterization of ZnO Nanocrystals

The ZnO NCs were synthesized based on the procedure of the references <sup>31 32 33</sup>. Structural properties were investigated using X-ray diffraction (XRD) (DRX-6000, Shimadzu) with monochromatic radiation Cu-K $\alpha_1$  ( $\lambda = 1.54056 \text{ \AA}$ ).

### Glyphotal TR<sup>®</sup> with ZnO Nanocrystals Solution

Glyphotal TR<sup>®</sup> is formed by Isopropylammonium salt of Glyphosate 648 g/L (64% m/v), N-(phosphonomethyl) Glycine acid equivalent: 480 g/L (48% m/v), and other ingredients: 721 g/L (72,10% m/v). Samples were prepared by dilution were the most concentrated solution was Glyphotal TR<sup>®</sup> [ $10^{-2}$  v/v] (which is usually used for soil for applications), which means that each volume unit of Glyphotal TR<sup>®</sup> was diluted in 99 parts of ultrapure water. ZnO NCs was always diluted at 1 $\mu$ g/100 $\mu$ L and add in this concentration at each Glyphotal TR<sup>®</sup> dilution. We used H<sub>2</sub>SO<sub>4</sub> and NaOH to perform pH changes.

### Fourier transform infrared spectroscopy (FTIR)

FTIR spectra of samples were recorded in the 4000-400 cm<sup>-1</sup> region using infrared spectrophotometer (Vertex 70, Bruker Optik) with a micro-attenuated total reflectance (ATR) accessory. The crystal material unit in the ATR unit was a diamond disc as an internal-reflection element. The sample penetration depth ranges between 0.1 and 2  $\mu$ m. Two  $\mu$ L of samples were dropped with a triple dental syringe to obtain FTIR spectra. The spectrum of air was used as a background in FTIR analysis. The samples spectrum was taken with 2 cm<sup>-1</sup> of resolution and 34 scans were performed to sample analysis.

### Scanning Electron Microscope (SEM)

The SEM images were performed using the electronic microscope (Carl Zeiss EVO MA10) with Energy Dispersive Spectroscopy (EDS) (Oxford

Instruments SDD detector) for investigated the compositional analyses by INCA analysis software. The SEM images were performed above a carbon attached to double-stick tape on aluminum stubs and coated with gold in a sputter coating apparatus in order to be viewed under the SEM and get information about how pH influence the dispersion of the ZnO NCs when interacting with glyphosate. We use 200  $\mu\text{L}$  of post-dried Glyphosate-ZnO [ $10^{-4}$  v/v] solution as the table below:

Table 1. Glyphosate-ZnO's proportions used to define the pH.

ZnO NCs (1 mg/mL)	Glyphosate ( $10^{-4}$ v/v)	H <sub>2</sub> SO <sub>4</sub> ( $\mu\text{L}$ )	NaOH ( $\mu\text{L}$ )	pH
10 $\mu\text{L}$	300 $\mu\text{L}$	18	0	0-1
20 $\mu\text{L}$	600 $\mu\text{L}$	4	0	3-4
10 $\mu\text{L}$	300 $\mu\text{L}$	0	0	6-7
30 $\mu\text{L}$	900 $\mu\text{L}$	0	1	9
10 $\mu\text{L}$	300 $\mu\text{L}$	0	10	13-14

#### Atomic Force Microscopy (AFM)

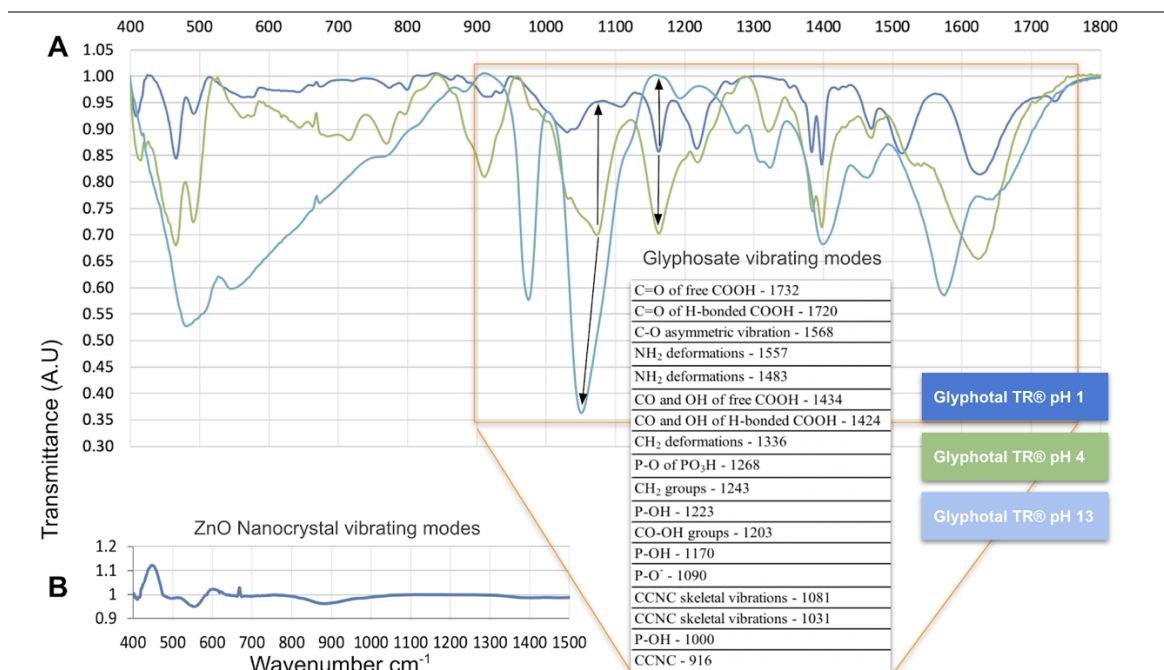
The AFM images were performed to view the possible interaction of glyphosate with ZnO NCs. To evaluate the formed complex we dropped 3  $\mu\text{L}$  of Glyphotal TR<sup>®</sup>-ZnO in ultrapure water [ $10^{-4}$  v/v] solution at a mica sheet and submitted it to the atomic force microscopy (Spm 9600, Shimadzu), a very-high-resolution scanning probe microscopy <sup>34</sup>. The control groups were the mica sheet and the nanofilm done by the Glyphotal TR<sup>®</sup> when overlapped the sheet.

## RESULTS AND DISCUSSION

### The pH effect on Glyphosate FTIR spectra

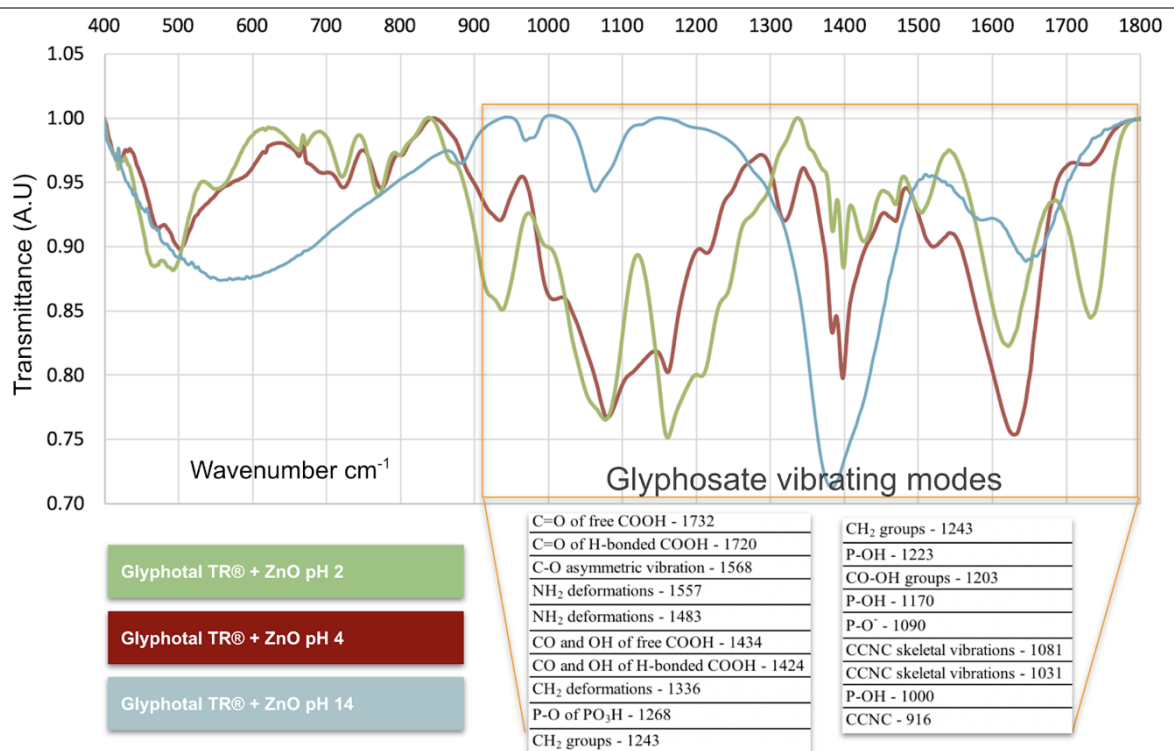
Some authors stated that the adsorption of this herbicide on soil and clay is not strongly dependent on pH <sup>12 35</sup> where the first stated it for pH ideally between 3.8 to 8.1, and the second from 4 to 6.5. However, others had concluded that increases in pH decrease the adsorption of Glyphosate <sup>36 37 38 39 40 41 42 43 44 45</sup>. We support these authors.

Glyphotal TR® and ZnO NCs (not solvated) were exploited in three different pH conditions using FTIR spectra as shown in Figure 1 and 2. ZnO IR absorption bands appear between 400 and 600 cm<sup>-1</sup>, corresponding to the Zn-O vibration mode <sup>46 47</sup>. For glyphosate, it was observed that some bands, e.g. 1170 cm<sup>-1</sup> reduce as the pH increases while the band at 1090 cm<sup>-1</sup> was concomitantly enhanced and dislocated when changes in pH occur. Normally, glyphosate has vibrational bands corresponding to  $\nu_s(\text{C-O})$ ,  $\nu_a(\text{P-OH})$  (antisymmetric and symmetric) vibration modes, respectively <sup>39</sup>. However, pH conditions change its protonation state, resulting in different vibrational modes, which undergo increments of intensity. In this way, ZnO Nanocrystal vibrating modes do not coincide with Glyphosate ones. Once glyphosate acts as a stronger buffer agent, it is very hard to reach an exact pH, so, we accept up to 0.5 difference between samples since it maintains the same protonated status.



**Chapter II, Figure 1. FTIR spectra of Glyphotal TR® in three different pH (A) and ZnO nanocrystals (B), all in ultrapure water [ $10^{-2}$  v/v]. The area highlighted in the spectrum corresponds to vibrational modes and chemical bonds of glyphosate spectra.**

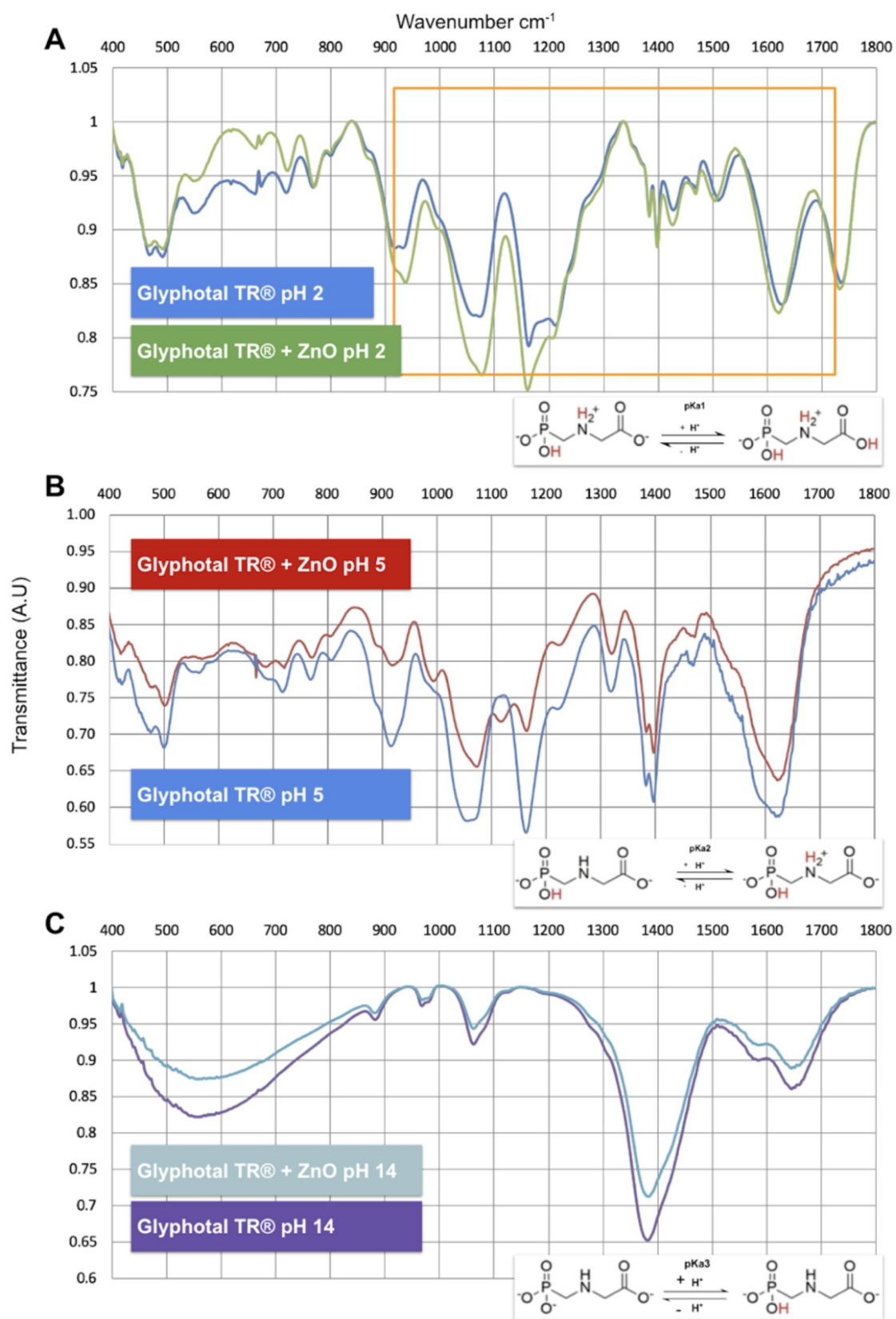
ZnO Nanocrystals formed a stronger interaction with Glyphosate at approximately 24 hours. Figure 2 compares the changes in vibrating modes of the Glyphosate- ZnO Nc in three different pH conditions.



**Chapter II, Figure 2. FTIR spectra of Glyphotal TR® when interacting with ZnO in three different pH, all in ultrapure water [ $10^{-2}$  v/v]. The area highlighted in the spectrum corresponds to vibrational modes and chemical bonds of glyphosate spectra.**

FTIR spectra changes under different pH on Glyphosate-ZnO Nanocrystals

Vibrational modes of Glyphosate and ZnO-Glyphosate complexes were compared under three different pH conditions (Figure 3), which allowed us to differentiate and detect all Glyphotal TR® with ZnO Nc.




Chapter II, Figure 3. Glyphotal TR® and Glyphosate-ZnO [10-2 v/v] spectra in 3 different pH.



The Heat Map that compares the strength of vibrational modes among groups is presented in Figure 4. Our Hypothesis is that the smaller the transmittance the more energy is absorbed in the structure, hence the interaction with other molecules becomes weaker. FTIR measures the amount of radiation a sample absorbs in each wavelength. Therefore, if a sample absorbs energy, the transmittance decreases. So, transmittance is the amount of energy which not is being absorbed after the laser reach a sample. In this way, each Glyphosate vibrational mode was compared with the same corresponding mode when interacts with ZnO NCs. We have normalized the spectral curve in relation to the vibrational mode with the smallest transmittance mode of each group, which are P-OH - 1170  $\text{cm}^{-1}$  at pH 2 and pH 5, and C-OH - 1424  $\text{cm}^{-1}$  at pH 14. Ratio represents the relation of transmittance of vibrational modes of the Glyphosate-ZnO NCs interaction with vibrational modes of Glyphosate alone.

	Glyphosate (pH 14)		Glyphosate (pH 5)		Glyphosate (pH 2)		RATIO		
	Without ZnO	With ZnO	Without ZnO	With ZnO	Without ZnO	With ZnO	ZnO/Gly (pH14)	ZnO/Gly (pH5)	ZnO/Gly (pH 2)
CO and OH of H-bonded COOH - 1424	1.000	1.000	0.866	0.929	0.876	0.848	1.000	1.072	0.969
CO and OH of free COOH - 1434	0.963	0.971	0.861	0.916	0.873	0.842	1.008	1.064	0.965
C-O asymmetric vibration - 1568	0.811	0.837	0.952	0.946	0.849	0.816	1.032	0.994	0.962
C=O of H-bonded COOH - 1720	0.763	0.799	0.805	0.860	0.921	0.887	1.047	1.068	0.964
C=O of free COOH - 1732	0.754	0.792	0.801	0.860	0.944	0.909	1.049	1.074	0.962
CO, OH groups - 1203	0.743	0.782	0.884	0.923	0.987	0.960	1.052	1.044	0.973
P-OH - 1170	0.738	0.777	1.000	1.000	1.000	1.000	1.054	1.000	1.000
P-OH - 1223	0.746	0.785	0.880	0.918	0.973	0.920	1.052	1.043	0.946
P-OH - 1000	0.734	0.774	0.839	0.962	0.886	0.853	1.055	1.146	0.963
P-O <sup>-</sup> - 1090	0.771	0.803	0.922	1.067	0.943	0.974	1.041	1.157	1.034
P-O of PO <sub>3</sub> H - 1268	0.770	0.803	0.814	0.860	0.868	0.833	1.043	1.056	0.960
CH <sub>2</sub> groups - 1243	0.752	0.790	0.847	0.883	0.923	0.887	1.049	1.042	0.961
CH <sub>2</sub> deformations - 1336	0.876	0.888	0.836	0.875	0.806	0.768	1.014	1.047	0.953
NH <sub>2</sub> deformations - 1557	0.800	0.827	0.922	0.922	0.836	0.800	1.035	1.000	0.956
NH <sub>2</sub> deformations - 1483	0.804	0.836	0.836	0.877	0.837	0.806	1.040	1.049	0.963
CCNC skeletal vibrations - 1081	0.782	0.810	0.975	1.081	0.975	1.000	1.036	1.108	1.026
CCNC skeletal vibrations - 1031	0.743	0.781	0.931	0.975	0.937	0.923	1.051	1.047	0.985
CCNC - 916	0.742	0.781	0.893	0.891	0.912	0.886	1.053	0.997	0.972

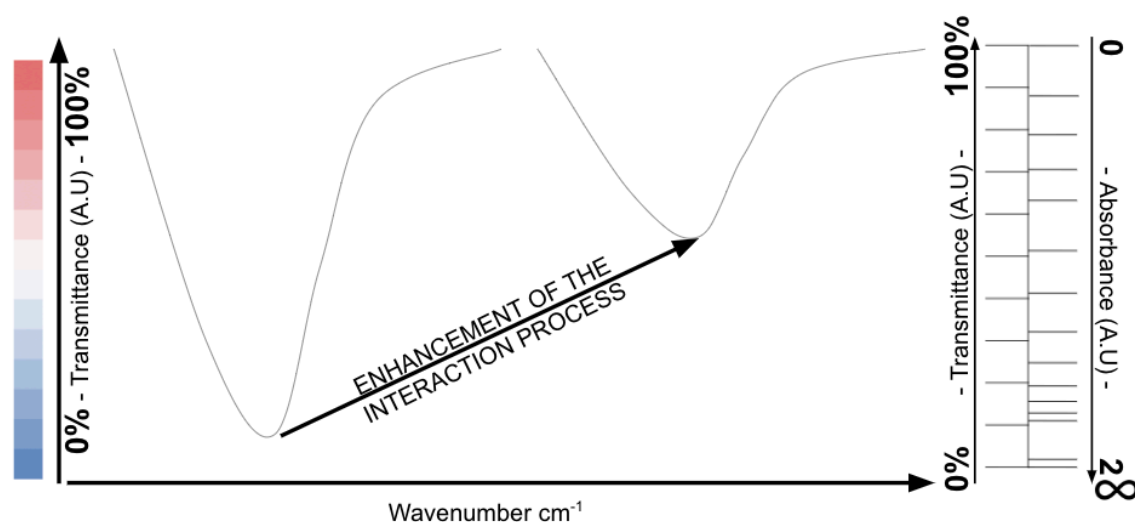
VERY REACTIVE  LITTLE REACTIVE

If: Ratio = 1, No observed changes; Ratio > 1, Movement loss; Ratio < 1, Movement gain

**Chapter II, Figure 4 Heat map of the transmittance's vibrations modes energy of Glyphosate [ $10^{-2}$  v/v] and Glyphosate-ZnO [ $10^{-2}$  v/v] interaction after spectra normalization. Ratio represents the relation between Glyphosate-ZnO and Glyphosate by pH evidencing the freedom and reactive structures in solution. As bluer, as more energy, as less interaction with another molecules.**

Once we are analyzing transmittance, if Ratio > 1, Glyphosate mixed with ZnO NCs promotes interaction. Ratio <1 means that before any interaction Glyphosate had greater energetic status on those vibrational modes. This way is

possible to visualize the enhancement for each vibrational mode, which is evidenced by the smaller vibrational modes of the ZnO-Glyphosate interaction in comparison to the glyphosate alone, so this molecular structure is strongly interacting with ZnO NCs. On the other hand, if it absorbs more energy, we can conclude that after interaction this structure is freer than before, as shown in Figure 5. A simple way to understand it is: If after reached by a FTIR laser, a structure have less movement, is because it is interacting strongly with other forces that restrict its movements. This way, to have the same previously vibrating status, a complexed structure, or a structure that is tightly interacting with other should need more energy. Therefore, more transmittance means less vibrational status.



*Chapter II, Figure 5. Schematic representations of the ZnO-Glyphosate interaction process. As transmittance decrease, as more energy was absorbed by the sample. The transmitted energy is detected by FTIR by vibrating mode of the structures. As more bonded as less a structure is able to vibrate. Hence, as bigger the transmittance as bigger interaction.*

However, in solution, Glyphosate molecules are aleatory disposed. FTIR laser do not reach all the molecules with the same intensity, and in the same direction. When Glyphosate interacts with ZnO, in accordance with our hypothesis, the nanocrystal promotes an alignment of the glyphosate's structures. Glyphosate molecules in solution are attracted to the adjacent surface of the NCs which has potential positive Zeta. This alignment makes the vibrational modes of each group be easily detected by FTIR once benefits the sum of each individual vibrational

status. The laser energy that promotes the vibration on a structure in a specific way can promote the same movement in another structure, once it is interlinked. Hence, the vibrating mode of this structure will be easily detected by FTIR. So, it could mean not that a structure is tightly interacting, but the equipment is detecting many structures that are vibrating in a similar way. To avoid this mistake, we use concentrate solution at  $[10^{-2} \text{ v/v}]$ . The chosen by this concentration came from previous analysis where we discovered that in low concentrations glyphosate could be detected by FTIR when interacting with ZnO. The ZnO-NC acting as a SERS-FTIR will be treated in a specific paper.

#### FTIR Glyphosate-ZnO Nanocrystals Spectra at pH 14

In this condition, glyphosate is totally deprotonated. All the vibrating modes loss vibrational energy when Glyphosate interacted with ZnO NCs, even groups that are not directly interacting with ZnO, as the skeletal structure CCNC ( $1081 \text{ cm}^{-1}$  and  $1031 \text{ cm}^{-1}$ ). We suppose that Glyphosate chelating on ZnO tightened by all reactive groups, being parallel to it.

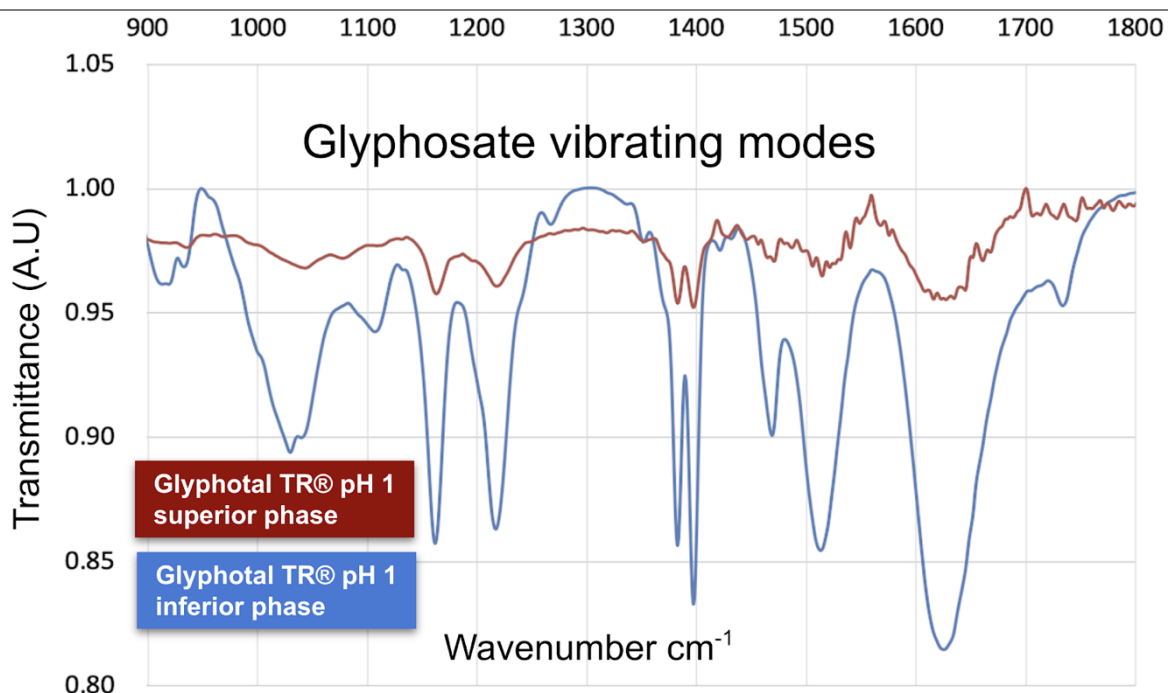
#### FTIR Glyphosate-ZnO Nanocrystals Spectra at pH 5

This is the pH that we can normally find Glyphosate on soils. Here, Glyphosate's phosphonic group  $\text{P-O}^-$  -  $1090 \text{ cm}^{-1}$  and  $\text{P-OH}$  -  $1000 \text{ cm}^{-1}$ , and CCNC skeletal vibrations -  $1081 \text{ cm}^{-1}$  present more vibrational energy than the same structures when interacting with Nanocrystals, and  $\text{P-OH}$  -  $1170 \text{ cm}^{-1}$ , CCNC -  $916 \text{ cm}^{-1}$  and C-O asymmetric vibration -  $1568 \text{ cm}^{-1}$  presents less energy. This is in accord with other studies that had already reported that Glyphosate bindings start on its phosphonic acid moiety <sup>12 23 24 25 26</sup>. In this protonation status, we already found a carboxyl group with evident chemical interaction with ZnO NCs, which restrict its movements. <sup>26</sup> demonstrated that the protonation pathway of glyphosate is performed through successive protonation sites starting from phosphonate oxygen, amino nitrogen, and finally carboxylate oxygen, in agreement with the most recent theoretical work in the literature <sup>48</sup> This theory is important because it confirms that the protonated site of glyphosate in pH range 7–8, is not on the amino but on the phosphonate group instead. We have found

amine group at pH 5 in according to the literature. However, we found the carboxyl group interacting in this pH, what should not be expected in accordance to <sup>26</sup>, unless we consider that <sup>49</sup> cited that if the phosphonic group is protected or bonded to another material, then zinc should bind to the carboxyl and amino groups. This conclusion was gotten studying inhibition mechanisms of Zn precipitation on Aluminum Oxide by Glyphosate. Because of this, the carboxyl vibrating mode is more evident.

#### FTIR Glyphosate-ZnO Nanocrystals Spectra at pH 2

In acid pH glyphosate salt and its components from the commercial formulation precipitated, as a result, a little spectrum was observed in the superior phase as shown in figure 6. However, in the presence of ZnO NCs, we did not see any precipitated, evidencing glyphosate interaction with ZnO NCs even at low pH conditions. Our personal observation that a saturated solution of 10 uL of ZnO NCs (solution 1mg mL<sup>-1</sup>) in 300 uL of Glyphotal TR<sup>®</sup> solubilize immediately with the addition of 4 uL of H<sub>2</sub>SO<sub>4</sub> 95% M.M. 98.07 <sup>26</sup> had already cited that the complex formation of glyphosate with metal cations in aqueous solution could increase the solubility and the mobility of the herbicide leaching it to deep layers and eventually into groundwater. Hence, acid media could speed up this process.



Chapter II, Figure 6. Glyphotal TR® vibrating modes after  $\text{H}_2\text{SO}_4$  addition showing a great concentration of glyphosate in the inferior phase.

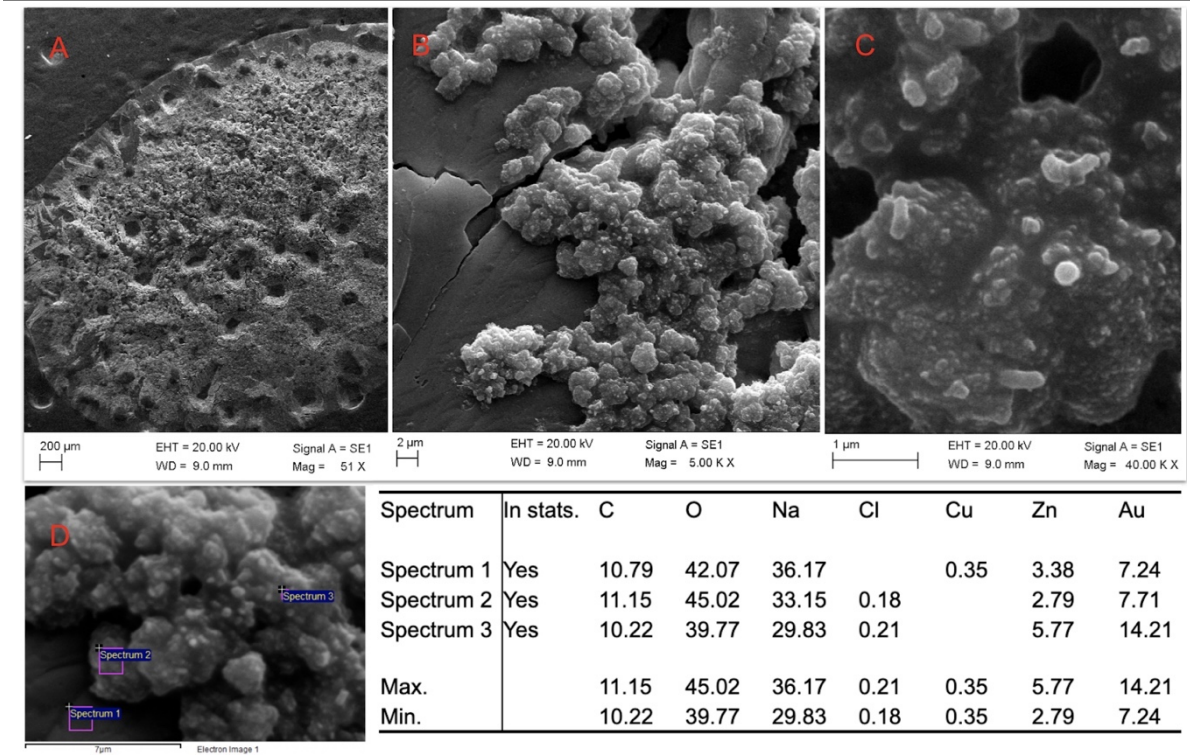
In this condition, glyphosate is totally protonated and just the phosphonic group -  $1090\text{ cm}^{-1}$  is supposed to be bonded on ZnO. The Glyphosate has less affinity to bind with ZnO and this could be evidenced in the figures below.

The micrometric level structure under different pH on Glyphosate-ZnO Nanocrystals

The interactions between Glyphosate and NC was confirmed by Energy-Dispersive X-Ray Spectroscopy (EDS) analysis of the scanning electron microscope (SEM)'s images. Figures 7 - 11 shows that the protonation pathway of glyphosate causes structural changes at a micrometric level where crystalloids forms are reached at more acid pH.

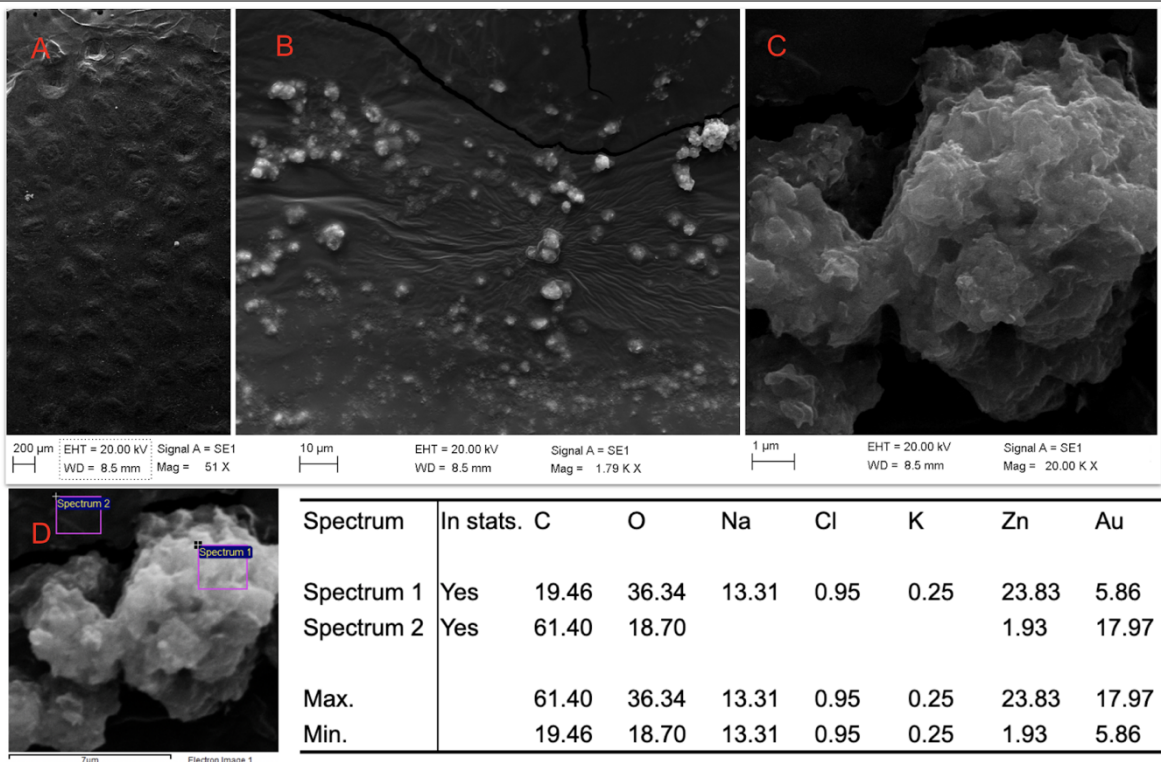
On Figures 7, 8 and 9 we supposed that glyphosate is surrounding bigger units of ZnO NCs interacting itself by charge affinity. The formation of aggregated nanocrystals is justified due to the increase in pH that decreases the repulsion interactions favoring agglomeration and subsequent nanocrystal erosion <sup>50</sup>.

Figure 8 show SEM images came from the supernatant portion of the solution on pH 9, and as you can see, even dispersed NCs are very concentrated on micro scale. The presence of large aggregates and small sizes of ZnO NCs is due to the fact that pH 9 is close to the point of zero charge for ZnO NCs <sup>50</sup>.

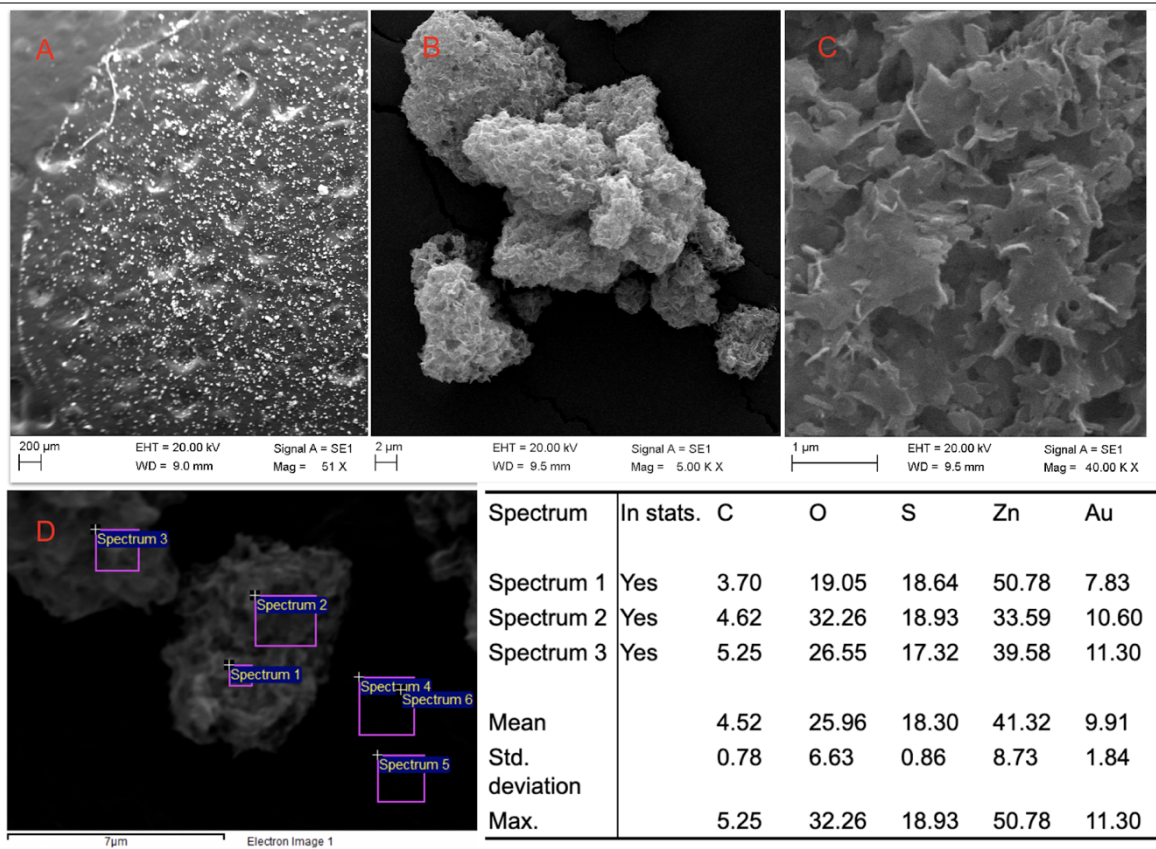


Chapter II, Figure 7. SEM of Glyphotal TR<sup>®</sup>-ZnO [ $10^{-4}$  v/v] at pH 13-14.

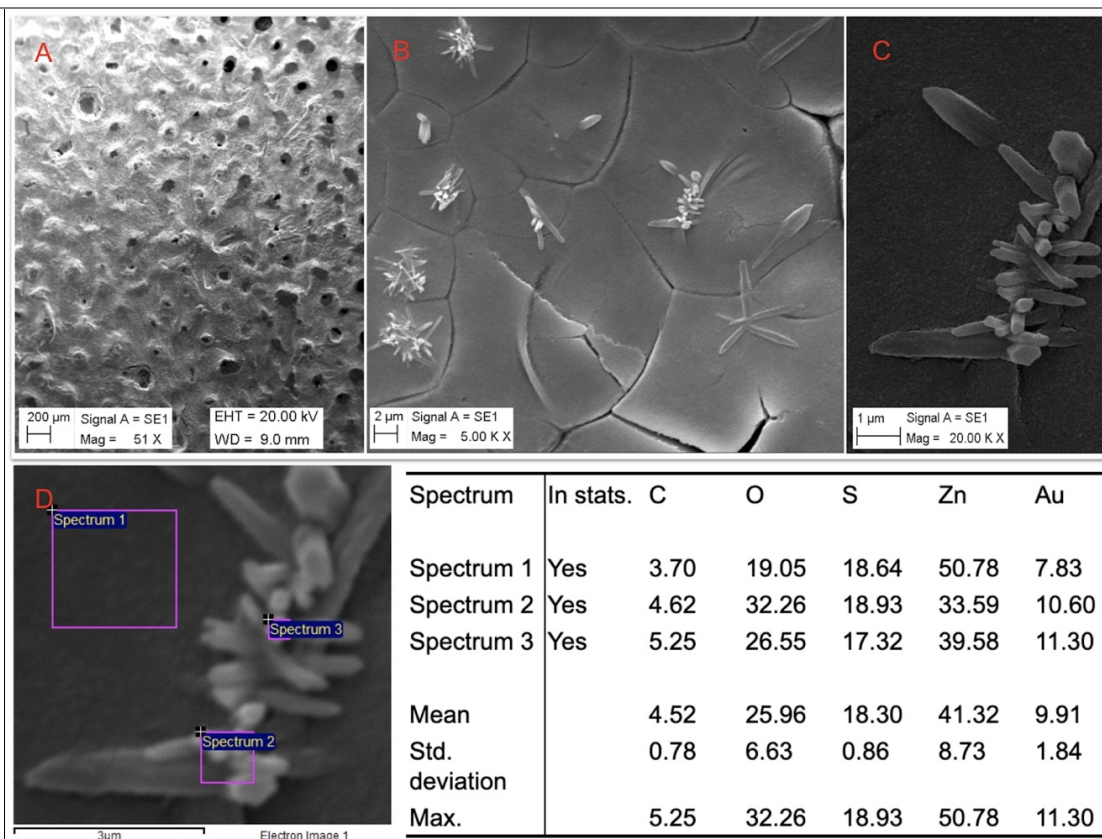




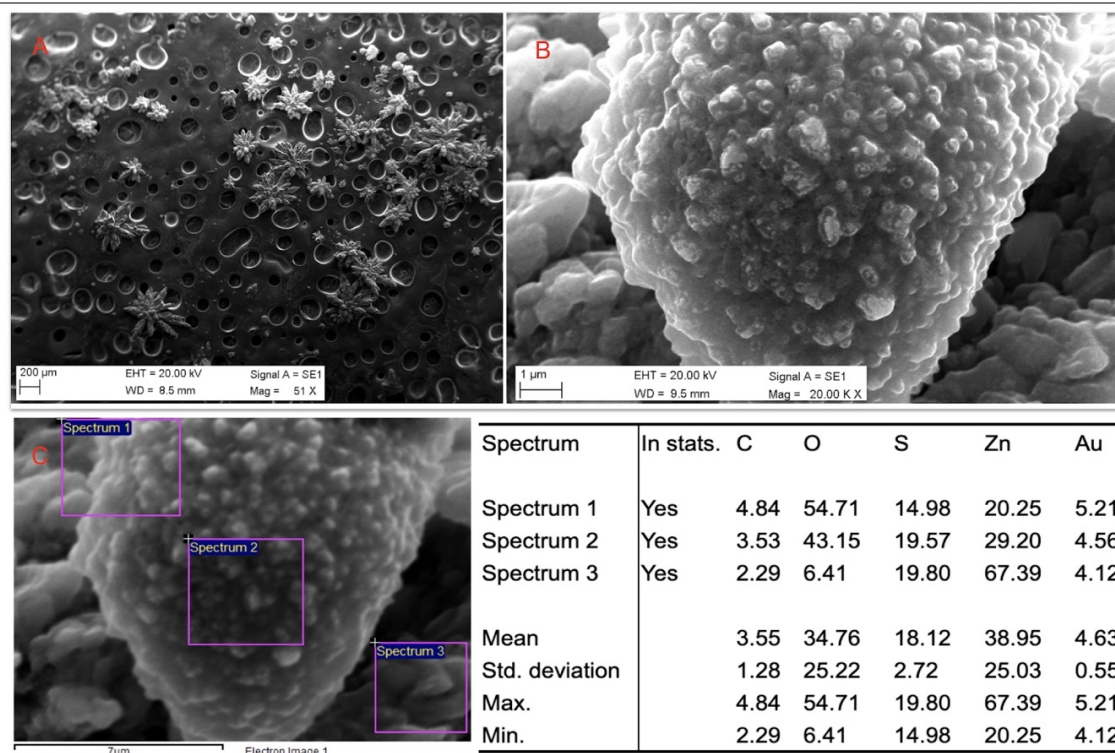
Chapter II, Figure 8. SEM of Glyphotal TR®-ZnO [ $10^{-4}$  v/v] pH 9.



Chapter II, Figure 9. SEM of Glyphotal TR®-ZnO [ $10^{-4}$  v/v] pH 6-7.



Chapter II, Figure 10 SEM of Glyphotal TR®-ZnO [ $10^{-4}$  v/v] pH 3-4.



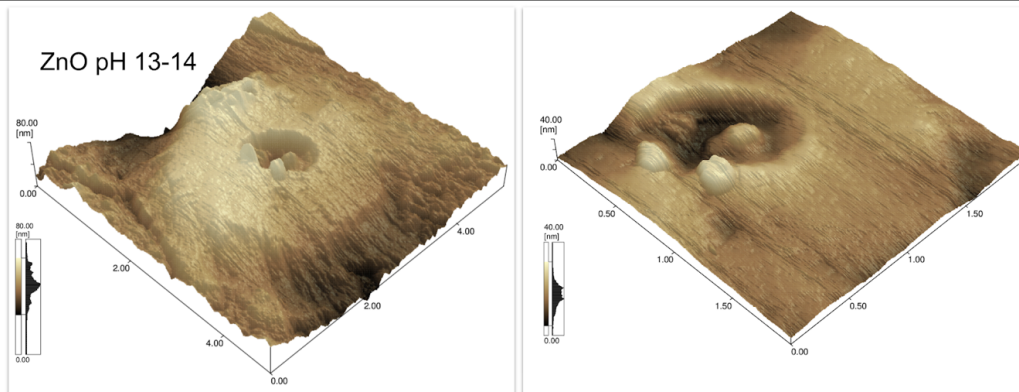
Chapter II, Figure 11. SEM of Glyphotal TR®-ZnO [ $10^{-4}$  v/v] pH 0-1. Like stars ZnO NCs are dispersed on the solution (A). Black holes are imperfections of the carbon tape. The end of a star is represented in (B) containing many ZnO NCs.



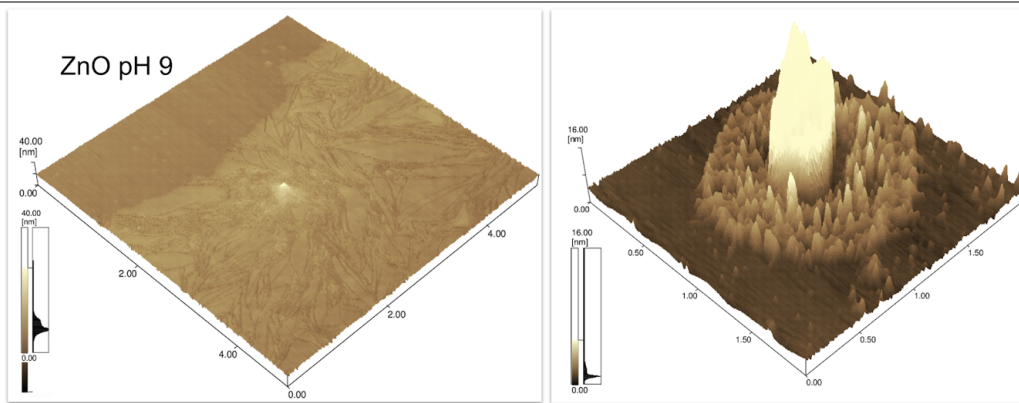
Figure 10 and 11 show stars structures in the SEM images. It is observed that ZnO NCs tend to attach to the tips making star-shaped structures. This result is justified once the ZnO NCs interact with the  $\text{PO}^-$  of glyphosate where the greatest charge accumulation occurs. The charge density is inversely proportional to the radius thus favors the formation of the star-shaped glyphosate-ZnO NCs accumulation. Some studies have shown that when the nanoparticles are in a star form occurs a surface enhancement intensification effect <sup>51</sup> <sup>52</sup>. Thus, this arrangement can favor an intensification of the glyphosate modes when in the presence of ZnO NCs. Therefore, the AFM and SEM images confirm the FTIR results of the intensification of the active modes of glyphosate-NC due to the star shape of the structures.

#### The nanometric level structure under different pH on Glyphosate-ZnO Nanocrystals

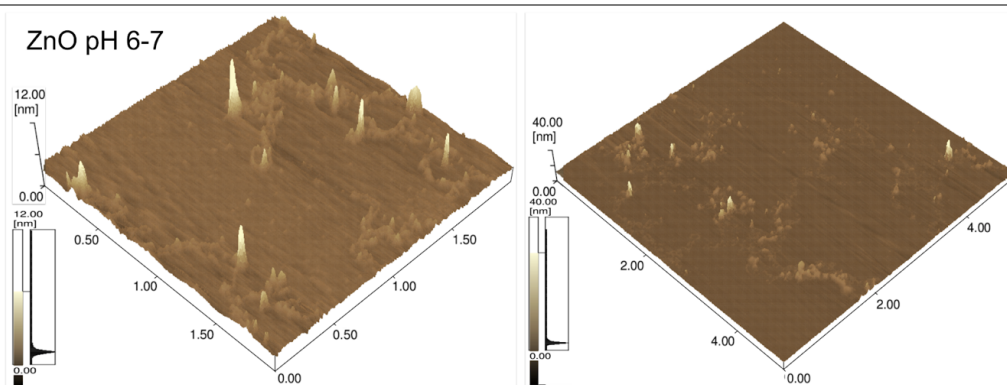
The interaction Glyphosate-Nanocrystals was already confirmed by Atomic Force Microscopy (AFM). Figures 12 - 16 show that the protonation pathway of glyphosate going from phosphonic group to carboxylic one causes structural changes at a nanometric level where vulcanoids forms are reached at more basic pH, while in the acid pH isolated nanocrystals can be identified.



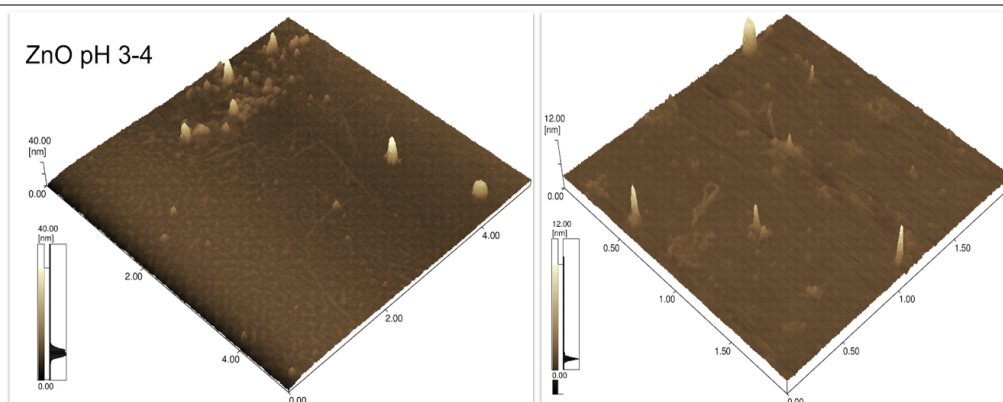
Chapter II, Figure 12. Figure 11. AFM of Glyphotal TR® and Glyphotal TR®-ZnO [ $10^{-4}$  v/v] pH 13-14.



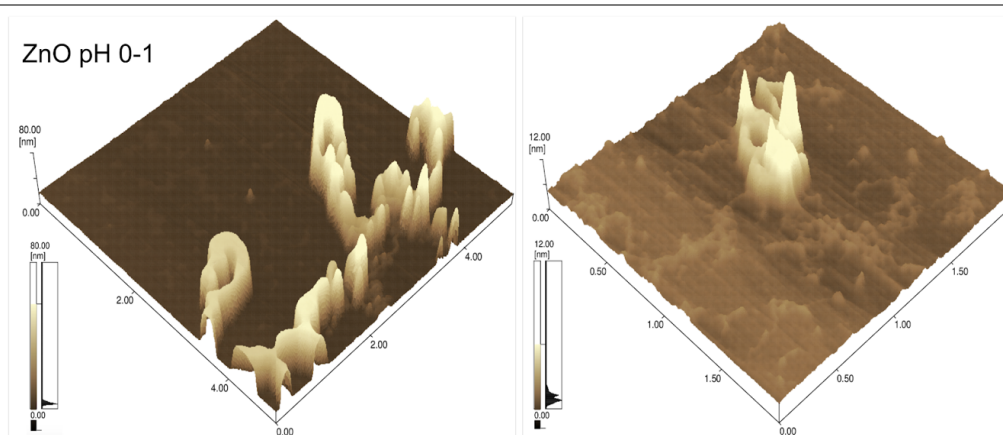
Chapter II, Figure 13. AFM of Glyphotal TR® and Glyphotal TR®-ZnO [ $10^{-4}$ v/v] pH 9.



Chapter II, Figure 14. AFM of Glyphotal TR® and Glyphotal TR®-ZnO [ $10^{-4}$  v/v] pH 6-7.



Chapter II, Figure 15. AFM of Glyphotal TR<sup>®</sup> and Glyphotal TR<sup>®</sup>-ZnO [10<sup>-4</sup> v/v] pH 3-4 at 4.00 μm<sup>2</sup> and 2.00 μm<sup>2</sup>.



Chapter II, Figure 16. AFM of Glyphotal TR<sup>®</sup> and Glyphotal TR<sup>®</sup>-ZnO [10<sup>-4</sup> v/v] pH 0-1 at 4.00 μm<sup>2</sup> and 2.00 μm<sup>2</sup>.

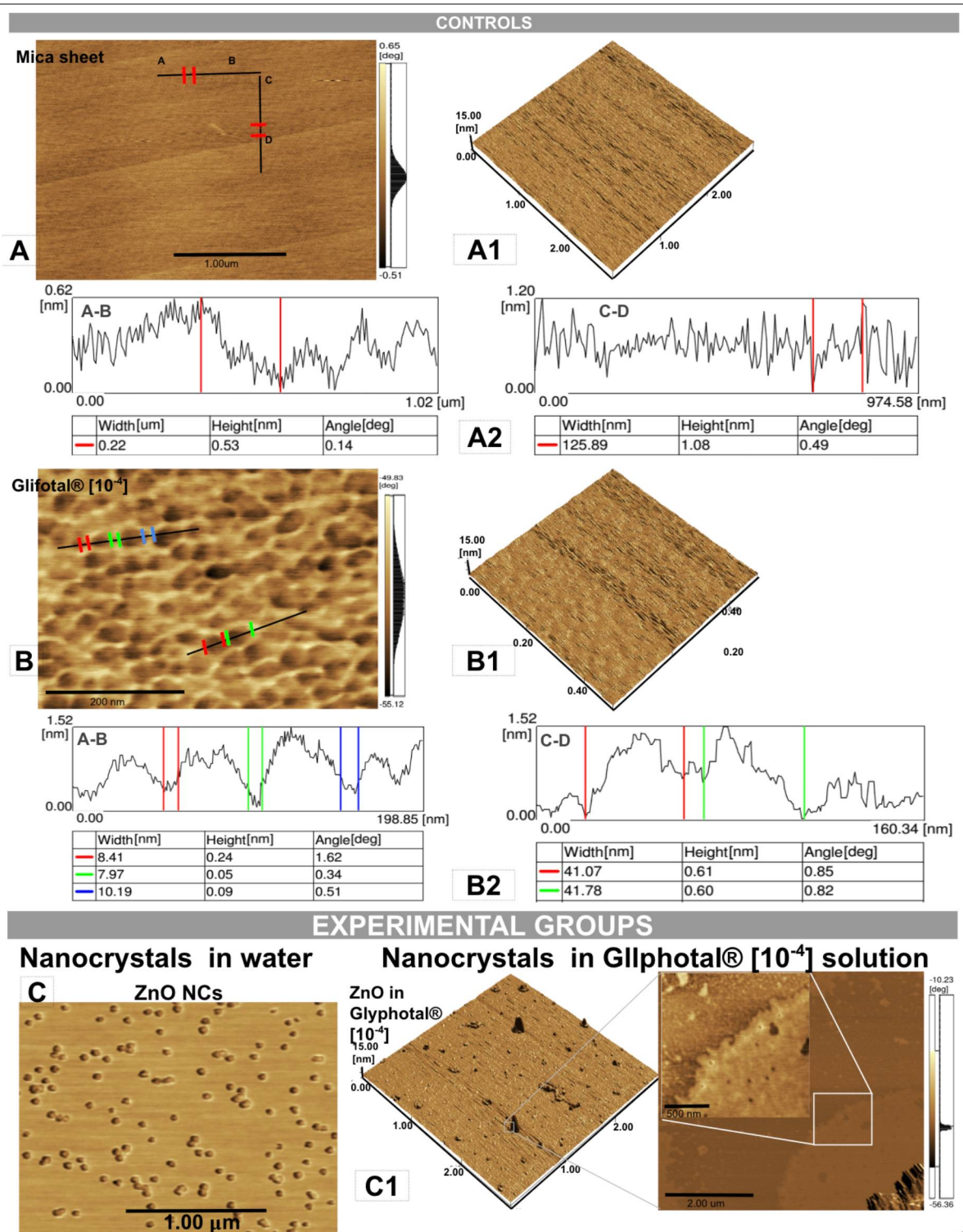
### A predicted model

ZnO NCs have a curious property that involves the ability to be activated by UV and visible light and form electron-hole pairs <sup>53</sup>. Because of this, anti-bactericidal properties <sup>54 55</sup> in water disinfection are associated with ZnO NCs once it causes the depolarization of the cell wall and subsequently the cell membrane, leaking the cell contents, and eventually cell death <sup>56</sup>. The full mechanism was presented by <sup>57</sup>, but basically, it happens because these nanocrystals can accumulate a positive charge on its surface. The affinity between ZnO and Glyphosate is due to the strong ability of the herbicide chelating on metals and the ZnO properties cited above. The Glyphosate protonation status can drastically influence how strong it will be the interaction with nanocrystals. Supported by previously cited literature and as shown in Figure 5, the phosphonic

group is the readiest to interact on ZnO in all pH. When glyphosates molecules interacting with ZnO NCs, above the pKa3, we suppose that the Glyphosate is like “lying down” on ZnO attracted by all its negative groups. In basic pH the Glyphosate’s attraction by ZnO are very strong promoting a fast agglomeration process, so fast that can wrap many nanocrystals forming precipitate pellets with the naked eye, clusters on SEM, and volcano forms at AFM.

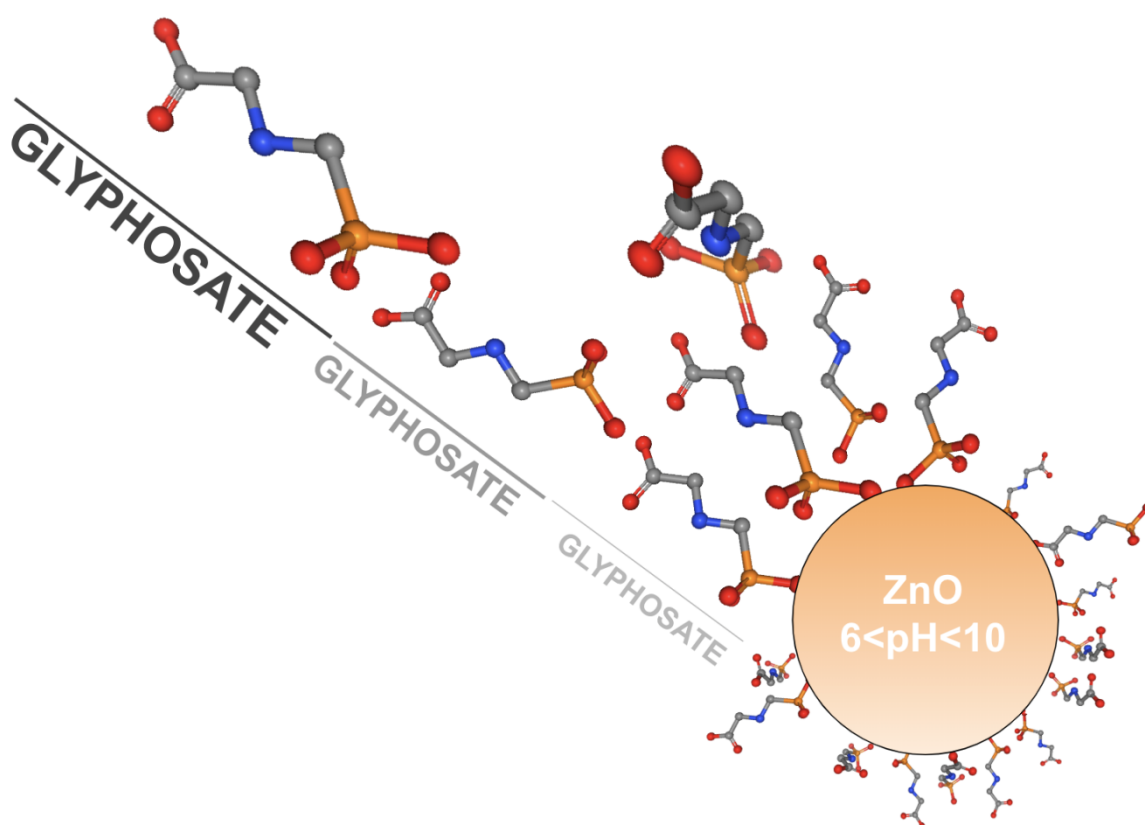
Although we do not present FTIR spectra in pH 7, between pKa3 and pKa2 is expected an intermediate loss of affinity for interact by amina group, as could be evidenced on pH 5. In this intermediate stage between pKa3 and pKa2 the Glyphosate unbind Amina group for the ZnO and fixes on the nanocrystal surface strongly by its phosphonic group as evidenced by  $1000\text{ cm}^{-1}$  and  $1090\text{ cm}^{-1}$  (Figure 5). Now Glyphosate is not more “lying down” on ZnO surface. It is expected an intermediary status where bonded by the  $\text{PO}_3^-$  the Glyphosate is disposed side by side in alignment creating a type of mycelial form. A Glyphosate cloud surges surround the Nanocrystal as evidenced by the image in Figure 17. Figure 17 shows AFM images of Glyphotal TR<sup>®</sup> and Glyphotal TR<sup>®</sup>-ZnO [ $10^{-4}$  v/v] in pH 6-7. The highlight of this Figure is to show the organizational structure of the herbicide without ZnO NCs and the aurea around ZnO NCs that we suppose that could be just glyphosate interacting through the phosphonic group on ZnO. The glyphosate molecule has three poles. As negative ones are the phosphonic acid and the carboxylic group, and the positive one the amino group. We assume that glyphosate arrays around the NCs are stabilized by multi-polar attractive forces.

No volcanic structures were seen on this pH and below. In this stage, we believe that electrostatic forces still influenced glyphosate to approximate to the nanocrystal even if no more space for covalent bonds exist. This lets to form a glyphosate cloud around the NC. Carboxylic vibrations are a result of the repel and attractive forces between carboxylic groups arranged size by size in the mycelium structure hypothesized represented in Figure 18.



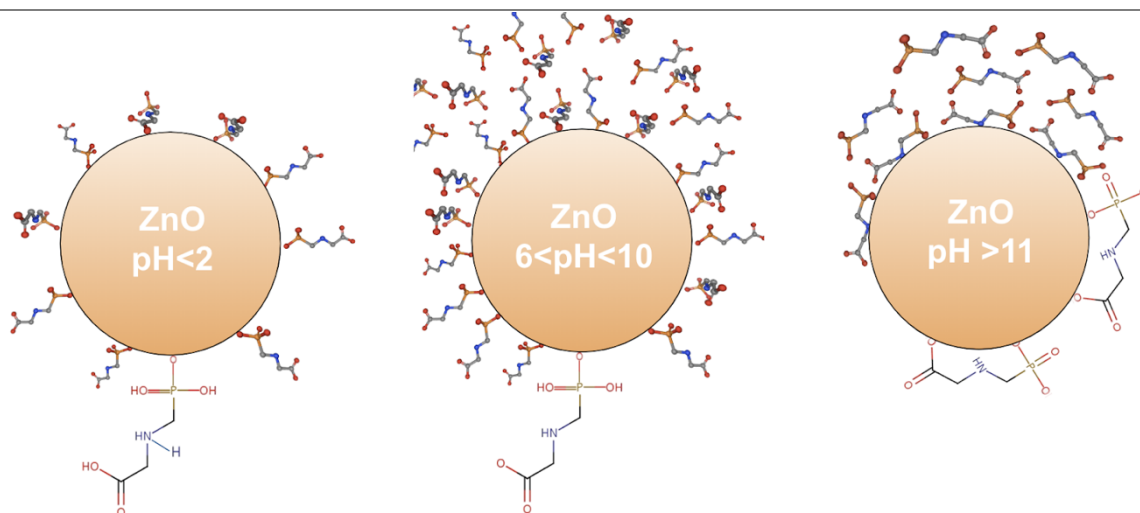
Chapter II, Figure 17. AFM of Gliphotal TR® and Gliphotal TR®-ZnO [ $10^{-4}$  v/v] pH 6-7.





*Chapter II, Figure 18. A hypothesis about glyphosate's clouds around ZnO NCs in pH 6-10.*

Going near to  $pK_{a2}$  the Glyphosate adopt more and more a mycelial-like structure around ZnO. Skeletal central structures transmit vibrational energy from ZnO while repel neighbors Glyphosates. Near to  $pK_1$ , all glyphosate structures are protonated. Hydrogen can access spaces where ZnO is big enough to reach. The binding sites competition favored hydrogenous, and then, the glyphosate clouds around the ZnO NC disappear. The ZnO electrostatic forces are enough to promote a thin film formed by Glyphosate held by its  $PO^-$  -  $1090\text{ cm}^{-1}$  on ZnO. In a low pH, the glyphosate multi-polar attractive forces are still stronger than electrostatic ZnO forces that maintain the nanocrystals together in water solution. The reaction is as slow as the nanocrystals can be reorganized in microcrystals. In acid pH, the visual reaction is the slowest and ZnO NCs that could be seen in neutral solutions, becomes invisible when interacts with Glyphosate. Figure 19 predicts how Glyphosate could be organized around ZnO based on FTIR vibrating modes as pH changes.



*Chapter II, Figure 19. Glyphosate-ZnO model in accordance to pH changes.*

The present observations probably must go in different way on other mediums. Previous studies already had describes that changes in the concentration of the background electrolyte affect the adsorption of glyphosate, e.g., on soils <sup>43</sup>, whereas glyphosate adsorption on goethite was only slightly influenced <sup>58 59</sup>.

However, this study is a proof of concept that could help in understanding the mechanisms involved, e.g., in glyphosate detection through derivatization process. Glyphosate detection on some chromatographic techniques diminishes the pH of medium to uncouple glyphosate and detect it, e.g. <sup>60 61 62</sup>. As we can see, even very low concentrations of glyphosate could still be detected in the presence of ZnO NCs.

## CONCLUSION

The vibrational mode of glyphosate is strongly influenced by pH conditions and our synthesized ZnO NCs can closely follow the vibration modes changes in the protonation of Glyphosate's pathway. We hypothesized that as much the Glyphosate vibrating modes detected by FTIR has more transmittance as much it is interacting with ZnO. So, comparing how much tithed is a structure as the glyphosate's protonation pathway changes, we can figure out the molecular behavior along this way. Phosphonic group is the strongest group to protonate and

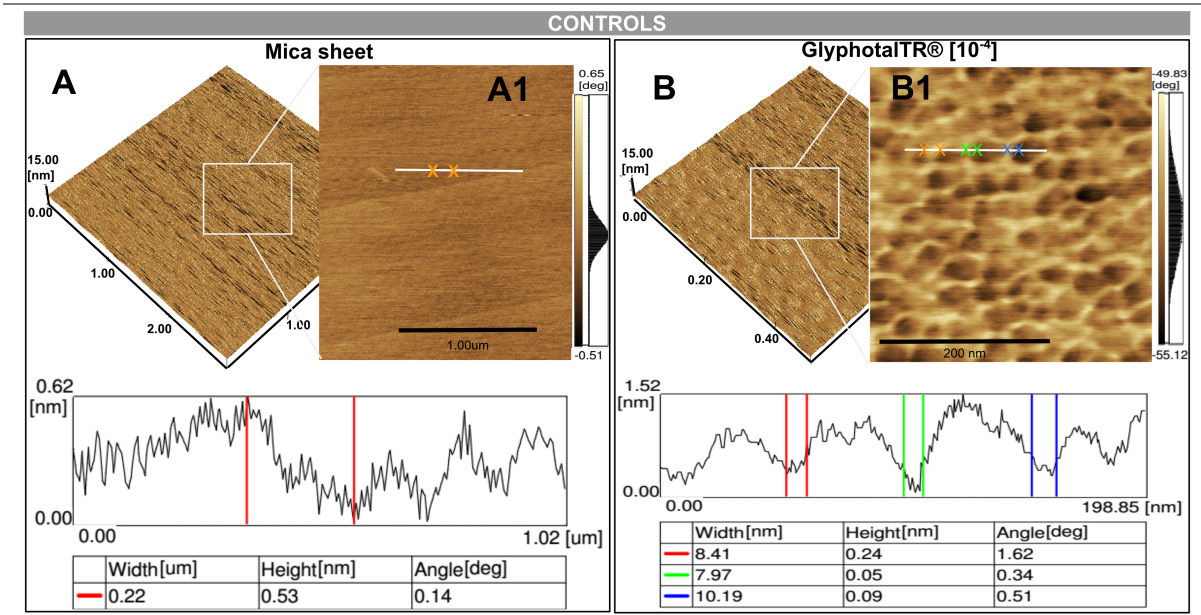
stay protonated as the pH cross the  $pK_{a3}$  to the acid direction. The amine group protonation makes Glyphosate, that was lying down on ZnO at  $pK_{a3}$ , become side by side in a mycelium like structure around ZnO. This structure allows the formation of a Glyphosate cloud around ZnO. Bellow  $pK_{a1}$  carboxylic group becomes protonated, ZnO exercises a few attractive forces and just the phosphonic acid is strong enough to bind on ZnO creating a thin film around it. This thin film individualizes the nanocrystal making it becomes very eluted in water. As Glyphosate-ZnO create many different structures according to the pH, we believe that ZnO NCs, in acid pH, has a potential to improve optical detection methods as spectrophotometry, photoluminescence, fluorescence, photoluminescence, etc., while the basic pH is better for e.g. like gravimetric methods. Neutral pH is ideal for a surface-sensitive technique to enhance Raman scattering and FTIR.

### Acknowledgements

The authors gratefully acknowledge the financial support of the Brazilian funding agencies, CNPq, CAPES, and FAPEMIG, for providing financial support to the National Institute of Science and Technology in Theranostics and Nanobiotechnology – INCT-TeraNano (CNPq/CAPES/FAPEMIG, grant numbers CNPq-465669/2014-0 and FAPEMIG-CBB-APQ-03613-17).



Supplements



Chapter II, Figure 20. Controls for AFM figures. A. Mica surface: The flattest known surface made by silica sheet. B. Glyphotal TR® above mica surface.

## References

- (1) Benbrook, C. M. Trends in Glyphosate Herbicide Use in the United States and Globally. *Environ Sci Eur* 2016, 28 (1), 3.
- (2) Giesy, J. P.; Dobson, S.; Solomon, K. R. Ecotoxicological Risk Assessment for Roundup® Herbicide. In *Reviews of Environmental Contamination and Toxicology*; Ware, G. W., Ed.; Reviews of Environmental Contamination and Toxicology; Springer New York, 2000; pp 35–120.
- (3) Organization, W. H.; Others. Glyphosate Environmental Health Criteria No. 159. *WHO, Geneva* 1994, 177.
- (4) Tsui, M. T. K.; Chu, L. M. Environmental Fate and Non-Target Impact of Glyphosate-Based Herbicide (Roundup®) in a Subtropical Wetland. *Chemosphere* 2008, 71 (3), 439–446.
- (5) Williams, G. M.; Kroes, R.; Munro, I. C. Safety Evaluation and Risk Assessment of the Herbicide Roundup and Its Active Ingredient, Glyphosate, for Humans. *Regul. Toxicol. Pharmacol.* 2000, 31 (2 Pt 1), 117–165.
- (6) Agency for Research on Cancer - Recuperado de [http://www. iarc. fr](http://www.iarc.fr), I.; 2015. IARC Monographs Volume 112: Evaluation of Five Organophosphate Insecticides and Herbicides. 2015.
- (7) Vereecken, H. Mobility and Leaching of Glyphosate: A Review. *Pest Manag. Sci.* 2005, 61 (12), 1139–1151.
- (8) Wang, Y. S.; Jaw, C. G.; Chen - Water, Y. L.; Air; Soil Pollution, &; 1994. Accumulation of 2, 4-D and Glyphosate in Fish and Water Hyacinth. *Springer* 1994.
- (9) Krüger, M.; Schledorn, P.; Schrödl - ... of Environmental & ..., W.; 2014. Detection of Glyphosate Residues in Animals and Humans. *pdfs.semanticscholar.org* 2014.

- (10) Rendon-von Osten, J.; Dzul-Caamal, R. Glyphosate Residues in Groundwater, Drinking Water and Urine of Subsistence Farmers from Intensive Agriculture Localities: A Survey in Hopelchén, Campeche, Mexico. *Int. J. Environ. Res. Public Health* 2017, 14 (6). <https://doi.org/10.3390/ijerph14060595>.
- (11) Glass, R. L. Adsorption of Glyphosate by Soils and Clay Minerals. *J. Agric. Food Chem.* 1987, 35 (4), 497–500.
- (12) Sprankle, P.; Meggitt, W. F.; Penner, D. Adsorption, Mobility, and Microbial Degradation of Glyphosate in the Soil. *Weed Sci.* 1975, 23 (3), 229–234.
- (13) Alloway, B. J. Zinc in Soils and Crop Nutrition. International Zinc Association Brussels 2004.
- (14) Singh, M. V.; Abrol, I. P. Transformation and Availability of Zinc in Alkali Soils. *Fert News* 1986, 31 (7), 17–27.
- (15) Smith, P. H.; Hahn, F. E.; Hugli, A.; Raymond, K. N. Crystal Structures of Two Salts of N-(phosphonomethyl)glycine and Equilibria with Hydrogen and Bicarbonate Ions. *Inorg. Chem.* 1989, 28 (11), 2052–2061.
- (16) Clarke, E. T.; Rudolf, P. R.; Martell, A. E.; Clearfield, A. Structural Investigation of the Cu (II) Chelate of N-Phosphonomethylglycine. X-Ray Crystal Structure of Cu (II)[O 2 CCH 2 NHCH 2 PO 3]·textperiodcentered Na (H 2 O) 3.5. *Inorganica Chim. Acta* 1989, 164 (1), 59–63.
- (17) Madsen, H. E. L.; Christensen, H. H.; Gottlieb-Petersen, C.; Andresen, A. F.; Smidsrød, O.; Pontchour, C.-O.; Phavanantha, P.; Pramatus, S.; Cyvin, B. N.; Cyvin, S. J. Stability Constants of Copper(II), Zinc, Manganese(II), Calcium, and Magnesium Complexes of N-(Phosphonomethyl)glycine (Glyphosate). *Acta Chem. Scand.* 1978, 32a, 79–83.
- (18) McBride, M.; Kung, K.-H. Complexation of Glyphosate and Related Ligands with Iron (III). *Soil Sci. Soc. Am. J.* 1989, 53 (6), 1668.

- (19) Shoval, S.; Yariv - Agrochimica, S.; 1981. Infrared Study of the Fine-Structures of Glyphosate and Roundup. *UNIV PISA VIA S MICHELE DEGLI ...* 1981.
- (20) Piccolo, A.; Celano, G. Modification of Infrared Spectra of the Herbicide Glyphosate Induced by pH Variation. *J. Environ. Sci. Health B* 1993, 28 (4), 447–457.
- (21) Caetano, M. S.; Ramalho, T. C.; Botrel, D. F.; da Cunha, E. F. F.; de Mello, W. C. Understanding the Inactivation Process of Organophosphorus Herbicides: A DFT Study of Glyphosate Metallic Complexes with  $Zn^{2+}$ ,  $Ca^{2+}$ ,  $Mg^{2+}$ ,  $Cu^{2+}$ ,  $Co^{3+}$ ,  $Fe^{3+}$ ,  $Cr^{3+}$ , and  $Al^{3+}$ . *Int. J. Quantum Chem.* 2012, 112 (15), 2752–2762.
- (22) Zhang, Y.; Gao, X.; Zhi, L.; Liu, X.; Jiang, W.; Sun, Y.; Yang, J. The Synergetic Antibacterial Activity of Ag Islands on ZnO (Ag/ZnO) Heterostructure Nanoparticles and Its Mode of Action. *J. Inorg. Biochem.* 2014, 130, 74–83.
- (23) Wauchope, D. Acid Dissociation Constants of Arsenic Acid, Methylarsonic Acid (MAA), Dimethylarsinic Acid (cacodylic Acid), and N-(phosphonomethyl)glycine (glyphosate). *J. Agric. Food Chem.* 1976, 24 (4), 717–721.
- (24) Chamberlain, K.; Evans, A. A.; Bromilow, R. H. 1-Octanol/Water Partition Coefficient ( $K_{ow}$ ) and  $pK_a$  for Ionisable Pesticides Measured by a pH-Metric Method. *Pestic. Sci.* 1996, 47 (3), 265–271.
- (25) Coutinho, C. F. B.; Mazo, L. H. Complexos Metálicos Com O Herbicida Glifosato: Revisão. *Química Nova* 2005, 28 (6), 1038.
- (26) Liu, B.; Dong, L.; Yu, Q.; Li, X.; Wu, F.; Tan, Z.; Luo, S. Thermodynamic Study on the Protonation Reactions of Glyphosate in Aqueous Solution: Potentiometry, Calorimetry and NMR Spectroscopy. *J. Phys. Chem. B* 2016, 120 (9), 2132–2137.

(27) Hance, R. J. Herbicide Usage and Soil Properties. *Plant Soil* 1976, 45 (1), 291–293.

(28) Thompson, D. G.; Cowell, J. E.; Daniels, R. J.; Staznik, B.; MacDonald, L. M. Liquid Chromatographic Method for Quantitation of Glyphosate and Metabolite Residues in Organic and Mineral Soils, Stream Sediments, and Hardwood Foliage. *J. Assoc. Off. Anal. Chem.* 1989, 72 (2), 355–360.

(29) Rueppel, M. L.; Brightwell, B. B.; Schaefer, J.; Marvel, J. T. Metabolism and Degradation of Glyphosate in Soil and Water. *J. Agric. Food Chem.* 1977, 25 (3), 517–528.

(30) Moraes, F. C.; Mascaro, L. H.; Machado, S. A. S.; Brett, C. M. A. Direct Electrochemical Determination of Glyphosate at Copper Phthalocyanine/Multiwalled Carbon Nanotube Film Electrodes. *Electroanalysis* 2010, 22 (14), 1586–1591.

(31) de Melo Reis, É.; de Rezende, A.; Santos - Food and Chemical ..., D. V.; 2015. Assessment of the Genotoxic Potential of Two Zinc Oxide Sources (amorphous and Nanoparticles) Using the in Vitro Micronucleus Test and the in Vivo Wing .... *Elsevier Oceanogr. Ser.* 2015.

(32) Sousa, C. J. A.; Pereira, M. C.; Almeida, R. J.; Loyola, A. M.; Silva, A. C. A.; Dantas, N. O. Synthesis and Characterization of Zinc Oxide Nanocrystals and Histologic Evaluation of Their Biocompatibility by Means of Intraosseous Implants. *Int. Endod. J.* 2014, 47 (5), 416–424.

(33) Morais, P. V.; Gomes, V. F.; Silva, A. C. A.; Dantas, N. O.; Schöning, M. J.; Siqueira, J. R. Nanofilm of ZnO Nanocrystals/carbon Nanotubes as Biocompatible Layer for Enzymatic Biosensors in Capacitive Field-Effect Devices. *J. Mater. Sci.* 2017, 52 (20), 12314–12325.

(34) Dantas, N. O.; Silva, A. S.; Silva - Optical Imaging ..., A.; 2012. Atomic and Magnetic Force Microscopy of Semiconductor and Semimagnetic

Nanocrystals Grown in Colloidal Solutions and Glass Matrices. *researchgate.net* 2012.

(35) Cheah, U. B.; Kirkwood, R. C.; Lum, K. Y. Adsorption, Desorption and Mobility of Four Commonly Used Pesticides in Malaysian Agricultural Soils. *Pestic. Sci.* 1997.

(36) Nomura, N. S.; Hilton, H. W. The Adsorption and Degradation of Glyphosate in Five Hawaiian Sugarcane Soils. *Weed Res.* 1977.

(37) McConnell, J. S.; Hossner, L. R. pH-Dependent Adsorption Isotherms of Glyphosate. *J. Agric. Food Chem.* 1985, 33 (6), 1075–1078.

(38) Morillo, E.; Undabeytia, T.; Maqueda, C.; Ramos, A. Glyphosate Adsorption on Soils of Different Characteristics. Influence of Copper Addition. *Chemosphere* 2000, 40 (1), 103–107.

(39) Sheals, J.; Sjöberg, S.; Persson, P. Adsorption of Glyphosate on Goethite: Molecular Characterization of Surface Complexes. *Environ. Sci. Technol.* 2002, 36 (14), 3090–3095.

(40) Cruz, L. H. da; Santana, H. de; Zaia, C. T. B. V.; Zaia, D. A. M. Adsorption of Glyphosate on Clays and Soils from Paraná State: Effect of pH and Competitive Adsorption of Phosphate. *Braz. Arch. Biol. Technol.* 2007, 50 (3), 385–394.

(41) Nicholls, P. H.; Evans, A. A. Sorption of Ionisable Organic Compounds by Field Soils. Part 2: Cations, Bases and Zwitterions. *Pestic. Sci.* 1991, 33 (3), 331–345.

(42) Morillo, E.; Undabeytia, T.; Maqueda, C. Adsorption of Glyphosate on the Clay Mineral Montmorillonite: Effect of Cu(II) in Solution and Adsorbed on the Mineral. *Environ. Sci. Technol.* 1997, 31 (12), 3588–3592.

(43) de Jonge, H.; Wollesen de Jonge, L. Influence of pH and Solution Composition on the Sorption of Glyphosate and Prochloraz to a Sandy Loam Soil. *Chemosphere* 1999, 39 (5), 753–763.

(44) de Jonge, H.; de Jonge, L. W.; Jacobsen, O. H.; Yamaguchi, T.; Moldrup, P. GLYPHOSATE SORPTION IN SOILS OF DIFFERENT pH AND PHOSPHORUS CONTENT. *Soil Sci.* 2001, 166 (4), 230.

(45) Gimsing, A. L.; Borggaard, O. K.; Bang, M. Influence of Soil Composition on Adsorption of Glyphosate and Phosphate by Contrasting Danish Surface Soils. *Eur. J. Soil Sci.* 2004, 55 (1), 183–191.

(46) Kołodziejczak-Radzimska, A.; Jesionowski, T. Zinc Oxide—From Synthesis to Application: A Review. *Materials* 2014, 7 (4), 2833–2881.

(47) Adil, S. F.; Assal, M. E.; Ali, R. Synthesis and Characterization of Silver Oxide and Silver Chloride Nanoparticles with High Thermal Stability. *Asian Journal of* 2013.

(48) Peixoto, M. M.; Bauerfeldt, G. F.; Herbst, M. H.; Pereira, M. S.; da Silva, C. O. Study of the Stepwise Deprotonation Reactions of Glyphosate and the Corresponding pKa Values in Aqueous Solution. *J. Phys. Chem. A* 2015, 119 (21), 5241–5249.

(49) Li, W.; Wang, Y.-J.; Zhu, M.; Fan, T.-T.; Zhou, D.-M.; Phillips, B. L.; Sparks, D. L. Inhibition Mechanisms of Zn Precipitation on Aluminum Oxide by Glyphosate: A <sup>31</sup>P NMR and Zn EXAFS Study. *Environ. Sci. Technol.* 2013, 47 (9), 4211–4219.

(50) Omar, F. M.; Aziz, H. A.; Stoll, S. Aggregation and Disaggregation of ZnO Nanoparticles: Influence of pH and Adsorption of Suwannee River Humic Acid. *Science of The Total Environment.* 2014, pp 195–201. <https://doi.org/10.1016/j.scitotenv.2013.08.044>.

(51) Hao, F.; Nehl, C. L.; Hafner, J. H.; Nordlander, P. Plasmon Resonances of a Gold Nanostar. *Nano Letters*. 2007, pp 729–732. <https://doi.org/10.1021/nl062969c>.

(52) James Holler, F.; Skoog, D. A.; Crouch, S. R.; Pasquini, C.; da Unicamp, E. *Princípios de análise instrumental*; 2009.

(53) Jones, N.; Ray, B.; Ranjit, K. T.; Manna, A. C. Antibacterial Activity of ZnO Nanoparticle Suspensions on a Broad Spectrum of Microorganisms. *FEMS Microbiol. Lett.* 2008, 279 (1), 71–76.

(54) Dimapilis, E. A. S.; Hsu, C.-S.; Mendoza, R. M. O.; Lu, M.-C. Zinc Oxide Nanoparticles for Water Disinfection. *Sustain. Environ. Res. SER* 2018, 28 (2), 47–56.

(55) Motshekga, S. C. *Application of Chitosan-Based Nanocomposites Containing Bentonite-Supported Silver and Zinc Oxide Nanoparticles for Bacterial Disinfection of Drinking Water*; 2016.

(56) Vijayaraghavan, R. Zinc Oxide Based Inorganic Antimicrobial Agents. *International Journal of Science Research* 2012, 1 (2), 35–46.

(57) Padmavathy, N.; Vijayaraghavan, R. Enhanced Bioactivity of ZnO Nanoparticles-an Antimicrobial Study. *Sci. Technol. Adv. Mater.* 2008, 9 (3), 035004.

(58) Gimsing, A. L.; Borggaard, O. K. EFFECT OF KCl AND CaCl<sub>2</sub> AS BACKGROUND ELECTROLYTES ON THE COMPETITIVE ADSORPTION OF GLYPHOSATE AND PHOSPHATE ON GOETHITE. *Clays Clay Miner.* 2001, 49 (3), 270–275.

(59) Barja, B. C.; Dos Santos Afonso, M. Aminomethylphosphonic Acid and Glyphosate Adsorption onto Goethite: A Comparative Study. *Environ. Sci. Technol.* 2005, 39 (2), 585–592.



(60) Waiman, C. V.; Avena, M. J.; Garrido, M.; Fernández Band, B.; Zanini, G. P. A Simple and Rapid Spectrophotometric Method to Quantify the Herbicide Glyphosate in Aqueous Media. Application to Adsorption Isotherms on Soils and Goethite. *Geoderma* 2012, 170, 154–158.

(61) Ibáñez, M.; Pozo, O. J.; Sancho, J. V.; López, F. J.; Hernández, F. Residue Determination of Glyphosate, Glufosinate and Aminomethylphosphonic Acid in Water and Soil Samples by Liquid Chromatography Coupled to Electrospray Tandem Mass Spectrometry. *J. Chromatogr. A* 2005, 1081 (2), 145–155.

(62) Guo, Z.-X.; Cai, Q.; Yang, Z. Determination of Glyphosate and Phosphate in Water by Ion Chromatography—inductively Coupled Plasma Mass Spectrometry Detection. *J. Chromatogr. A* 2005, 1100 (2), 160–167.

## CAPÍTULO III

### Application of ZnO Nanocrystals as a Surface-Enhancer FTIR for Glyphosate Detection

Journal: Analytica Chimica Acta  
Manuscript ID: ACA-19-2307  
Manuscript Status: Submitted

## Application of ZnO Nanocrystals as a Surface-Enhancer FTIR for Glyphosate Detection

Anderson L. Valle<sup>a</sup>, Anielle, C. A. Silva<sup>b,c</sup>, Noelio O. Dantas<sup>b,c</sup>, Francielli, C. C. Melo<sup>a</sup>, Robinson Sabino-Silva<sup>d</sup>, Cleumar da Silva Moreira<sup>f</sup>, Luciano P. Rodrigues<sup>e\*</sup>, Luiz R. Goulart<sup>a\*</sup>

<sup>a</sup> Nanobiotechnology Laboratory, Institute of Genetics and Biochemistry, Federal University of Uberlândia, Uberlândia, MG, Brazil.

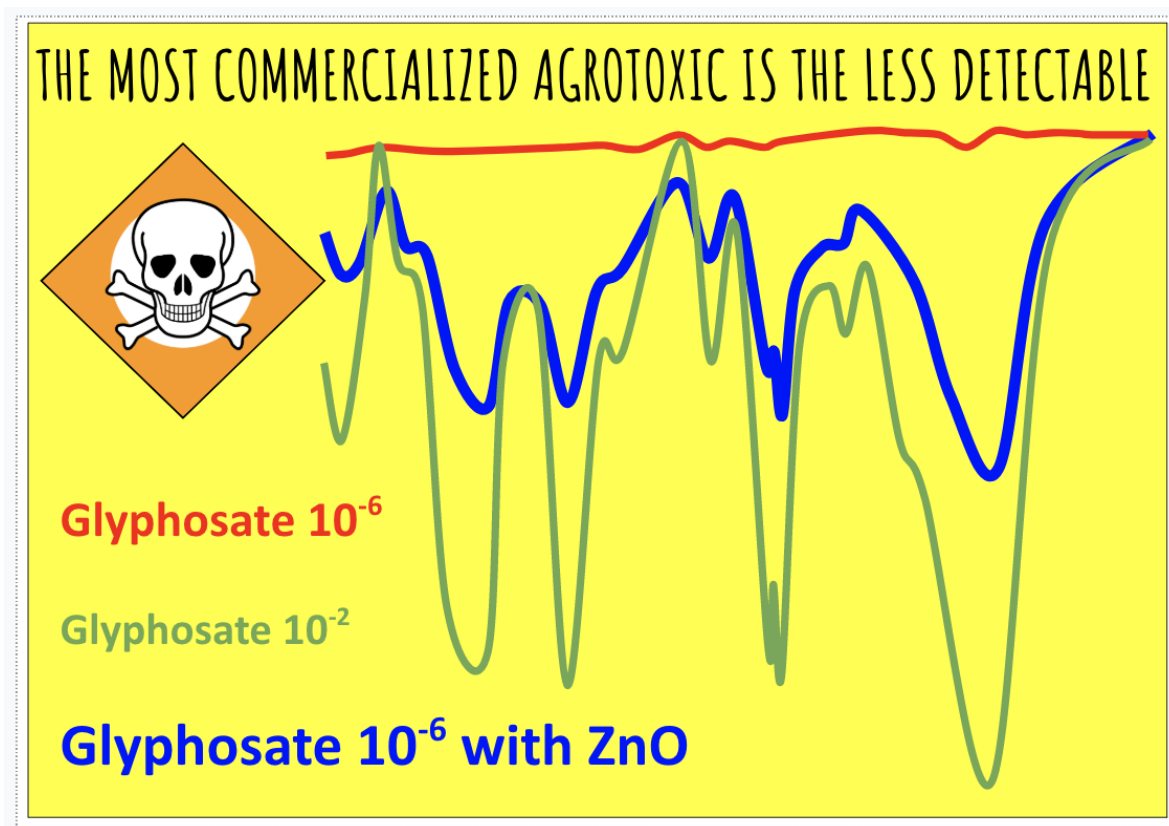
<sup>b</sup> Laboratory of New Insulating and Semiconductors Materials, Institute of Physics, Federal University of Uberlândia, Uberlândia, MG, Brazil.

<sup>c</sup> Laboratory of New Nanostructured and Functional Materials, Institute of Physics, Federal University of Alagoas, Maceió, AL, Brazil.

<sup>d</sup> Institute of Biomedical Sciences, Uberlândia, MG, Brazil.

<sup>e</sup> Institute of Engineering, Science and Technology, Federal University of Jequitinhonha and Mucuri's Valleys, Janaúba, MG, Brazil.

<sup>f</sup> Electrical Engineering, Federal Institute of Paraíba, João Pessoa, PB, Brazil.



## ABSTRACT

Glyphosate detection and quantification is still a challenge. After an extensive literature review, we have observed that the Fourier transform infrared spectroscopy (FTIR) had not been used for detection or quantification yet. The interaction of zinc oxide (ZnO), silver oxide (Ag<sub>2</sub>O), Ag-doped with ZnO:Ag<sub>2</sub>O nanocomposites (Ag doped with ZnO + Ag<sub>2</sub>O NCs) with glyphosate was analysed at a FTIR to determine whether nanomaterials could be used as signal enhancers of glyphosates. Results were further supported by atomic force microscopy (AFM) imaging. ZnO nanocrystals provoked a surface enhancement FTIR (SE-FTIR) for commercial solutions of glyphosate with 10,000-fold signal amplification when the ZnO:Glyphosate interaction is formed. In another way strong chelating properties of Ag may disturb the signal and makes difficult glyphosate FTIR identification. Briefly, we have shown for the first time the SE-FTIR for Glyphosate as a proof-of-concept, which may be explored for detection of other molecules based on nanocrystals affinity.

**Keywords:** Nanocomposites, FTIR enhancement, FTIR spectroscopy, Silver Oxide, Zinc Oxide.

## HIGHLIGHTS

- Specific zinc oxide nanocrystals are potent FTIR spectral-enhancer for samples with glyphosate.
- Silver oxide nanocrystals have higher chelating properties for sensors and recovery of glyphosate from environment.

## INTRODUCTION

Glyphosate [(N-phosphonomethyl) Glycine] is the most worldwide commercialized herbicide, representing billions of tons [1]. It has been used dramatically since genetically modified glyphosate-resistant crops were introduced late in the 20<sup>th</sup> century [2]. Commercial formulation of glyphosate, as GLYPHOTAL TR®, consists of isopropyl amine salt and the surfactant polyoxyethylene amine added according to the manufacturer to increase its efficiency [3]. This herbicide was considered “toxicologically harmless” for animals and the environment [4] [5] [6] due to its degradability by soil microbes and binding ability to soil colloids [7]. But nowadays, it is back on focus due to its carcinogenic effects, according to the International Agency for Research on Cancer, based on evidence from agriculture exposure and laboratory animal data [8].

While discussions about human safety is ongoing, the environmental future may point to a different path, once new studies have indicated its potential to accumulate in the environmental water [9], fish [10], cows, hares, rabbits, humans [11] and others [12]. Although many articles have correlated endocrines and toxics effects of glyphosate, it has been suggested that the presence of adjuvants is even more toxic than the herbicide, and enhances its toxicity [13], bioavailability and/or bioaccumulation [14].

Actually, there are more than eighty methods to detect glyphosate [15]; however, its detection and quantification is generally expensive and slow, which means that governmental control measures are ineffective. The European Union (EU) authorities have performed regular monitoring of glyphosate in cereals since 2010, but the challenge in testing glyphosate residues on imported genetically modified soybeans (GMS) still remains, and in this scenario, Brazil is one of the biggest GMS producers. Even in Europe, only a small number of testing laboratories are able to detect glyphosate [16].

The glyphosate's capacity to adsorb strongly on clay minerals [17] and organic or mineral particles in water [18][19] and its high affinity to metal cations impose great difficulty to detect it without pretreatment methods [20]. The behavior

of glyphosate has been examined by several research groups showing the tendency of transitions in some trivalent metal ions and divalent alkaline-earth to form 1:1 (e.g. Ca(II) and Cu(II) [21],[22]) and 2:1 metal chelates with glyphosate in solution [23]. Using density functional theory molecular modeling methods showed that zinc is the most stable to form tetrahedral and octahedral complexes with glyphosate, with the following affinity dominance:  $Zn > Cu > Co > Fe > Cr > Al > Ca > Mg$  [24].

It is known that most agricultural soils contain Zn ( $10\text{--}300\text{ mg kg}^{-1}$ ) [25], and that the increase in the use of glyphosate have an effect in the availability of this metal on soils [26]. On the other hand, the interaction of glyphosate with Ag has been barely discussed, and has been generally used only for biosensing purposes [27], [28], [29].

Zinc is normally found complexed with oxygen (ZnO), which is widely used as an additive in several products and materials applied in foods [30] and for pollutants' degradation [31]. ZnO nanoparticles can be amorphous or crystalline, with the difference that nanocrystals are highly stable and do not present genotoxicity, unlike amorphous nanoparticles [32]. Therefore, ZnO nanocrystals may open new opportunities for biomedical applications, including biosensors [33], [34], [35].

The oxides make Ag ions more stable and consequently more biocompatible. It is found in two forms, monovalent ( $Ag_2O$ ) and bivalent (AgO) cations. The activity of silver in the  $Ag_2O$  form is shape-dependent [36], and its increased biocompatibility and reduced cytotoxicity is reached through immobilization in nanotubular walls [37] or even through other nanostructures [38]. AgO is an empirical formula that suggests that silver is in the +2 oxidation state, which is repelled by a magnetic field [39].

In this investigation, we have analyzed the interaction of ZnO,  $Ag_2O$ , and Ag-doped ZnO hybrid nanocomposites (Ag-doped ZnO + AgO NCs) with glyphosate and possible implications in biosensing applications. These interactions were investigated by Fourier transform infrared spectroscopy (FTIR)

and atomic force microscopy (AFM), and we have shown for the first time that ZnO can be used as an FTIR enhancer enabling technology for glyphosate detection.

## MATERIALS AND METHODS

### Synthesis and Characterization of Nanocrystals

The ZnO nanocrystals were synthesized as described elsewhere [32], [40], [35] and patented in according to process number BR 10 2018 007714 7 - Instituto Nacional da Propriedade Industrial. The concentrations of silver during synthesis, labeled as x, were 0, 0.3 and 1.0 wt% relative to zinc (ZnO:xAg). Structural properties were investigated using X-ray diffraction (XRD) (DRX-6000, Shimadzu) with monochromatic radiation Cu-K $\alpha$ 1 ( $\lambda$  = 1.54,056 Å). We also used the Fourier transform infrared spectroscopy (FTIR) and atomic force microscopy (AFM) for characterization of samples ZnO:xAg.

### Characterization of the GLYPHOTAL TR<sup>®</sup> with Nanocrystals

Samples were prepared from a 10<sup>-2</sup> (v/v) dilution of GLYPHOTAL TR<sup>®</sup> (1:100 ultrapure water) that is composed. NCs were also diluted in ultrapure water (10 mg mL<sup>-1</sup>), which was properly mixed with GLYPHOTAL TR<sup>®</sup> dilutions to demonstrate enhancement properties. To demonstrate chelant properties, NCs were also diluted in ultrapure water (1.5 mg mL<sup>-1</sup>).

### Fourier transform infrared spectroscopy (FTIR)

Samples' spectra were recorded in 4000-400 cm<sup>-1</sup> range using FTIR spectrophotometer (Vertex 70, Bruker Optik) with a micro-attenuated total reflectance (ATR) accessory. The crystal material in the ATR unit was a diamond disc as an internal-reflection element. The sample penetration depth ranges between 0.1 and 2  $\mu$ m. Two  $\mu$ L of samples were dropped with a triple dental syringe to obtain FTIR spectra. The air spectrum was used as a background in the FTIR analysis. The samples spectra analyses were obtained with 2 cm<sup>-1</sup> of resolution and 34 scans.



## Atomic force microscopy (AFM)

The AFM images were performed to view the interaction of GLIFOTAL with NCs. To evaluate the interaction, we have dropped 3  $\mu\text{L}$  of GLYPHOTAL TR<sup>®</sup>-NC [ $10^{-4}$  (v/v)] solution onto the mica sheet surface and submitted to the Atomic Force Microscopy (AFM) with a very-high-resolution scanning probe [41]. Control groups were mica sheet and the nanofilm formed by GLYPHOTAL TR<sup>®</sup> when sheets were overlapped.

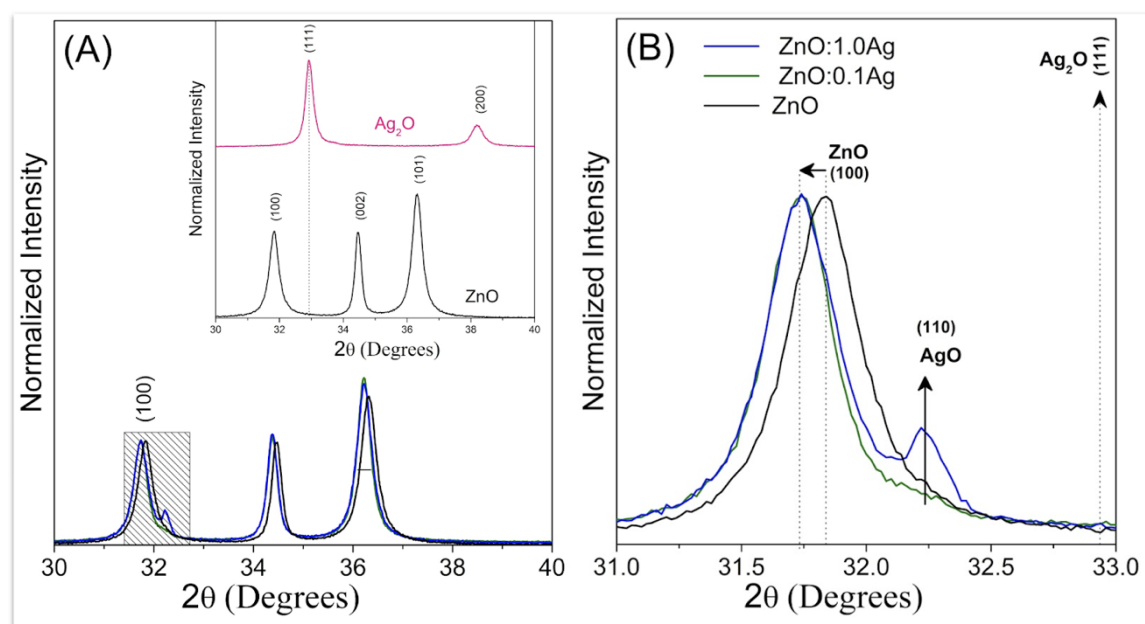
## Enhancement properties analysis

The FTIR spectra were obtained to investigate the glyphosate interactions with its commercial formulation (GLYPHOTAL TR<sup>®</sup>) and four types of nanocrystals (ZnO; ZnO:0.3Ag; ZnO:1Ag; Ag<sub>2</sub>O) in different dilutions. GLYPHOTAL TR<sup>®</sup> is formed by Isopropylammonium N-(phosphonomethyl) Glycine: 480 g L<sup>-1</sup> (48% m/v), acid equivalent: 360 g L<sup>-1</sup> (36% m/v) and other ingredients: 673,4 g L<sup>-1</sup> (67,34% m/v). It is classified as systemic, substituted Glycine chemical group, soluble concentrated, and pKa: < 2, 2.6, 5.6, 10.6.

## RESULTS

In order to investigate the interactions, we have mixed GLYPHOTAL TR® with the four previous cited nanocrystals in ultrapure water at four dilutions in ultrapure water:  $[10^{-2} \text{ (v/v)}]$  (which is usually used for soil applications),  $[10^{-4} \text{ (v/v)}]$ ,  $[10^{-6} \text{ (v/v)}]$  and  $[10^{-8} \text{ (v/v)}]$  or simply  $10^{-2}$ ,  $10^{-4}$ ,  $10^{-6}$ ,  $10^{-8}$ . To analyze the samples, 2  $\mu\text{L}$  of the GLYPHOTAL TR®-NC solutions were placed onto the FTIR crystal using a triple dental syringe, which was further dried at the environment temperature.

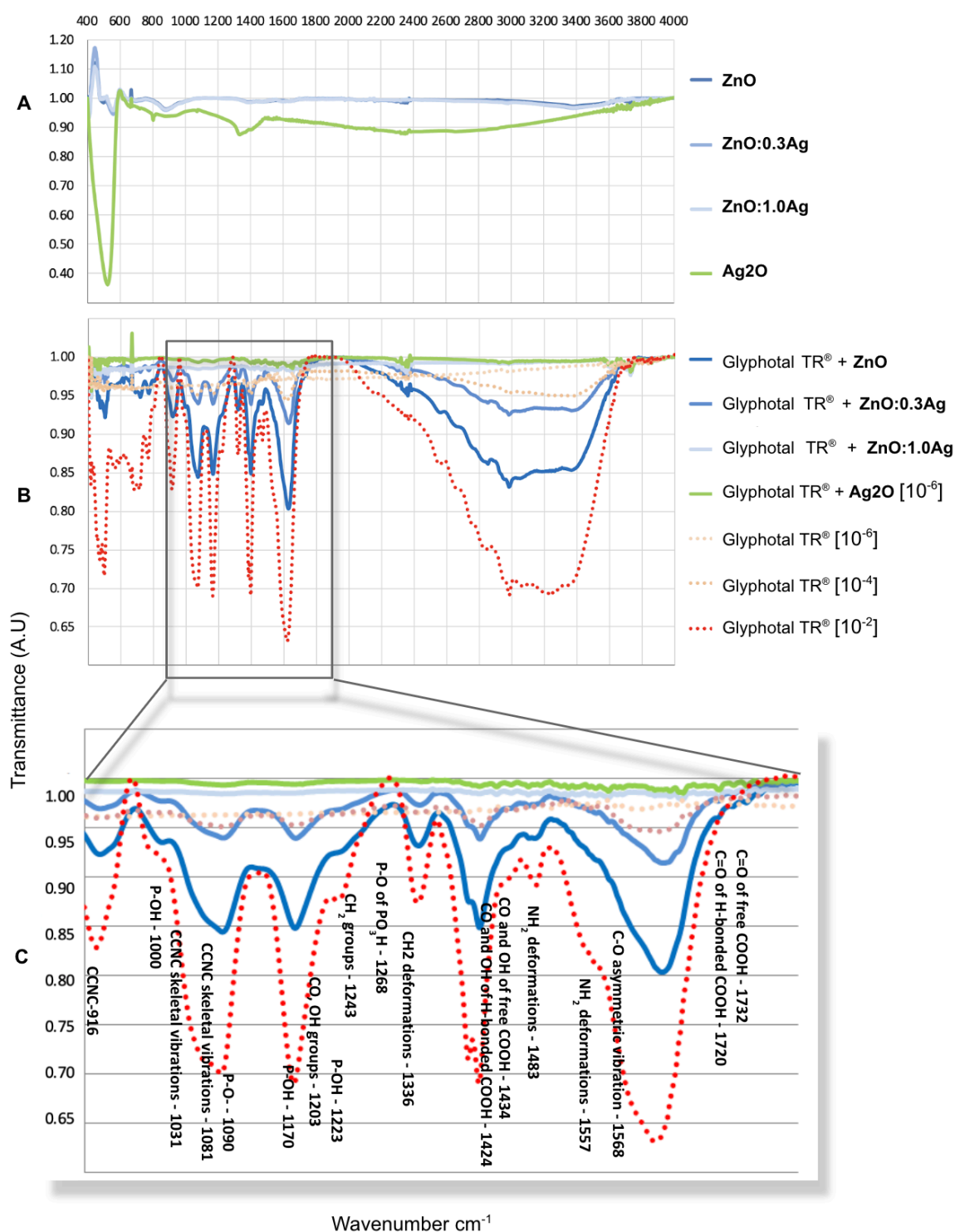
Figure 1 shows the XRD patterns of nanocrystals at room temperature. On Figure 1(A) its specific Bragg diffraction peaks show diffraction patterns of ZnO correlated with the wurtzite crystal structure (JCPDS 36-1451). The silver oxide standards correspond to the cubic crystalline structure of  $\text{Ag}_2\text{O}$  nanocrystals (JCPDS 76-1393). The average sizes of ZnO and  $\text{Ag}_2\text{O}$  nanocrystals are 28 nm and 30 nm, respectively. In order to investigate the effect of Ag incorporation into ZnO, a zoom performed around the peak 100 shows shifts on smaller angles relative to the ZnO peak (100) in Ag-doped samples, as shown in Figure 1(B). This result confirms the substitution of zinc by silver into the crystalline structure of ZnO, since  $\text{Ag}^{+2}$  has a larger ionic radius (1.26 Å) than  $\text{Zn}^{+2}$  (0.74 Å). The second magnification shows a typical AgO peak (JCPDS 43-1038) at a molar ratio of 1 Ag. The AgO percentage in the sample is 22.4. So, in this sample it was formed by a nanocomposite formed of Ag-doped ZnO and AgO NCs.



*Chapter III, Figure 1. (A) XRD of ZnO, Ag-doped ZnO and Ag<sub>2</sub>O nanocrystals. (B) The inset shows a zoom around the peak (100) of ZnO.*

Figure 2 shows the FTIR spectra of (A) the studied nanocrystals, (B) GLYPHOTAL TR<sup>®</sup> in three different dilutions ( $10^{-2}$ ,  $10^{-4}$ ,  $10^{-6}$  v/v) and the GLYPHOTAL TR<sup>®</sup>-NCs interaction at concentration ( $10^{-6}$ ), and (C) a zoom delimiting glyphosate on GLYPHOTAL TR<sup>®</sup> spectrum. Between 400-600  $\text{cm}^{-1}$  in (A) the characteristic bands were represented related to Zn-O and Ag-O bonds [42], [43]. These bands have a very low intensity compared to GLYPHOTAL TR<sup>®</sup>.

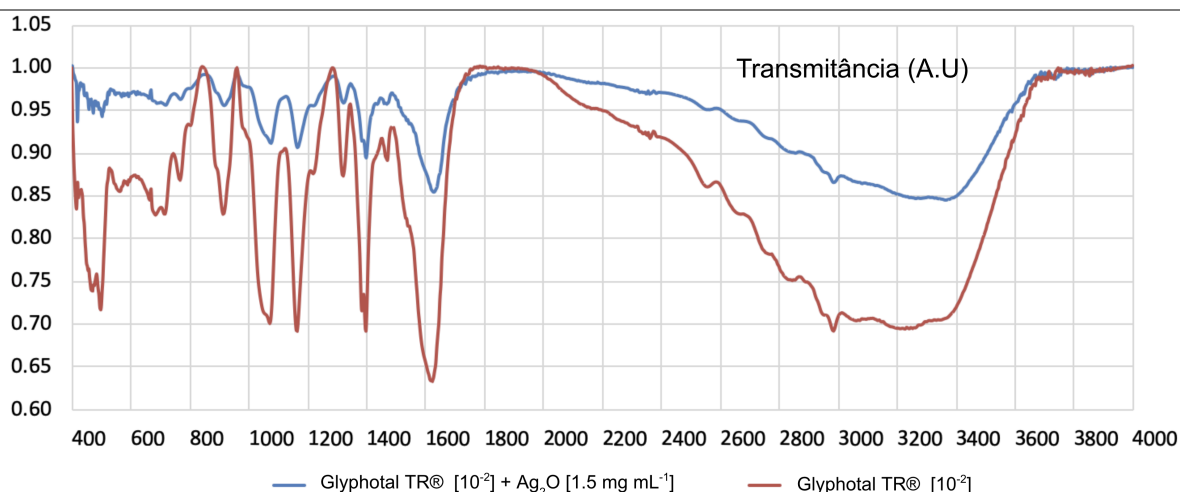
The enhancement properties were evidenced when ZnO nanocrystals were added to the GLYPHOTAL TR<sup>®</sup> solutions diluted at  $10^{-6}$  ( $480 \text{ ng mL}^{-1}$ ) in which bands were as visible as those diluted at  $10^{-3}$  without NCs. On the other hand, as the Ag had been added to the ZnO NC structure, the less vibratory frequency was detected, achieving its maximum with Ag<sub>2</sub>O NCs.



Chapter III, Figure 2. A) ZnO, ZnO:0.3Ag, ZnO:1.0Ag and Ag<sub>2</sub>O. (B) Glyphotal TR® at [10<sup>-2</sup> v/v], [10<sup>-4</sup> v/v] and [10<sup>-6</sup> v/v], and Glyphotal TR®-NCs interacted at 10<sup>-6</sup> v/v, (C) zoom of the glyphosate in Glyphotal TR® spectra.

At the opposite way, when the concentration of silver was increased, evidenced by nanocomposites and Ag<sub>2</sub>O NC, the enhancement properties did not

occur, achieving its maximum with Ag<sub>2</sub>O NCs. To demonstrate this property, Figure 3 shows that even a low Ag<sub>2</sub>O NC concentration is able to reduce FTIR vibrational signal.



**Chapter III, Figure 3. FTIR nanocrystals' spectra comparison of Glyphotal TR® at [10<sup>-2</sup> v/v] and Glyphotal TR®- Ag<sub>2</sub>O.**

We were able to show all glyphosate's groups through FTIR structural vibration frequencies' modes. Table 1 shows the frequency mode of each molecular group that compose glyphosate, and their frequency mode changes when interacted with each nanocrystal, and the differences (Ratio) for each NC considering the most and least diluted concentrations of Glyphotal TR® (10<sup>-6</sup>/10<sup>-2</sup>). Each bond that composes the molecular structure of each glyphosate functional group, after interactions with NCs, may present higher or less energy. So, each color represents the vibrational status of a specific bond. Blue represents the highest frequency, while red the lowest one. R is the Pearson's correlation among the referred NC and the respective glyphosate vibrational status, what has been characterized as the correlator. The closer to 1 the greater the positive correlation with the correlator. The first three columns composed by Glyphotal TR® in different concentrations show analytical limitations of the technique without nanomaterials, since just 10<sup>-2</sup> dilution could be observed. In this group, Glyphotal TR® (10<sup>-2</sup>) showed high vibrational modes at peaks 1568, 1557, 1170, 1081 and 1031 cm<sup>-1</sup>. The interaction of the four types of nanocrystals with the most diluted Glyphotal TR® solution showed that while ZnO enhanced the vibrational status of the herbicide, Ag<sub>2</sub>O diminished it. To understand where the nanocrystal was

bonded to the glyphosate structure, we have calculated the peak ratios for the NCs with the lower dilution (Ratio) for each vibrational mode. So, the Ratio's columns represent the NCs columns divided by the Glyphotal TR<sup>®</sup> (10<sup>-2</sup>) column.

				R=0.95	R=0.94	R=0.60	R=0.50	
A		Glyphosate [10 <sup>-6</sup> ]	Glyphosate [10 <sup>-4</sup> ]	Glyphosate [10 <sup>-2</sup> ]	ZnO [10 <sup>-6</sup> ]	ZnO AgO 0.3 [10 <sup>-6</sup> ]	ZnO AgO 1.0[10 <sup>-6</sup> ]	Ag2O [10 <sup>-6</sup> ]
CO and OH of H-bonded COOH - 1424								
	1424	0.743	0.745	0.808	0.780	0.745	0.730	0.724
CO and OH of free COOH - 1434								
	1434	0.742	0.743	0.802	0.775	0.742	0.730	0.724
C-O asymmetric vibration - 1568								
	1568	0.740	0.749	0.961	0.810	0.754	0.731	0.726
C=O of H-bonded COOH - 1720								
	1720	0.738	0.734	0.733	0.740	0.731	0.730	0.725
C=O of free COOH - 1732								
	1732	0.738	0.733	0.728	0.738	0.730	0.730	0.724
CO, OH groups - 1203								
	1203	0.746	0.748	0.823	0.784	0.746	0.729	0.722
P-OH - 1170								
	1170	0.747	0.756	1.000	0.843	0.765	0.731	0.724
P-OH - 1223								
	1223	0.746	0.747	0.820	0.778	0.743	0.729	0.722
P-OH - 1000								
	1000	0.748	0.746	0.785	0.770	0.737	0.730	0.722
P-O - 1090								
	1090	0.747	0.754	0.882	0.822	0.757	0.731	0.724
P-O of PO3H - 1268								
	1268	0.746	0.742	0.731	0.747	0.731	0.729	0.722
CH2 groups - 1243								
	1243	0.746	0.745	0.771	0.765	0.738	0.729	0.722
CH2 deformations - 1336								
	1336	0.746	0.744	0.772	0.755	0.734	0.729	0.722
NH2 deformations - 1557								
	1557	0.737	0.742	0.908	0.796	0.751	0.733	0.728
NH2 deformations - 1483								
	1483	0.742	0.740	0.774	0.753	0.734	0.730	0.723
CCNC skeletal vibrations - 1081								
	1081	0.748	0.757	0.971	0.844	0.764	0.731	0.725
CCNC skeletal vibrations - 1031								
	1031	0.748	0.752	0.952	0.808	0.750	0.730	0.723
CCNC - 916								
	916	0.749	0.750	0.868	0.780	0.742	0.730	0.722
					Improvement on signal quality			

B

	Ratio and Great group Color Map				Ratio and Great group Color Map			
	ZnO[10 <sup>-6</sup> ]/ Glyphosate [10 <sup>-2</sup> ]	ZnO AgO 0.3 [10 <sup>-6</sup> ]/ Glyphosate [10 <sup>-2</sup> ]	ZnO AgO 1.0[10 <sup>-6</sup> ]/ Glyphosate [10 <sup>-2</sup> ]	Ag2O[10 <sup>-6</sup> ]/ Glyphosate [10 <sup>-2</sup> ]	ZnO[10 <sup>-6</sup> ]/ Glyphosate [10 <sup>-2</sup> ]	ZnO AgO 0.3 [10 <sup>-6</sup> ]/ Glyphosate [10 <sup>-2</sup> ]	ZnO AgO 1.0[10 <sup>-6</sup> ]/ Glyphosate [10 <sup>-2</sup> ]	Ag2O[10 <sup>-6</sup> ]/ Glyphosate [10 <sup>-2</sup> ]
CO and OH of H-bonded COOH - 1424	0.965	0.922	0.904	0.896	0.965	0.922	0.904	0.896
CO and OH of free COOH - 1434	0.966	0.926	0.911	0.903	0.966	0.926	0.911	0.903
C-O asymmetric vibration - 1568	0.842	0.784	0.761	0.755	0.842	0.784	0.761	0.755
C=O of H-bonded COOH - 1720	1.010	0.997	0.997	0.989	1.010	0.997	0.997	0.989
C=O of free COOH - 1732	1.013	1.002	1.002	0.994	1.013	1.002	1.002	0.994
CO, OH groups - 1203	0.952	0.906	0.886	0.877	0.952	0.906	0.886	0.877
P-OH - 1170	0.843	0.765	0.731	0.724	0.843	0.765	0.731	0.724
P-OH - 1223	0.949	0.907	0.890	0.881	0.949	0.907	0.890	0.881
P-OH - 1000	0.980	0.938	0.930	0.919	0.980	0.938	0.930	0.919
P-O - 1090	0.932	0.859	0.829	0.821	0.932	0.859	0.829	0.821
P-O of PO3H - 1268	1.022	1.001	0.997	0.987	1.022	1.001	0.997	0.987
CH2 groups - 1243	0.992	0.958	0.946	0.937	0.992	0.958	0.946	0.937
CH2 deformations - 1336	0.979	0.951	0.944	0.935	0.979	0.951	0.944	0.935
NH2 deformations - 1557	0.876	0.826	0.808	0.802	0.876	0.826	0.808	0.802
NH2 deformations - 1483	0.972	0.948	0.943	0.934	0.972	0.948	0.943	0.934
CCNC skeletal vibrations - 1081	0.869	0.787	0.753	0.746	0.869	0.787	0.753	0.746
CCNC skeletal vibrations - 1031	0.848	0.788	0.767	0.759	0.848	0.788	0.767	0.759
CCNC - 916	0.899	0.855	0.841	0.832	0.899	0.855	0.841	0.832

Chapter III, Figure 4. Energy color scale. A compares the signal intensity of different Glyphosate and Glyphosate -NCs. As more colored as mor intensity. B compares the signal intensity of the

---

*Glyphosate-NCs and Glyphosate at 10<sup>-2</sup> (v/v) solution. The left table all Glyphosate-NCs structures were compared among them. As bluer more evident the signal. The right table compares the structures of each Nanocrystal among itself.*

---

The AFM images of the samples are shown in Figure 4. The images for the control group showed a very smooth surface and the roughness for GLYPHOTAL TR<sup>®</sup>. The right panels show transects of the AFM bidimensional images. At the experimental groups, we were able to show different structures formed by those nanoparticles when associated with Glyphotal TR<sup>®</sup>.

ZnO in water was commonly found ungrouped and dispersed on water, and in association with Glyphotal TR<sup>®</sup>. This specific interaction is evidenced by a single unit, and not as a cluster. Differently, the interaction formed with more than 1% of Ag in water are always seen as clusters, but when associated with GLYPHOTAL TR<sup>®</sup> it forms volcanic-like structures.

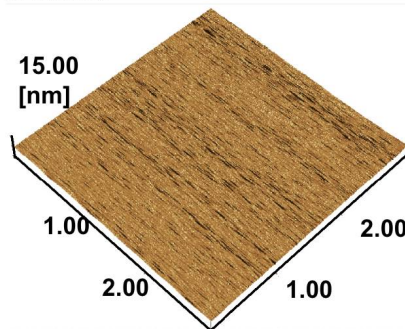
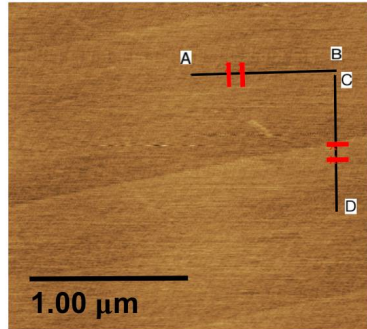
In water, it was observed that nanocrystals presented different degrees of aggregation. While ZnO and ZnO:0.3Ag were well dispersed, the ZnO:1Ag and Ag<sub>2</sub>O were not. In addition, the ZnO:1Ag image confirms that the nanocomposite is a hybrid NC with different sizes. These results are in agreement with the X-ray diffractograms, confirming the presence of the hybrid nanocomposite (Ag-doped ZnO + AgO NCs).



## CONTROL GROUPS

**A**

**Mica sheet**



0.62 [nm]

Width[nm]

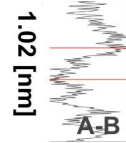
0.22

Height[nm]

0.53

Angle[deg]

0.14



1.20 [nm]

Width[nm]

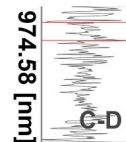
125.89

Height[nm]

1.08

Angle[deg]

0.49



1.52 [nm]

Width[nm]

8.41

7.97

Height[nm]

0.24

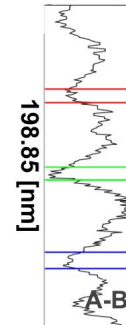
0.05

Angle[deg]

1.62

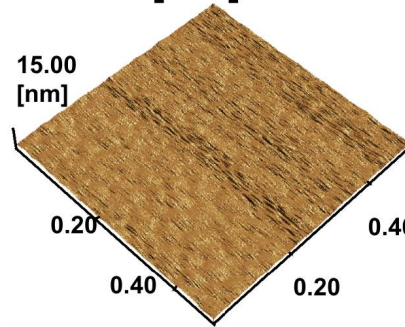
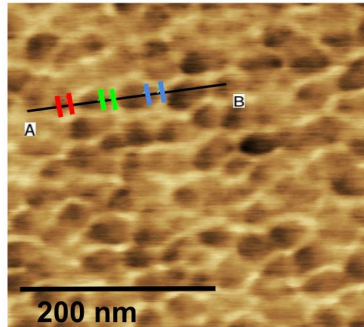
0.34

0.51



**B**

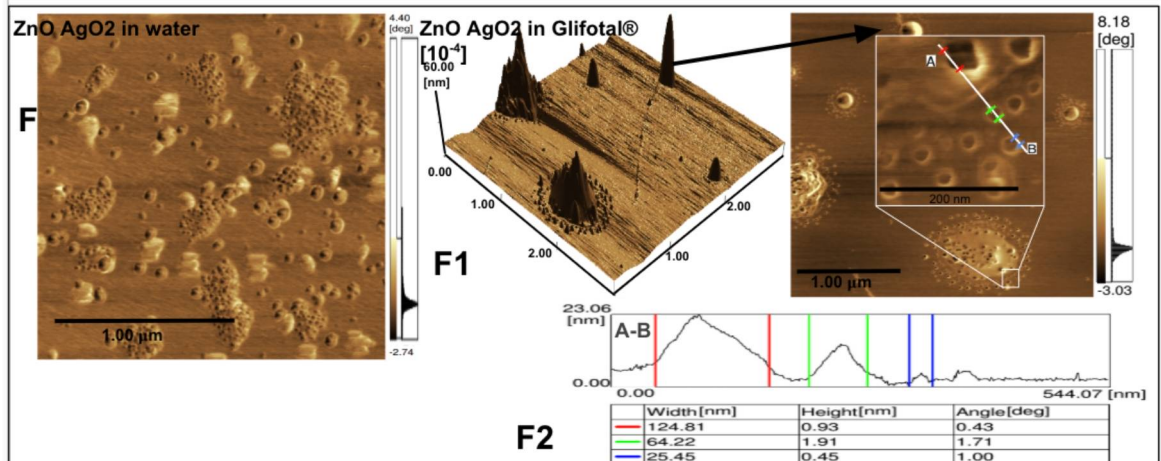
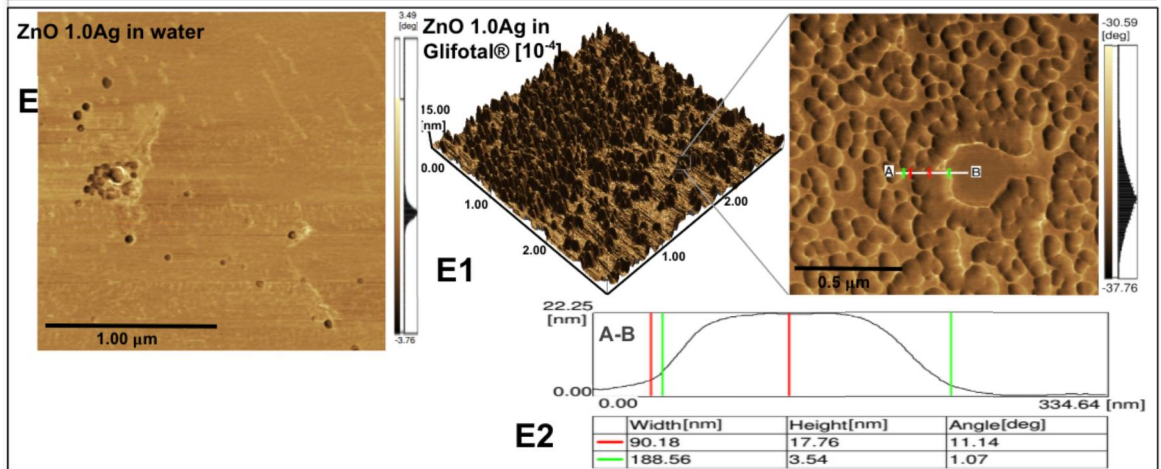
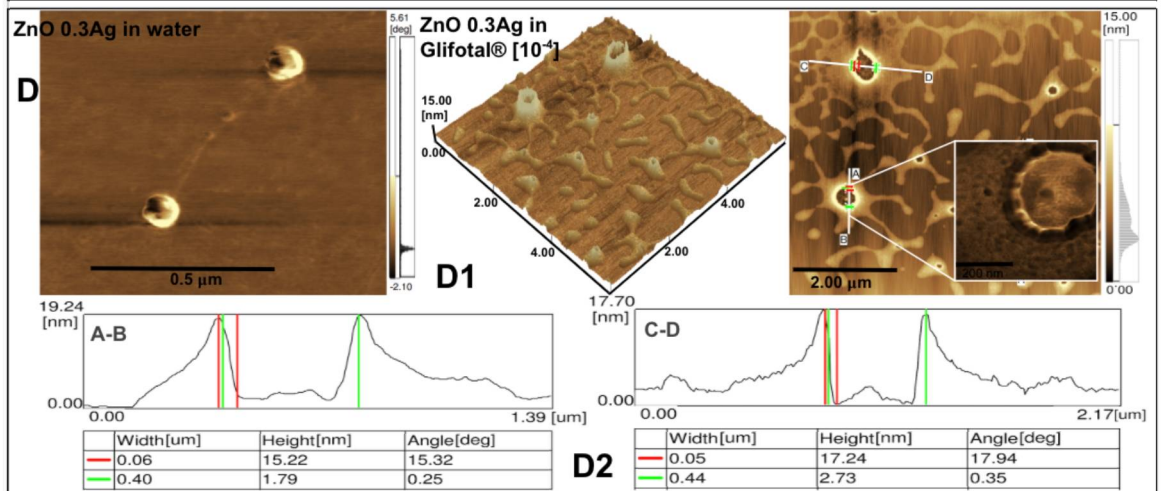
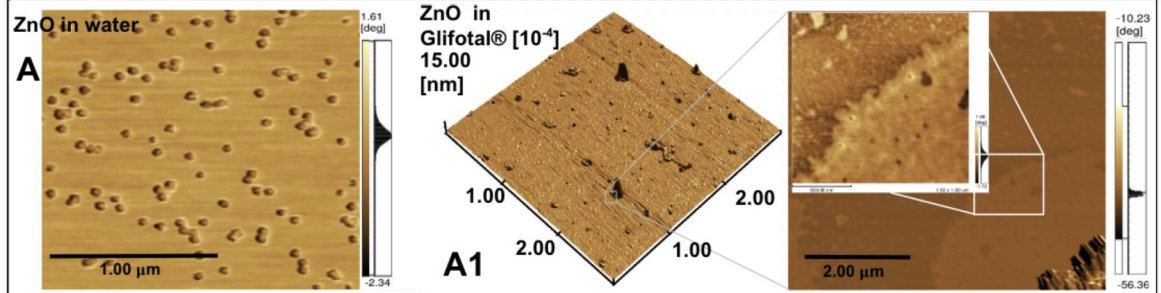
**Glifotal TR® [10<sup>-4</sup>] solution**





## Nanocrystals in water

## Nanocrystals in Glifotal TR® [10<sup>-4</sup>] solution



## DISCUSSION

Glyphosate detection and quantification is expensive and slow [44,45]. There is an ineffective governmental control because glyphosate cannot be detected by multiresidue methods. The impact of this knowledge gap on the health system and public economy is unknown. Hence, the concept of the “glyphosate's paradox” was raised, which means that besides glyphosate being the most widely used agrochemical in the world, it is also the most hardly determined by analytical methods [7,46].

The regulatory rules regarding the maximum residue limit (MRL) for both crops and water adopted by each country differ significantly. For example, the largest value established by the United State Environmental Protection Agency (EPA) for soybean was 20 mg kg<sup>-1</sup>. Independently of the structure or activity of the compound, the European Union has set the MRL of pesticides in 0.1 ng mL<sup>-1</sup>, while the EPA's MRL, established in terms of persistence and toxicity of each pesticide individually, was 700 ng mL<sup>-1</sup> [47]. The Canadian Drinking Water Guideline recommends an MRL of 280 ng mL<sup>-1</sup>, and the Brazilian Surveillance Agency (ANVISA) an MRL of 500 ng mL<sup>-1</sup>. It is important to emphasize that analyses on current approvals by the EU and USA regarding glyphosate's levels suggest that the established acceptable daily intake levels are inaccurate and dangerously high [48], especially because agencies used information provided by studies performed by the industries. All these facts have raised questions about how safe glyphosate levels are, which is further complicated by the fact that many technical approaches present Limits of Detection (LODs) that are far away from Agency's control interest.

In this way, we have shown in this investigation for the first time that the ZnO nanocrystal may be used as an enhancing agent for the FTIR glyphosate detection methodology. The opposite effect was observed as the Ag ion was incorporated into the NCs, since the Ag ion functioned as a chelating agent on

glyphosate leading to a full signal suppression when Ag<sub>2</sub>O was mixed. Interestingly, we have also shown for the first time that both ZnO and Ag<sub>2</sub>O NCs mixed in water have almost no effect on FTIR, suggesting that the ZnO NC did impact the glyphosate structure inducing a differential vibrational mode.

It is known that ZnO interacts with glyphosate and has a direct effect on environment impacting the nutrient uptake and translocation by “non-target” plants more than Fe and Mn [49], reducing weed control between 43 and 59 percent if done in the same solution before application, reducing biomass of Zn in 88 to 96 percent when applied alone or reducing 41 percent of the Zn biomass in co-application [50]. Foliar absorption is too widely reduced when glyphosate is applied in solution with Zn, Ca, Fe, Mg and Mn [51]. Comparing N, P, K, Cu and Zn, the most decreased foliar nutrient level observed post-glyphosate application was N and Zn, and both were correlated with glyphosate concentration [52], [53]. At sunflower, it reduces the absorption and translocation of radiolabeled Fe<sup>59</sup>, Zn<sup>65</sup> e Mn<sup>54</sup> [49], [54]. Plants intoxicated by glyphosate present the same morphological alterations as those observed for N, B, Fe and Zn deficiency [55],[56],[57],[58]. These reports not only corroborate our findings, but also indicate that the strong interaction of Zn with glyphosate may be a problem for glyphosate detection in soils. It remains to be demonstrated if the ZnO nanocrystals would have stronger binding affinity than the Zn ions found in the soil.

After interaction with a nanocrystal, some glyphosate structures diminished their vibrational status, while others have shown increased vibrational modes, probably indicating free groups without bond formation. The lowest vibrational frequency at ZnO-Glyphosate was found at the C=O of free COOH and C=O of H bonded COOH, and at second place at the NH<sub>2</sub> and P-O of PO<sub>3</sub>H. When Glyphotal TR<sup>®</sup> was not interacted with nanocrystals, its vibrational status was low at 1732 cm<sup>-1</sup>, but increased in 1% when interacted with ZnO.

These data suggest that while Ag is fully interacting with glyphosate in a less or more strong binding, ZnO is not bond to the corresponding 1732 cm<sup>-1</sup>, 1720 cm<sup>-1</sup> and 1268 cm<sup>-1</sup> wavenumber regions. The stronger bonds were related to the 1568 cm<sup>-1</sup>, 1557 cm<sup>-1</sup>, 1170 cm<sup>-1</sup>, 1081 cm<sup>-1</sup> and 1031 cm<sup>-1</sup> wavenumber

peaks. Ratio shows that interactions containing Ag are stronger than with ZnO. This can also be observed in AFM images, especially showing the volcanic structures formed when Ag interacted with glyphosate. On the other hand, glyphosate molecules are aggregated around ZnO. In both cases, the NC aggregate not only glyphosate, but everything that compose GLYPHOTAL TR®. This interaction is strong enough to retrieve all nanocrystals, water, surfactants or any other material at the surface of the mica sheet.

We suggest that glyphosate aggregation is assembled as a net structure, aligning glyphosate molecule threads around ZnO NC (nucleus). This alignment starts probably from structures that are less free, corresponding to the bands at  $1031\text{ cm}^{-1}$ ,  $1081\text{ cm}^{-1}$ ,  $1179\text{ cm}^{-1}$ ,  $1557\text{ cm}^{-1}$ , and  $1568\text{ cm}^{-1}$ . These structures interact directly with nanocrystals creating an alignment that coordinate the arrangement of glyphosate molecules in a pairwise fashion, even those that cannot interact directly with the nanocrystals, probably created by a differential charge in the first molecules bonded to the NC. Analogously, the bands at  $1732\text{ cm}^{-1}$ ,  $1720\text{ cm}^{-1}$  and  $1268\text{ cm}^{-1}$  remained less interaction. However, the peak at  $1170\text{ cm}^{-1}$  can be attributed by the presence of  $\text{R-PO(OH)}_2$ . This group has the capacity to form strong complexes with metal that may result in adsorption, photodegradation, biodegradation processes and the formation of soluble and insoluble complexes [24].

It is reported in the literature that the use of ZnO-NC decorated on the surface of multiwalled carbon nanotubes can enhance electrochemiluminescence signals to detect glyphosate [59]. The detection could reach limits lower than  $1\text{ }\mu\text{mol L}^{-1}$ . In addition, these methods are cheaper, faster, and more sensitive than many spectroscopic tests. Besides, a sensor for detecting pesticides in water, using the photoluminescence intensity of ZnCdSe quantum dot has also been developed [60]. However, to our knowledge, our investigation is the first to report the use of ZnO as an FTIR-enhancer to improve detection of glyphosate. These results demonstrated that glyphosate infrared modes can be intensified probably due to the organizational interaction between glyphosate and nanocrystals.

There are accurate and sensitive technologies related to atomic absorption spectrometry, electrothermal atomization atomic absorption spectrometry [61],[62], flame atomic absorption spectrometry [63],[64],[65], and fading spectrophotometry. All of them suffer from the requirement of well-established laboratory settings, high complexity, and long testing times. Theoretically, all these spectrophotometric techniques could have their minimum limit of detection enhanced by ZnO-NC.

On the other hand, the chelating ability of glyphosate by the NC is directly proportional to the Ag concentration. We suggest that the Ag binds to phosphonate and carboxylate groups making them to vibrate in the FTIR in a very restrictive manner. Comparing our results with the PVP-capped silver nanocubes system for glyphosate removal from water [66], we corroborated those results in many aspects, and it is possible that our  $\text{Ag}_2\text{O}$  NC could also be efficiently used for glyphosate removal from water too. The difference between our work and the later one is that while they have shown different absorption peaks for glyphosate FTIR spectra for the PVP-capped silver nanocubes binding, our  $\text{Ag}_2\text{O}$ -NC was quite stable and homogeneous, suggesting that our NC has efficiently immobilized glyphosate.

This hypothesis explains the “volcanic like” structures formed with Ag. It works by aggregating glyphosate, and the empty nucleus of the volcanic-like structure is explained by this aggregation behavior. In water, it is very hard to maintain ungrouped  $\text{Ag}_2\text{O}$ , because of charge interactions. When an  $\text{Ag}_2\text{O}$  NC enters in contact with glyphosate, a chelate formed, and glyphosate gradually replaces its uncharged bonds by ionic ones. In Figure 5F, small isolated  $\text{Ag}_2\text{O}$ -NCs are separated from the main  $\text{Ag}_2\text{O}$ -NC aggregates, which is then surrounded by glyphosate.

For this reason, we believe that  $\text{Ag}_2\text{O}$ -NCs could also be used to promote glyphosate removal from water, e.g in an Ag-magnetic core shell. A photoluminescence study [66] has previously shown that silver nanocubes degrade glyphosate present in drinking water. The study confirmed that silver nanoparticles can fully degrade glyphosate, evidenced by the intensity of photoluminescence spectra that gradually decreased as the glyphosate

concentration diminished [67], concluding that the adsorption of the amine group of glyphosate is bonded onto silver nanocrystals, leading to the aggregation of Ag<sub>2</sub>O-NCs.

The characterization of the glyphosate removal is not simple, mainly because it was never found in a non-complexed form in non-laboratorial situations. It means that it needs to be firstly unbonded. Fortunately, the interaction between glyphosate and other metals are pH dependent [68],[69],[70,71],[72],[73],[74],[70],[71]. Glyphosate exists in a zwitterion form with adjuvants or surfactants in order to improve its activity. It is an aminophosphonic analogue of the natural amino acid glycine, and so, can be protonated, presenting different ionic states depending on pH. It has a carboxylic acid and an amino group, the first one and the phosphonic acid can be ionized and the second can be protonated [75]. Glyphosate assume the following protonation states: pKa<sub>1</sub> = 0.47, pKa<sub>2</sub> = 5.69, and pKa<sub>3</sub> = 11.81 [76], where at pH 6.0 both phosphonate and amino group are ionized [77], suggesting that strategies of glyphosate separation or purification based on pH changes are possible.

Finally, glyphosate has more than one thousand analogues [78], but there are only two very similar analogues, which are as effective to the same extent as glyphosate is, the N-hydroxy-glyphosate and N-amino-glyphosate [79]. Once the phosphonates adsorb very strongly onto almost all mineral surfaces [80], we believe that the ZnO enhancing properties could also be applied to them. On the other hand, we do not expect the same for amino-carboxylates, in which interactions with mineral surfaces are weak, especially at near neutral pH [80].

## CONCLUSION

In this investigation, we have shown that ZnO nanocrystals can be used as signal enhancer of vibrational frequencies in FTIR, even if it is in solution with its unknown adjuvants. The specific characteristics of this nanomaterial may also be used to improve other spectroscopic methods. We have also shown a very high chelating properties of Ag<sub>2</sub>O, which may be used to develop strategies

for glyphosate recovery from the environment, either for purification or sensing purposes.

## References

- [1] C.M. Benbrook, Trends in glyphosate herbicide use in the United States and globally, *Environ Sci Eur.* 28 (2016) 3. doi:10.1186/s12302-016-0070-0.
- [2] J.P. Giesy, S. Dobson, K.R. Solomon, Ecotoxicological Risk Assessment for Roundup® Herbicide, in: G.W. Ware (Ed.), *Reviews of Environmental Contamination and Toxicology*, Springer New York, 2000: pp. 35–120. doi:10.1007/978-1-4612-1156-3\_2.
- [3] M.T.K. Tsui, L.M. Chu, Aquatic toxicity of glyphosate-based formulations: comparison between different organisms and the effects of environmental factors, *Chemosphere.* 52 (2003) 1189–1197. doi:10.1016/S0045-6535(03)00306-0.
- [4] W.H. Organization, Others, Glyphosate environmental health criteria No. 159, WHO, Geneva. 177 (1994).
- [5] M.T.K. Tsui, L.M. Chu, Environmental fate and non-target impact of glyphosate-based herbicide (Roundup®) in a subtropical wetland, *Chemosphere.* 71 (2008) 439–446. doi:10.1016/j.chemosphere.2007.10.059.
- [6] G.M. Williams, R. Kroes, I.C. Munro, Safety evaluation and risk assessment of the herbicide Roundup and its active ingredient, glyphosate, for humans, *Regul. Toxicol. Pharmacol.* 31 (2000) 117–165. doi:10.1006/rtph.1999.1371.
- [7] †. Miguel Ángel González-Martínez, †. Eva María Brun, †. Rosa Puchades, †. Ángel Maquieira, ‡. Kristy Ramsey, ‡. Fernando Rubio\*, Glyphosate Immunosensor. Application for Water and Soil Analysis, *Anal. Chem.* 77 (2005) 4219–4227. doi:10.1021/ac048431d.



[8] I. Agency for Research on Cancer - Recuperado de <http://www.iarc.fr>, 2015, IARC Monographs Volume 112: evaluation of five organophosphate insecticides and herbicides, (2015).

[9] H. Vereecken, Mobility and leaching of glyphosate: a review, *Pest Manag. Sci.* 61 (2005) 1139–1151. doi:10.1002/ps.1122.

[10] Y.S. Wang, C.G. Jaw, Y.L. Chen - Water, Air, & Soil Pollution, 1994, Accumulation of 2, 4-D and glyphosate in fish and water hyacinth, Springer. (1994). <http://www.springerlink.com/index/T3M4821Q7R761V18.pdf>.

[11] M. Krüger, P. Schledorn, W. Schrödl - ... of Environmental & ..., 2014, Detection of glyphosate residues in animals and humans, Pdfs.semanticscholar.org. (2014). <https://pdfs.semanticscholar.org/78f1/ca9c4e4db7a404c58dff82b5e8822dad7b42.pdf>.

[12] J. Rendon-von Osten, R. Dzul-Caamal, Glyphosate Residues in Groundwater, Drinking Water and Urine of Subsistence Farmers from Intensive Agriculture Localities: A Survey in Hopelchén, Campeche, Mexico, *Int. J. Environ. Res. Public Health*. 14 (2017). doi:10.3390/ijerph14060595.

[13] G. Chaufan, I. Coalova, M.D.C. Ríos de Molina, Glyphosate commercial formulation causes cytotoxicity, oxidative effects, and apoptosis on human cells: differences with its active ingredient, *Int. J. Toxicol.* 33 (2014) 29–38. doi:10.1177/1091581813517906.

[14] S. Richard, S. Moslemi, H. Sipahutar, N. Benachour, G.-E. Seralini, Differential effects of glyphosate and roundup on human placental cells and aromatase, *Environ. Health Perspect.* 113 (2005) 716–720. <http://www.ncbi.nlm.nih.gov/pubmed/15929894>.

[15] A.L. Valle, F.C.C. Mello, R.P. Alves-Balvedi, L.P. Rodrigues, L.R. Goulart, Glyphosate detection: methods, needs and challenges, *Environ. Chem. Lett.* (2018). doi:10.1007/s10311-018-0789-5.

[16] M.E. Poulsen, H.B. Christensen, S.S. Herrmann, Proficiency test on incurred and spiked pesticide residues in cereals, *Accredit. Qual. Assur.* 14 (2009) 477–485. doi:10.1007/s00769-009-0555-2.

[17] R.J. Hance, Herbicide usage and soil properties, *Plant Soil.* 45 (1976) 291–293. <http://www.jstor.org/stable/42947022>.

[18] D.G. Thompson, J.E. Cowell, R.J. Daniels, B. Staznik, L.M. MacDonald, Liquid chromatographic method for quantitation of glyphosate and metabolite residues in organic and mineral soils, stream sediments, and hardwood foliage, *J. Assoc. Off. Anal. Chem.* 72 (1989) 355–360. <http://www.ncbi.nlm.nih.gov/pubmed/2708285>.

[19] M.L. Rueppel, B.B. Brightwell, J. Schaefer, J.T. Marvel, Metabolism and degradation of glyphosate in soil and water, *J. Agric. Food Chem.* 25 (1977) 517–528. doi:10.1021/jf60211a018.

[20] F.C. Moraes, L.H. Mascaro, S.A.S. Machado, C.M.A. Brett, Direct Electrochemical Determination of Glyphosate at Copper Phthalocyanine/Multiwalled Carbon Nanotube Film Electrodes, *Electroanalysis.* 22 (2010) 1586–1591. doi:10.1002/elan.200900614.

[21] P.H. Smith, F.E. Hahn, A. Hugi, K.N. Raymond, Crystal structures of two salts of N-(phosphonomethyl)glycine and equilibria with hydrogen and bicarbonate ions, *Inorg. Chem.* 28 (1989) 2052–2061. doi:10.1021/ic00310a010.

[22] E.T. Clarke, P.R. Rudolf, A.E. Martell, A. Clearfield, Structural investigation of the Cu (II) chelate of N-phosphonomethylglycine. X-ray crystal structure of Cu (II)[O 2 CCH 2 NHCH 2 PO 3]textperiodcentered Na (H 2 O) 3.5, *Inorganica Chim. Acta.* 164 (1989) 59–63. <http://www.sciencedirect.com/science/article/pii/S0020169300808762>.

[23] H.E.L. Madsen, H.H. Christensen, C. Gottlieb-Petersen, A.F. Andresen, O. Smidsrød, C.-O. Pontchour, P. Phavanantha, S. Pramatus, B.N. Cyvin, S.J. Cyvin, Stability Constants of Copper(II), Zinc, Manganese(II), Calcium,

and Magnesium Complexes of N-(Phosphonomethyl)glycine (Glyphosate), *Acta Chem. Scand.* 32a (1978) 79–83. doi:10.3891/acta.chem.scand.32a-0079.

[24] M.S. Caetano, T.C. Ramalho, D.F. Botrel, E.F.F. da Cunha, W.C. de Mello, Understanding the inactivation process of organophosphorus herbicides: A DFT study of glyphosate metallic complexes with  $\text{Zn}^{2+}$ ,  $\text{Ca}^{2+}$ ,  $\text{Mg}^{2+}$ ,  $\text{Cu}^{2+}$ ,  $\text{Co}^{3+}$ ,  $\text{Fe}^{3+}$ ,  $\text{Cr}^{3+}$ , and  $\text{Al}^{3+}$ , *Int. J. Quantum Chem.* 112 (2012) 2752–2762. <http://onlinelibrary.wiley.com/doi/10.1002/qua.23222/full>.

[25] B.J. Alloway, Zinc in soils and crop nutrition, (2004). <http://www.topsoils.co.nz/wp-content/uploads/2014/09/Zinc-in-Soils-and-Crop-Nutrition-Brian-J.-Alloway.pdf>.

[26] M.V. Singh, I.P. Abrol, Transformation and availability of zinc in alkali soils, *Fert News*. 31 (1986) 17–27.

[27] L. Polavarapu, J. Pérez-Juste, Q.-H. Xu, L.M. Liz-Marzán, Optical sensing of biological, chemical and ionic species through aggregation of plasmonic nanoparticles, *J. Mater. Chem.* 2 (2014) 7460–7476. doi:10.1039/C4TC01142B.

[28] K.A. Rawat, R.P. Majithiya, J.V. Rohit, H. Basu, R.K. Singhal, S.K. Kailasa,  $\text{Mg}^{2+}$  ion as a tuner for colorimetric sensing of glyphosate with improved sensitivity via the aggregation of 2-mercapto-5-nitrobenzimidazole capped silver nanoparticles, *RSC Adv.* 6 (2016) 47741–47752. doi:10.1039/C6RA06450G.

[29] R.E. De Góes, M. Muller, J.L. Fabris, Spectroscopic Detection of Glyphosate in Water Assisted by Laser-Ablated Silver Nanoparticles, *Sensors* . 17 (2017). doi:10.3390/s17050954.

[30] M. Rao, T. Okada, ZnO nanocrystals and allied materials, (2014). <http://link.springer.com/content/pdf/10.1007/978-81-322-1160-0.pdf>.

[31] M.A. Fox, M.T. Dulay, Heterogeneous photocatalysis, *Chem. Rev.* 93 (1993) 341–357. doi:10.1021/cr00017a016.

[32] É. de Melo Reis, A. de Rezende, D.V. Santos - Food and Chemical ..., 2015, Assessment of the genotoxic potential of two zinc oxide sources (amorphous and nanoparticles) using the in vitro micronucleus test and the in vivo wing ..., Elsevier Oceanogr. Ser. (2015). <http://www.sciencedirect.com/science/article/pii/S0278691515300168>.

[33] J. Hussein, M. El-Banna, T.A. Razik, M.E. El-Naggar, Biocompatible zinc oxide nanocrystals stabilized via hydroxyethyl cellulose for mitigation of diabetic complications, Int. J. Biol. Macromol. (2017). doi:10.1016/j.ijbiomac.2017.09.056.

[34] Y. Zhang, T.R. Nayak, H. Hong, W. Cai, Biomedical applications of zinc oxide nanomaterials, Curr. Mol. Med. 13 (2013) 1633–1645. <https://www.ncbi.nlm.nih.gov/pubmed/24206130>.

[35] P.V. Morais, V.F. Gomes, A.C.A. Silva, N.O. Dantas, M.J. Schöning, J.R. Siqueira, Nanofilm of ZnO nanocrystals/carbon nanotubes as biocompatible layer for enzymatic biosensors in capacitive field-effect devices, J. Mater. Sci. 52 (2017) 12314–12325. doi:10.1007/s10853-017-1369-y.

[36] X. Wang, H.-F. Wu, Q. Kuang, R.-B. Huang, Z.-X. Xie, L.-S. Zheng, Shape-dependent antibacterial activities of Ag<sub>2</sub>O polyhedral particles, Langmuir. 26 (2010) 2774–2778. doi:10.1021/la9028172.

[37] H. Cao, Silver Nanoparticles for Antibacterial Devices: Biocompatibility and Toxicity, CRC Press, 2017. <https://market.android.com/details?id=book-HTkkDwAAQBAJ>.

[38] J.-J. Lin, W.-C. Lin, S.-D. Li, C.-Y. Lin, S.-H. Hsu, Evaluation of the antibacterial activity and biocompatibility for silver nanoparticles immobilized on nano silicate platelets, ACS Appl. Mater. Interfaces. 5 (2013) 433–443. doi:10.1021/am302534k.

[39] A.F. Wells, Structural inorganic chemistry, Oxford University Press, USA, 1984.

[https://books.google.com/books/about/Structural\\_inorganic\\_chemistry.html?hl=&id=IQfwAAAAMAAJ](https://books.google.com/books/about/Structural_inorganic_chemistry.html?hl=&id=IQfwAAAAMAAJ).

[40] C.J.A. Sousa, M.C. Pereira, R.J. Almeida, A.M. Loyola, A.C.A. Silva, N.O. Dantas, Synthesis and characterization of zinc oxide nanocrystals and histologic evaluation of their biocompatibility by means of intraosseous implants, *Int. Endod. J.* 47 (2014) 416–424. doi:10.1111/iej.12164.

[41] N.O. Dantas, A.S. Silva, A. Silva - Optical Imaging ..., 2012, Atomic and magnetic force microscopy of semiconductor and semimagnetic nanocrystals grown in colloidal solutions and glass matrices, Researchgate.net. (2012). [https://www.researchgate.net/profile/Ernesto\\_Neto/publication/233639440\\_Atomic\\_and\\_Magnetic\\_Force\\_Microscopy\\_of\\_Semiconductor\\_and\\_Semimagnetic\\_Nano\\_crystals\\_Grown\\_in\\_Colloidal\\_Solutions\\_and\\_Glass\\_Matrices/links/0deec51b9eb2642c33000000.pdf](https://www.researchgate.net/profile/Ernesto_Neto/publication/233639440_Atomic_and_Magnetic_Force_Microscopy_of_Semiconductor_and_Semimagnetic_Nano_crystals_Grown_in_Colloidal_Solutions_and_Glass_Matrices/links/0deec51b9eb2642c33000000.pdf).

[42] A. Kołodziejczak-Radzimska, T. Jesionowski, Zinc Oxide—From Synthesis to Application: A Review, *Materials* . 7 (2014) 2833–2881. doi:10.3390/ma7042833.

[43] M.R.H. Siddiqui, S. Adil, M. Assal, R. Ali, Synthesis and characterization of silver oxide and silver chloride nanoparticles with high thermal stability, *Asian J. Chem.* (2013). [https://www.researchgate.net/profile/M\\_R\\_Siddiqui/publication/235766964\\_Synthesis\\_and\\_Characterization\\_of\\_Silver\\_Oxide\\_and\\_SilverChloride\\_Nanoparticles\\_with\\_High\\_Thermal\\_Stability/links/00b49521f0e0fd5bbf000000.pdf](https://www.researchgate.net/profile/M_R_Siddiqui/publication/235766964_Synthesis_and_Characterization_of_Silver_Oxide_and_SilverChloride_Nanoparticles_with_High_Thermal_Stability/links/00b49521f0e0fd5bbf000000.pdf).

[44] M. Ibáñez, O.J. Pozo, J.V. Sancho, F.J. López, F. Hernández, Re-evaluation of glyphosate determination in water by liquid chromatography coupled to electrospray tandem mass spectrometry, *J. Chromatogr. A.* 1134 (2006) 51–55. doi:10.1016/j.chroma.2006.07.093.

[45] M.P.G. de Llasera, L. Gómez-Almaraz, L.E. Vera-Avila, A. Peña-Alvarez, Matrix solid-phase dispersion extraction and determination by high-performance liquid chromatography with fluorescence detection of residues of

glyphosate and aminomethylphosphonic acid in tomato fruit, *J. Chromatogr. A.* 1093 (2005) 139–146. doi:10.1016/j.chroma.2005.07.063.

[46] M. Cuhra, T. Bøhn, P. Cuhra, Glyphosate: Too Much of a Good Thing?, *Front. Environ. Sci. Eng. China.* 4 (2016) 28. doi:10.3389/fenvs.2016.00028.

[47] T.W. Winfield, Determination of Glyphosate in Drinking Water by Direct-aqueous-injection HPLC, Post-column Derivatization, and Fluorescence Detection: Test Method 547, US Environmental Protection Agency, 1990.

[48] M. Antoniou, M. Habib, C.V. Howard, R.C. Jennings, C. Leifert, R.O. Nodari, C.J. Robinson, J. Fagan, Teratogenic effects of glyphosate-based herbicides: divergence of regulatory decisions from scientific evidence, *J Environ Anal Toxicol S.* 4 (2012) 2161–0525. <http://moraybeedinosaurs.co.uk/neonicotinoid/Teratogenic%20Effects%20of%20Glyphosate-Based%20Herbicides.pdf>.

[49] S. Eker, L. Ozturk, A. Yazici, B. Erenoglu, V. Romheld, I. Cakmak, Foliar-applied glyphosate substantially reduced uptake and transport of iron and manganese in sunflower (*Helianthus annuus* L.) plants, *J. Agric. Food Chem.* 54 (2006) 10019–10025. doi:10.1021/jf0625196.

[50] D.M. Scroggs, A.S.M. Stewart, D.K. Miller, B.R. Leonard, J.L. Griffin, D.C. Blouin, Response of Weeds to Zinc-Glyphosate Mixtures, *La. Agric.* 51 (2008). [http://www.lsuagcenter.com/NR/rdonlyres/10DDB771-C862-4417-9DD6-DFD3907A2416/50555/Louisiana\\_Agriculture\\_Summer\\_2008\\_web.pdf](http://www.lsuagcenter.com/NR/rdonlyres/10DDB771-C862-4417-9DD6-DFD3907A2416/50555/Louisiana_Agriculture_Summer_2008_web.pdf).

[51] M.L. Bernards, K.D. Thelen, D. Penner, R.B. Muthukumaran, J.L. McCracken, Glyphosate interaction with manganese in tank mixtures and its effect on glyphosate absorption and translocation, *Weed Sci.* 53 (2005) 787–794. doi:10.1614/WS-05-043R.1.

[52] A.C. França, M.A.M. Freitas, L. D'Antonino, C.M.T. Fialho, A.A. Silva, M.R. Reis, C.P. Ronchi, Nutrient content in arabica coffee cultivars

subjected to glyphosate drift, *Planta Daninha*. 28 (2010) 877–885. doi:10.1590/S0100-83582010000400021.

[53] Y.-J. Wang, D.-M. Zhou, R.-J. Sun, L. Cang, X.-Z. Hao, Cosorption of zinc and glyphosate on two soils with different characteristics, *J. Hazard. Mater.* 137 (2006) 76–82. doi:10.1016/j.jhazmat.2006.02.032.

[54] L. Ozturk, A. Yazici, S. Eker, O. Gokmen, V. Römheld, I. Cakmak, Glyphosate inhibition of ferric reductase activity in iron deficient sunflower roots, *New Phytol.* 177 (2008) 899–906. doi:10.1111/j.1469-8137.2007.02340.x.

[55] E. Malavolta, Manual de nutrição mineral de plantas, Agronômica Ceres, 2006. <http://www.sidalc.net/cgi-bin/wxis.exe/?IsisScript=INIA.xis&method=post&formato=2&cantidad=1&expresion=mfn=022855>.

[56] D.W. Franzen, J.H. O'Barr, R.K. Zollinger, Interaction of a Foliar Application of Iron HEDTA and Three Postemergence Broadleaf Herbicides with Soybeans Stressed from Chlorosis, *J. Plant Nutr.* 26 (2003) 2365–2374. doi:10.1081/PLN-120025465.

[57] V. Römheld, V. Romheld, M.G. Guldner, T. Yamada, L. Öztürk, L. Ozturk, İ. Çakmak, I. Cakmak, G. Neumann, Relevance of glyphosate in the rhizosphere of non-target plants in, in: Kluwer, 2005: pp. 476–477. <http://research.sabanciuniv.edu/1579/> (accessed June 25, 2017).

[58] L.D. Tuffi Santos, C.H. de Siqueira, N.F. de Barros, F.A. Ferreira, L.R. Ferreira, A. Ferreira Lopes Machado, Crescimento e concentração de nutrientes na parte aérea de eucalipto sob efeito da deriva do glyphosate, *Cerne*. 13 (2007). <http://www.redalyc.org/html/744/74413401/>.

[59] S. Bozorgzadeh, B. Haghighi, Enhanced electrochemiluminescence of ZnO nanoparticles decorated on multiwalled carbon nanotubes in the presence of peroxydisulfate, *Microchim. Acta*. 183 (2016) 1487–1492. doi:10.1007/s00604-016-1785-8.

[60] N.A. Bakar, M.M. Salleh, A.A. Umar, M. Yahaya, The detection of pesticides in water using ZnCdSe quantum dot films, *Advances in Natural Sciences: Nanoscience and Nanotechnology*. 2 (2011) 025011. doi:10.1088/2043-6262/2/2/025011.

[61] C.J. Miles, H.A. Moya, Extraction of glyphosate herbicide from soil and clay minerals and determination of residues in soils, *J. Agric. Food Chem.* 36 (1988) 486–491. doi:10.1021/jf00081a020.

[62] J.V. Sancho, F.J. López, F. Hernández, E.A. Hogendoorn, P. van Zoonen, Rapid determination of glufosinate in environmental water samples using 9-fluorenylmethoxycarbonyl precolumn derivatization, large-volume injection and coupled-column liquid chromatography, *J. Chromatogr. A*. 678 (1994) 59–67. doi:10.1016/0021-9673(94)87074-8.

[63] T.V. Nedelkoska, G.K.-C. Low, High-performance liquid chromatographic determination of glyphosate in water and plant material after pre-column derivatisation with 9-fluorenylmethyl chloroformate, *Anal. Chim. Acta*. 511 (2004) 145–153. doi:10.1016/j.aca.2004.01.027.

[64] C. Hidalgo, C. Rios, M. Hidalgo, V. Salvadó, J.V. Sancho, F. Hernández, Improved coupled-column liquid chromatographic method for the determination of glyphosate and aminomethylphosphonic acid residues in environmental waters, *J. Chromatogr. A*. 1035 (2004) 153–157. <http://www.ncbi.nlm.nih.gov/pubmed/15117086>.

[65] Z.H. Kudzin, D.K. Gralak, J. Drabowicz, J. Luczak, Novel approach for the simultaneous analysis of glyphosate and its metabolites, *J. Chromatogr. A*. 947 (2002) 129–141. <http://www.ncbi.nlm.nih.gov/pubmed/11873992>.

[66] S. Sarkar, R. Das, PVP capped silver nanocubes assisted removal of glyphosate from water—A photoluminescence study, *J. Hazard. Mater.* 339 (2017) 54–62. doi:10.1016/j.jhazmat.2017.06.014.



[67] M. Muneer, C. Boxall, Photocatalyzed Degradation of a Pesticide Derivative Glyphosate in Aqueous Suspensions of Titanium Dioxide, *Int. J. Photoenergy*. 2008 (2008) 1–7. doi:10.1155/2008/197346.

[68] J.S. McConnell, L.R. Hossner, pH-Dependent adsorption isotherms of glyphosate, *J. Agric. Food Chem.* 33 (1985) 1075–1078. doi:10.1021/jf00066a014.

[69] J.S. McConnell, L.R. Hossner, pH-dependent adsorption isotherms of glyphosate [Erratum to document cited in CA103(25):208751y], *J. Agric. Food Chem.* 39 (1991) 824–824. doi:10.1021/jf00004a043.

[70] J. Sheals, M. Granström, S. Sjöberg, P. Persson, Coadsorption of Cu(II) and glyphosate at the water-goethite ( $\alpha$ -FeOOH) interface: molecular structures from FTIR and EXAFS measurements, *J. Colloid Interface Sci.* 262 (2003) 38–47. doi:10.1016/S0021-9797(03)00207-8.

[71] J. Sheals, S. Sjöberg, P. Persson, Adsorption of Glyphosate on Goethite: Molecular Characterization of Surface Complexes, *Environ. Sci. Technol.* 36 (2002) 3090–3095. doi:10.1021/es010295w.

[72] K. Dideriksen, S.L.S. Stipp, The adsorption of glyphosate and phosphate to goethite: a molecular-scale atomic force microscopy study, *Geochim. Cosmochim. Acta.* 67 (2003) 3313–3327. doi:10.1016/s0016-7037(02)01369-8.

[73] E. Morillo, T. Undabeytia, C. Maqueda, A. Ramos, Glyphosate adsorption on soils of different characteristics. Influence of copper addition, *Chemosphere*. 40 (2000) 103–107. <https://www.ncbi.nlm.nih.gov/pubmed/10665451>.

[74] V. Subramaniam, P.E. Hoggard, Metal complexes of glyphosate, *J. Agric. Food Chem.* 36 (1988) 1326–1329. doi:10.1021/jf00084a050.

[75] P.J. Chenier, *Survey of Industrial Chemistry*., Springer US, 2002. doi:10.1007/978-1-4615-0603-4.

[76] M.M. Peixoto, G.F. Bauerfeldt, M.H. Herbst, M.S. Pereira, C.O. da Silva, Study of the stepwise deprotonation reactions of glyphosate and the corresponding pKa values in aqueous solution, *J. Phys. Chem. A*. 119 (2015) 5241–5249. doi:10.1021/jp5099552.

[77] B. Liu, L. Dong, Q. Yu, X. Li, F. Wu, Z. Tan, S. Luo, Thermodynamic Study on the Protonation Reactions of Glyphosate in Aqueous Solution: Potentiometry, Calorimetry and NMR spectroscopy, *J. Phys. Chem. B*. 120 (2016) 2132–2137. doi:10.1021/acs.jpcc.5b11550.

[78] L. Pollegioni, E. Schonbrunn, D. Siehl, Molecular basis of glyphosate resistance--different approaches through protein engineering, *FEBS J*. 278 (2011) 2753–2766. <http://onlinelibrary.wiley.com/doi/10.1111/j.1742-4658.2011.08214.x/full>.

[79] B.K. Singh, *Plant amino acids: biochemistry and biotechnology*, CRC Press, 1998. [https://books.google.com/books?hl=en&lr=&id=b53DpRRHZtsC&oi=fnd&pg=PR3&dq=Plant%2BAmino%2BAcids%2BBiochemistry%2Band%2BBiotechnology&ots=-\\_PX9ZZRQD&sig=IhKe\\_T1ncbTrmwj7kdZrMLoc6Fk](https://books.google.com/books?hl=en&lr=&id=b53DpRRHZtsC&oi=fnd&pg=PR3&dq=Plant%2BAmino%2BAcids%2BBiochemistry%2Band%2BBiotechnology&ots=-_PX9ZZRQD&sig=IhKe_T1ncbTrmwj7kdZrMLoc6Fk).

[80] A.T. Stone, M.A. Knight, B. Nowack, Speciation and Chemical Reactions of Phosphonate Chelating Agents in Aqueous Media, in: *Chemicals in the Environment*, American Chemical Society, 2002: pp. 59–94. doi:10.1021/bk-2002-0806.ch004.

## CAPÍTULO IV

### Smartphone-based surface plasmon resonance device for glyphosate detection

Journal: Sensors and Actuators Reports  
Manuscript ID:  
Manuscript Status: in submission.

---

*Smartphone-based surface plasmon resonance device for  
glyphosate detection*

---

Carmonizia da Silva Freire<sup>\*1</sup>, Anderson Luis Valle<sup>\*2</sup>, Alessandro Falqueto<sup>1</sup>, Luiz Ricardo Goulart<sup>2</sup>, Eliton Souto de Medeiros<sup>3</sup>, Carlos Alberto de Souza Filho<sup>4</sup>, Rossana Moreno Santa Cruz<sup>1</sup>, Kaline do Nascimento Ferreira<sup>3</sup>, Luciano P. Rodrigues<sup>5</sup>, and Cleumar da Silva Moreira<sup>1\*\*</sup>,

1 Electrical Eng Graduate Program, Federal Institute of Paraíba, João Pessoa - PB, Brazil.

2 Institute of Biotechnology, Federal University of Uberlândia, Uberlândia - MG, Brazil.

3 Material Eng Graduate Program Federal Institute of Paraíba, João Pessoa - PB, Brazil.

4 Electrical Engineering Department Federal University of Paraíba, João Pessoa - PB, Brazil

5 Institute of Engineering, Science and Technology, Federal University of Jequitinhonha and Mucuri's Valleys, MG, Brazil.

\*\* Correspondent Author. cleumarmoreira@gmail.com]

\* Co-First Author

## ABSTRACT

Glyphosate is a widely used herbicide on many agricultural crops due to its high efficiency to control weeds. Recent studies have proven that glyphosate can cause acute and chronic damage to the human health. Simple, real time, and portable methods for detection and quantification of glyphosate remains a challenge. Actually, current techniques require expensive resources without any possibility of real time detection. Here, a smartphone-based surface plasmon resonance (SPR) device is proposed for glyphosate detection. CuO nanoparticles have been added to glyphosate samples diluted in ultra-pure water solutions to enhance its detection. Source and detection apparatus were coupled to a smartphone. Detection of the herbicide could be performed in different pH and concentration levels. An enhancement of sensitivity was observed in acidic solutions reaching a dilution of  $10^{-8}$  (v/v). This novel smartphone based SPR device for glyphosate detection presented increased sensitivity and all the other favorable biosensor features, such as ease of use, portability, and real-time analysis.

**Keywords:** Glyphosate, Biosensor, SPR, Smartphone, Biochip.

## INTRODUCTION

Glyphosate [(N-phosphonomethyl) Glycine] is a non-selective and post-emergent herbicide widely used in crop control due to its high weeding efficiency [1, 2]. Since its ability to chelate in the soil, which gives it a non-mobility feature, and the ability to be degraded by fungi, it is supposed to create a toxicologically harmless status. However, in 2012, the European Glyphosate Task Force (GTF) published a list of 285 scientific citations dealing with its toxicological effects, including the growth of wheat-infecting fungi [3] and over 30 plant diseases [4]. The historic carefree worldwide use of glyphosate and glyphosate resistant transgenic crops coupled with the fact that there are many considerations that make glyphosate a difficult molecule to detect have created the "glyphosate paradox". This paradox means that the most widely used agrochemical in the

world is one of the most rarely determined. Various methods and techniques of detection for the glyphosate exist, such as: chromatography techniques (liquid chromatography, gas chromatography, ion chromatography, chromatography-mass spectrometry) [5], methods of absorption and emission [6], surface-enhanced Raman scattering [7], spectroscopic optical nuclear magnetic resonance [8], chemiluminescence-molecular imprinting sensor [9], electrochemical sensors amperometric and voltammetric [10, 11], capillary electrophoresis [9], enzyme-linked immunosorbent assays [12], cell biosensor [9] and cross-responses from multiple sensors [13].

Nevertheless, none of the glyphosate detection methods present a unique device with the following features: high sensitivity, portability, applicability for real samples, reproducibility, fast response, specificity, high selectivity, stability, low cost, and possibility to be operated by a non-specialized user, as the actual glucometers [9]. In this way, smartphone-based biosensors are a good alternative for remote applications providing simple, fast, and low-cost detection devices [14].

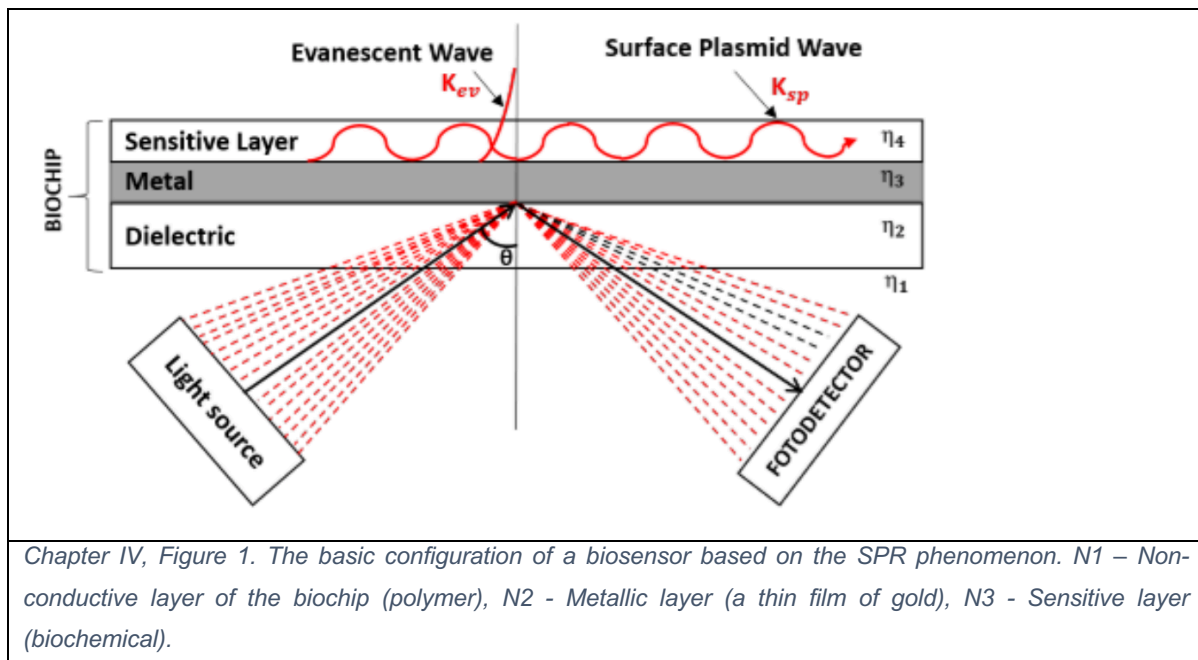
Smartphones are affordable, inexpensive gadgets with embedded technology, such as high-performance processors, high-megapixel CCD camera, touch screen, multiplayer system, Bluetooth, WIFI [15]. Recent studies have pointed out

the use of smartphones on the development of optical devices applied for chemical and biological analyses [16, 17]. One of these optical devices is based on the surface plasmon resonance spectroscopy, having some advantageous features that lead to higher sensitivity, selectivity, and simplicity.

Recently, an SPR-based smartphone device was applied for glyphosate detection [18]. It has used a prism as the optical substrate, a red input source was generated on the smartphone screen, and the image was detected by the frontal camera. Experimental results of this device [18] are here presented, considering different samples of glyphosate diluted in ultra-pure water with different pH values. The sensing scheme relied on the interaction between silver nanoparticles produced by laser ablation in an aqueous solution of sodium citrate. This forms a stable colloid with the analyte during the measurement time span. The Raman spectra of samples reached a limit of detection of 1.7 mg/L of Glyphosate in water. The glyphosate dilution ranged from  $10^{-2}$  to  $10^{-8}$ , and our device detected the herbicide in the lower level of dilution, i.e.,  $10^{-8}$ . Moreover, at the acidic pH, the sensitivity increased when compared to a basic solution.

## THEORETICAL BACKGROUND

### SPR technique



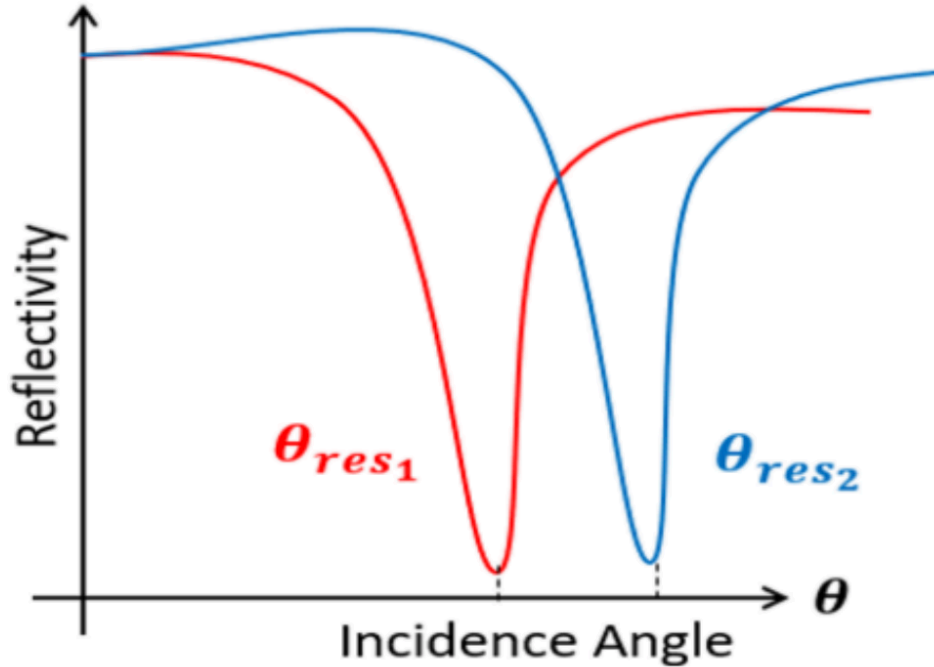
Surface plasmon resonance (SPR) is a well-known technique used at the design of chemical and biological sensors. A metal-dielectric interface (Fig. 1) is the basic element of an SPR sensor, where the metal is a nanolayer, being normally a noble metal such as gold, silver and copper, and the dielectric is the substance or solution to be investigated. Additionally, an optical substrate is used to match the propagation constants of the electromagnetic waves of the metal (called surface plasmon polaritons) to the incoming photons [19, 20].

When the input polarized light beam hits on the dielectric-metal interface (N1 /N2), certain or all quantity of light is absorbed, and another part is re- flected. When the surface plasmon resonance conditions are reached, an evanes- cent electric field is generated. Its amplitude changes accordance the distance to the metal-dielectric interface, having higher values on the interface. There- fore, SPR sensors exhibit high sensitivities to the interface changes, especially for small molecules, which explains the wide research and proposal of devices for environmental applications and diseases detection [21, 20].

The resonance occurs at a specific angle, called the resonance angle ( $\theta_{Res}$ ), which represents the point where the wavevectors of the incoming photons



( $k_{ev}$ ) and the surface plasmons ( $k_{sp}$ ) have the same amplitudes. This leads to a reflectivity value  $R$  minimum at  $\theta_{RES}$ , which is represented in Fig. 2.



*Chapter IV, Figure 2. SPR characteristic curve. Reflections in function of the angle of incidence. For each sensitive layer type, we have a refractive index associated with a different resonance angle (res).*

An overview of Smartphone-based SPR sensors

The first smartphone-based SPR detection system was proposed in 2013 [22]. The central SPR coupler disposable system for this implementation is compatible with Lab-on-a-chip (LOC) technology and temporarily adheres to the surface of the phone screen during measurement. The apparatus performs the coupling and conditioning the screen illumination and directs the image of the SPR to the camera of the phone. After analysis, the device can be removed and discarded, leaving the phone intact.

The work developed by [23] presents a spectrometer developed from the use of the integrated camera of the smartphone. This instrument performs detection as a biosensor of photonic crystal without labels. Its platform was made with a plastic substrate, which is attached to a standard glass microscope slide, and that can be easily removed and replaced.

The work presented by [15] develops a technique that uses the camera of the smartphone as a spectroscopic sensor of evanescent-coupled waves. Also, it uses simple optical components, such as the smartphone camera converted as a spectrometer and a prism glass. The main advantages of this proposed sensing technique are its reduced size, portability. and cost-effectiveness.

The work developed by [24] reports the construction of a portable fiber biosensor based on the resonance of surface plasmons using a smartphone as the detection platform. The instrumentation developed in this project allows its application to a wide range of analytes.

The work developed by [25] brings a prototype of an SPR sensor system in optical fiber designed for smartphones. In this project, the flashlight and the rear camera of the smartphone device are used, avoiding the use of electrical components external to the system.

The project developed by [26] exposes a sensitive and portable SPR platform for the screening of high-risk pesticides using highly sensitive nanoplasmonic biochips integrated into a smartphone.

The work done by [27] implements a measuring instrument using a plastic optical fiber based on smartphone technology, whose purpose is to measure the refractive index of liquids.

The research developed by [28] has led to a surface plasmon resonance platform integrated with a smartphone for use in the field with high throughput bio-detection using inexpensive and disposable SPR substrates which are produced by commercial disc metal coating Blu-ray.

The work presented by [19] brings a portable optical biosensor system that uses light sensor coupled to the smartphone. In this project, an added sensor in the smartphone is considered as an alternative optical receiver instead of the conventional optical analysis device. The sensor can respond to ambient light over a wide range of wavelengths, including the visible and infrared spectrum.

The design developed by [29] describes a mobile biosensing apparatus based on the integration of a microfluidic device with a smartphone. The system is built as an integrated test kit, which includes microfluidic chips, a smartphone-based imaging platform, applications developed for image capture and data analysis, and a set of reagents and accessories to perform the analysis test.

The work presented by [30] reports a SPR biosensor platform based on smart- phones with a grating coupler. This device offers the advantage of portability and simplicity, attractive features for point-of-care application and remote sens- ing of biomedical and environmental targets.

The majority of the analyzed papers, the approach is built as a proof of concept rather than real applications.

## MATERIAL AND METHODS

### Smartphone-based SPR sensor

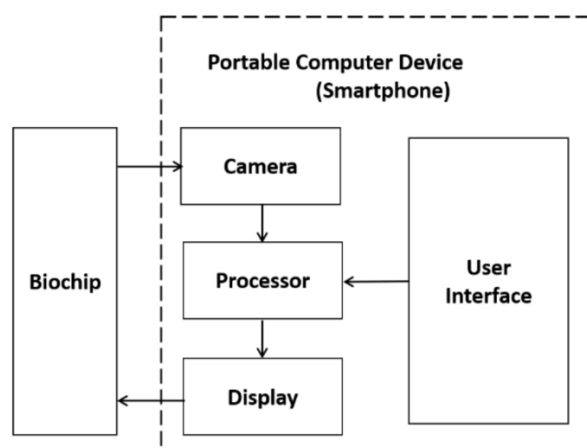
Recently, an ordinary smartphone was used to perform analytical measurements, and then to work as an optical biosensor based on the SPR effect [21]. The surface phenomena is studied through the monitoring changes in the refractive index of the substance under analysis. Fig. 3 shows the platform used in our experiments.

The light source, photodetector, processor and device/user interface of the smartphone were employed to the development of the proposed device. A commercial SPR sensor was used to interact with the glyphosate samples, the VIR biochip [31]. Nevertheless, the modularity of the platform allows the use of other biochips. The input and output signals were generated and detected, respectively, by a software developed in Android Studio. Fig. 4 shows the proposed device.

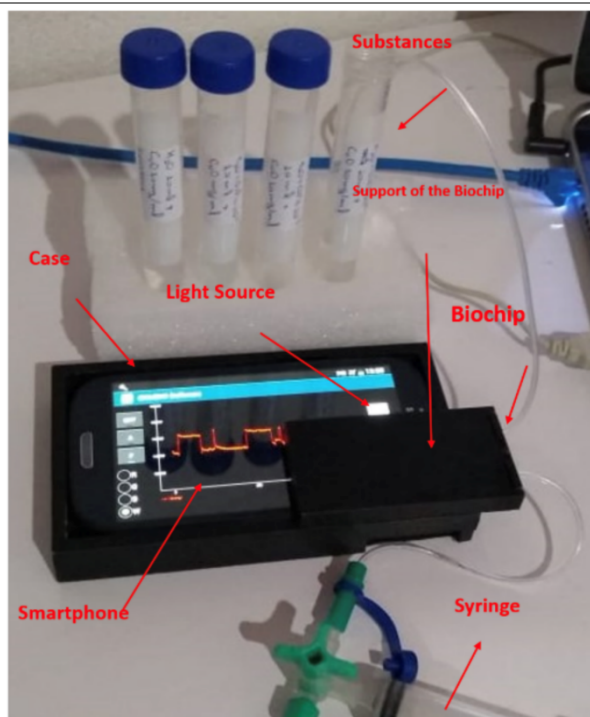
The proposed system features a modular, case-shaped structure for attaching the smartphone to the platform, which is totally portable and flexible, and can be used with various biochips. There is a slot in the smartphone case to attach the biochip holder and the flow cell.

The operation of the portable SPR device starts by the insertion of the samples, which are in plastic tubes. This insertion is done by means of capillaries connected to a flow cell present in the center of the biochip. The fluidic transport is provided by a commercial syringe. After each analysis, the system starts a cleaning and rinsing cycle, and then starts a new analysis.

The smartphone screen exhibit incoming light signal for the sensor, which enters in the SPR sensor. It is totally reflected, and the outgoing signal is captured by the camera of the smartphone. The captured images are stored in the internal memory of the smartphone, and processed to extract the necessary information at the SPR analysis.



*Chapter IV, Figure 3. Portable multi-analytic detection platform hardware architecture. Camera - photodetector, Processor - image processing, Display - light source, User Interface (Display) - information input and output and Biochip - Transducer (converts biochemical signal to electrical signal).*



*Chapter IV, Figure 4. Smartphone-based Portable Multi-analytical SPR Biosensor Device. The screen of the smartphone sends the signal that light in the entrance of the biochip is transmitted to its exit and captured by the camera of the smartphone in image form. The captured images are stored in the internal memory of the smartphone and processed, for extraction of the characteristic information to the SPR technique of analysis.*

## Samples

Glyphosate was tested from its commercial formulation, Glyphotal TR<sup>®</sup>. It is formed by Isopropylammonium salt of Glyphosate 648 g L<sup>-1</sup> (64% m/v), N-(phosphonomethyl) Glycine acid equivalent: 480 g L<sup>-1</sup> (48% m/v), and other ingredients: 721 g L<sup>-1</sup> (72,10% m/v). Samples were prepared by dilution were the most concentrated solution was Glyphotal TR<sup>®</sup> 10<sup>-2</sup> (v/v) that represents 4.8 ppm, to the most diluted 10<sup>-8</sup> (v/v) (0.00000048 ppm). Nanoparticles was always diluted at 1g/1000 mL and add in this concentration at each Glyphotal TR<sup>®</sup> dilution. We used H<sub>2</sub>SO<sub>4</sub> and NaOH to perform pH changes. The influence of the addition of different metallic nanoparticles to the substances, containing glyphosate, was also investigated, and the effects to a lower or higher detection capacity, according to the used metal.

## Microscopy Analysis of the Glyphosate-CuO interaction

To check the characteristics of the formed complex accordance to the pH changes, SEM images were collected by an electronic microscope (Carl Zeiss EVO MA10) associated to an Energy Dispersive Spectroscopy (EDS) (Oxford Instruments SDD detector). Compositional analyses were performed by the INCA Tools for Measurements software (INCA V7.2 Service Pack.13.2, ETAS GmbH, Stuttgart, Germany). At the SEM images, a carbon was attached to double-stick tape on aluminum stubs and coated with gold in a sputter coating apparatus. The complex was diluted at the concentration of (10<sup>-2</sup> v/v). AFM images were also performed by the SPM 9600, Shimadzu, a very high-resolution scanning probe microscopy. A 3 L of GlyphotalTR<sup>®</sup>-CuO was dropped in ultrapure water [10<sup>-4</sup> v/v] solution at a mica sheet.

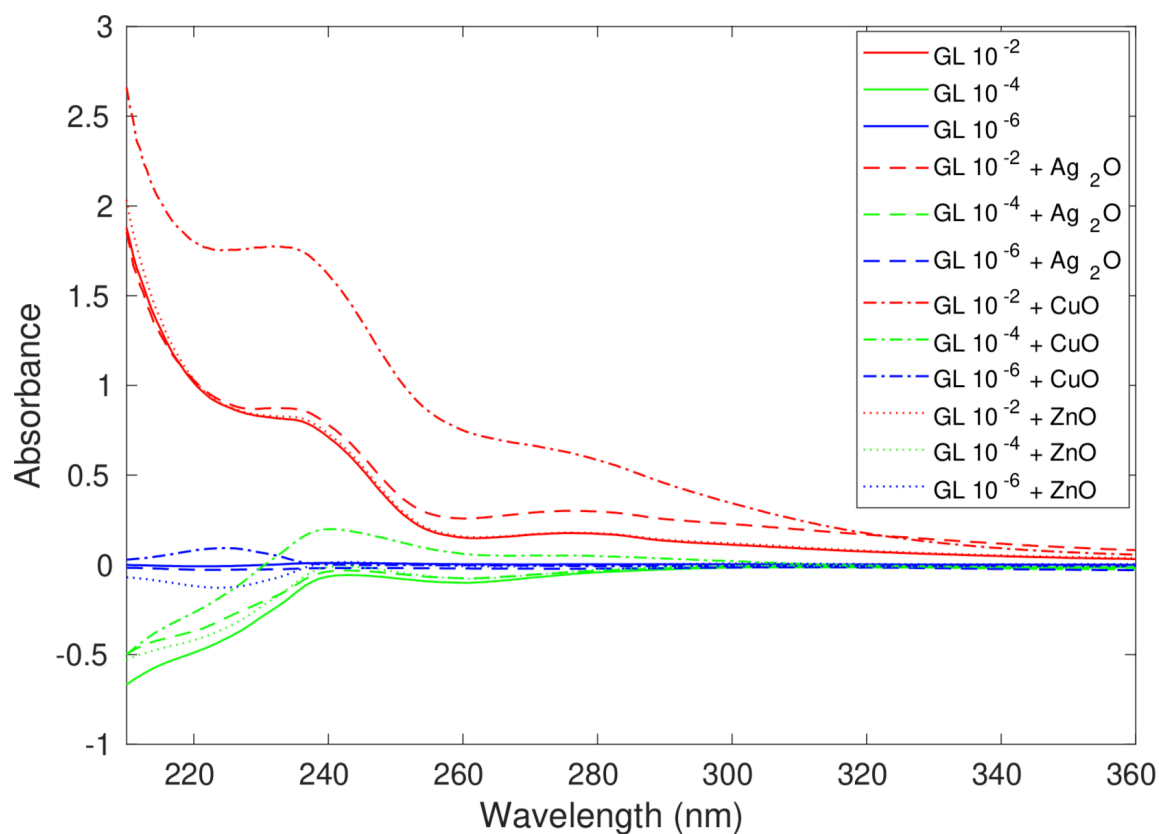
### Analysis of the absorbance spectrum of glyphosate samples

A UV-1800 Shimadzu UV Spectrophotometer was used to verify the characteristics of glyphosate through the UV-Visible range. A quartz cuvette with a 10 mm optical path was employed.

## EXPERIMENTAL RESULTS

Glyphosate samples at the dilutions of  $10^{-2}$  (which is usually used for soil for applications),  $10^{-6}$  and  $10^{-8}$  (v/v) (hardly detected by other devices [22]) in ultrapure water have been used. In order to measure the Glyphosate's enhancement signal, and the consequent measurement of their affinities, it was added ZnO, Ag<sub>2</sub>O and CuO nanoparticles.

Fig. 5 shows the absorption spectra of glyphosate (GL) at the dilutions of  $10^{-2}$ ,  $10^{-4}$  and  $10^{-6}$  (v/v) in ultrapure water (UP), with and without the influence of the nanoparticles of the Ag<sub>2</sub>O (silver oxide), CuO (copper oxide) and ZnO (zinc oxide). The absorption spectra of the pesticide are remarkably identified at the dilutions of  $10^{-2}$  (v/v), whose dilution is generally applied to the soil [9] which is of the initial interest to this application.





---

*glyphosate-containing samples. Acronyms: UP - ultrapure water, GL - glyphosate, Ag<sub>2</sub>O - silver oxide nanoparticle, CuO-nanoparticle of copper oxide and ZnO - nanoparticle of zinc oxide. The red curves represent the samples with glyphosate in the dilution of 10<sup>-2</sup> (v/v), the green curves represent the samples with glyphosate in the dilution of 10<sup>-4</sup> (v/v) and the blue curves represent the samples with glyphosate in the dilution of 10<sup>-6</sup> (v/v). Full line curves are related to samples without the influence of nanoparticles, dashed curves with the influence of Ag<sub>2</sub>O nanoparticles, traces curves with points with the influence of CuO nanoparticles and dotted curves with the influence of ZnO nanoparticles.*

---

The results for copper oxide (CuO) have pointed out to be the most efficient in the amplification of the absorbance signal. On the other hand, dilutions of 10<sup>-4</sup> and 10<sup>-6</sup> (v/v) showed no absorbance at the range of ultraviolet light, leading to new techniques, which will allow new types of analyses in smaller dilutions, such as the analysis of glyphosate in food.

Glyphosate at 10<sup>-6</sup> (v/v) with CuO nanoparticles presented the best results and were analyzed under different pH values. In this process, the following samples were analyzed:

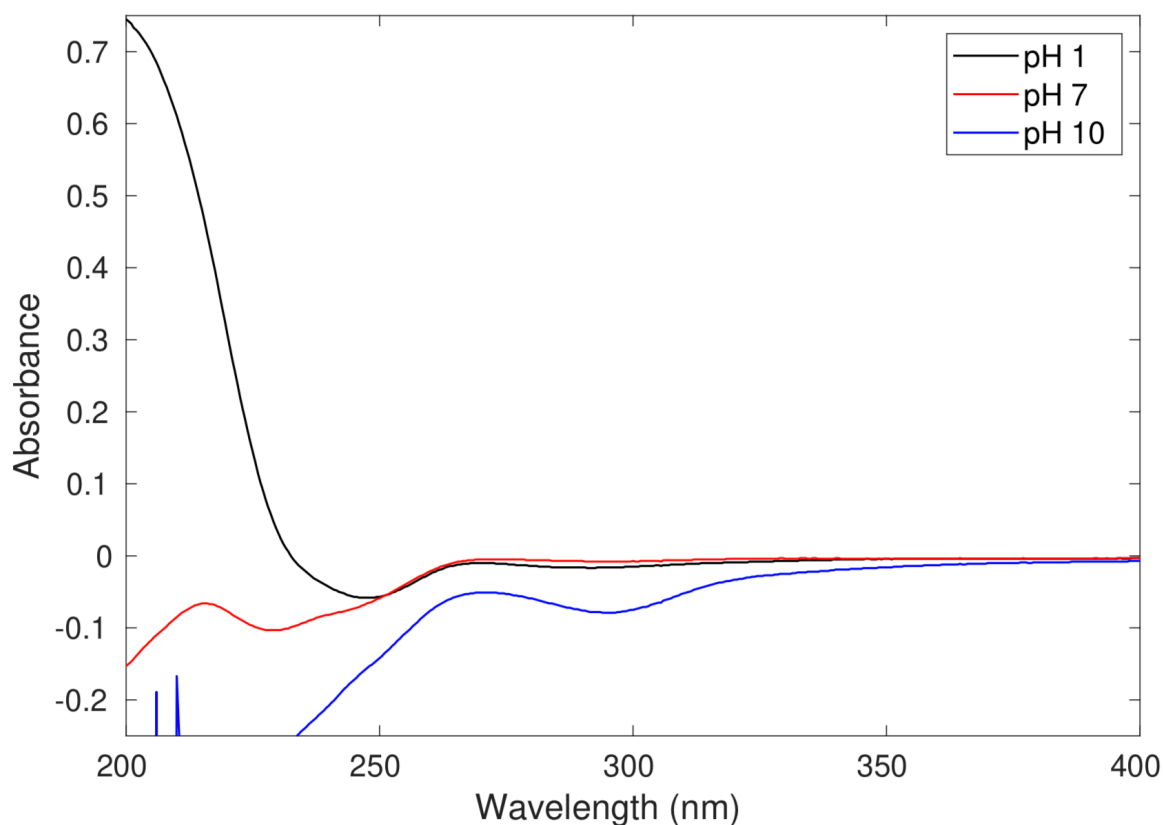
- Acidic solution (pH = 1): ultrapure water, glyphosate, copper oxide, and sulfuric acid;
- Neutral solution (pH = 7): ultrapure water, glyphosate, and copper oxide;
- Basic solution (pH = 10): ultrapure water, glyphosate, copper oxide and, sodium hydroxide.

Fig. 6 shows the results obtained by UV-Vis instrument considering the analysis of samples under pHs. The results indicated a significant increase in the absorbance signal for the acidic solution at a dilution of 10<sup>-6</sup> (v/v), when compared to the signal depicted in Fig. 5.

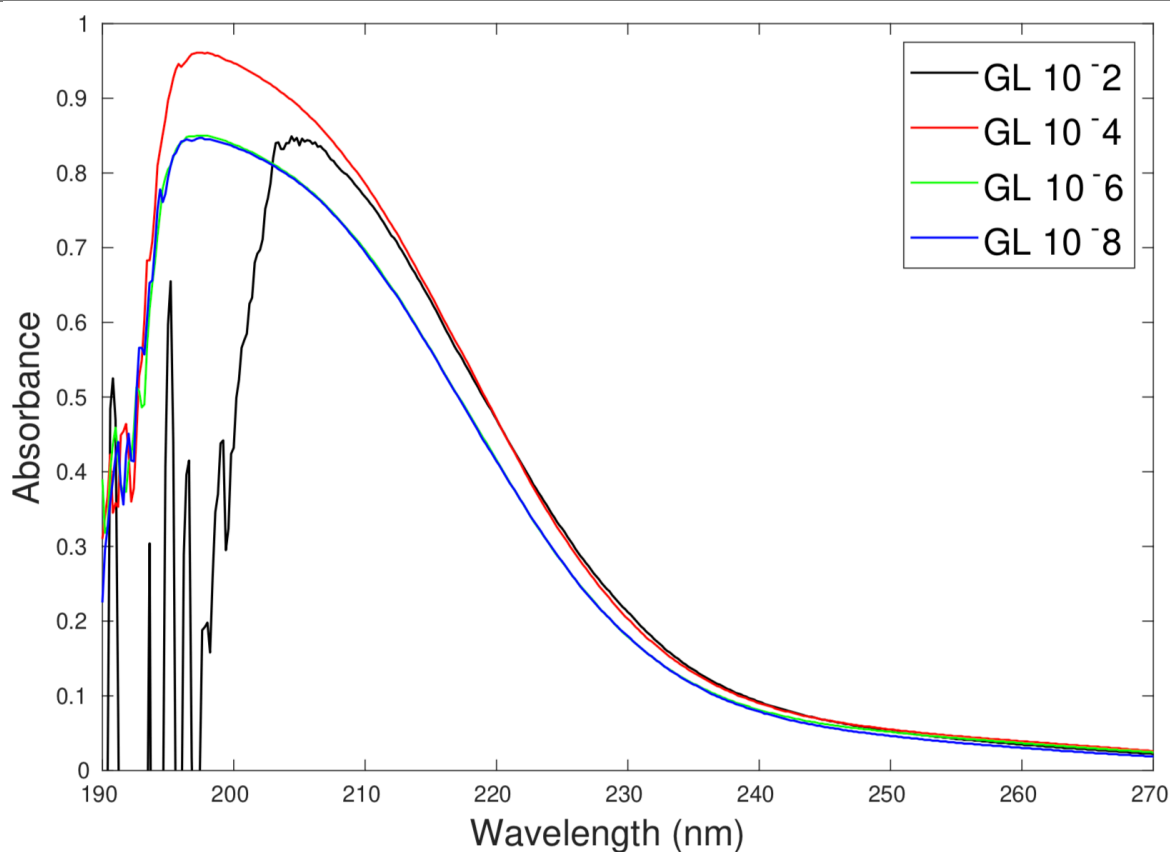
Fig. 6 evidences the influence of pH as a pre-treatment technique for the detection of glyphosate when coupled to copper oxide (CuO) nanoparticles, using a Shimadzu UV- 1800 operating at the range of 190 nm to 400 nm.

Investigations of the effect of pH 1 (acid) on ultraviolet-visible spectroscopy analysis at the dilutions of  $10^{-2}$ ,  $10^{-4}$ ,  $10^{-6}$  and  $10^{-8}$  (v/v) of glyphosate with CuO nanoparticles in ultrapure water are shown in Fig. 7.

In this study, it was possible to identify pesticide absorbance spectra at all acidic dilutions. For dilutions up to  $10^{-6}$  (v/v), the absorbance of glyphosate with the nanoparticles exhibited the same behavior, demonstrating that at very low concentrations the equipment has similar sensitivity. For dilutions of  $10^{-4}$  (v/v), an increase in the intensity of the spectrum occurs, and for the dilutions of  $10^{-2}$  (v/v) the spectrum presented the same profile. However, shifting the characteristic peak to the region of lower energy, result concatenated with the increase in the concentration of the species, which reduces the average distance between molecules to the extent of modifying the absorption capacity of the pesticide.



*Chapter IV, Figure 6. Investigation of the influence of pH on the absorbance spectrum of substances containing glyphosate at a dilution of  $10^{-8}$  (v/v) and copper oxide nanoparticles. Following the legend: pH 1 - acid, pH 7 - neutral, pH 10 - basic.*



*Chapter IV, Figure 7. Investigation of the influence of pH 1-acid in UP-ultrapure water on the absorbance spectrum of glyphosate-containing substances in the dilutions of  $10^{-2}$ ,  $10^{-4}$ ,  $10^{-6}$  and  $10^{-8}$  (v/v) and CuO-oxide nanoparticles copper.*

### Performance analysis

The preliminar tests were carried out with the objective to check the biosensor performance, for different solutions with and without the presence of glyphosate.

Cobalt Ferrite nanoparticles ( $\text{CoFe}_2\text{O}_4$ ) were also used. Fig. 7 and Fig. 8 depict the analysis of three different substances (concentration of 100 g), which follows:

- Ultrapure water (UP);
- Ultrapure water and, cobalt ferrite;
- Ultrapure water, cobalt ferrite and glyphosate.

The analysis was developed by using the RGB channels of the smartphone camera. Therefore, for each channel (R, G and B) the measurements were collected through some image processing techniques.

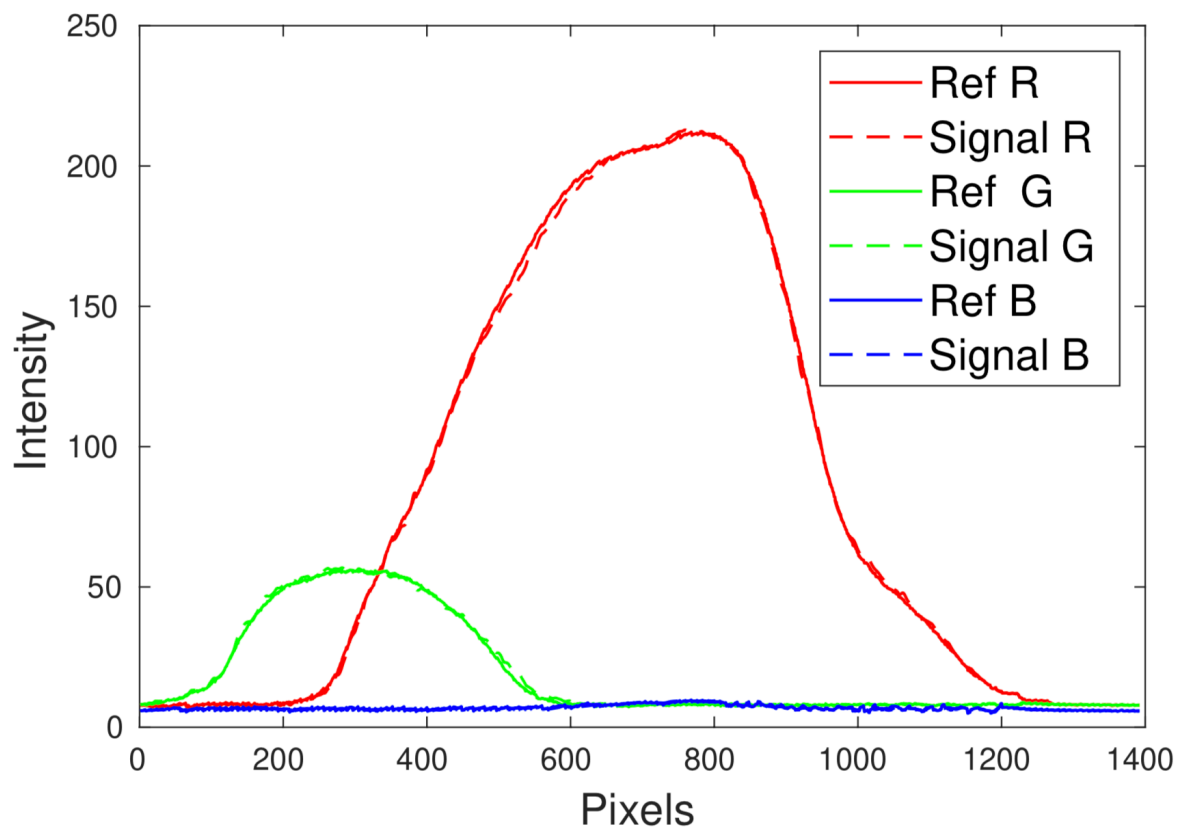
Fig. 8 illustrates the intensity curves of the pixels for each channel (R, G and B) of the signal. In this case, the SPR effect can be observed with a signal attenuation (Channel R) relative to the reference signal (REF R channel), as a result of the absorption of light. It also confirms that the SPR phenomenon occurs for the samples and can be observed by signal attenuation regarding the R channel and can be better observed from the analysis of this channel.

After analyzing and verifying the intensity variation of the pixels for the channels (R, G and B) of the images, the energy of the signal is calculated, given by the variation of the intensity of the pixels as a function of the samples.

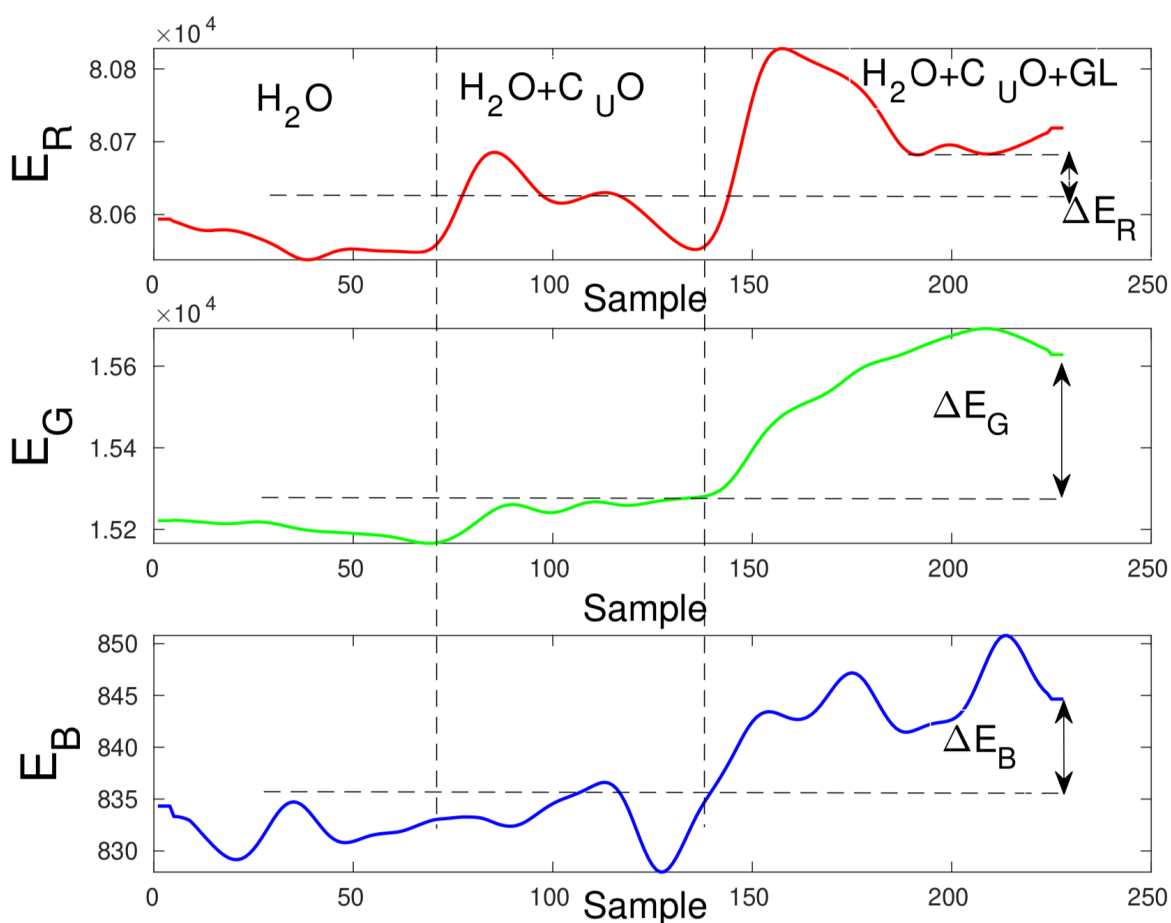
Fig. 9 shows the investigation of the energy curves for each channel (R, G and B) of the images resulting from the analysis of the substances.

The intensity of the signal increases with the increase of the refractive index of the substances. It is also noted that there is a difference in the signal amplitude for each substance identified in the image.

From the information related to the behavior of glyphosate in the presence of nanoparticles (Fig. 5), the substances containing the CuO nanoparticles were selected (presented the best result) to be analyzed by means of the device. Fig. 10 shows the graph of the signal energy at different dilutions for the copper oxide nanoparticles.



*Chapter IV, Figure 8. Curves resulting from the analysis of the intensity of the pixels of the images. Following the legend: REF - Reference signals of the pixels intensity for the channels (R, G and B). Signal - signals of the intensity of the pixels relative to the analysis of the samples for the channels (R, G and B).*

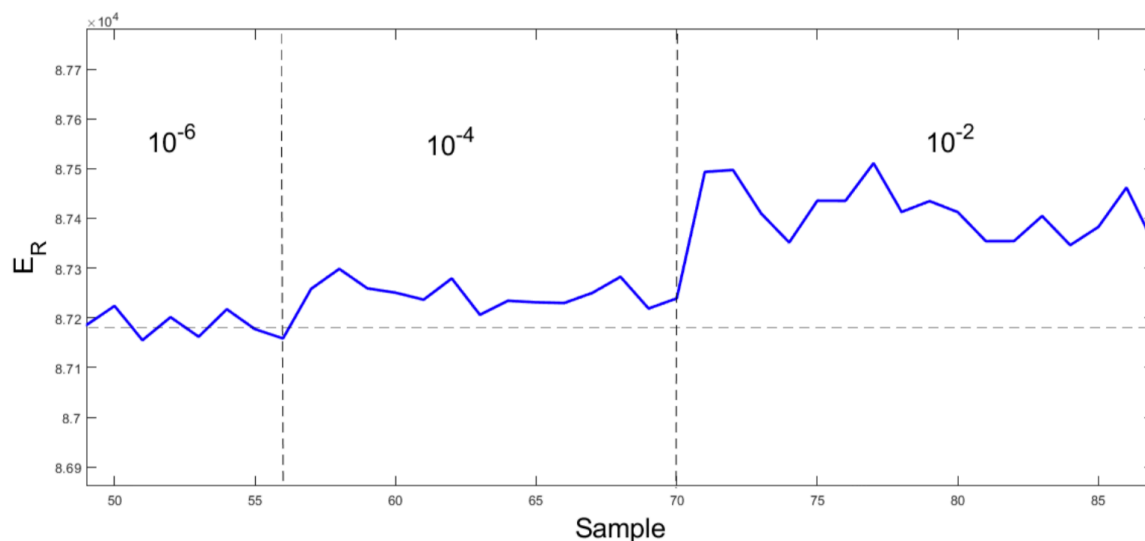


**Chapter IV, Figure 9.** Curves of the energy signals for the channels (R, G and B) of the images resulting from the analysis of the substances.  $\Delta E_R$  - Energy variation for the red channel.  $\Delta E_G$  - Energy variation for the green channel.  $\Delta E_B$  - Energy variation for the blue channel.

Results presented in Fig. 10 agree with those ones presented in Fig. 9, whereby increasing the refractive index, the energy also increases. As can be seen in Fig. 10, the proposed device distinguished the different concentrations of glyphosate, in which high sensitivity was evidenced for small dilutions.

To evaluate the performance of the proposed system, an average of 50 samples of the signal energy, for each used concentration value, was obtained by the smartphone ( $E_R$ ). UV-Vis analysis was used as standard references. The peaks of the obtained absorbance signal ( $M_{axAbs}$ ) were analyzed for each concentration, and results are depicted in Fig. 11.

The obtained results from the biosensor platform have the same behavior as the conventional laboratory instrument (UV-Vis), which indicates coherence of measurements.



*Chapter IV, Figure 10. Energy signal curve for the red channel of the images resulting from the analysis of the samples containing different concentrations of the glyphosate and CuO nanoparticle.*

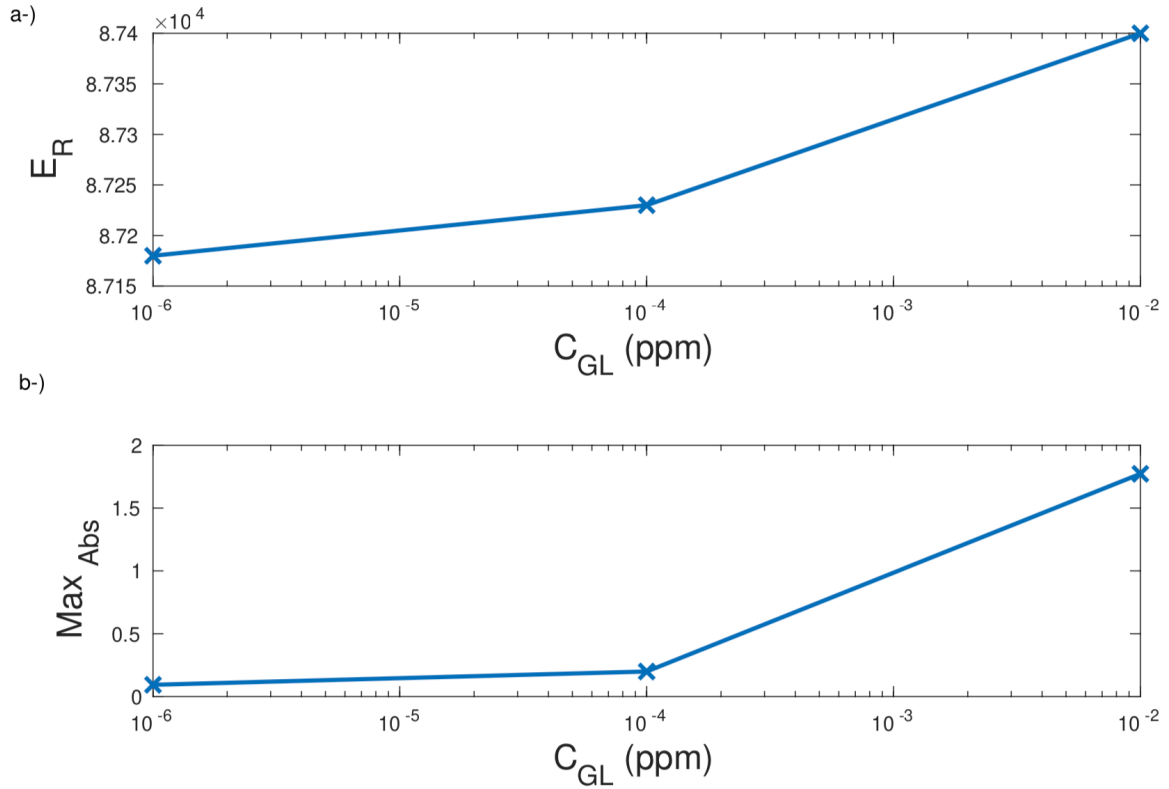
To analyze the response of the portable platform to acid pH glyphosate solutions, the same methodology was applied for a neutral solution. CuO nanoparticle solutions were sequenced for dilutions  $10^{-8}$ ,  $10^{-6}$ ,  $10^{-4}$  and  $10^{-2}$  (v/v) of Glyphosate, and results with acidic pH are shown in Fig. 12.

It can be seen from Fig. 12 that their  $E_R$  increases when the dilution is  $10^{-4}$  (v/v). This behavior was also observed at UV-Vis experiments. For values between  $10^{-8}$  to  $10^{-6}$  (v/v), the sensor response is even more pronounced than the UV-Vis approach.

When the transition occurs from  $10^{-4}$  to  $10^{-2}$  (v/v), there is a change in the output signal dynamics, with a diminished  $E_R$  value. Although this behavior is not desired, the same response was verified in the maximum absorbance value obtained by UV-Vis. This result comes from the fact that acidic pH amplified the response of the sensor, which means that solutions with very high concentrations may be far from the measurement range of the sensor.

The change to acidic pH allowed the measurement of  $10^{-8}$  (v/v) dilution, which was not possible with neutral pH. This result proves that amplification of the

response signal occurs due to the change of neutral pH to the acidic pH, already observed in the results shown in Fig. 6.



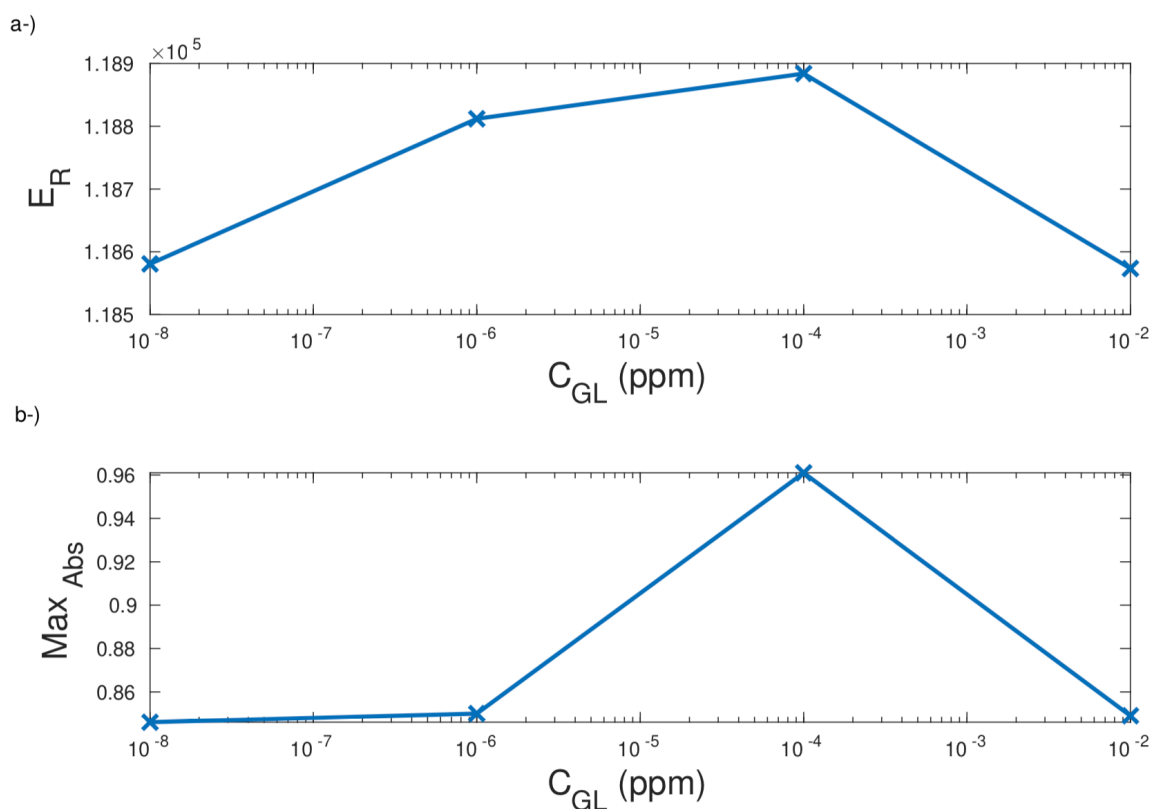
**Chapter IV, Figure 11. Signals referring to the analysis of samples containing glyphosate in the solutions of  $10^{-6}$ ,  $10^{-4}$  and  $10^{-2}$  (v/v) in neutral pH. a-) Signal obtained by the biosensor platform presented the energy of the channel (R) in relation to the concentration of glyphosate. b-) Signal obtained by UV-Vis showing the maximum absorbance in relation to the glyphosate concentration.**

In order to evaluate the pH effects on the response of the sensor, the sensitivity of the instrument in relation to the solution dilution was determined by using the following equation,

$$S_{C_{GL}}^y = \frac{\Delta y}{\Delta C_{GL}}$$

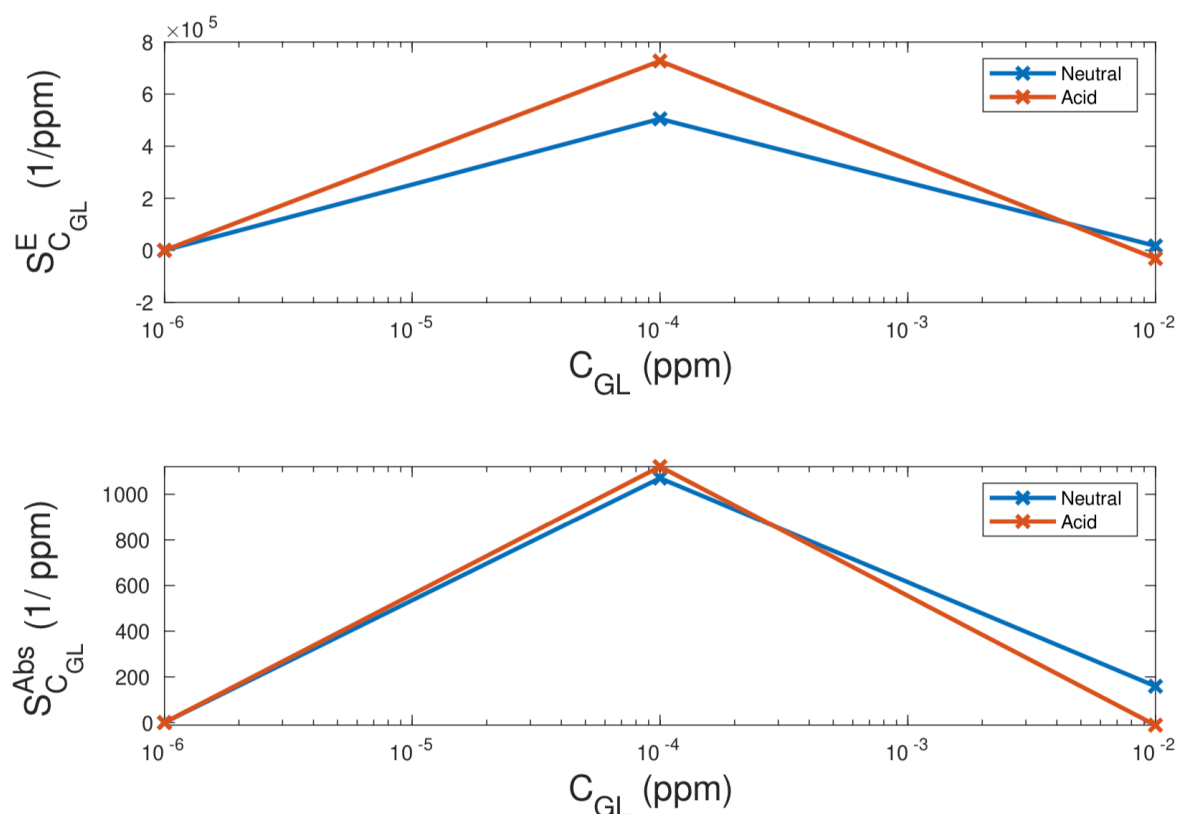
where for the proposed system, the output signal  $y$  and the energy value  $ER$  and for the UV-Vis the maximum absorbance value  $Max_{Abs}$ . The results obtained are shown in Fig.13.





**Chapter IV, Figure 12.** Signals pertaining to the analysis of glyphosate-containing samples in the dilutions of  $10^{-8}$ ,  $10^{-6}$ ,  $10^{-4}$  and  $10^{-2}$  (v/v) in acidic pH. a-) Signal obtained by the biosensor platform presented the energy of the channel (R) in relation to the glyphosate concentration. b-) Signal obtained by UV-Vis showing the maximum absorbance in relation to glyphosate concentration.

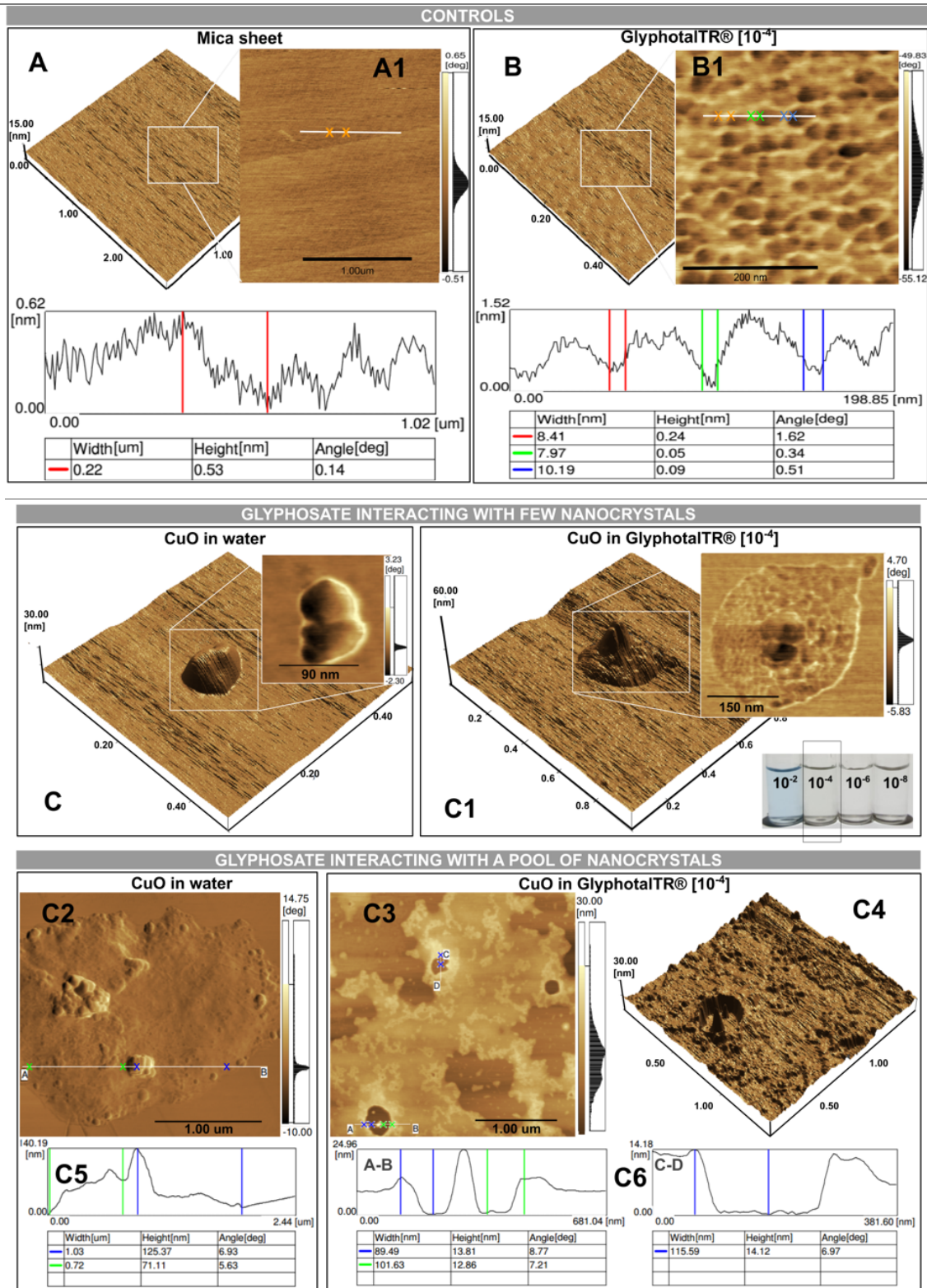
Therefore, when we use an acidic solution, the sensor presneed a higher sensitivity compared to that for a neutral solution, when a dilution of  $10^{-4}$  was considered. This increase in the sensitivity was verified for both UV-Vis and proposed SPR sensor. Nevertheless, when the dilution was of  $10^{-2}$  (v/v), a decrease in the sensitivity of the proposed platform and the UV-Vis was observed. This occurred to the extrapolation of the response range of the used equipment.



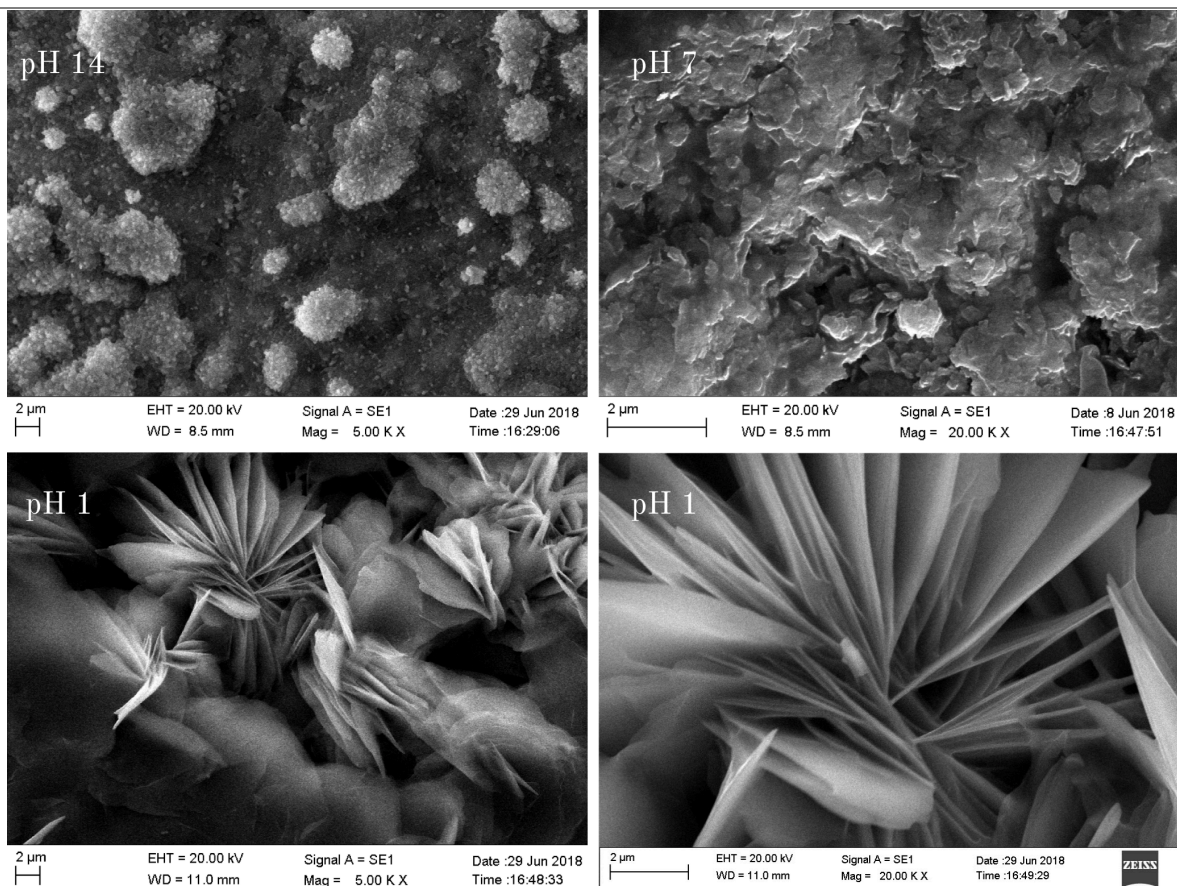
**Chapter IV, Figure 13.** Calculated sensitivity to the sample analysis with glyphosate diluted at dilution of  $10^{-6}$ ,  $10^{-4}$  and  $10^{-2}$ , considering acidic and neutral pH. a-) Calculated sensitivity for the proposed sensor. b-) Calculated sensitivity for UV-Vis approach.

The Fig. 14 shows the AFM of the Glyphosate interaction with CuO at  $10^{-4}$  in the pH 6. The interaction Glyphosate-CuO NCs was confirmed by Energy-Dispersive XRay Spectroscopy (EDS) analysis of the scanning electron microscope (SEM)s images conformer Fig. 15.

Thus, it is expected that at acidic media CuO is bound to Glyphosate by one of the tridentate complexes, which promotes a molecular restructuring where stellar forms are highlighted, as shown in Fig. 15A, which does not happen in neutral and basic media, Fig. 15B and 15C, respectively.



*Chapter IV, Figure 14 AFM of the (A) mica sheet used to support (B) Glyphosate, (C1 and C2) CuO nanocrystals in water and (C3 and C4) Glyphosate-CuO interacted.*



**Chapter IV, Figure 15. SEM of Glyphotal TR-CuO ( $10^{-2}$  v/v) in pH 1, 6 and 14. Like stars CuO nanocrystals are shown interacted with Glyphosate. The starry structure is missed as the pH increases. EDS results: mean - C (65.15), O (16.87), Cu (12.63), Au (5.35); Std. deviation: C (3.17), O (2.39), Cu (3.31), Au (0.44).**

## DISCUSSION

Although most of the available equipments fail to detect glyphosates without pretreatment due to its high affinity and complexation with metal cations [11], the presented smartphone-based surface plasmon resonance device was able to detect the herbicide in a very low concentration. Even in the Europe, with the highest restriction of glyphosate use (0.0001 ppm), only a small number of testing laboratories are able to detect this chemical [32]. Once  $\text{Cu}^{+2}$  is extensively used for agricultural purposes as a fungicide, being frequently added together with glyphosate and is present in fertilizers, sewage sludge, and other wastes, when  $\text{Cu}^{+2}$  was present, it is observed a drastic reduction in the concentration of free glyphosate due to the interaction, as indicated by [33] and [34]. So, it does not mean that Glyphosate is not present on the environment, but it can have been not detected. The herbicide and  $\text{Cu}^{+2}$  are strongly adsorbed on goethite (an iron-bearing hydroxide mineral), and the formed interaction is affected by pH and by the presence of the other.

There are a tendency of transitions and some trivalent metal ions, and divalent alkaline-earth to form 1:1 (e.g.  $\text{Ca(II)}$  and  $\text{Cu(II)}$ ) [35], [36] and 2:1 metal chelates with Glyphosate in solution [33]. Using DFT molecular modeling methods was showed that there is a stability order for tetrahedral and octahedral complexes between metals and Glyphosate as  $\text{Zn} > \text{Cu} > \text{Co} > \text{Fe} > \text{Cr} > \text{Al} > \text{Ca} > \text{Mg}$  [38].

The pH effect on the adsorption of  $\text{Cu}^{+2}$  and other metals for adsorbents of variable charge has been previously reported. The work developed in [39] found that the percentage of  $\text{Cu}^{+2}$  adsorbed on an iron oxyhydroxide decreased by about 80% when pH decreased from 6 to 4.75. Also, others [40] found similar behavior in the adsorption of  $\text{Cu}^{+2}$  on an oxisol soil.

The FT-IR analysis of glyphosate-Cu complex in pH 7.0 showed that the formation of the complex disappear the band at  $911\text{ cm}^{-1}$ , which was assigned to the P-OH group and, instead, a new band appears at approximately  $945\text{ cm}^{-1}$  due to the P-OCu group [41]. These authors did not found absorption

bands corresponding to the secondary amine group of glyphosate due to their overlapping with carboxylate bands, but [42] compared the spectral parameters for the complex and concluding that were consistent with  $1N_3O$  coordination in the equatorial ligand positions. Others [43] consider that the coordination via nitrogen and that in copper-glycine complexes would be analogous. In [41] a sharp absorption band at  $3236\text{ cm}^{-1}$  in the metal-herbicide complex is reported, and this is consistent with a square-planar geometry complex where copper was coordinated to the non-protonated amine N, phosphonate, and carboxylate moieties and an additional water molecule as proposed by [43]. [41] also found the bands at  $3455$  and  $3381\text{ cm}^{-1}$  probably hydrate OH stretching bands. In this way, glyphosate functions act as a tridentate ligand in the complex via amine nitrogen, carboxylic, and phosphonate [44]. [34] propose that in this way exist a coordination by one amino group and two negatively charged donor groups, with the formation of two chelate rings. On pH 4.0, the bidentate complex is protonated on the amine group [33] and non-protonated nitrogen makes direct bonding with Cu [43].

$\text{Cu}^{+2}$  was also used to develop a simple, label-free colorimetric method based on the inhibition of the peroxidase-like activity of  $\text{Cu}^{+2}$  able to detect glyphosate [45].  $\text{Cu}^{+2}$  was also used in voltammetric test, that concluded that the complex has two absorption bands from ultraviolet to visible light (200 to 1000 nm) [46]. They concluded that once glyphosate does not have a chromophoric group in its structure, it absorbs light up to 200 nm [47], but in  $\text{Cu}^{+2}$  solution, the band at 231 nm is evident as a result of the charge metal-glyphosate transfer where the herbicide sends an electron. Probably in this process, the electrons on the amino group are involved [48]. Those authors purpose that glyphosate as part of the  $\text{Cu}^{+2}$  complex occupies 3 of the 6 positions in a distorted octahedral (Jahn-Teller Distortion). This octahedron is completed by three water molecules. Glyphosate does not present electrochemical response on Hanging mercury drop electrode (HMDE electrode) [49] unless it is complexed with  $\text{Cu}^{+2}$  through reduction to Cu [46].



Combining the geometric shape, we also hypothesized that the formation of the NCs-CuO interaction promotes an orbital overlap capable of stimulating the electromagnetic field, which leads to an increasing plasmon. It is noteworthy that in the acid medium we have protonated glyphosate in the amine functional group and excess  $H^+$  ions in the medium that are ideal conditions for electron transfer. We believe these factors would promote a P-type doping, considerably amplifying the magnitude of the electromagnetic field, allowing detection of glyphosate at a dilution of  $10^{-8}$  (v/v) equivalent to  $0.0005 \text{ ng mL}^{-1}$ . Very sensitive chromatographic methods were used to reach detection limits of this magnitude, such as LC-SPE-ESI/ MS / MS [50].

In this way, it is expected that in acid medium CuO interacts with glyphosate by one of the tridentate complexes, what promotes a molecular restructuring where star forms are evidenced. Some studies have shown that when the nanoparticles are in a star form occurs a surface-enhanced Raman spectroscopy (SERS) intensification effect [51], [52]. SERS-sensors are considered as best device for non-destructive molecular analysis considering reliability, sensibility and selectivity. Unfortunately, its applicability is rather limited due to the lack of highly sensitive SERS platforms with good stability and reproducibility. Because of this the use of many SERS platforms has been coupled with metal nanoparticles.

The acquired morphology by some nanoparticles is the key applications in (SERS) because the resonant excitation of plasmons can dramatically amplify the electric field near the nanoparticle surface, which is exploited in the present device [53], [54], [55], [56]. This strongly contributes to the enhancement of the sensitivity of the plasmon resonance to the local dielectric environment.

Others [51] show that a nanostar have the electric field enhancements for excitation of the plasmon resonances as a result from the plasmon's hybridization and characteristics of the nanoparticle core, as already conclude by [57], [58]. In this way, they conclude that tip plasmons composed the low energy bonding nanostar plasmons with a finite contribution of the core plasmons. The interaction core/tip plasmon increases the excitation of the bonding plasmons enhancing the local electric field.

## CONCLUSIONS

A SPR-based sensor based on smartphone was proposed here to detect glyphosate in aqueous solutions. The results indicated the feasibility of the proposed sensor, with advantages of portability, ease of use, real time operation, which results in a more effective control of the use of this herbicide in the agricultural crops.

Selection of the appropriate nanoparticle (CuO) greatly improve the response of the equipment, allowing to identify the presence of this herbicide even in diluted in the order of  $10^{-6}$  (v/v).

The proposed smartphone system was able to measure dilution up to  $10^{-8}$  (v/v) of glyphosate, when using an acidic solution. A greater variation was proposed on the proposed sensor approach when compared to UV-Vis one, at the dilutions of  $10^{-4}$  (v/v). The results show that the proposed solution is then capable of measuring low levels of glyphosate concentration, similar to those found in soils ( $10^{-2}$  (v/v)) and in foods ( $10^{-6}$  (v/v)).

A best pretreatment technique and optimum concentration of the samples are under investigation, and then can lead to a way to minimize the herbicide effects in the environment and the mankind live.



## References

- [1] A. Junior, T. Santos, N. Brito, M. Ribeiro, Glyphosate: properties, toxicity, uses and legislation, *Química Nova* 25 (4) (2002) 589–593.
- [2] C. F. B. Coutinho, L. F. M. Coutinho, L. H. Mazo, S. L. Nixdorf, C. A. P. Camara, F. M. Lanças, Direct determination of glyphosate using hydrophilic interaction chromatography with coulometric detection at copper microelectrode, *Analytica chimica acta* 592 (1) (2007) 30—35. doi:10.1016/j.aca.2007.04.003.
- [3] G. Johal, D. Huber, Glyphosate effects on diseases of plants, *European Journal of Agronomy* 31 (3) (2009) 144 – 152. doi:https://doi.org/10.1016/j.eja.2009.04.004.
- [4] M. W. Ho, B. Cherry, Glyphosate tolerant crops bring diseases and death, *Science in Society* 47 (2010) 12–15.
- [5] N. F. Zelenkova, N. G. Vinokurova, Determination of glyphosate and its biodegradation products by chromatographic methods, *Journal of Analytical Chemistry* 63 (9) (2008) 871–874. doi:10.1134/S106193480809013X.
- [6] H. U. Lee, D. U. Jung, L. J. H, et al, Detection of glyphosate by quantitative analysis of fluorescence and single dna using dna-labeled fluorescent magnetic core–shell nanoparticles, *Sensors and Actuators B: Chemical* 177 (2013) 879 – 886. doi:https://doi.org/10.1016/j.snb.2012.11.075.
- [7] H. Torul, Boyaci, U. Tamer, Attomole detection of glyphosate by surface- enhanced raman spectroscopy using gold nanorods, *J Pharm Sci* 35 (4) (2010) 179–184.
- [8] B. Cartigny, N. Azaroual, M. Imbenotte, et al, Determination of glyphosate in biological fluids by <sup>1</sup>h and <sup>31</sup>p nmr spectroscopy, *Forensic Science International* 143 (2) (2004) 141 – 145. doi:https://doi.org/10.1016/j.forsciint.2004.03.025.

[9] A. Valle, F. Mello, R. Alves-Balvedi, L. Rodrigues, L. Goulart, Glyphosate detection: methods, needs and challenges, *Environmental Chemistry Letters* 17 (1) (2019) 219–317.

[10] J. Stutz, Development of electrochemical platform for differential analysis of commercial herbicides based on glyphosate (Master Thesis, 2016).

[11] F. C. Moraes, L. H. Mascaro, S. A. S. Machado, C. M. A. Brett, Direct electrochemical determination of glyphosate at copper phthalocyanine/multiwalled carbon nanotube film electrodes, *Electroanalysis* 22.

[12] F. Rubio, et al, Comparison of a direct elisa and an hplc method for glyphosate determinations in water, *Journal Of Agricultural And Food Chemistry* 51 (3) (2003) 691–696. doi:10.1021/jf020761g.

[13] S. Liu, H. Che, K. Smith, L. Chen, Contamination event detection using multiple types of conventional water quality sensors in source water, *Environ. Sci.: Processes Impacts* 16 (2014) 2028–2038. doi:10.1039/C4EM00188E.

[14] D. Zhang, Q. Liu, Biosensors and bioelectronics on smartphone for portable biochemical detection, *Biosensors and Bioelectronics* 75 (2016) 273–284. doi:https://doi.org/10.1016/j.bios.2015.08.037.

[15] S. Dutta, A. Choudhury, P. Nath, Evanescent wave coupled spectroscopic sensing using smartphone, *IEEE Photonics Technology Letters* 26 (6) (2014) 568–570. doi:10.1109/LPT.2013.2297700.

[16] A. Roda, E. Michelini, M. Zangheri, M. D. Fusco, D. Calabria, P. Simoni, Smartphone-based biosensors: A critical review and perspectives, *TrAC Trends in Analytical Chemistry* 79 (2016) 317 – 325. doi:https://doi.org/10.1016/j.trac.2015.10.019.

[17] T. Alawsi, Z. Al-Bawi, A review of smartphone point-of-care adapter design, *Engineering Reports* 1 (2) (2019) e12039. doi:10.1002/eng2.12039.

[18] C. d. Silva Freire, C. da Silva Moreira, C. A. de Souza Filho, R. Moreno Santa Cruz, A. Falqueto, A. L. Valle, L. R. Goulart, E. Souto de Medeiros, K. d. Nascimento Ferreira, Application of a smartphone-based spr platform for glyphosate detection, in: 2019 IEEE Sensors Applications Symposium (SAS), 2019, pp. 1–6. doi:10.1109/SAS.2019.8706024.

[19] Y. M. Park, Y. D. Han, H. J. Chun, H. C. Yoon, Ambient light-based optical biosensing platform with smartphone-embedded illumination sensor, *Biosensors and Bioelectronics* 93 (2017) 205–211.

[20] L. C. Oliveira, C. da Silva Moreira, C. Thirstrup, E. U. K. Melcher, A. M. N. Lima, H. Neff, A surface plasmon resonance biochip that operates both in the angular and wavelength interrogation modes, *IEEE Transactions on Instrumentation and Measurement* 62 (5) (2018) 1223–1232.

[21] C. A. d. Souza Filho, A. M. N. Lima, H. Neff, Smartphone based, portable optical biosensor utilizing surface plasmon resonance, in: 2014 IEEE International Instrumentation and Measurement Technology Conference (I2MTC) Proceedings.

[22] M. C. Preechaburana, Gonzalez, A. Suska, D. Filippini, Surface plasmon resonance chemical sensing on cell phones, *Sensors*.

[23] D. Gallegos, et al, Label-free biodetection using a smartphone, *Lab Chip* 13 (2013) 2124–2132. doi:10.1039/C3LC40991K.

[24] Y. Liu, Q. Liu, S. Chen, F. Cheng, H. Wang, W. Peng, Surface plasmon resonance biosensor based on smart phone platforms, *Sci Rep* 5 (2015) 1–9.

[25] Z. Chen, S. Chengjun, L. Zewei, L. Kunping, Y. Xijian, Z. Haimin, L. Yongxin, D. Yixiang, Fiber optic biosensor for detection of genetically modified food based on catalytic hairpin assembly reaction and nanocomposites assisted signal amplification, *Sensors and Actuators B: Chemical* 254 (2018) 956 – 965. doi:https://doi.org/10.1016/j.snb.2017.07. 174.

[26] K. L. Lee, et al, Nanoplasmonic biochips for rapid label-free detection of imidacloprid pesticides with a smartphone, *Biosensors and Bioelectronics* 75 (2016) 88–95. doi:<https://doi.org/10.1016/j.bios.2015.08.010>.

[27] Instrumento para medição de índice de refração a fibra óptica plástica baseado em tecnologia de smartphone (2017).

[28] H. Guner, et al, A smartphone based surface plasmon resonance imaging (spri) platform for on-site biodetection, *Sensors and Actuators B: Chemical* 239 (2017) 571–577. doi:<https://doi.org/10.1016/j.snb.2016.08.061>.

[29] K. Yang, et al, Mkit: A cell migration assay based on microfluidic device and smartphone, *Biosensors and Bioelectronics* 99 (2018) 259–267. doi:<https://doi.org/10.1016/j.bios.2017.07.064>.

[30] J. Zhang, I. Khan, Q. Zhang, X. Liu, J. Dostalek, B. Liedberg, Y. Wang, Lipopolysaccharides detection on a grating-coupled surface plasmon resonance smartphone biosensor, *Biosensors and Bioelectronics* 99 (2018) 312 – 317. doi:<https://doi.org/10.1016/j.bios.2017.07.048>. URL <http://www.sciencedirect.com/science/article/pii/S0956566317304943>.

[31] C. Thirstrup, W. Zong, M. Borre, H. Neff, H. Pedersen, G. Holzhueter, Diffractive optical coupling element for surface plasmon resonance sensors, *Sensors and Actuators B: Chemical* 100 (3) (2004) 298 – 308. doi:<https://doi.org/10.1016/j.snb.2004.01.010>.

[32] P. M. E, C. H. B, H. S. S, Proficiency test on incurred and spiked pesticide residues in cereals, *Accredit Qual Assur* 14.

[33] R. J. Motekaitis, A. E. Martell, Metal chelate formation by n-phosphonomethylglycine and related ligands, *Journal of Coordination Chemistry* 14.

[34] P. G. Daniele, C. D. Stefano, E. Prenesti, S. Sammartano, Copper(ii) complexes of n-(phosphonomethyl)glycine in aqueous solution: A thermodynamic and spectrophotometric study, *Talanta* 45.

[35] F. E. H. A. H. Smith, Paul H., K. N. Raymond, Crystal structures of two salts of n-(phosphonomethyl)glycine and equilibria with hydrogen and bicarbonate ions, *Inorganic Chemistry* 28.

[36] E. T. Clarke, P. R. Rudolf, A. E. Martell, A. Clearfield, Structural investigation of the cu (ii) chelate of n-phosphonomethylglycine, *Inorganica Chimica Acta* 164.

[37] H. E. Madsen, H. H. Lundager, C. Christensen, A. F. Gottlieb-Petersen, O. S. Andresen, C.-O. Pontchour, P. Phavanantha, S. Pramatus, B. N. Cyvin, S. J. Cyvin, Stability constants of copper(ii), zinc, manganese(ii), calcium, and magnesium complexes of n-(phosphonomethyl)glycine (glyphosate), *Acta Chemica Scandinavica* 32a.

[38] M. S. Caetano, T. C. Ramalho, D. F. Botrel, E. F. F. da Cunha, W. C. de Mello, Understanding the inactivation process of organophosphorus herbicides: A dft study of glyphosate metallic complexes with  $\text{Zn}^{2+}$ ,  $\text{Ca}^{2+}$ ,  $\text{Mg}^{2+}$ ,  $\text{Cu}^{2+}$ ,  $\text{Co}^{3+}$ ,  $\text{Fe}^{3+}$ ,  $\text{Cr}^{3+}$ , and  $\text{Al}^{3+}$ , *Journal of Quantum Chemistry* 112.

[39] M. M. Benjamin, , J. O. Leckie, Multiple-site adsorption of cd, cu, zn, and pb on amorphous iron oxyhydroxide, *Journal of Colloid and Interface Science* 79 (1) (1981) 209–221.

[40] J. J. Msaky, R. Calvet, Metal chelate formation by n-phosphonomethylglycine and related ligands, *Soil Science* 150.

[41] T. Undabeytia, M. V. Cheshire, D. Mephail, Ftir study of glyphosate-copper complexes, *Journal of Agricultural and Food Chemistry* 50.

[42] T. Undabeytia, M. V. Cheshire, D. Mephail, Interaction of the herbicide glyphosate with copper in humic complexes, *Chemosphere* 32.

[43] M. B. McBride, Electron spin resonance study of copper ion complexation by glyphosate and related ligands, *Soil Science Society of America Journal* 55.

[44] W. E. Dubbin, G. Sposito, M. Zavarin, X-ray absorption spectroscopic study of cu-glyphosate adsorbed by microcrystalline gibbsite, *Soil Science* 165.

[45] Y. Chang, Z. Zhang, J. Hao, W. Yang, J. Tang, Understanding the inactivation process of organophosphorus herbicides: A dft study of glyphosate metallic complexes with  $\text{Zn}^{2+}$ ,  $\text{Ca}^{2+}$ ,  $\text{Mg}^{2+}$ ,  $\text{Cu}^{2+}$ ,  $\text{Co}^{3+}$ ,  $\text{Fe}^{3+}$ ,  $\text{Cr}^{3+}$ , and  $\text{Al}^{3+}$ , *Sensors and Actuators B* 228.

[46] C. F. B. Coutinho, L. H. Mazo, Estudo voltamétrico e espectrofotométrico do complexo Cu(ii)-glifosato, *Pesticidas: Revista de Ecotoxicologia E Meio Ambiente* 17.

[47] K. Sato, J.-Y. Jin, T. Takeuchi, T. Miwa, K. Suenami, Y. Takekoshi, S. Kanno, Integrated pulsed amperometric detection of glufosinate, bialaphos and glyphosate at gold electrodes in anion-exchange chromatography, *Journal of Chromatography A*.

[48] R. L. Glass, Metal complex formation by glyphosate, *Journal of Agricultural and Food Chemistry* 32.

[49] R. F. Teofilo, E. L. Reis, C. Reis, G. A. da Silva, L. T. Kubota, Experimental design employed to square wave voltammetry response optimization for the glyphosate determination, *Journal of the Brazilian Chemical Society* 15.

[50] M. Ibanez, O. J. Pozo, S. J. V, F. J. Lopez, F. Hernandez, Re-evaluation of glyphosate determination in water by liquid chromatography coupled to electrospray tandem mass spectrometry, *J Chromatogr A*. 17.

[51] F. Hao, C. Nehl, J. H. Hafner, P. Nordlander, Plasmon resonances of a gold nanostar, *Nano Letters* 50.

[52] F. James Holler, D. A. Skoog, S. R. Crouch, C. Pasquini, Plasmon resonances of a gold nanostar, *Princípios de Análise Instrumental*.

[53] R. D. Averitt, D. Sarkar, N. J. Halas, Plasmon resonance shifts of au-coated a2s nanoshells: Insight into multicomponent nanoparticle growth, Phys. Rev. Lett. 78.

[54] T. R. Jensen, M. D. Malinsky, C. L. Haynes, R. P. van Duyne, Nanosphere lithography: Tunable localized surface plasmon resonance spectra of silver nanoparticles, J. Phys. Chem. B 104.

[55] S. Link, M. A. El-Sayed, Spectral properties and relaxation dynamics of surface plasmon electronic oscillations in gold and silver nanodots and nanorods, J. Phys. Chem. B 103.

[56] K. L. Kelly, E. Coronado, L. L. Zhao, S. G. C, The optical properties of metal nanoparticles: The influence of size, shape, and dielectric environment, J. Phys. Chem. B 107.

[57] E. Prodan, C. Radloff, N. J. Halas, P. Nordlander, A hybridization model for the plasmon response of complex nanostructures, Science 302.

[58] H. Wang, D. W. Brandl, P. Nordlander, N. J. Halas, Plasmonic nanostructures: Artificial molecules, Accounts of Chemical Research.

If you reached this point, I'm glad! We are on the way to building a better world.